RSC Advances

REVIEW

View Article Online
View Journal | View Issue



Cite this: *RSC Adv.*, 2025, **15**, 41724

# Synthetic strategies towards benzothiazole-based compounds of therapeutic potency: experimental, investigational and approved drugs

Reham A. Mohamed-Ezzat [a] and Galal H. Elgemeie *[b]

Received 5th June 2025
Accepted 29th August 2025

DOI: 10.1039/d5ra03993b

rsc.li/rsc-advances

Benzothiazoles play significant roles in modern therapeutical chemistry owing to their significant effects and their integration into various pharmaceutical agents for treating critical diseases. Several approved, investigational, and experimental benzothiazole-based drugs have been accomplished. Novel strategies targeting therapeutical benzothiazoles and up-to-date synthetic strategies of anti-neurodegenerative, anti-inflammatory, antitumor, anti-microbial, and anti-viral benzothiazoles are well-recognized and reviewed. The biological investigations of the newly synthesized compounds are emphasized. This comprehensive review is considered as a valuable source in drug discovery and development.



## 1. Introduction

The wide range of biological and pharmacological actions of benzothiazole-based compounds, such as their anti-cancer,

[a]*Chemistry of Natural and Microbial Products Department, Pharmaceutical and Drug Industries Research Institute, National Research Centre, Dokki, Cairo, Egypt*
[b]*Chemistry Department, Faculty of Science, Helwan University, Cairo, Egypt. E-mail: elgemeie@yahoo.com*

**Assoc. Prof. Reham A. Mohamed-Ezzat**

*Reham Amgad Mohamed-Ezzat, PhD in Organic Chemistry, Associate Professor of Therapeutic Chemistry at Chemistry of Natural & Microbial Products Department, Pharmaceutical & Drug Industries Research Institute, National Research Centre, Cairo, Egypt. She got her BSc (2010) in Chemistry & Biochemistry-Faculty of Science. She was awarded her MSc (2015) & PhD degree of science in organic chemistry in 2019 from Helwan University. She has published books and articles in international journals in the field of bio-organic and medicinal chemistry. She also published many conferences presentations. She has experience in the field of design and synthesis of new molecules of medicinal application, as well as the implementation of novel strategies in the syntheses of bioactive compounds. She is a member in the Egyptian Chemical Society, and in the Egyptian Society for Basic Sciences. E-mail: reham_amgad_2010@yahoo.com; ra.mohamed-ezzat@nrc.sci.eg.*

**Prof. Galal H. Elgemeie**

*Galal H. Elgemeie is the author of over 300 Scientific International papers on Heterocyclic Chemistry and Medicinal Chemistry. He was awarded the degree of Doctor of Science (DSc) in 2004. His research interests include the development and mechanistic understanding of organic reactions and their application to the synthesis of antimetabolic agents. He was an international elected member of the Scientific Board of the International Basic Sciences Programme (IBSP), UNESCO, in Paris, France. He was a postdoctoral fellow of the Alexander von Humboldt Foundation in Germany, the Fulbright in USA, the British Council in England, and then the German Research Foundation (DFG) in Germany. He supervised several cooperation projects with the European Community under the TEMUPS programme, Prof. Elgemeie was nominated as one of the leading scientists of the COMSTECH in the year 2009 Report. Prof. Elgemeie's research activities have received many awards including The African Union Scientific Award "Continental Scientific Award" in Science and Technology, The ISESCO Scientific Award and The Egypt State Honor Award "NILE", among many others. E-mail: elgemeie@yahoo.com; Galal_elgemeie@science.helwan.edu.eg.*

anti-inflammatory, anti-viral, anti-malarial, anti-tubercular, anti-diabetic, and neuroprotective activities, have garnered a lot of interest.[1–5] They are useful candidates in drug discovery because of their adaptable heterocyclic framework, which allows interaction with a variety of molecular targets. The therapeutic value of benzothiazole derivatives in addressing important signaling pathways and disease mechanisms has been shown in recent research. Novel benzothiazole derivatives, for example, have shown promise as GPR183 antagonists for the treatment of inflammatory bowel disease (IBD)[6] and as strong inhibitors of phosphoinositide 3-kinase γ (PI3Kγ), which is linked to inflammatory and autoimmune diseases.[7] Additional derivatives have the potential to treat cell death-related disorders as they preferentially inhibit RIPK1, a regulator of necroptosis.[8]

Benzothiazole scaffolds have been investigated for the synthesis of agents that target Huntington's and Alzheimer's diseases in neurodegenerative diseases.[9–15] By blocking Hsp90, TRPC3/6, androgen receptors, glutathione peroxidase, and kinases including SCD and CLK, other benzothiazole analogs have also demonstrated effectiveness against a variety of cancer types.[16–24]

Compounds that target HSV-1, HCV, USP7, NS3/4A, and SARS-CoV-2 are used in antiviral applications; many inhibitors have been found to block Mpro and spike protein interactions.[25–29] Other derivatives have showed anti-trypanosomal activity, with enhanced *in vivo* efficacy through optimal structural alterations, and benzothiazole-based DHFR inhibitors have shown promise in bacterial infections.[30–40] Benzothiazoles have other applications, including molecular imaging and photodynamic treatment.[41,42] Notably, boron-containing benzothiazoles have demonstrated promise in glioma treatment using boron neutron capture therapy (BNCT),[43] while 68Ga-labeled benzothiazole derivatives have been developed for imaging amyloid β plaques in cerebral amyloid angiopathy (CAA).[44] On the whole, benzothiazole derivatives are effective molecules in both therapeutic and diagnostic medicine due to their structural adaptability and pharmacological range. Clinically relevant molecules for a variety of disorders may result from their ongoing optimization and evaluation.[45–51]

## 2. Benzothiazole-based approved drugs

### 2.1. Riluzole

Riluzole **1** (Rilutek as marketed by Sanofi) (Fig. 1) is a glutamate antagonist utilized as anti-convulsants and used to treat to amyotrophic lateral sclerosis.[52] Riluzole is an activator of the TREK-1 channel and has been used clinically for a long time to treat almost all individuals with amyotrophic lateral sclerosis. It has a strong analgesic impact in a number of models of inflammatory and neuropathic pain. It's interesting to note that

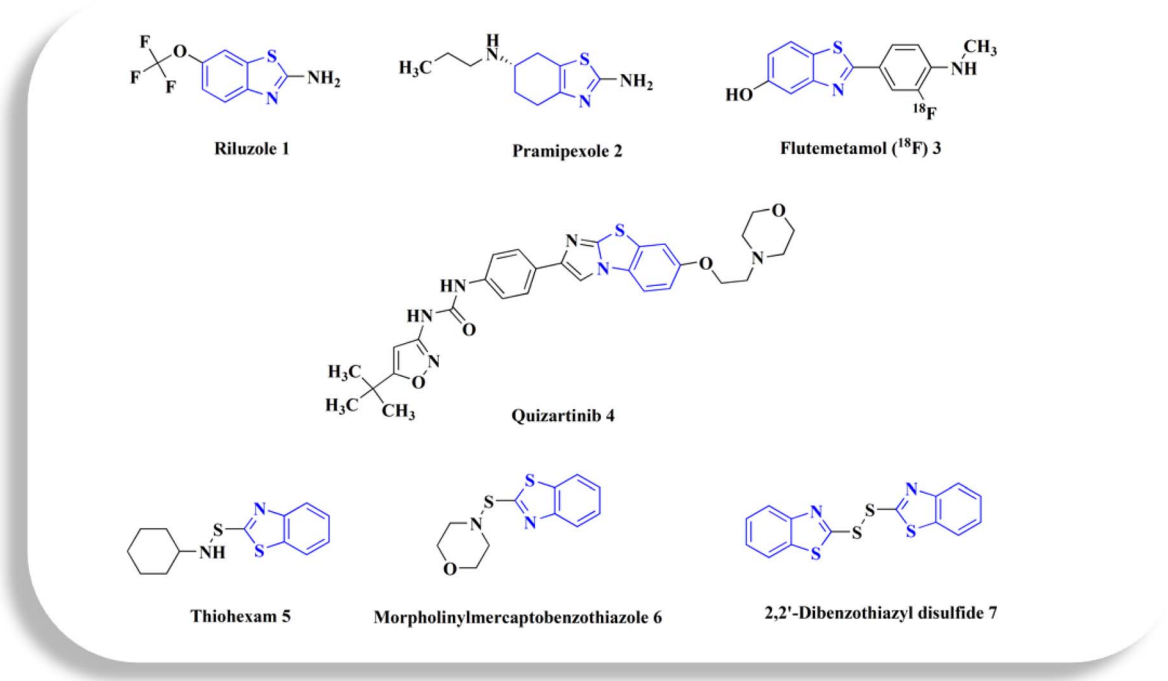


Fig. 1 Benzothiazole-based drugs.

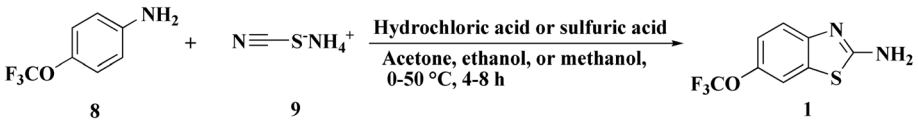


8 9 1

Scheme 1 Synthesis of riluzole 1.

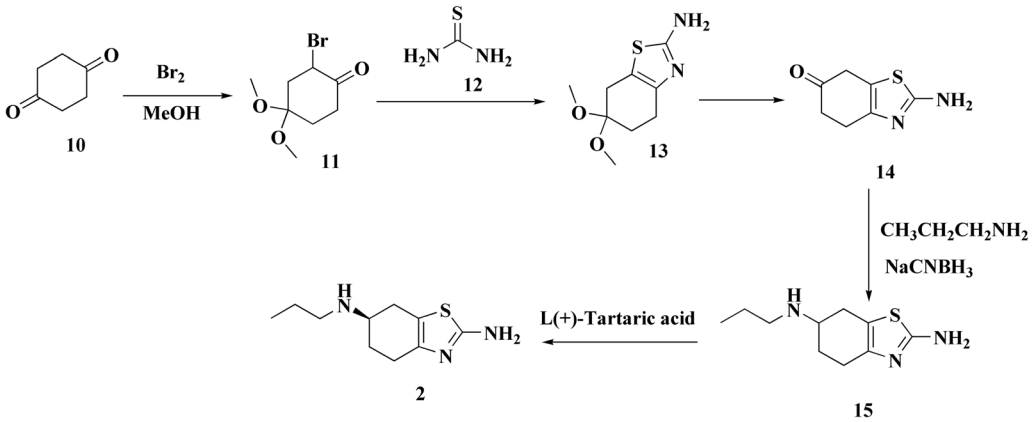


10 11 13 14 15 2

Scheme 2 Synthesis of pramipexole 2.

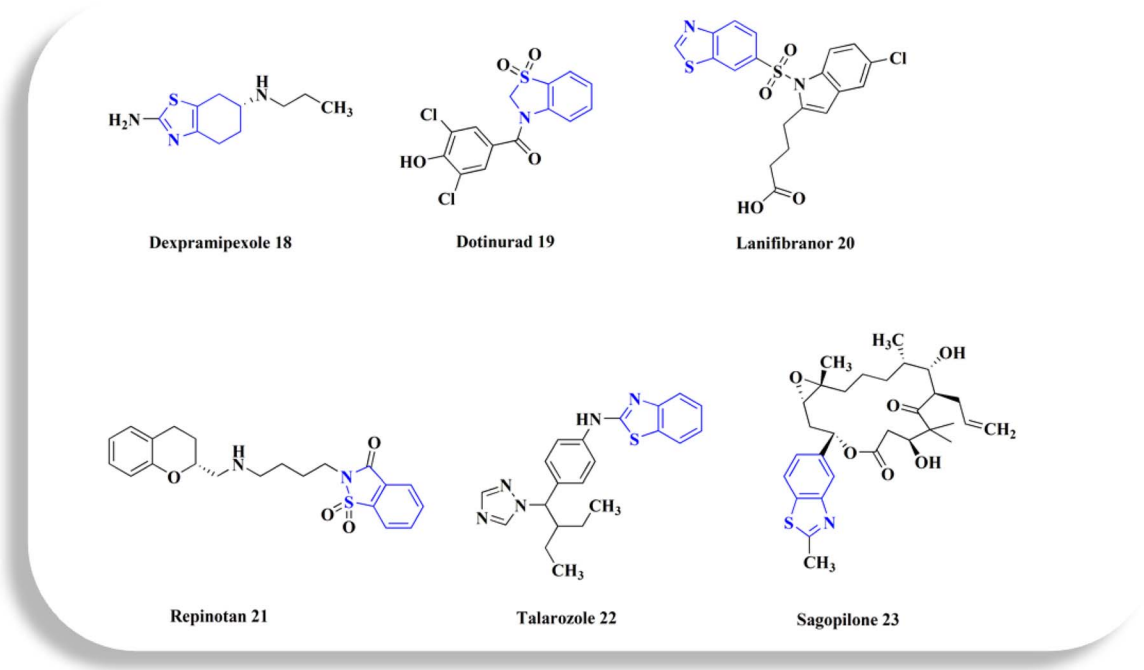


Fig. 2 Benzothiazole-based investigational drugs.

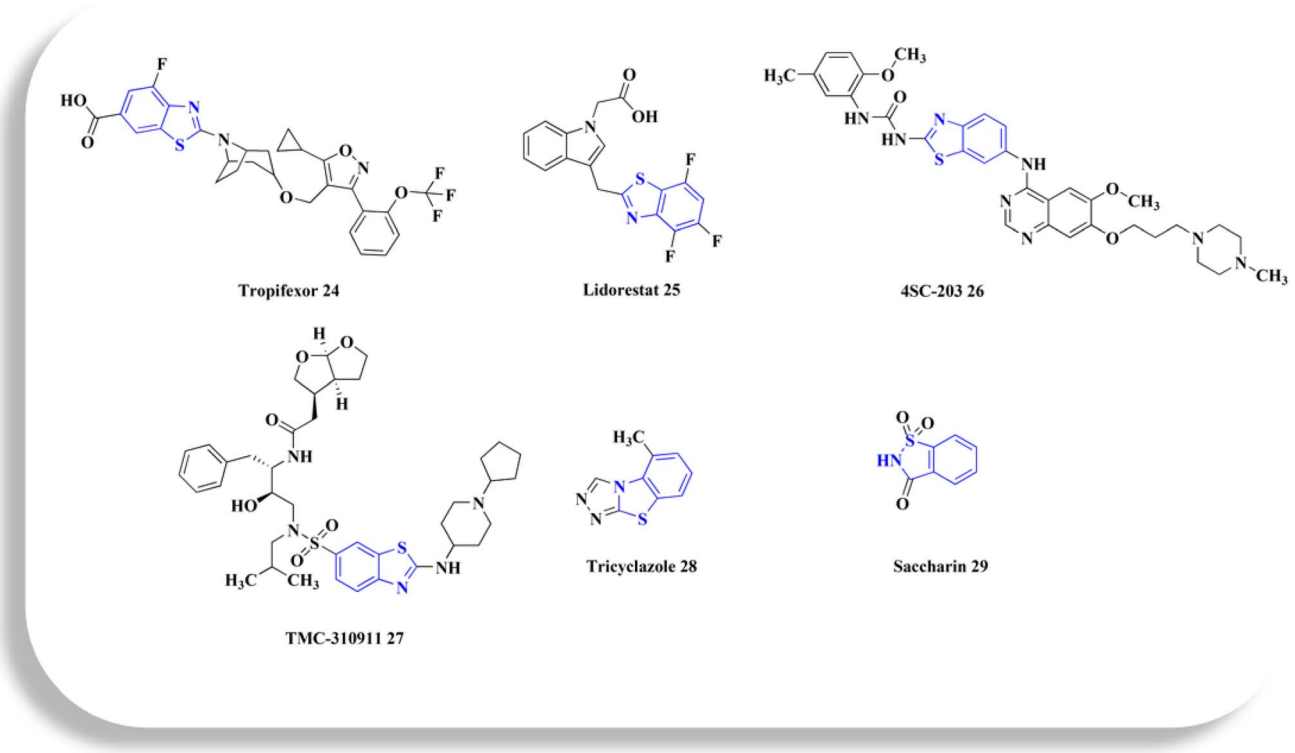


Fig. 3 Benzothiazole-based investigational drugs.

riluzole inhibits proliferation as well. The riluzole's effects on bone pain that induced by prostate cancer were analyzed. Prostate cancer (PCa) cell viability has also been shown to be dramatically reduced *in vitro* by riluzole treatment. In addition, riluzole's antiproliferative action causes cancer cells to express more TREK-1 channels.[53]

Riluzole (**1**) was prepared through reacting 4-trifluoromethoxyaniline (**8**) with ammonium thiocyanate (**9**) in acidic condition (Scheme 1).[54]

### 2.2. Pramipexole

Pramipexole **2** (Fig. 1) is an anti-parkinsonian drug used in treating parkinsonism and restless leg syndrome.[55]

The preparation of the pramipexole dihydrochloride proceeds from the 4-acetamidocyclohexanone and starts *via* bromination then thiourea cycliation and eventually transformation to generate the pramipexole (Scheme 2). An enhanced process uses aminocyclohexanol as the starting material and incorporates safer chemicals and fewer steps to increase efficiency and lessen environmental impact.[56]

### 2.3. Flutemetamol ($^{18}$F)

Flutemetamol ($^{18}$F) **3** (Fig. 1) is a PET scanning radiopharmaceutical containing the radionuclide fluorine-18. Estimating the density of β amyloid neuritic plaque in the brain by Positron Emission Tomography (PET) imaging is recommended for adult patients experiencing cognitive impairment who are being assessed for Alzheimer's disease (AD) or other potential causes of cognitive loss.[57] As a radiotracer, the $^{18}$F-flumetamol has a strong affinity for brain amyloid plaques, is capable of differentiating AD cases from controls, and has strong histopathological neuritic amyloid plaque density concordance.[58]

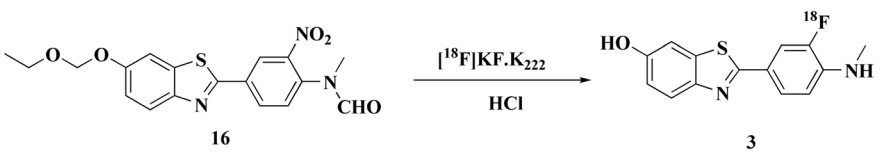


Scheme 3 Synthesis of flutemetamol ($^{18}$F) **3**.

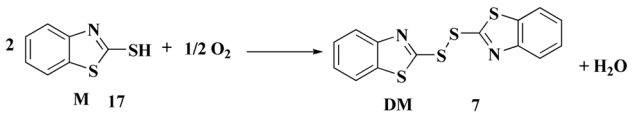


Scheme 4 Synthesis of 2,2′-dibenzothiazyl disulfide 7.



Flutemetamol ($^{18}$F) is produced by a nucleophilic aromatic substitution reaction between [$^{18}$F]fluoride and a nitro precursor. The synthesis pathway is described in detail below (Scheme 3).[59]

### 2.4. Quizartinib

Quizartinib **4** (Fig. 1) is an oral and active fms-like tyrosine kinase 3 inhibitor (FLT3 inhibitor) and it is the 1$^{st}$ drug developed precisely targeting FLT3. Quizartinib is a highly potent, 2$^{nd}$-generation, selective, type 2 FLT3 inhibitor. In patients with newly diagnosed AML that was FLT3-ITD-positive, phase-1/2 trials revealed that quizartinib plus chemotherapy demonstrated anti-leukaemic effectiveness with a tolerable safety profile. The drug was also effective when used separately following allo-HCT31. Additionally, in the phase 3 QuANTUM-R trial, quizartinib monotherapy increased overall survival compared to salvage chemotherapy in the relapsed or refractory circumstances.[60]

### 2.5. Thiohexam

Thiohexam **5**, 2-(cyclohexylaminothio)benzothiazole (Fig. 1), is considered as a rubber cure accelerator. It is an identified dermatological sensitizer and allergen as well.[52]

### 2.6. Morpholinylmercaptobenzothiazole

The 2-(morpholin-4-ylsulfanyl)-1,3-benzothiazole **6** (Fig. 1)[52] an be synthesized *via* the oxidative condensation of the 2-mercaptobenzothiazole and morpholine. This drug also known as the 2-(morpholinothio)-benothiazole. Sodium hypochlorite (NaOCl) is frequently used as the oxidizing agent in this reaction.

2-(Morpholinothio)-benothiazole is a sealant has demonstrated efficacy against cancerous cells *in vitro*. By interfering with the formation of disulfide bonds, 2-(morpholinothio)-benothiazole interacts with the cell nuclei and stops DNA synthesis. According to *in vivo* research, 2-(morpholinothio)-benzothiazole can be utilized as a sealant for brain injuries because it is not absorbed into the bloodstream. Additionally, it might have antiangiogenic properties, which could explain why it inhibits EGF.[61]

### 2.7. 2,2′-Dibenzothiazyl disulfide

2,2′-Dibenzothiazyl disulfide **7** (Fig. 1) is an accelerator utilized in processing plastic regeneration and the process of synthetic rubber & natural rubber. It is also a dermatological sensitizer and allergen.[52]

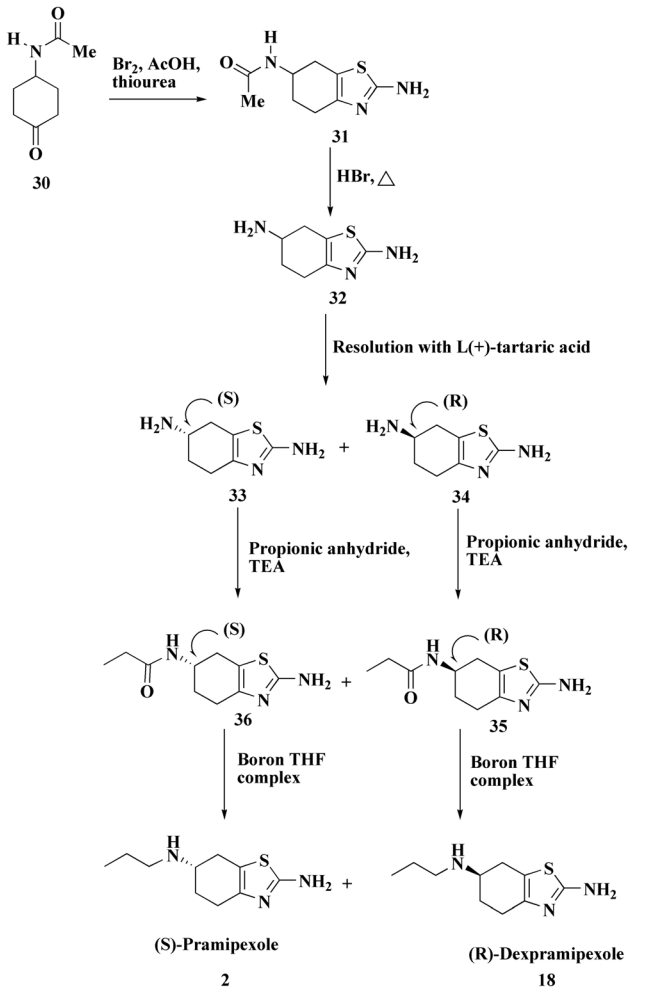


Scheme 5 Synthesis of dexpramipexole **18**.

The process for synthesizing 2,2′-dithiodibenzothiazole is accomplished *via* catalyzing the oxidation of the molecular oxygen (Scheme 4). A transition metal salt and molecule with N or O acting as a ligand make up the procedure. In order to synthesize 2,2′-dithiobis(benzothiazole), the complex is utilized as a catalyst to react benzothiazole-2-thiol with a solvent for one to thirty hours in an oxygen or air atmosphere at a pressure. The catalyst utilized in this invention is free of precious metals, has multiple uses, produces less waste, is eco-friendly, and has promising industrial applications. Its synthesis process is straightforward, and its catalytic activity and reaction efficiency are high. The synthesis reaction product has a high degree of selectivity and minimal by-products, and no base, acid, or other additives are required.[62]

Another method for preparing dibenzothiazyl disulfide involves using hydrogen peroxide to oxidize mercaptobenzothiazole in an aqueous suspension. The oxidation is carried out with the use of ethylenediaminetetraacetic acid (EDTA) or a derived alkali metal salt.[63]

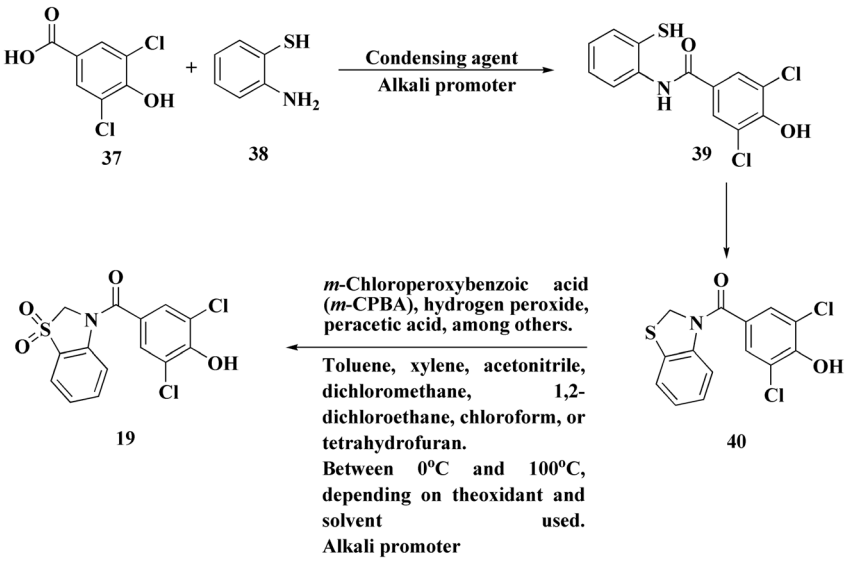


Scheme 6 Synthesis of dotinurad **19**.

## 3. Benzothiazole-based investigational drugs

### 3.1. Dexpramipexole

Dexpramipexole **18**, (Fig. 2) (6*R*)-*N*6-propyl-4,5,6,7-tetrahydro-1,3-benzothiazole-2,6-diamine, is under clinical investigation (trial no. NCT01511029).

Dexpramipexole, an orally bio-available aminobenzothiazole that was originally developed for treating amyotrophic lateral sclerosis, verified an important dose dependent eosinophil lowering effect.[64] Synthesis of dexpramipexole **18** is accomplished as depicted in Scheme 5.[65]

### 3.2. Dotinurad

Dotinurad **19** (Fig. 2) is under clinical trial NCT03372200. It is considered as a selective urate reabsorption inhibitor that specifically inhibits URAT1. Recently developed as a potent uricosuric drug.[66,67] It is widely utilized in clinical practice in Japan to treat hyperuricemia in Japan.[68–70]

The invention of dotinurad preparation reveals the technique that starts with 2-aminobenzenethiol and proceeds to produce a target product dortinode *via* a series of reactions, including condensation, cyclization, oxidation, and similar processes (Scheme 6). A benzoxazole intermediate is synthesized by cyclizing a 2-aminophenol derivative with an acid chloride or a benzoic acid derivative. Introducing substituents necessary for dotinurad's action by functionalizing the benzoxazole ring by halogenation or alkylation. The whole dotinurad molecule is furnished by coupling the functionalized benzoxazole intermediate with other elements.

Easy access to raw materials, speed, ease of use, cost effectiveness, environmental preservation, and adaptability for large scale industrial production are all advantages of the preparation process.[71]

### 3.3. Lanifibranor

Lanifibranor (Fig. 2), **20** 4-[1-(1,3-benzothiazole-6-sulfonyl)-5-chloro-1*H*-indol-2-yl]butanoic acid, is under clinical trial's investigations under number NCT03008070.[52] Inflammatory,

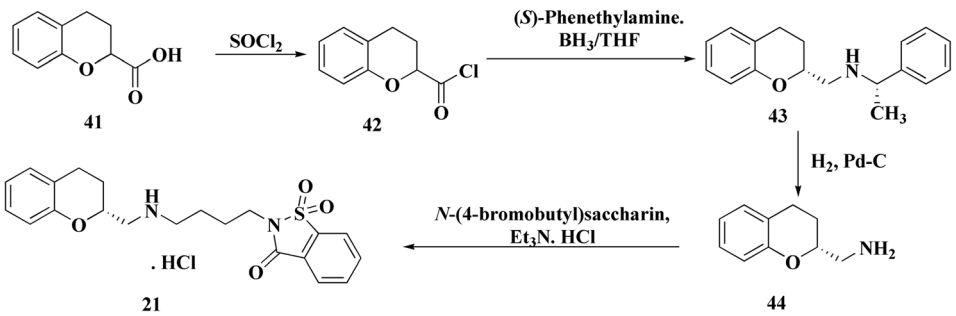


Scheme 7 Synthesis of repinotan **21**.

metabolic, and hepatic fibrotic pathways are modulated by the panperoxisome proliferator activated receptor (PPAR) agonist lanifibranor in the pathogenesis of non-alcoholic steatohepatitis (NASH).[72,73]

### 3.4. Repinotan

Repinotan **21** (Fig. 2) is a selective, high affinity, full agonist of the 5HT1A receptor sub-type with neuroprotective features.[52]

Repinotan, also known as BA X3702, is a highly effective agonist for the 5-hydroxytryptamine1A (5HT1A) receptor subtype, which is extensively expressed in cortical tissue. In a rat permanent middle cerebral artery occlusion model, repinotan has been demonstrated to lower extracellular glutamate by approximately 50% when compared to untreated animals. Repinotan has currently been studied in a number of clinical investigations for acute ischemic stroke due to the positive experimental results.[74]

Synthesis of repinotan (**21**) is depicted, as shown in Scheme 7, chroman-2-carboxylic acid (**42**) is treated with thionyl chloride to create acid chloride (**34**). When **34** reacts with (*S*)-phenethylamine, a 1 : 1 mixture of diastereomers is produced. The mixture is separated (fractional crystallized) to provide the required epimer with high optical purity. The amide is then reduced with diborane to yield benzyl amine (**43**), which is then hydrogenolyzed to provide (*R*)-2-(aminomethyl)chroman (**44**). Repinotan (**21**) is obtained by alkylating **44** with *N*-(4-bromobutyl)saccharin and is separated as the hydrochloride salt.[75]

### 3.5. Talarozole

Talarozole **22** (Fig. 2) has been clinically investigated for treating cutaneous inflammation and psoriasis.[52] Under a license from Johnson & Johnson, it was developed *via* Barrier Therapeutics Inc., as a selective and potent inhibitor of cytochrome

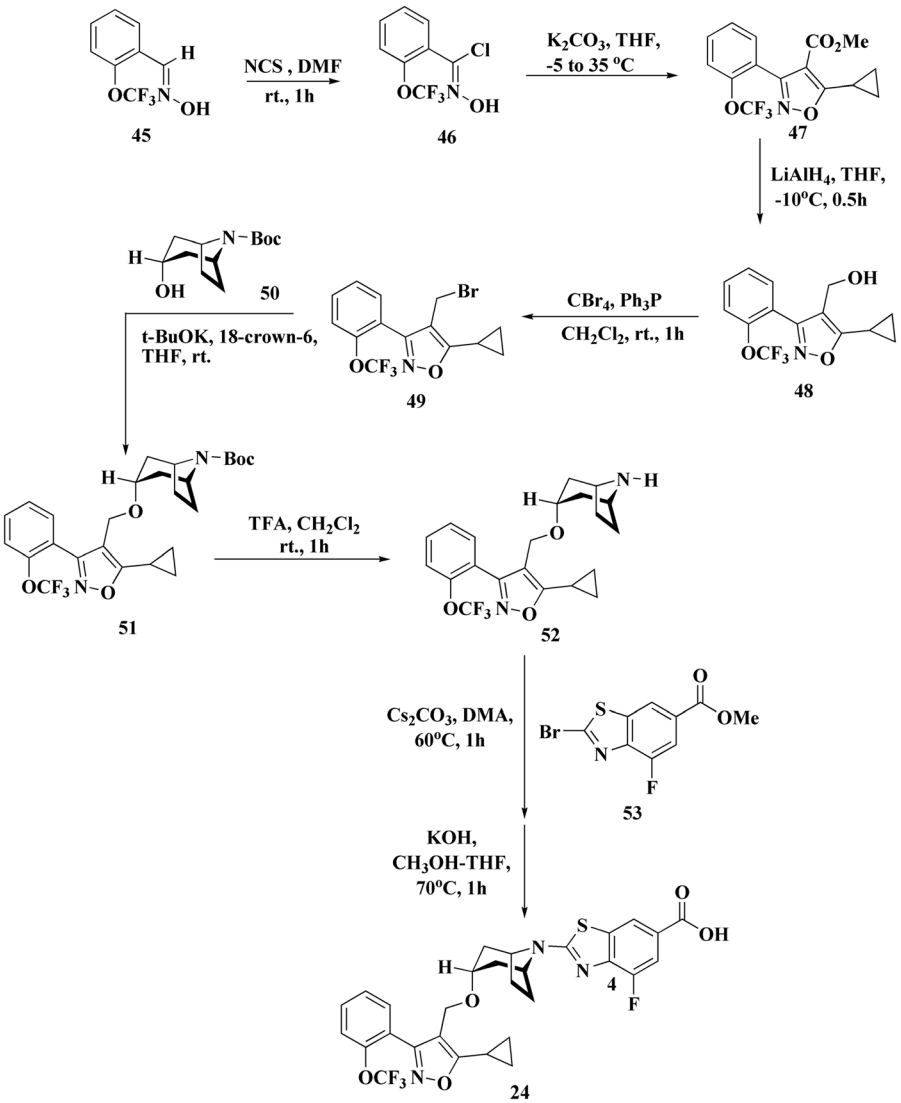


Scheme 8 Synthesis of tropifexor **24**.

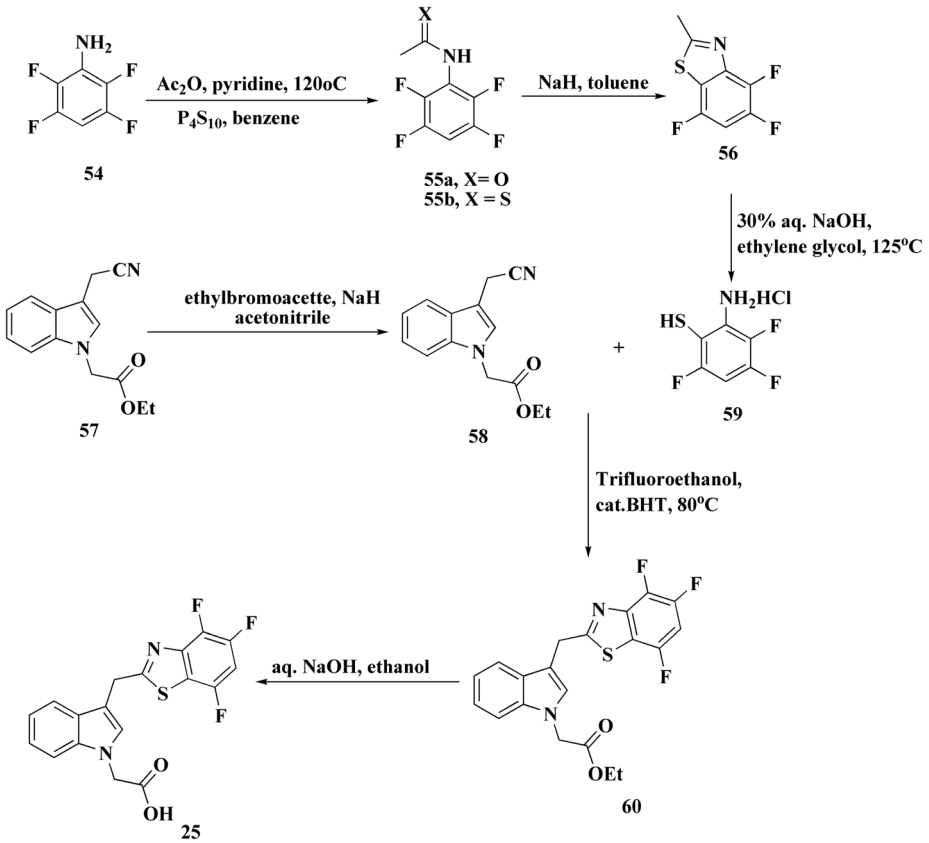


Scheme 9 Synthesis of lidorestat **25**.

P450 26-mediated breakdown of endogenous all *trans*-retinoic acid for treating acne and psoriasis.[76]

### 3.6. Sagopilone

Sagopilone **23** (ZK219477, Fig. 2) is an epothilone analogue[77] (16 member ring macrolides) that works against tumor cell lines resistant to many drugs. It has shown therapeutically effective in treating a number of solid tumors, including melanoma and ovarian cancer.[78] Also, it has been used in trials for treating of CNS disease, neoplasms, and breast cancer.

### 3.7. Tropifexor

Tropifexor **24** (Fig. 3), 3-[2-(trifluoromethoxy)phenyl]-1,2-oxazol-4-yl}methoxy)-8-azabicyclo[3.2.1]octan-8-yl]-4-fluoro-1,3-benzothiazole, is under clinical investigation (trial no. NCT02516605).

Tropifexor, LJN452, is a nonbile acid FXR agonist with subnanomolar activity due to a special bicyclic nortropine-substituted benzothiazole carboxylic acid moiety that has been optimized for improved fit into the ligand-binding domain of FXR.[79] In rodent models of non-alcoholic steatohepatitis (NASH)[79,80] and cholestasis,[81] tropifexor shown greater effectiveness than OCA and effectively regulated FXR-target genes in the intestine and liver. Tropifexor exhibits a pharmacokinetic profile in humans[82] and has demonstrated active FXR target engagement through transient & dose dependent rises in fibroblast growth factor 19 in healthy volunteers[82] and patients with NASH[83,84] and primary bile acid diarrhea.[85,86]

One important modulator of bile acid synthesis, conjugation, and transport is the farnesoid X receptor (FXR). An FXR antagonist called tropifexor (LJN452) is presently undergoing phase 2 trials to treat nonalcoholic steatohepatitis and cholestatic liver disorders. The reaction of the nitrile oxide obtained from the removal of HCl from **46** with $\beta$-keto ester to produce isoxazole **47** in a 52% yield is a crucial step in the synthesis shown in Scheme 8.[87,88]

### 3.8. Lidorestat

Investigations to identify therapy for the compliations of chronic diabetes lead to the discovery of a new series of highly effective and selective 3-[(benzothiazol-2-yl)methyl]indole-*N*-alkanoic acid aldose reductase inhibitors. 3-[(4,5,7-Trifluorobenzothiazol-2-yl)methyl]indole-*N*-acetic acid (lidorestat **25**, Fig. 3) as a lead compound inhibits aldose reductase ($IC_{50}$ of 5 nM), while being 5400 fold less potent against aldehyde

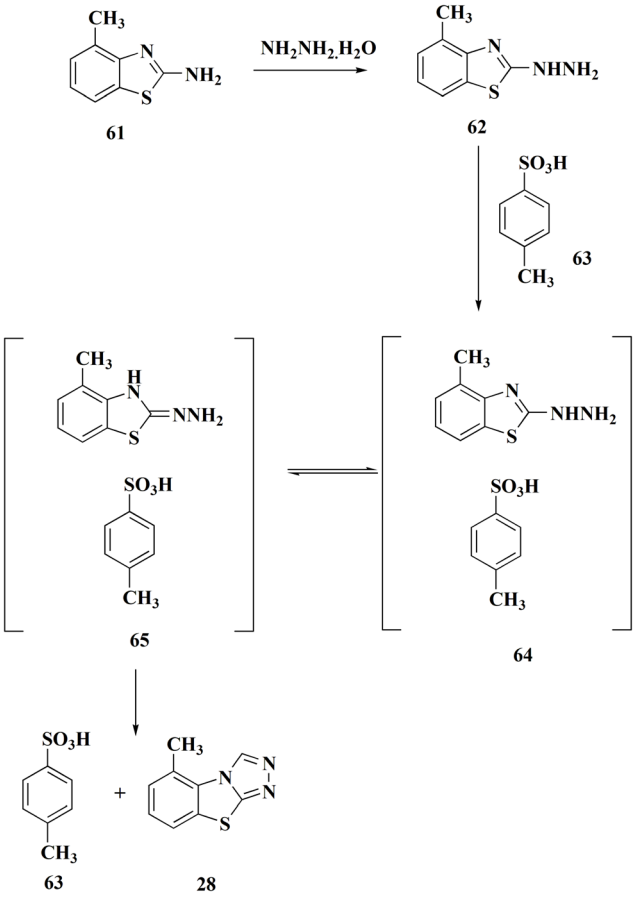


Scheme 10 Synthesis of tricyclazole **28**.

reductase which is an associated enzyme elaborated in the detoxification of reactive aldehydes. In the five-day STZ induced diabetic rat model, it reduces nerve & lens sorbitol levels (ED50s of 1.9 & 4.5 mg per kg per d po).[89,90]

The synthesis of lidorestat comprises the construction to the benothiazole scaffold, then linking it with indole core are accomplished in Scheme 9.[91]

### 3.9. 4SC-203

4SC-203 **26** (Fig. 3) has been utilized in investigational trials for treating acute myeloid leukemia.

4SC-203 is a new small molecule selective spectrum kinase inhibitor of the benzothiazole chemical class that exhibits a unique selectivity profile against ALK, AXL, VEGF-R2, FAK, FLT3, FLT3 mutants, & TRK receptors in both *in vitro* estimations with an inhibitory potency on cell line growth in the low nM range. Furthermore, 4SC-203 has demonstrated a strong antitumor impact in acute myeloid leukemia (AML) related *in vivo* models in preclinical investigations. 4SC-203 demonstrated favorable pharmacokinetic characteristics and was well tolerated over the whole concentration range tested in a first-in-man study with healthy volunteers.[92]

### 3.10. TMC-310911

TMC-310911 **27** (ASC-09; furan-3-yl *N*-[(2*S*,3*R*)-3-hydroxy-4-[*N*-(2-methylpropyl)2-[(1-cyclopentylpiperidin-4-yl)amino]-1,3-benzothiazole, Fig. 3) is an investigational protease inhibitor. Its potential application to HIV-1 infections is being researched. Significant efficacy against many HIV-1 strains, comprising multi PI-resistant strains, has been demonstrated by TMC-310911.[52] TMC310911 is a new protease inhibitor (PI) for HIV-1 that shares structural similarities with darunavir (DRV) but has enhanced virological properties.[93]

### 3.11. Tricyclazole

The 5-methyl-1,2,4-triazolo(3,4-*b*)benzothiazole, tricyclazole **28** (Fig. 3) is synthesized from 2-hyrazino 4-methyl benzothiazole.

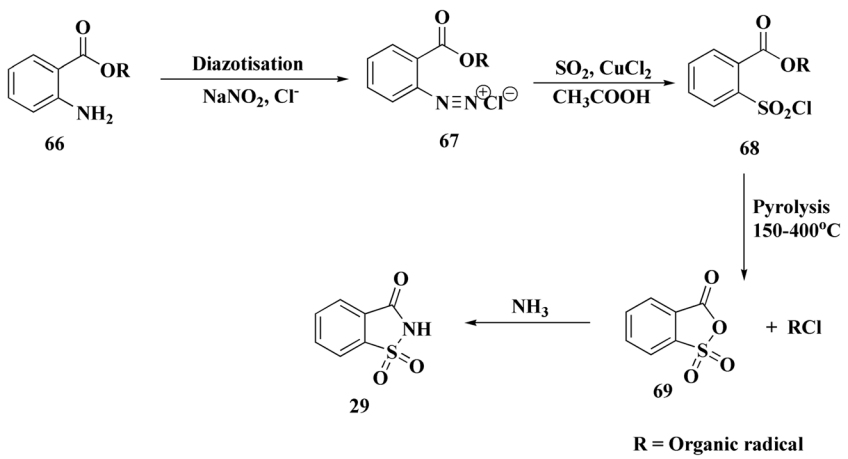


Scheme 11 Synthesis of saccharin **29**.

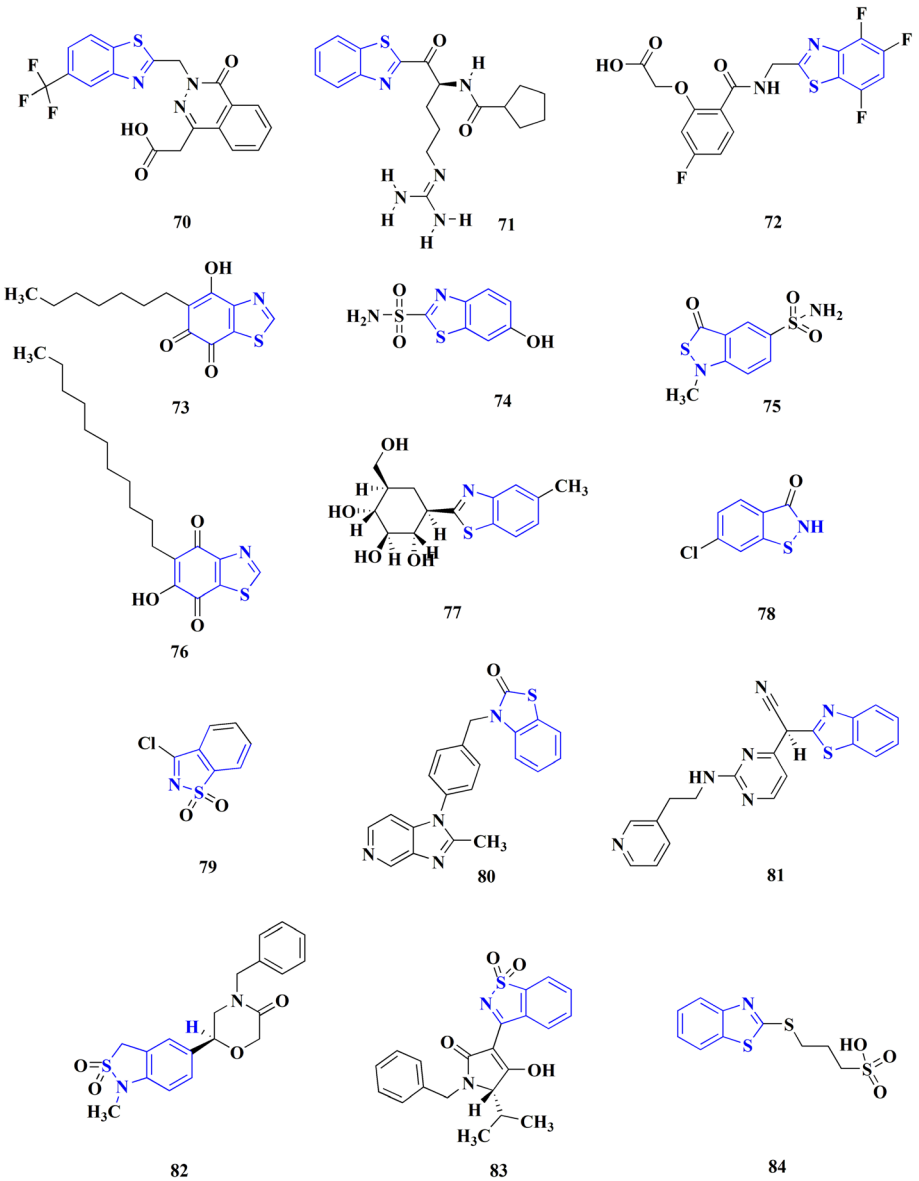


Fig. 4 Benzothiazole-based experimental drugs.

2-Hydrazine 4-methyl benzothiazole is prepared by reacting amino compound (**61**) with hydrazine hydrate in the presence of MEG and hydrochloric acid (Scheme 10). The condensation process with formic acid is carried out in the presence of acid promotor catalyst. The final product is isolated in aqueous slurry form by dumping solvent-free molton stirrable mass in precooled water. This is an improved, efficient, and environmentally safe method for producing tricyclazole useful fungicide for rice blast in aqueous slurry form.[94]

### 3.12. Saccharin

Saccharin **29** (Fig. 3), 2,3-dihydro-1lambda6,2-benzothiazole-1,1,3-trione, has been investigated for treating hyperglycemia and hypertension.[95]

A process for the preparation of saccharin by reacting an aqueous hydrochloric acid solution of *o*-methoxy-carbonylbenzenediazonium chloride with sulfur dioxide. Oxidation then reaction with ammonia afforded saccharin (Scheme 11).[96]

## 4. Benzothiazole-based experimental drugs

Many structures containing benzothiazoles were designed and synthesized, they revealed remarkble biological activities and are under pre-clinical and clinical investigations such as Zopolrestat **70** which acts as an active competitive GLO1

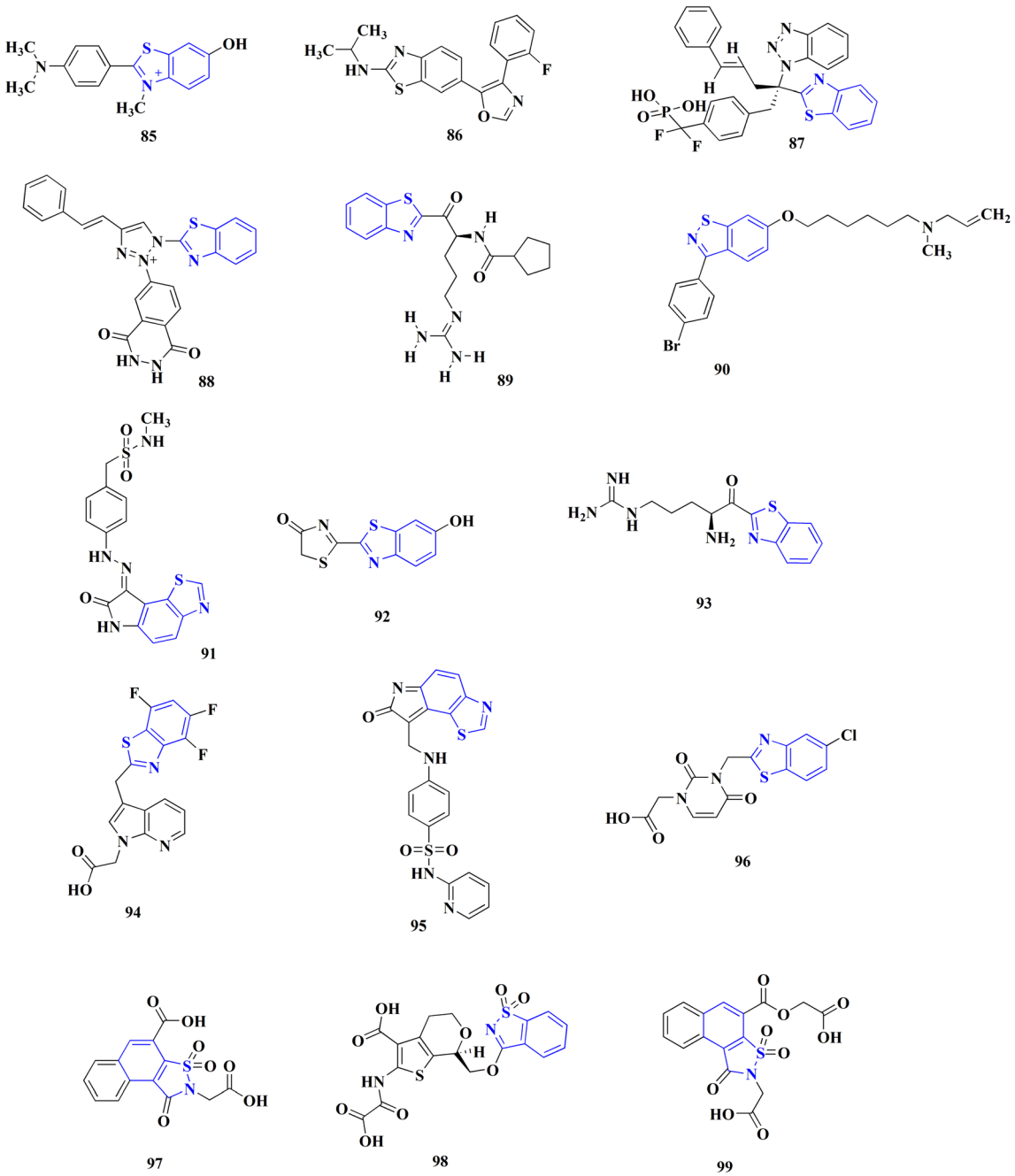


Fig. 5 Benzothiazole-based experimental drugs.

inhibitor which is currently in phase-III clinical trials.[97] Many other experimental drugs were developed which are depicted in Fig. 4 and 5 such as RWJ-56423,[98] IDD552[99] 6-hydroxy-5-undecyl-4,7-benzothiazoledione, 5-heptyl-6-hydroxy-1,3-benzothiazole-4,7-dione, 2-(beta-D-glucopyranosyl)-5-methyl-1,3,4-benzothiazole, pseudosaccharin chloride, 1-methyl-3-oxo-1,3-dihydro-benzo[C]isothiazole-5-sulfonic acid amide, ticlatone, CP-271485, CP-94707, (2*S*)-1,3-benzothiazol-2-yl{2-[(2-pyridin-3-ylethyl)amino]pyrimidin-4-yl}ethanenitrile, 3-(2-benzothiazolylthio)-1-propanesulfonic acid, RWJ-51084.[52]

# 5. Main molecular targets and mechanism of benzothiazole-based drugs (investigational & approved drugs)

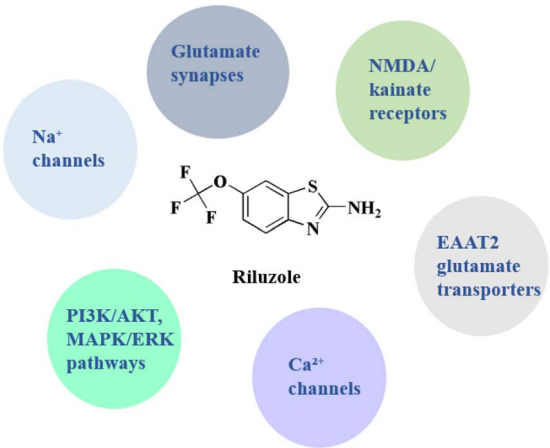


**Riluzole**

- Riluzole targeting presynaptic voltage-gated sodium channels, it inhibits Nav channels, which lowers neuronal excitability. Its effect is to limit excitotoxicity and decrease glutamate release[100,101]
- It targeted glutamate synapses, it reduces synaptic glutamate release through $Na^+$ channel blocking; it indirectly targeting the glutamate synapses; through preventing glutamate-induced excitotoxicity, a major contributing factor to ALS, in neurons[102]
- It modulates NMDA & kainate receptors targeting postsynaptic NMDA and kainate-type glutamate receptors; *via* non-competitive antagonism; riluzole diminishes excitatory toxicity and calcium influx[103]
- It enhances the glutamate clearance through targeting the glial glutamate transporters (*e.g.*, EAAT2/GLT-1). It acts indirectly to upregulate the transporter expression, promoting the glutamate reuptake, to reduce the extracellular excitotoxin buildup[104]
- It modulate calcium channels *via* targeting the high voltage-activated calcium channels, it inhibits calcium influx during the depolarization, reducing the neurotransmitter exocytosis[105]
- Concerneing the neurotrophic/survival pathways (PI3K/AKT, MAPK/ERK), riluzole targeting the intracellular pro-survival signaling indirectly through stimulating pathways supporting the neuronal viability & plasticity[106]

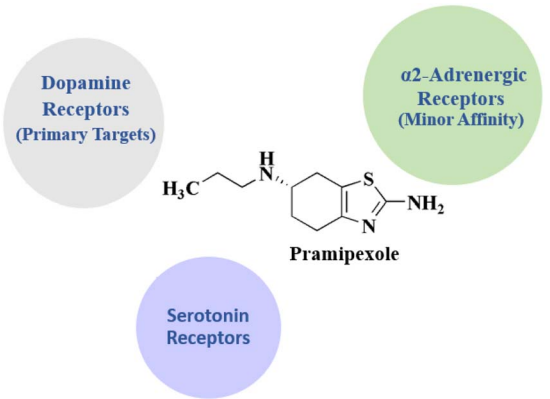


**Pramipexole**

- Pramipexole binds with high affinity to the dopamine $D_3$ receptor (DRD3), making it its primary receptor target
- It also considered as an agonist at $D_2$ receptors (DRD2), with some extent lower affinity
- Pramipexole displays moderate affinity for $D_4$ receptor (DRD4)
- Pramipexole indicated very low to negligible binding to serotonin (5-$HT_1$A/1B/1D) & $\alpha_2$-adrenergic receptors
- The main mechanism that pramipexole reduces motor symptoms in Parkinson's disease and restless legs syndrome (RLS) is by activating $D_2$-like dopamine receptors, particularly $D_3$ and $D_2$. Its $D_3$ predilection might also have neuroprotective and mood-regulating benefits, although $D_4$ and other minor affinities have little therapeutic value[107]

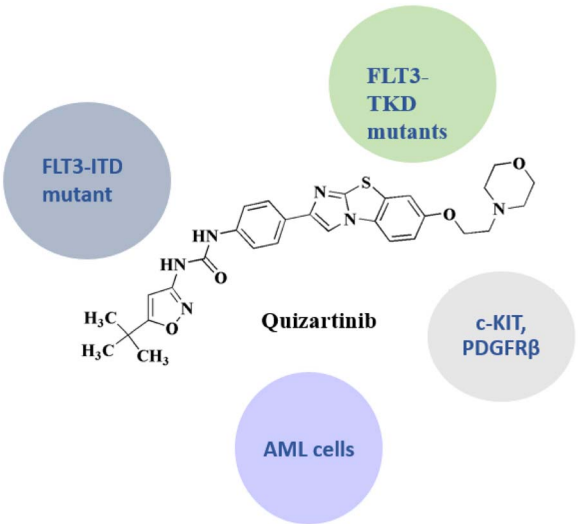


**Quizartinib**

- FLT3 (FMS-like tyrosine kinase 3) is the primary target of Quizartinib. Its mechanism is as follows: It binds to the inactive conformation of FLT3. It inhibits autophosphorylation and downstream signaling. It blocks pathways, and causes FLT3-ITD-positive AML cells to undergo apoptosis[108]
- FLT3 mutations associated with resistance

Mechanisms of resistance: mutations in FLT3-TKD, such as D835Y and F691L, decrease binding affinity. Alternative signaling pathways are upregulated. The effectiveness of monotherapy is limited by resistance; combination therapy is being researched[109]

- Low-level off-target kinase inhibition: Limited inhibition of other kinases such as c-KIT, PDGFRβ, RET. It may have mild off-target effects and contribute to myelosuppression[110]
- Clinically used in treating acute myeloid leukemia (AML) with FLT3-ITD mutation; FDA clearance (2023): To treat newly diagnosed FLT3-ITD AML in conjunction with chemotherapy (brand name Vanflyta®). It is orally administrated[111,112]

(*Contd.*)

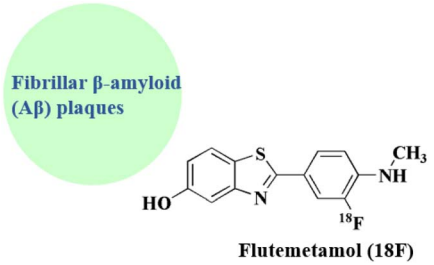

Flutemetamol (18F)

**Flutemetamol ($^{18}$F)**

• The principal molecular target of flutemetamol ($^{18}$F) is the fibrillar *β*-amyloid (*Aβ*) plaques. The structure that is being targeted is the cross *β*-sheet conformation in insoluble *Aβ* aggregates

• There is no discernible binding to soluble or monomeric Aβ forms; instead, there is high-affinity, selective binding to dense-core amyloid plaques[113]

Imaging mechanism and brain uptake:

• PET imaging is made possible by the radiotracer fluorine-18 isotope. It efficiently penetrates the blood–brain barrier (BBB)[114]

It does not interact with neurotransmitter receptors or intracellular signaling pathways; solely used for diagnostic purposes; not therapeutic

• It is used in amyloid pathology detection and measurement in mild cognitive impairment, Alzheimer's disease, and indeterminate etiology dementia[115]

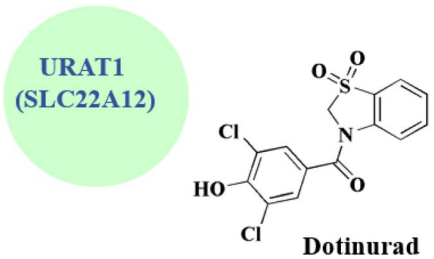

Dotinurad

**Dotinurad**

• URAT1 (SLC22A12) is the primary molecular target of Dotinurad. It is encoded by the SLC22A12 gene and is located in the proximal renal tubular cells' apical membrane. It acts as a selective inhibitor and promotes uricosuria, or increased excretion of uric acid, by preventing the renal tubule from reabsorbing uric acid into the bloodstream. It has the effect of lowering serum uric acid levels without substantially altering other renal transporters[116]

• It increases its effectiveness and decreases off-target effects by specifically inhibiting URAT1 without substantially altering other renal urate transporters like OAT1/3 or ABCG2 (ref. 117)

• Pharmacodynamic and clinical impacts:

It reduces blood uric acid levels in both hyperuricemia patients and healthy individuals in a dose-dependent manner

It is favorable, with a low incidence of hepatic or renal side effects compared to previous uricosurics like benzbromarone; half-life: around 10 hours, permitting once-daily dosing[118,119]

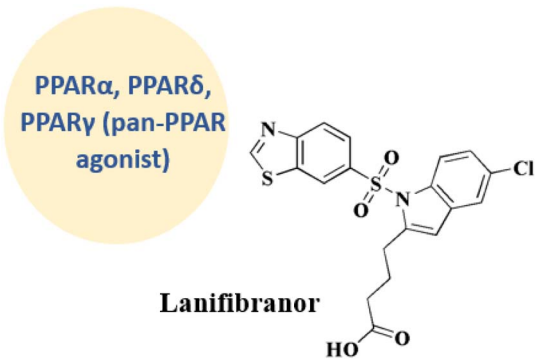

Lanifibranor

**Lanifibranor**

• Lanifibranor has a triple agonist action on PPARα, PPARδ, and PPARγ, and impact on metabolic and inflammatory pathways[120] Lanifibranor modulates gene expression *via* PPARs[121,122]

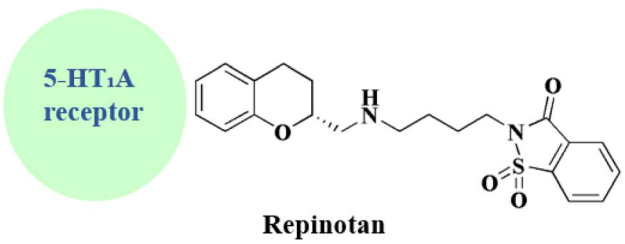

Repinotan

**Repinotan**

• Mechanism of action & preclinical neuroprotection: Up to five hours after a stroke, repinotan dramatically decreased the infarct volume in rats

• Mechanism: excitotoxic damage is decreased by high-affinity 5 $HT_1$A receptor agonism[123]

• In a clinical trial in early stage: BRAINS study

IV repinotan (0.5–2.5 mg per day) is being evaluated in a phase II trial for acute stroke. It displayed some non-significant favorable trends and tolerability[124]

(*Contd.*)

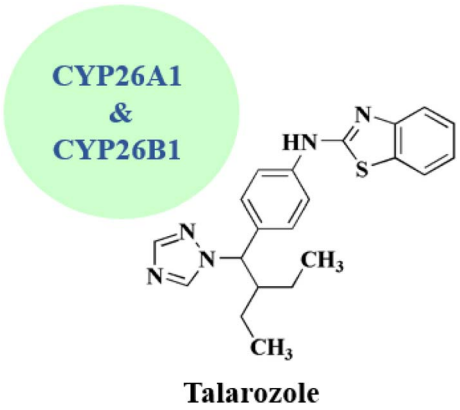


Talarozole

**Talarozole**

- Talarozole (R115866) is consiered as a selective and active CYP26A1/B1 inhibitor with nanomolar potency[125]
- Talarozole exhibits anti-inflammatory effects of in joint cartilage injury models[126]

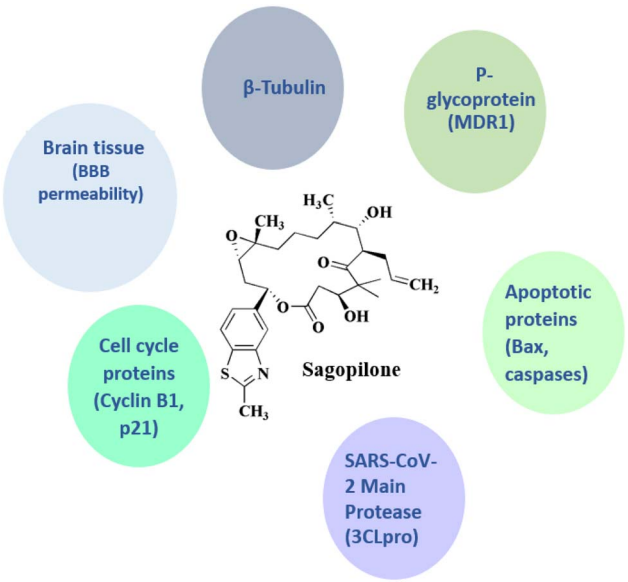


Sagopilone

**Sagopilone**

- Sagopilone's primary target is the $\beta$-tubulin (microtubules). $\beta$-Tubulin is a key structural protein of microtubules. Its mechanism is to attach to the taxane-binding site on $\beta$-tubulin, stimulate tubulin polymerization, and stabilize microtubules against depolymerization. Cell cycle arrest at the $G_2$/M phase and apoptosis in proliferating tumor cells are the results of this disturbance of mitotic spindle dynamics[127]
- Regarding the multidrug resistance proteins (*e.g.*, *P*-glycoprotein/MDR1) sagopilone is not a target, although *P*-glycoprotein (ABCB1) recognizes it poorly
- Sagopilone circumvents a major chemoresistance mechanism by maintaining cytotoxic activity in MDR1-overexpressing cancer cells, in contrast to taxanes[128]
- Even though $\beta$-tubulin is the only direct molecular target, sagopilone has downstream effects that include indirect modulation of the pro-apoptotic pathways, cell cycle regulators, and the activation of mitotic checkpoints[129]
- Blood–brain barrier penetration: Unlike paclitaxel and other microtubule drugs, sagopilone penetrates the brain. This enables the targeting of brain malignancies like glioblastoma
- This impacts therapeutic value even though it is a pharmacokinetic characteristic rather than a receptor interaction[130]

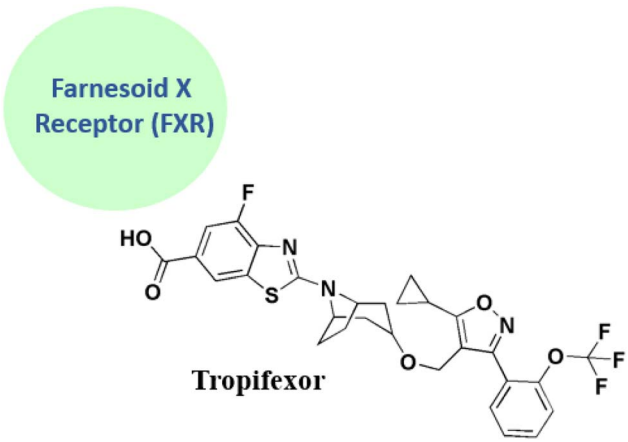


Tropifexor

**Tropifexor**

- Tropifexor is considered as a highly selective FXR agonist[131]
- According to a pre-clinical study in NASH models it demonstrates anti-fibrotic & anti-steatotic effects through FXR activation in rodents[132]
- FXR-tropifexor structural interaction is detected as its crystal structure insights into FXR-ligand binding specificity is provided[133]
- Tropifexor's dose-dependent reduction in liver fat and ALT, along with adverse effects (LDL rise, pruritus), is reported in the FLIGHT-FXR trial, a clinical study in NASH[134]

(*Contd.*)

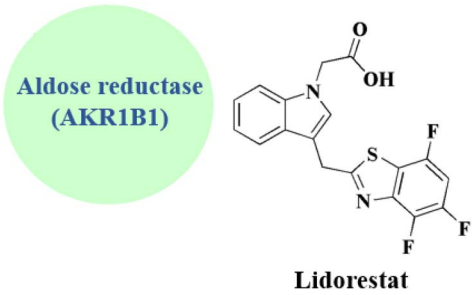


**Lidorestat**

- Lidorestat is considered as an aldose reductase (AKR1B1) selective competitive inhibitor
- Lidorestat binds to the active site of aldose reductase (AKR1B1), preventing the conversion of glucose to sorbitol, the initial and rate-limiting step in the polyol pathway. Aldose reductase (AKR1B1) is the primary and direct target. It is a member of the aldo-keto reductase superfamily. It acts as a selective and strong competitive inhibitor. When this route is overactivated under hyperglycemic settings, tissues like the heart, kidney, retina, and nerves experience oxidative stress, sorbitol buildup, osmotic damage, and secondary inflammation
- Aldose reductase inhibition aims to stop the development of diabetes complications, including cardiomyopathy and nephropathy, without interfering with regular glucose metabolism[135]

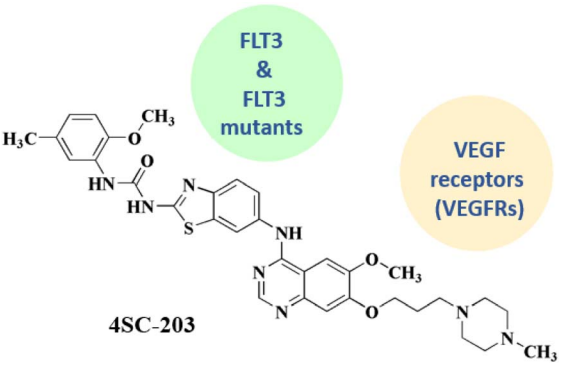


**4SC-203**

- Official declaration of the start of a clinical trial characterizes 4SC 203 as a selective kinase inhibitor that primarily targets VEGF receptors and FLT3 (including mutant versions). Pharmacokinetics, safety, and tolerability were evaluated in a clinical trial[136]

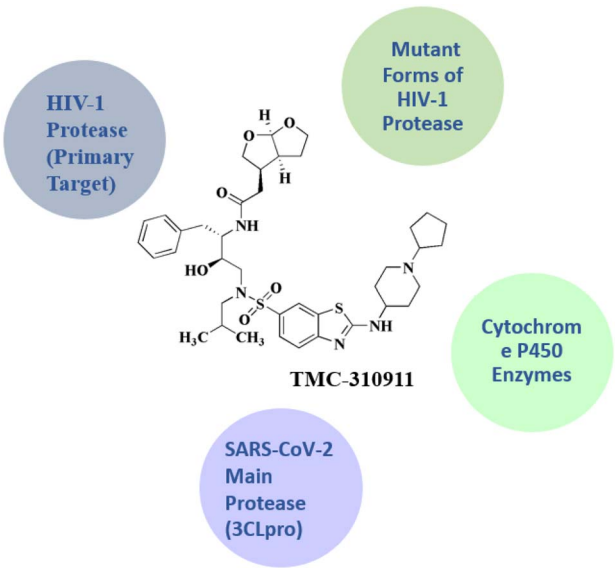


**TMC-310911**

- HIV-1 aspartyl protease (EC 3.4.23.16) is the target of TMC-310911. It acts as a competitive inhibitor
- TMC-310911 binds to the active site of the HIV-1 protease enzyme, preventing the cleavage of viral gag and gag-pol polyproteins into functional proteins (*e.g.*, capsid, reverse transcriptase, integrase, protease).When this process is disrupted, immature, non-infectious virions are formed[137]
- It targets HIV-1 protease variants with resistance mutations; it preserves inhibitory activity against numerous drug-resistant HIV strains; TMC-310911 was designed especially to preserve effectiveness against HIV strains that are resistant to multiple drugs along with an enhanced genetic barrier to resistance[138]
- It targeted the cytochrome P450 enzymes; they act as a substrate and a mild inhibitor; it is relevant because similar to darunavir, ritonavir or cobicistat boosting is necessary for TMC-310911 to enhance plasma exposure through CYP3A4-mediated metabolic inhibition. It might also impact how other drugs that are co-administered and processed by CYP3A4 are metabolized[139]
- The main protease of SARS-CoV-2 (3CLpro): a potential or investigative target
- TMC-310911 targets SARS-CoV-2's 3-chymotrypsin-like protease (Mpro, 3CLpro); it ats as a weak inhibitor (*in vitro* and *in silico* research)
- TMC-310911's protease-inhibitory scaffold led to its evaluation as a repurposing candidate during the COVID-19 pandemic. Nevertheless, there was no compelling preclinical or clinical data to support substantial anti-SARS-CoV-2 efficacy[140]

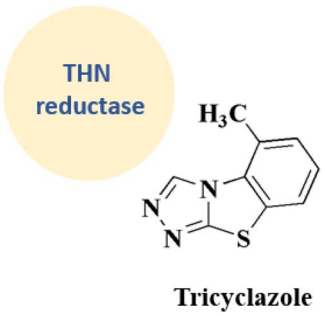


**Tricyclazole**

- Tricyclazole's known enzyme target is tetrahydroxynaphthalene reductase (THN reductase)
- Its mechanism of action depend on the 1,8-dihydroxynaphthalene melanin route, or DHN-melanin production pathway; primarily in fungi like alternaria alternata and magnaporthe oryzae
- A crucial stage in the biosynthesis of fungal melanin is the reduction of 1,3,6,8-tetrahydroxynaphthalene (THN) to scytalone, which is catalyzed by the enzyme THN reductase, which is inhibited by tricyclazole. The following functions of this melanin are essential: protection against oxidative stress and host immunological responses; appressorium turgor pressure, which is necessary for host penetration

Because THN reductase is blocked, fungi are unable to synthesize melanin and are unable to effectively penetrate plant tissue, which reduces their virulence and pathogenicity[141,142]

(*Contd.*)

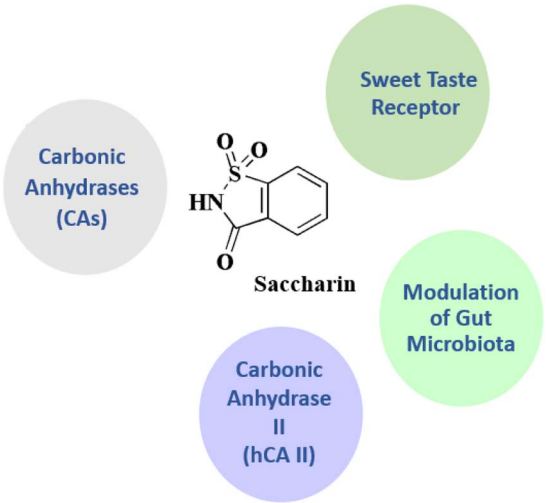


**Saccharin**

- Saccharin targets the carbonic anhydrases (CAs) particularly the human carbonic anhydrase isoenzymes, hCA IX and XII
- CAs are zinc metalloenzymes that regulate pH and are overexpressed in cancers. Saccharin and its derivatives have shown specific inhibition of tumor-associated CAs, especially CA IX, making them intriguing anticancer leads[143,144]
- It targets sweet taste receptor, saccharin binds and activates the sweet taste receptor complex (T1R2 + T1R3), specifically connecting with extracellular Venus flytrap domains. It targets the G-protein coupled receptor (GPCR) T1R2/T1R3. Its sweetening ability stems from this.[145,146] It target human carbonic anhydrase II (hCA II) as a weak inhibitor; saccharin can weakly inhibit hCA II, suggesting a broad CA interaction, although less selectively than for hCA IX/XII[147]
- Saccharin modulate the gut microbiota, it indirect interacts with gut microbial species (*e.g.*, clostridium, bacteroides); it has modulatory effect on microbiota composition and function; long-term exposure to saccharin can result in dysbiosis of the gut microbiota, which is associated with metabolic changes and glucose intolerance[148,149]

## 6. Synthetic strategies for novel anti neurodegenerative benzothiazoles

### 6.1. Oxadiazole-benzothiazole based analogues

The synthesis of the imidazopyridine-based benzothiazole–oxadiazole analogs as anti-Alzheimer's agents was accomplished in Scheme 12. Treatment of 6-fluoroimidazo[1,2-*a*] pyridine-3-carbaldehyde **100** with carbamylhydrazine in methylalchlol in the presence of ethanoic acid, under reflux yielded the hydrazine based intermediate **101**. Further reaction of the latter intermediate with potassium carbonate and iodine to access the cyclized intermediate **102**, under reflux condition. Synthesizing the imidazopyridine-based benzothiazole–oxadiazole hybrid **105** was accomplished *via* treating intermediate **102** with the substituted benzothiazole. These analogs were accessed *via* reacting 2-benzothiazolethiol (MBT) with several substituted 2-bromo-1-phenylethanone.[150]

The efficiency of these compounds was estimated comparable to donepezil as a standard drug ($IC_{50}$ value 19.90 ± 2.40 μM for BuChE & 14.47 ± 1.20 μM for AChE). The new scaffolds displayed potency in a range of $IC_{50}$ value 6.40 ± 1.80 μM for AChE and 6.70 ± 1.65 μM & 41.65 ± 7.20 μM for AChE & 44.65 ± 7.40 μM for BuChE. Compound **105** with $IC_{50}$ value 6.40 ± 1.80 μM for BuChE and 6.70 ± 1.65 μM for AChE was considered as the strutural optimization of the compounds with the maximum inhibition as the result of the presence of small-sized

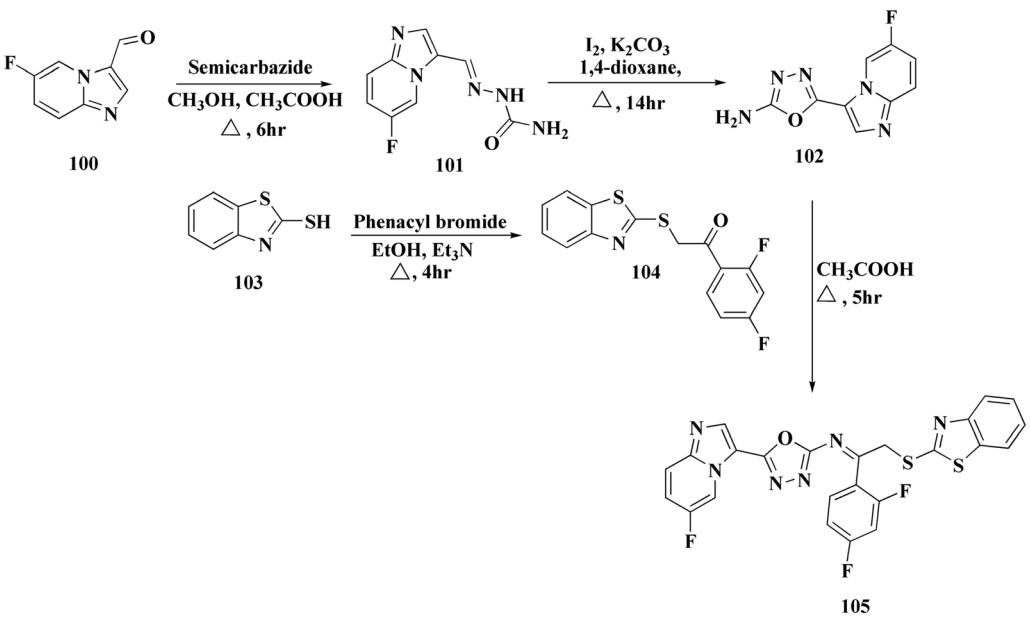


Scheme 12 Synthesis of imidazopyridine-based benzothiazole–oxadiazole.

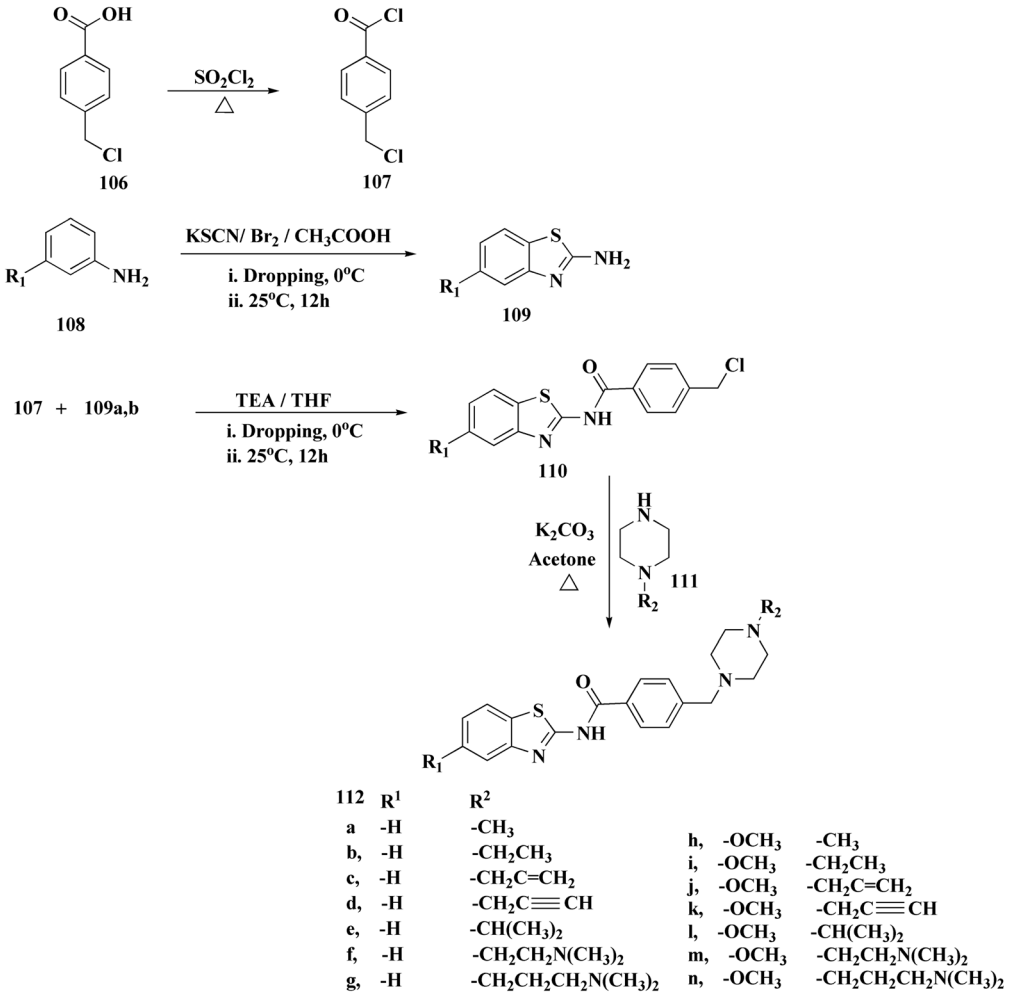


Scheme 13 Synthesis of substituted benzamides.

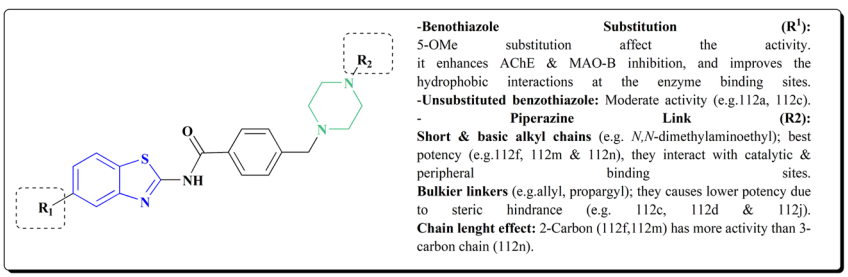


Fig. 6 Structure–activity relationship of compound **112**.

and the highly electro-negative fluoro scaffolds that inhibite the enzymes *via* the formation of hydrogen bonds.

### 6.2. Piprazine–benzothiazole based analogues

The usage of dual acetylcholinesterase (AChE) monoamine oxidase B inhibitors is a novel strategy in treating Alzheimer's disease. New compounds were designed and synthesized to target those enzymes. Novel compounds comprising piperazine and benzothiazole was synthesized as depicted in Scheme 2. 4-Chloromethylbenzoyl chloride **107** was synthesized utilizing sulfinyl chloride. 2-Benzothiazolamine **109a–b** analogs were synthesized *via* ring closure reaction utilizing brome soln. The substituted benzamides **110a–b** were accessed *via* reacting 4-chloromethyl benzoyl chloride **107** and 2-benzothiazolamine **110a–b.** Compounds **110a,b** & piperazine analogs were allowed to react to afford compounds **112a–n** (Scheme 13).[151]

The inhibitory potential of all compounds against butyrylcholinesterase (BChE), AChE, MAO-A & MAO-B was estimated utilizing an *in vitro* fluorometric procedure. In addition, the inhibitory effect of the potent compounds on amyloid-beta (Ab) aggregation was estimated *in vitro*. Biological investigation revealed that compounds **112a**, **112d**, **112f**, **112h**, **112k** & **112m**

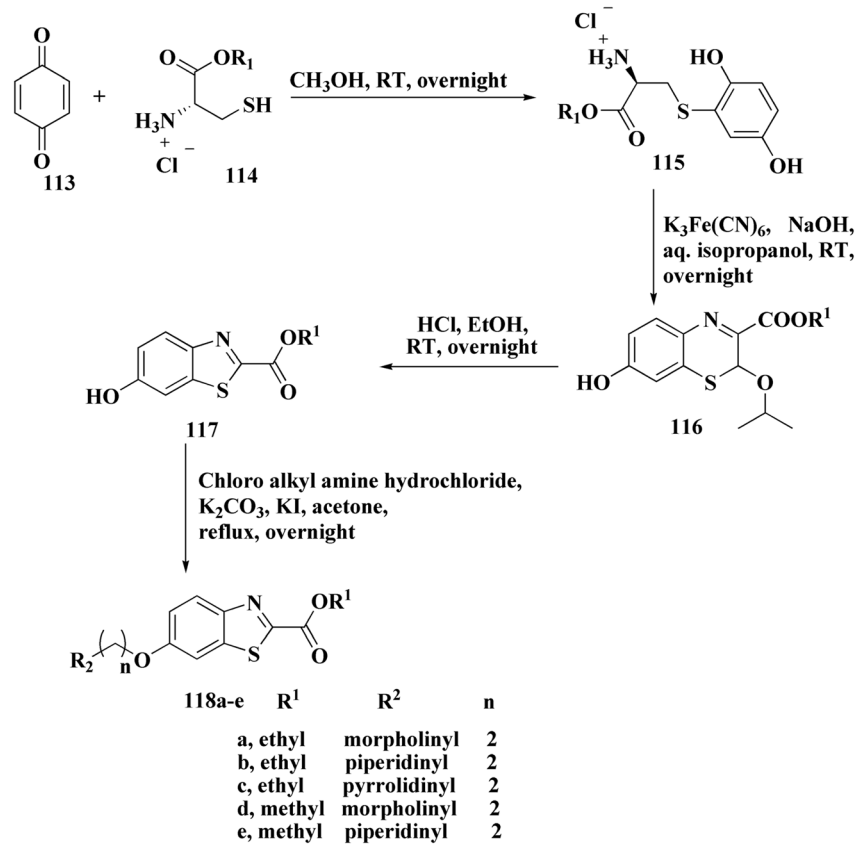


Scheme 14 Synthesis of methyl/ethyl 6-hydroxybenzothiazole-2-carboxylates.

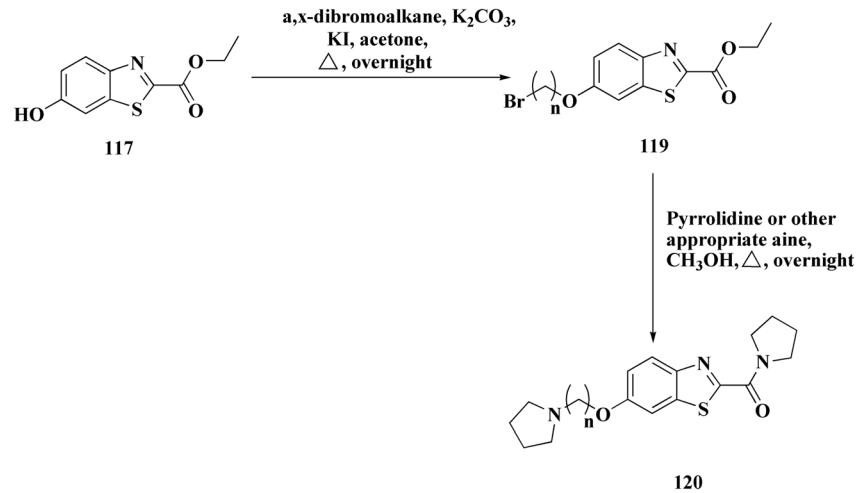


Scheme 15 Synthesis of methyl/ethyl 6-hydroxybenzothiazole-2-carboxylates.

exhibited significant potency against MAO-B & AChE enzymes (Fig. 6). Compound **112f** inhibited MAO-B and AChE enzyme with $IC_{50}$ values of 23.4 to 1.1 nM & 40.3 to 1.7 nM. It was found that compound **112f** may inhibit AChE & MAO-B enzymes potentially, besides the capability to inhibit the beta amyloid plaques's formation accumulated in the brains of AD patients. *In silico* investigations correspondingly support the resultant bioactivity. Compound **112f** induced a strong interaction with the active site of the two enzymes. The interaction of flavin adenine dinucleotide (FAD) with compound **112f** in the active site of the MAO-B enzyme active site is an exciting discovery.

It is presumed that multi-targeted directed ligands (MTDLs) which interact with various targets related to Alzheimer's disease (AD), might offer an enhanced therapeutic alternative than utilizing the "one-target, one-molecule" strategy. Novel benzothiazole-based analogs were described as a privileged moiety for histamine H3 receptor ligands (H3R). The most affine compound, the propyloxy-linked benzothiazole analog

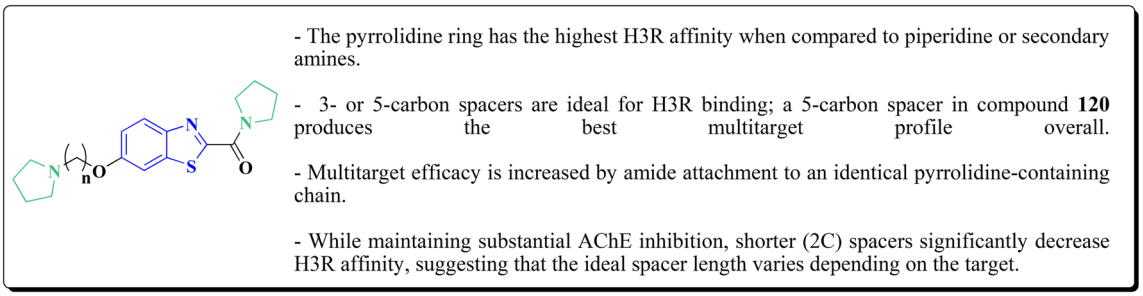


Fig. 7 Structure–activity relationship of compound **120**.

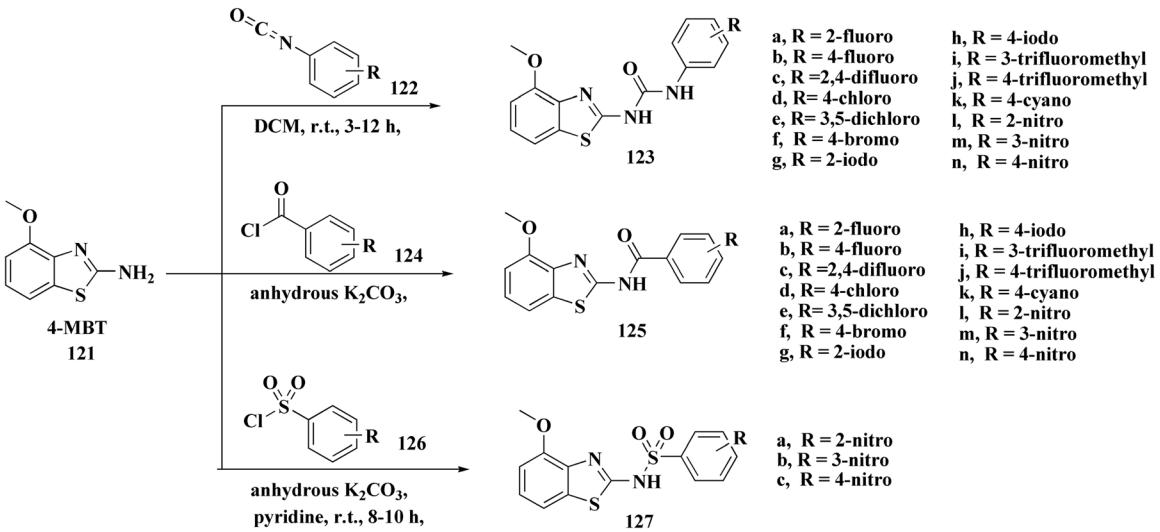


Scheme 16 Synthesis of substituted benzothiazol-2-amine.

**112b**, exhibited a $K_i$ value of 0.012 lM. The multi-targeting potential of these H3R ligands towards AChE, BuChE & MAO-B enzymes was estimated to afford compound **112f** as the furthermost promising MTDL with a Ki value of 0.036 lM at H3R and $IC_{50}$ values of 6.7 mM, 2.35 mM, & 1.6 mM towards AChE, BuChE, & MAO-B. These results propose that compound **112f** can be a structural optimization for novel multitargeting anti-AD agents.[151]

The methyl/ethyl 6-hydroxybenzothiazole-2-carboxylate was synthesized as depicted in Schemes 14 & 15. The quinone was reacted with cysteine methyl/ethyl ester hydrochloride *via* Michael addition to give the hydroquinone. Then, the oxidation of the hydroquinone intermediate using potassium ferric hexacyanoferrate afforded the benzothiazine analog. The further contraction to benzothiazole ring in acidic medium gave compounds **117a** & **117b**. This mechanism was suggested to occur through benzothiazine ring hydrolysis to afford a mercapto-aldehyde analog, intramolecular attack inorder to form the contracted ring, which was followed by oxidation and decarboxylation of the aldehyde group. Compounds **117a** ($R^1 = CH_3$) & **117b** ($R^1 = CH_2CH_3$) were allowed to reflux with various chloroalkyl amines to afford compounds **118**. The 6 hydroxybenzothiazole-2-carboxylate methyl ester (**117a**) was reacted with the α,ω-dibromoalkane to yield an ether in the presence of potassium iodide and potassium carbonate to give compounds **119**, which were then reacted with the methyl ester of various aromatic amino acids under reflux to afford compounds **120**.[152]

The struture–activity relationship of compound **120** is shown in Fig. 7. Regarding the H3R binding model, the Glu176 and protonated pyrrolidine nitrogen form a salt bridge. Phe163-CH–π interaction adds extra CH–π with Trp341. Glu176 (CH···O), Cys88 (CH···S), and Arg351 (carbonyl group) are hydrogen bonds. With an essential ionic connection to Glu176, the binding mode is similar to those of known inverse agonists (ABT-239, JNJ5207852).

Crystal structure of AChE complexed with PDB ID: 4EY5 indicated that the pyrrolidine ring is near the anionic site and catalytic triad. The molecule is held in place by CH–π interactions with Tyr337, cation–π interactions with Trp86, and hydrogen bonds with Glu202 and Phe295.

In case of Inhibition of MAO-B the compound probably entails binding inside the hydrophobic substrate cavity; compound **120** demonstrates MAO-B selectivity over MAO-A, which could be related to amide orientation and spacer length.[152]

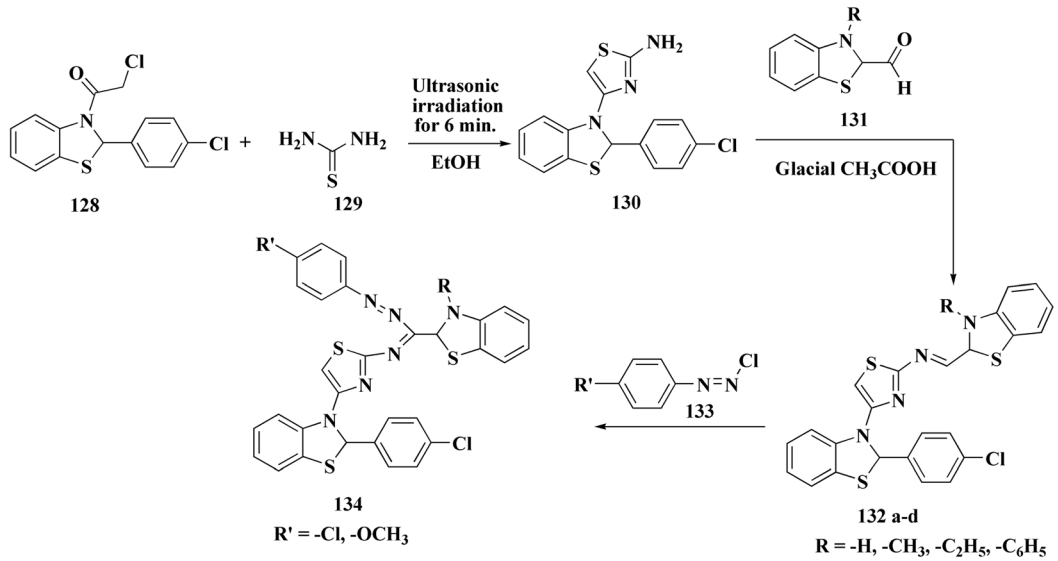


Scheme 17 Synthesis of the substituted 2-hydrobenzothiazole-2-carboxamidines.

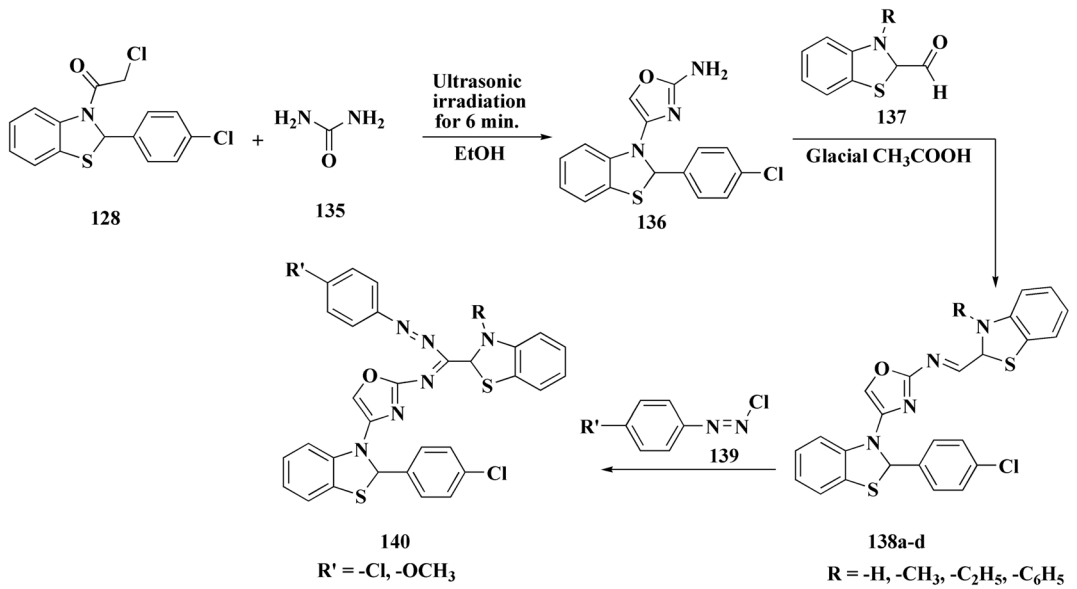


Scheme 18 Synthesis of benzothiazole-2-carboxamidine derivatives.

### 6.3. Benzothiazoles linked with substituted aromatics

α-Synuclein (α-syn) & Tau aggregates are the key histopathological hallmarks in Parkinson's disease (PD), Alzheimer's disease (AD), and many other neurodegenerative diseases. Alternatively, misfolding of α-synuclein is considered as a distinguishing feature in PD & dementia with Lewy bodies (DLB). Targeting of proteinaceous oligomers & aggregates remains challenging.

The benzothiazole-based compounds were synthesized utilizing the structural hybridization approach among the benzothiazole cyanine dye & the diphenyl pyrazole analog that revealed anti-aggregation potency towards α-syn & 2N4R tau. The targetedcompounds were synthesized utilizing 4-methoxy-1,3-benzothiazol-2-amine (4-MBT). To synthesize compounds comprising the urea linker, the phenyl isocyanate in a quantitative amount was utilized in methylene chloride. The sulfonamide or the amido counterparts were furnished using benzene sulfonyl chloride or benzoyl chloride, in the presence of pyridine and anhydrous potassium carbonate (Scheme 16).[153]

The antiaggregation impact of the compounds was investigated utilizing the thioflavin-T fluorescence assay, whereas transmission electron microscopy was used for the detection of fibrils utilizing the ThT assay *via* the accomplishment of a time course research. Meanwhile, the photoinduced cross-linking of the unmodified protein assay (PICUP assay) was utilized to identify the formation of oligomers.

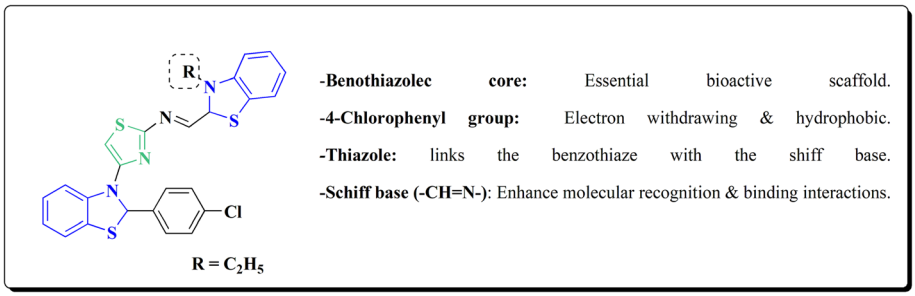


Fig. 8 Structure–activity relationship of compound **132c**.

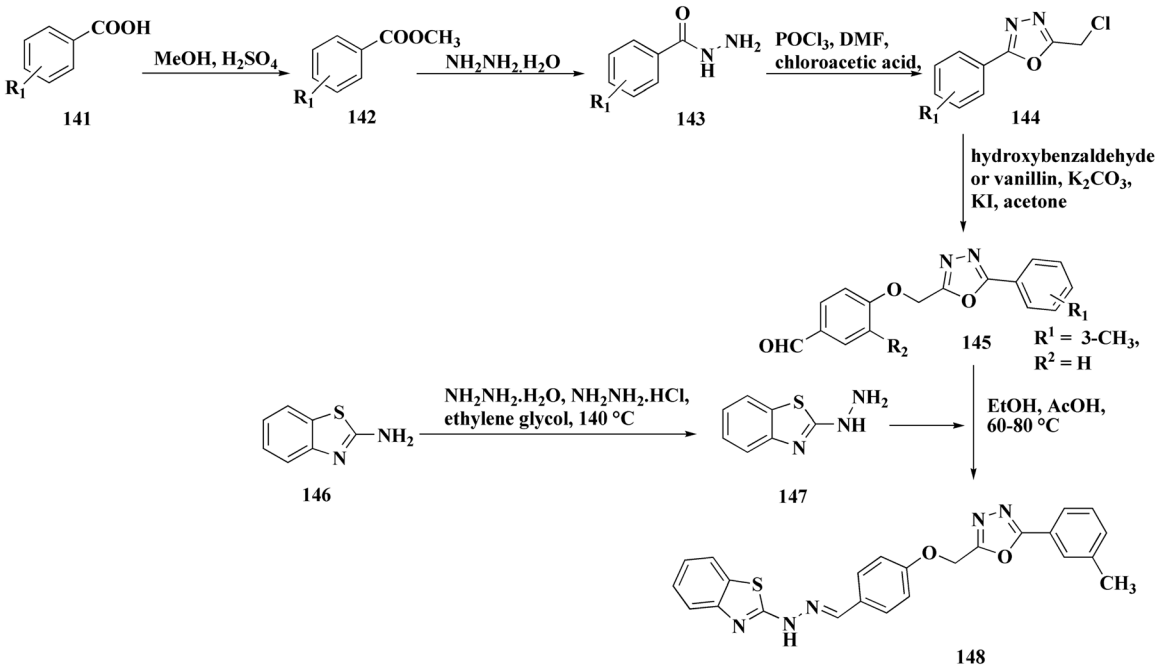


Scheme 19 Synthesis of benzothiazole-1,3,4-oxadiazole conjugates.

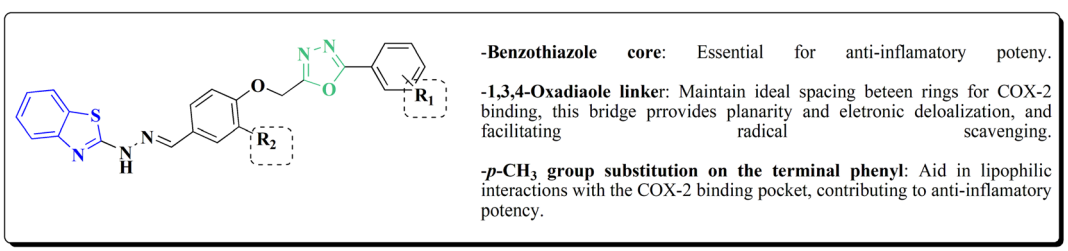


Fig. 9 Structure–activity relationship of compound **148**.

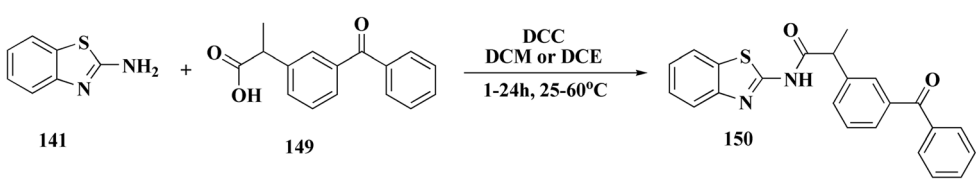


Scheme 20 Synthesis of 2-aminobenzothiazole analogs.

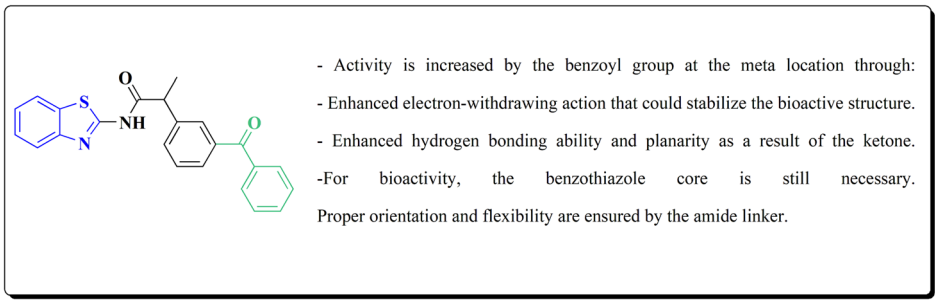


Fig. 10 Structure–activity relationship of compound **150**.

## 7. Synthetic strategies for novel anti-inflammatory benzothiazoles

### 7.1. Thiazole–benzothiazole based analogues

Non-Steroidal bioactive heterocyclic compounds **132**, **134** & **140** were synthesized starting from the 2-chloro-1-(2-(4-chlorophenyl)benzothiazol-3(2*H*)-yl) ethanone **128**. These novel compounds were estimated for their analgesic, anti-inflammation, ulcerogenic, acute toxicity & free-radical scavenging action as compared to reference drugs in the albino rats. At a dose of 50 mg per kg p.o. compound **132c** showed more potency than reference drug.

The synthesis of 2-chloro-1-(2-(4-chlorophenyl)benzothiazol-3(2*H*)-yl) ethenone (**128**) was started *via* reacting 2-(4-chlorophenyl)-2,3-dihydrobenzothiazole with chloroacetyl chloride. The latter compound was reacted with thiourea to generate the substituted (benzothiazol-3(2*H*)-yl)thiazol-2-amine (**130**). Further reaction of compounds **130** with the substituted hydrobenzothiazole-2-carboxaldehyde to generate compound **132** which on further reaction with diazonium salts **133** furnished the substituted 2-hydrobenzothiazole-2-carboxamidine **134** (Scheme 17).[154]

### 7.2. Oxazole–benzothiazole based analogues

The reaction of compound **77** with urea afforded compound **136**. The latter compound was reacted with 3-substituted-2-hydrobenzothiazole-2-carboxaldehyde to produce the substituted (benzothiazol-2-yl)methylene)oxazol-2-amine **138** which on further reaction with the substituted aniline synthesized the benzothiazole-2-carboxamidine derivative **140** (Scheme 18, Fig. 8).[154]

### 7.3. Oxadiazole–benzothiazole based analogues

Benzothiazole analogs bearing a 1,3,4-oxadiazole scaffold were synthesized (Scheme 19) and investigated for their anti-

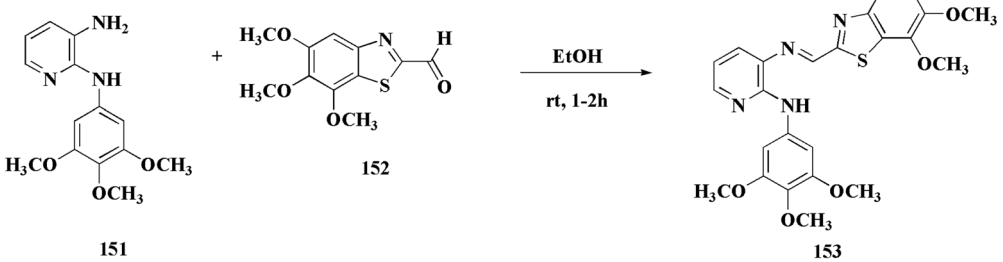


Scheme 21 Synthesis of 2-anilinopyridinyl-benzothiazoles.

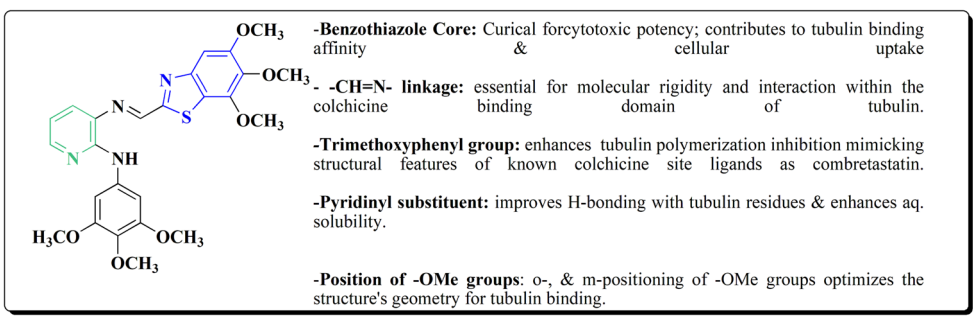


Fig. 11 Structure–activity relationship of compound **153**.

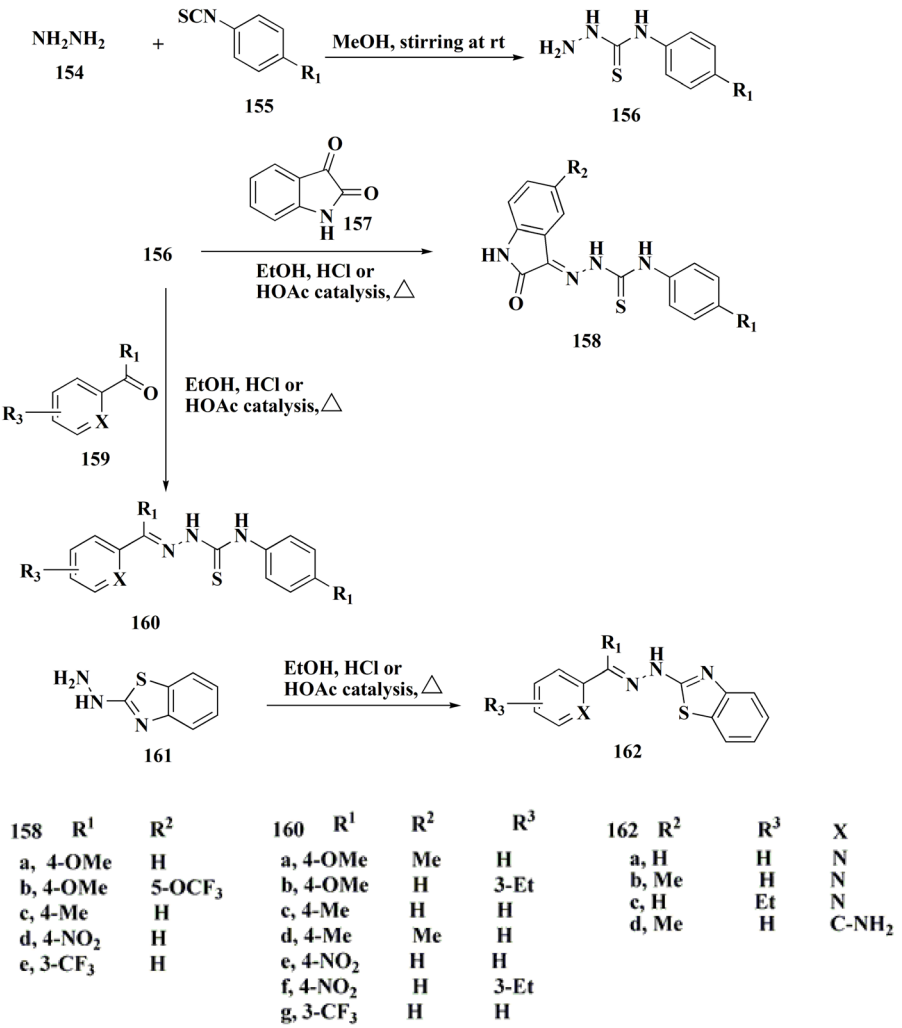


Scheme 22 Synthesis of hydrazinobenzothiazoles.

inflammatory and anti-oxidant potencies (Fig. 9). Compound **148** possessed high radical scavenging efficacies using the ABTS+% bioassay. Upon anti-inflammatory assessments, compound **148** exhibited good potency with 57.35% inhibition after intraperitoneal administration, which was more active than indomethacin as a reference drug. Molecular modeling investigations were carried out to estimate the binding mode of compound **148** as a representative structure into COX-2 enzyme. *In vitro* enzyme investigation indicated that compound **148** displayed its anti-inflammatory potency *via* COX-2 inhibition.[155]

### 7.4. Benzothiazoles linked with substituted aromatics

Several benzothiazoles have utility as anti-inflammatory agents.[156,157] It was also reported that 2-aminobenzothiazole was combined with a variety of profens to synthesize a number of novel compounds **150** (Scheme 20, Fig. 10). When their biological activities were examined *in vitro*, they had strong anti-oxidant and anti-inflammatory properties that were on scale with those of common reference compounds. The findings demonstrate the compounds' potent affinity for HSA and

-Several derivatives across three fundamental scaffolds: arylhydrazones, hydrazino-benzothiazoles, and thiosemicarbazones

-Isatin ß thiosemicarbazones exhibited MDR cell selectivity and collateral sensitivity.

-NNS/NNN donor chelators are more effective than ONS chelators irrespective of the examined cell lines' resistance status

**Thiosemicarbazones:** Strong cytotoxicity and MDR selectivity were demonstrated by isatin-ß thiosemicarbazones.

**-Hydrazinobenzothiazoles:** No intrinsic collateral sensitivity; moderate potency.

**-Arylhydrazones:** Mildly effective; less specific for MDR cells.

Fig. 12 Structure–activity relationship of compounds 158–162.

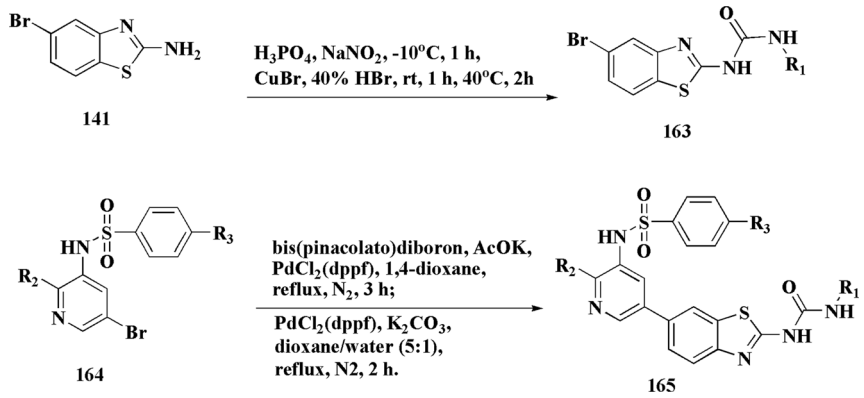


Scheme 23 Synthesis of substituted sulfonylaminopyridin-(5-yl)benzo[*d*]thiazol-2-yl)urea.

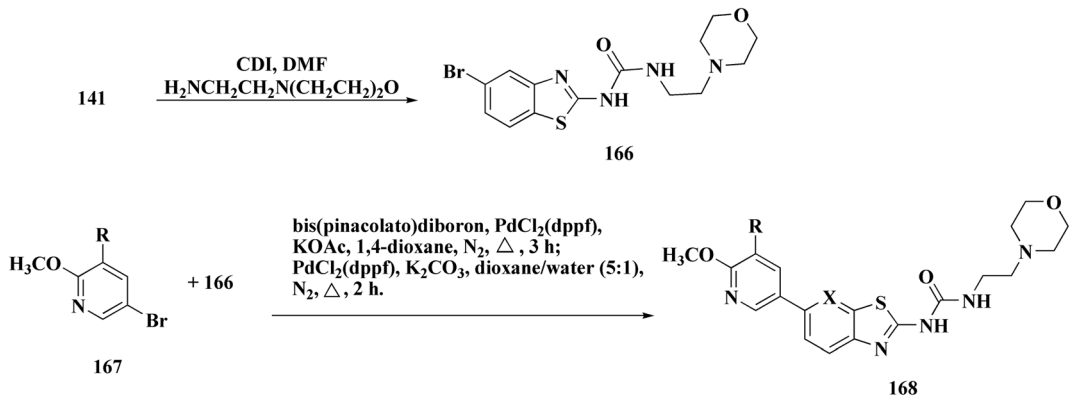


Scheme 24 Synthesis of substituted (benzo[*d*]thiazol-2-yl)urea.

encouraging biological activity. The experimental findings and *in silico* calculations support the new hybrid compound between 2-ABT and ketoprofen 150, which shows great promise. With an $IC_{50}$ of 60.24 μg $mL^{-1}$, compound **150** has the highest hydrogen peroxide scavenging activity of all the compounds examined. Additionally, compound **150** has better anti-inflammatory action than the conventional ibuprofen (76.05 μg $mL^{-1}$), with an $IC_{50}$ of 54.64 μg $mL^{-1}$.[158]

# 8. Synthetic strategies for novel antitumor benzothiazoles

## 8.1. Benzothiazoles linked with heterocyclic compounds

**8.1.1. Deaza-pyrimidine–benzothiazole based analogues.** Compound **151** was reacted with compound **152** to generate compounds **153** (Scheme 21). The anticancer potential of the compounds was evaluated. The compound **153** displayed high

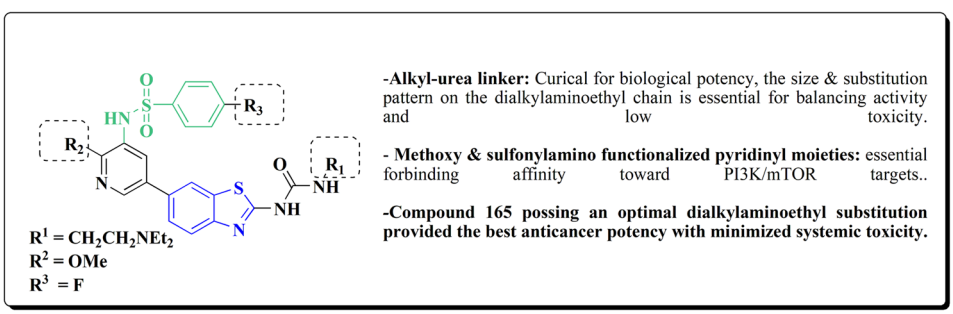


Fig. 13 Structure–activity relationship of compound **165**.

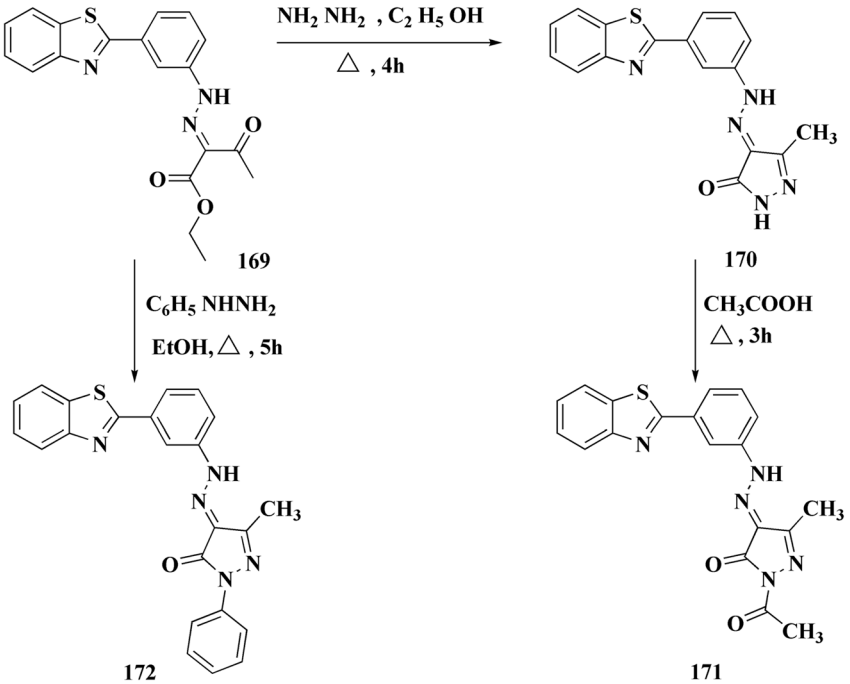


Scheme 25 Synthesis of pyrazole–benzothiazole conjugates.

antiproliferative potency ($GI_{50}$ value of 3.8 μM) against the cell line DU145.[159]

In this study, a series of 2-anilinopyridinyl-benzothiazole Schiff bases were rationally designed by molecular modeling, and key compounds—particularly **153**, featuring a trimethoxy substituent on the benzothiazole ring—exhibited superior binding energies at the tubulin colchicine binding site (even outperforming the reference ligand E7010). These derivatives disrupted mitotic spindle assembly by inhibiting tubulin polymerization, causing a cell-cycle arrest at the $G_2$/M phase. Biologically, compound **153** (Fig. 11) induced apoptosis through mitochondrial pathways (*e.g.* loss of mitochondrial membrane potential, caspase-3 activation, and Annexin V binding), consistent with microtubule destabilization leading to programmed cell death.

In another approach, the thiosemicarbazones were generated through an acid catalyzed Schiff base condensation of the thiosemicarbazide **156** with the corresponding ketone. Compound **156** were synthesized from the isothiocyanates upon reaction with hydrazine. The picolinylidene, acetaniline and salicylidene hydrazinobenzothiazoles **162** were accessed by reacting 2-hydrazinobenzothiazole with the keto components under acid catalyzed conditions (Scheme 22; Fig. 12).[160]

2-Amino-6-bromobenzothiazole was allowed to react with alkylamine and CDI to afford compounds **163**. The intermediate **164** was reacted with intermediate **163** and bis(pinacolato)diboron to generate compounds **165** (Schemes 23 & 24).[161,162]

The anti-proliferative potencies of the compounds were tested *in vitro* against MCF-7, HCT116, A549 and U87 MG cell lines. The compounds with high anti-proliferative potency were examined for their oral toxicity and their inhibitory effect against mTORC1and PI3Ks. Compound **165** (Fig. 13) can efficiently inhibit tumor growth in a study using a mice S180 homograft model. These results propose that this compound can act as potent anticancer agents and PI3K inhibitors.[162]

**8.1.2. Pyrazole–benzothiazole based analogues.** Pyrazoles have various biological potencies,[163–166] its conjugations with benzothiazoles enhance their activities.[167] Novel benzothiazole substituted pyrazole derivatives were synthesized. Compound

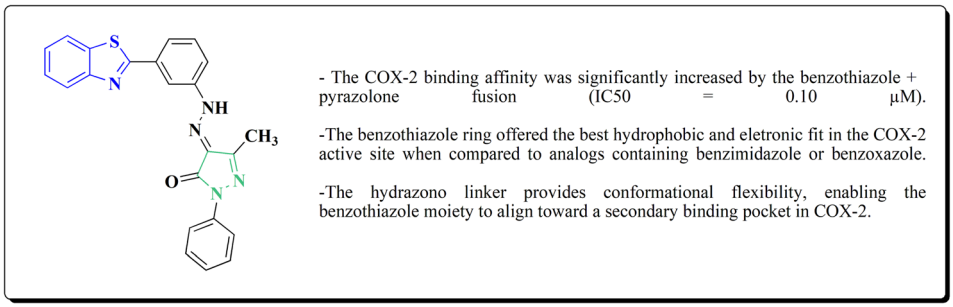


Fig. 14 Structure–activity relationship of compound **172**.

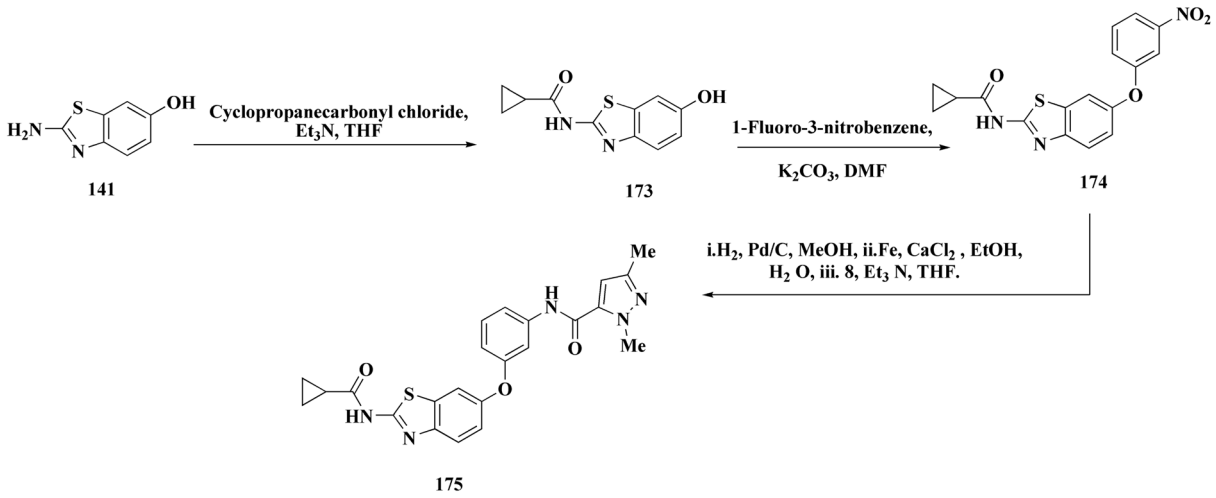


Scheme 26 Synthesis of substituted dimethyl-1*H*-pyrazole-5-carboxamide.

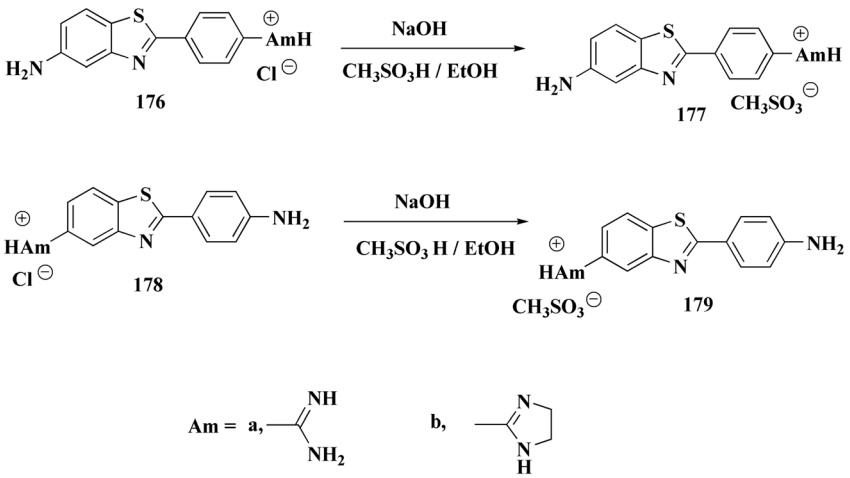


Scheme 27 Synthesis of benzothazole mesylate salts 177b–179b.

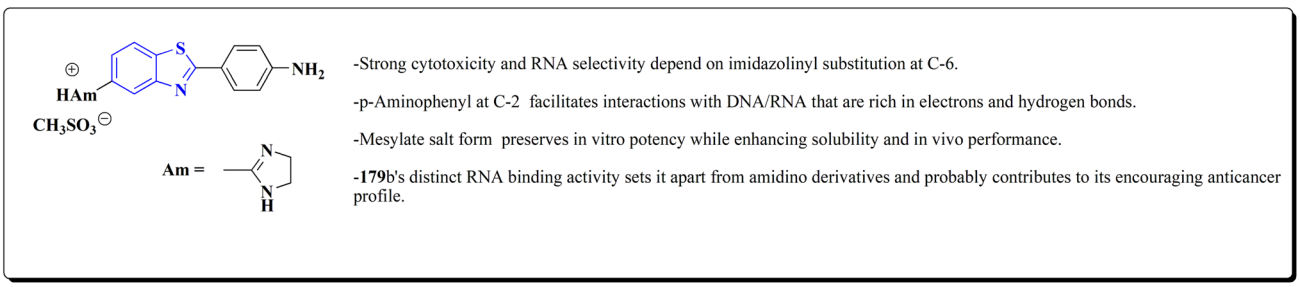


Fig. 15 Structure–activity relationship of compound 179.

**169** was furnished as accomplished in Scheme 25. Then the synthesis of the pyrazolone derivatives **171** was generated by refluxing compound **169** with hydrazine hydrate. Acetylation of compounds **170** yielded the substituted acetyl pyrazolone **171**. Additionally, reacting compound **169** with phenylhydrazine afforded the phenylpyrazolone **172**.[167]

The compounds were examined for their anti-proliferative potency against A549 and MCF-7 cell lines. The obtained findings revealed that the benzothiazolopyrazoloylpyrazolone derivative **172** was the most active COX-2 inhibitor as comparable to celecoxib (Fig. 14).[167]

Furthermore, the synthesis of the 1,3-benzothiazole derivative **175** was outlined in Scheme 26. Acylation of compound **30** with the cyclopropanecarboxylic acid chloride generated **173**, which was reacted with the substituted nitrobenzene to afford compound **174**. Reduction of the latter compound **174** and

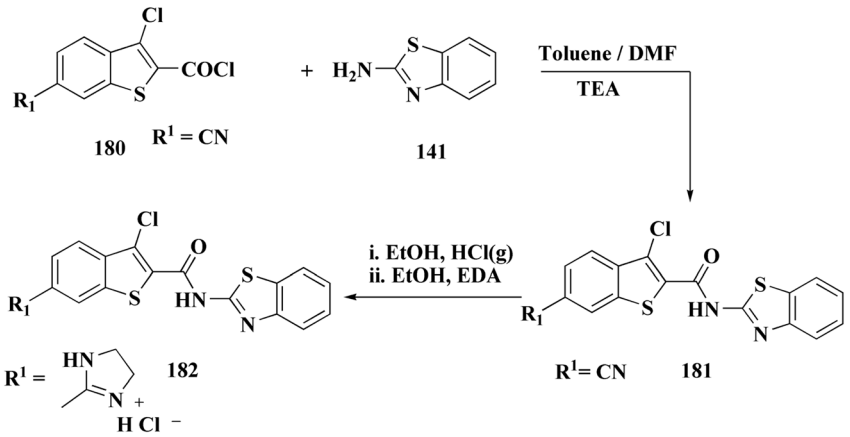


Scheme 28 Synthesis of benzothiazolebenzo[*b*]thieno-2-carboxamides.

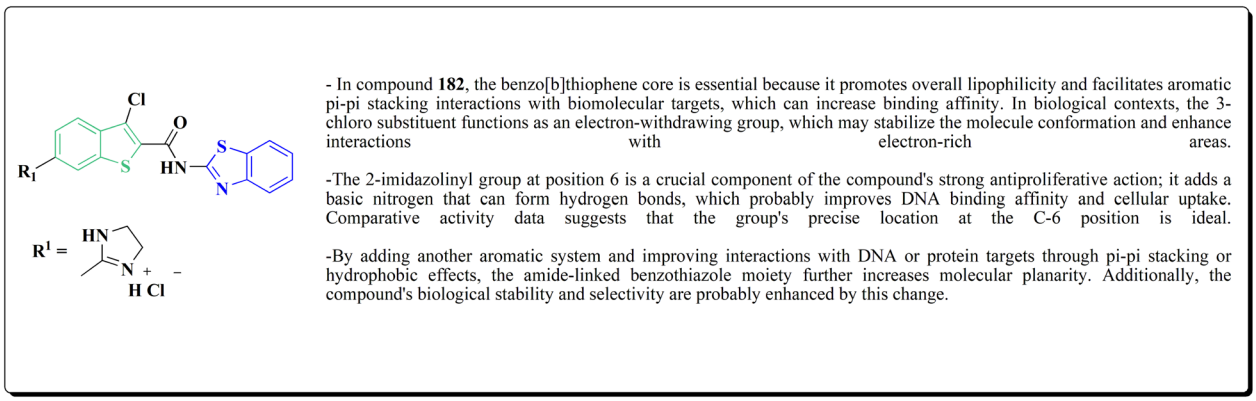


Fig. 16 Structure–activity relationship of compound **182**.

further acylation with acid chloride yielded compound **175.** The compounds indicated strong inhibitory activity against VEGFR2 kinase.[168]

**8.1.3. Imidazole–benzothiazole based analogues.** Hydrochloride salts **176** were transformed to mesylate salts **177**, as accomplished in Scheme 27. Mesylate salts **177** were synthesized through the corresponding free bases. The free bases as intermediates were isolated after the addition of sodium hydroxide solution, and transformed into mesylates *via* treating their ethanolic solutions with mesylic acid. The amidine scafold was then protonated and the salts **177b–179b** were accessed as monocationic mesylates.

The *in vitro* investigations of benzothiazoles revealed antiproliferative potency on a panel of human cancer cell lines.[169]

Without compromising *in vitro* potency, conversion from hydrochloride to mesylate salt significantly increases water solubility and bioavailability. The mesylate derivative of **179b** (Fig. 15) is better for *in vivo* application because it has substantial cytotoxic effects on tumor cells while having little acute oral toxicity.

Mode of DNA/RNA binding: -dual binding is indicated in **179b:** ds-RNA intercalation, binding of minor grooves to AT-rich DNA, unique among the derivatives under study in terms of distinct single-stranded RNA (ss-RNA) binding.

Its cytotoxic selectivity is probably influenced by this selective binding profile.

Correlation of biological activity: using a variety of cancer cell lines, **179b** consistently shown cytotoxic action. Its capacity to bind RNA more effectively than amidino analogs coincides with its action, indicating a molecular connection between RNA recognition and antitumor efficacy.[169]

In parallel, the benzothiazolebenzo[*b*]thieno-2-carboxamides **181** were generated. Compound **180** were reacted with 2-aminobenzothiazoles to afford the corresponding carboxamides **181.** Compounds **181** underwent an acidic Pinner reaction to yield the imidazolinyl substituted derivatives **182.** Monosubstituted carboxamides bearing 2imidazolinyl group on benzothiazole nuclei were synthesized through the condensation of compound **180** with 2-amino-6-(2imidazolinyl)benzothiazole **141** (Scheme 28).

The antiproliferative activities were estimated *in vitro* against human cancer cell lines. The effective potency against HeLa cells was showed for compound **182** ($IC_{50} = 1.16$ μM) (Fig. 16).[170]

The bioactive benzothiazole and 1,2,3-triazole moieties were integrated into a single molecular framework for the investigation of their anticancer potential using an effective Cu(I)-catalyzed alkyne–azide cycloaddition (CuAAC) technique.

Therefore, by 1,3-dipolar cycloaddition of different substituted and unsubstituted benzothiazole azides **185** with corresponding *O*-propargylated benzylidene derivatives, a novel series of 1,2,3-triazole–benzothiazole conjugates **188** with

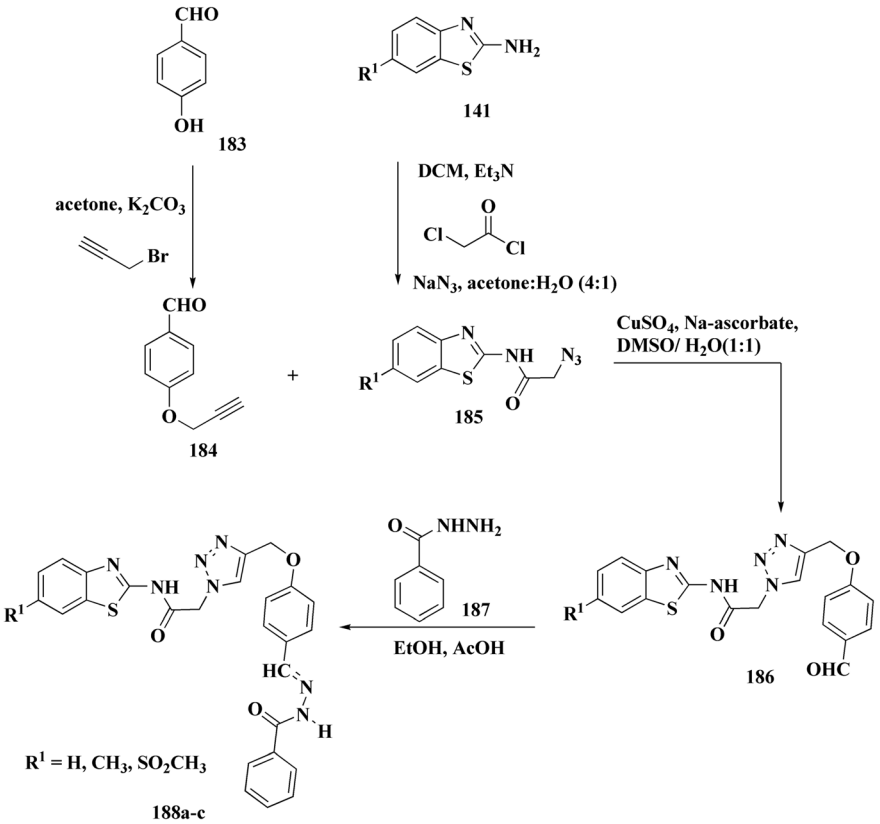


Scheme 29 Synthesis of thiosemicarbazone based benzothiazole-1,2,3-triazole derivatives **188a–c**.

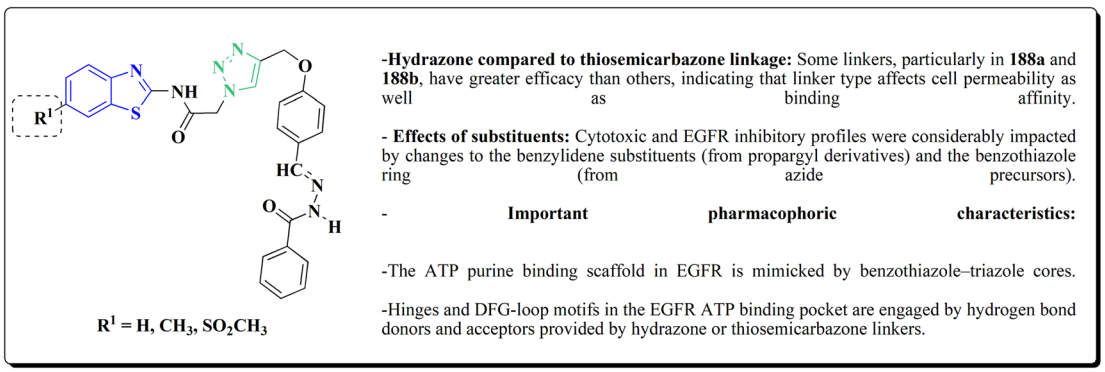


Fig. 17 Structure–activity relationship of compound **188**.

hydrazone or thiosemicarbazone linkages was successfully designed and synthesized (Scheme 29).

Compounds **188a–c** demonstrated high anticancer activity, especially against the T47D breast cancer cell line, while maintaining acceptable safety profiles in normal cells, according to a biological study of these compounds against three human cancer cell lines. Additionally, compounds **188a** and **188b** showed remarkable anti-proliferative potential by dramatically inhibiting the two-dimensional migration of lung cancer cells in a concentration-dependent manner. Interestingly, the $IC_{50}$ values of compounds **188a**, **188b**, and **188c** were 0.69, 1.16, and 4.82 μM, respectively.

These results were corroborated by molecular docking experiments, which demonstrated that **188a** and **188b** have substantial binding affinities to the EGFR active site. These findings collectively imply that compounds **188a** and **188b** are excellent candidates for the synthesis of chemotherapeutic drugs that target EGFR.[171]

Against T47 D cells, compounds **188a–188c** (Fig. 17) demonstrated the strongest cytotoxic effects: $IC_{50}$ values: ≈0.69 μM for **188a**, 1.16 μM for **188b**, and 4.82 μM for **188c**, at matched concentration, it demonstrated >96% inhibition in a favorable comparison to erlotinib ($IC_{50}$ = 1.3 μM). Safety profiling on normal (non-cancerous) cells found $IC_{50}$ values >500 μM, indicating low toxicity and a high therapeutic window.

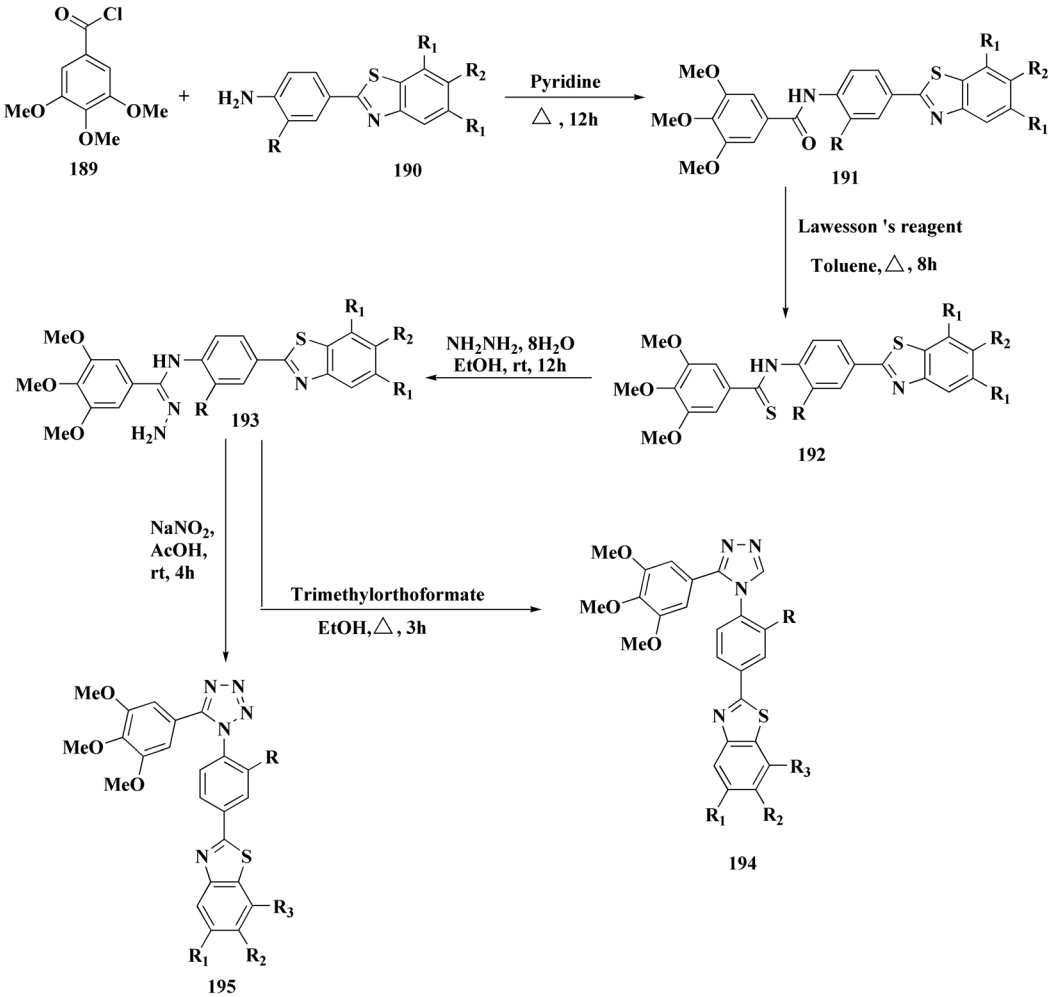


Scheme 30 Synthesis of amidrazones **193** & combretastatin-benzothiazole analogs.

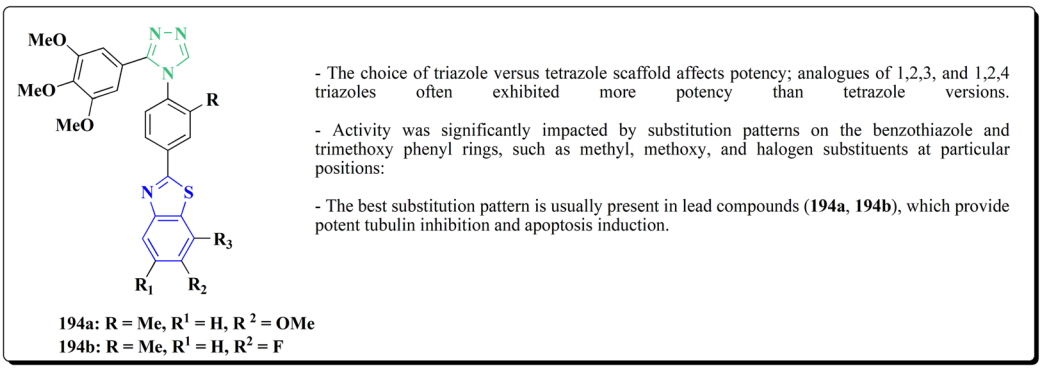


Fig. 18 Structure–activity relationship of compound **194**.

The mechanism of **188a** and **188b** as EGFR inhibitors was supported by molecular docking, which revealed that they have substantial binding affinities for the EGFR active site.

**8.1.4. Tetrazole–benzothiazole based analogues.** Colchicine site binding tubulin inhibitors were prepared as outlined in Scheme 30. Synthesis of the tetrazoles **194** and **195.** The 2-(4-aminophenyl) benzothiazoles **190** were reacted with the benzoyl chloride **189** to afford the substituted benzothiazole amides **191** which upon further treatment with Lawesson's reagent affords thioamides **192.** The reaction of thioamides with hydrazine hydrate yields amidrazones **193.** The intramolecular cyclization was carried out using trimethylorthoformate in the presence of catalytic amount of sulphuric acid giving the targeted cis restricted 1,2,4-triazoles **194,** whereas 1,2,3,4-tetrazoles **195** were obtained as shown in Scheme 30.

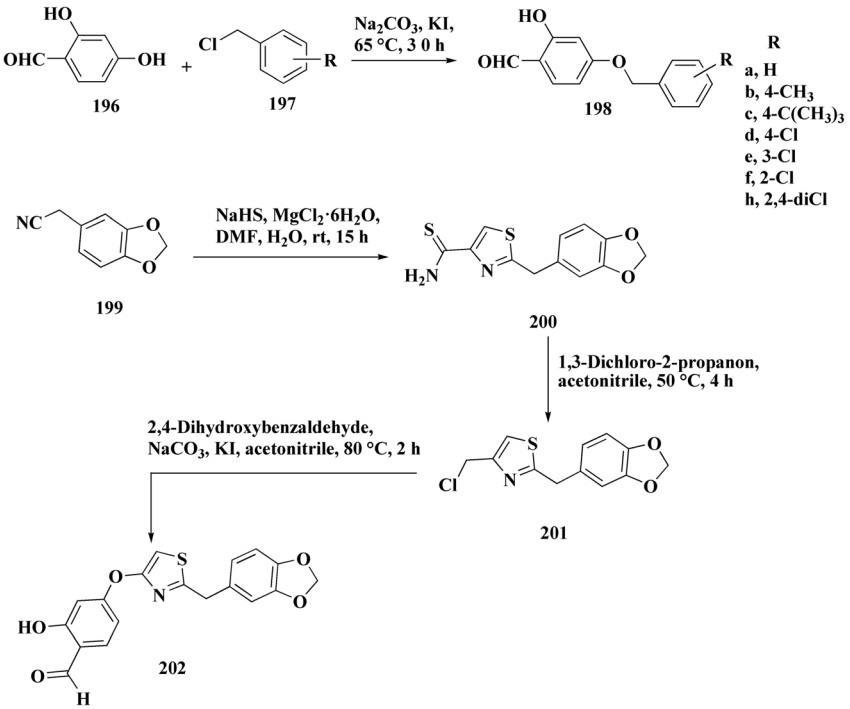


Scheme 31 Synthesis substituted thiazole derivative **202**.

These compounds were tested for their antiproliferative potency against cancer cell lines. The most active compounds **194a,b** (Fig. 18) indicated an antiproliferative effect as compared to that of Combretastatin A-4 (CA-4).[172]

They induced cell-cycle arrest (mitotic arrest) in the G-/M phase. Immunocytochemistry and tubulin polymerization tests validate the disruption of microtubule dynamics. Western blot experiments showed increased tubulin in the soluble

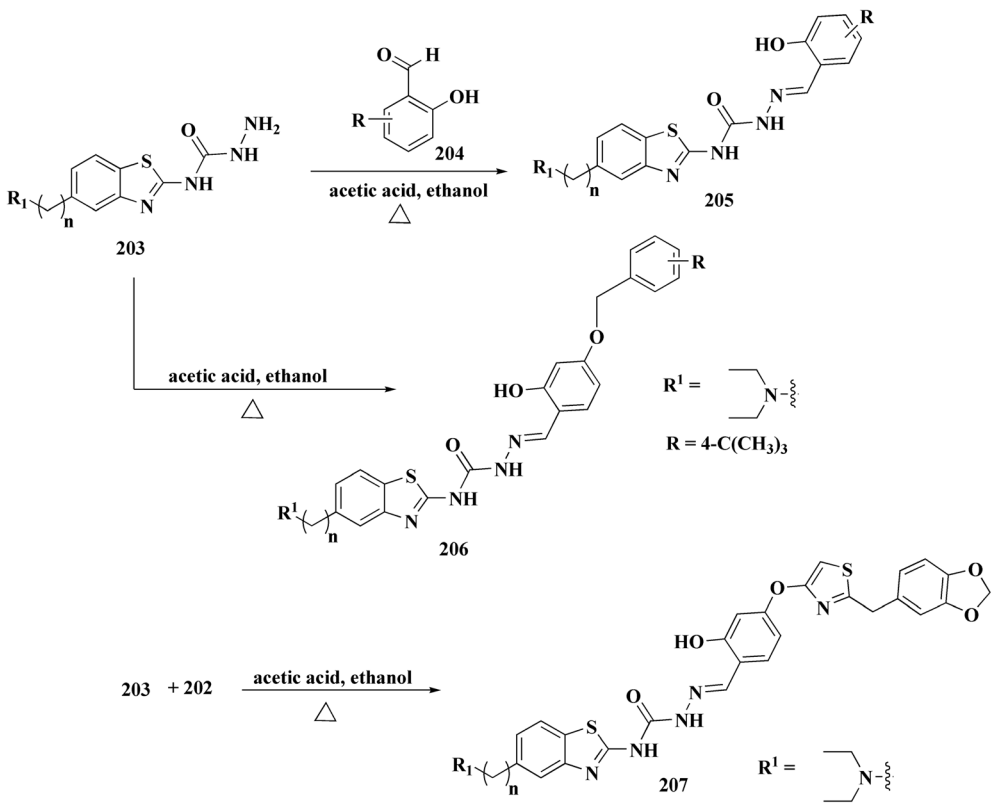


Scheme 32 Synthesis of substituted hydrazinecarboxamides.

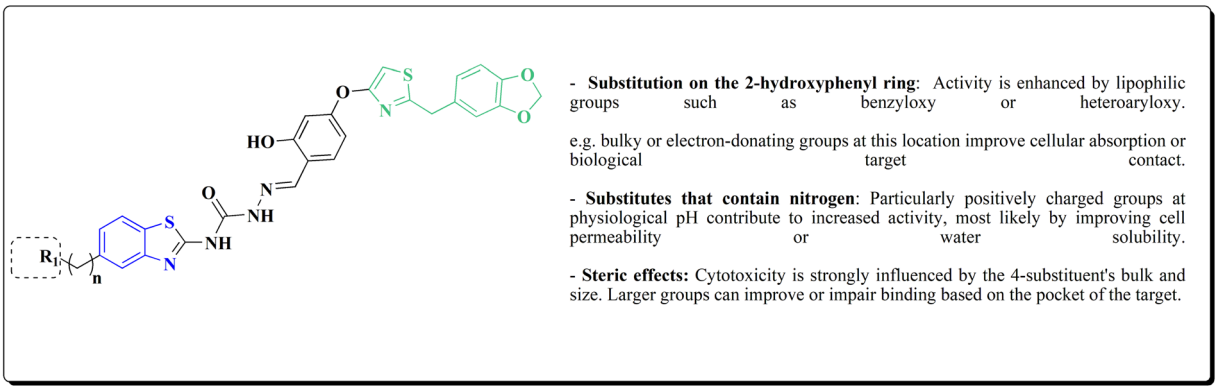


Fig. 19 Structure–activity relationship of compound **207**.

fraction, which is consistent with depolymerization. Molecular docking and colchicine-competitive binding tests confirm that they bind at the colchicine site in a manner comparable to Combretastatin A-4 (CA 4).

After mitotic arrest, these compounds cause apoptotic cell death, as demonstrated by these compounds induce apoptotic cell death following mitotic arrest, confirmed by: hoechst nuclear staining, mitochondrial membrane potential loss, Annexin-V-FITC positivity, activation of caspase-3, ROS generation.

**8.1.5. Thiazole–benzothiazole based analogues.** The benzyloxy 2-hydroxybenzaldehydes **198** were furnished through the reaction of 2,4-dihydroxy benzaldehyde with substituted benzylchloride. 1,3-Benzodioxole-5-acetonitrile was allowed to react with sodium sulfide to access compound **200**, which was then reacted with 1,3-dichloroacetone to give compound **201.**[173] Compound **202** was synthesized through the reaction of 4-hydroxysalicylaldehyde with compound **201.** Its worthy to note that the salicylaldehyde analogs have anticancer potencies.[174,175] The desired compounds **205**, **206** and **207** were furnished through the reaction of compound **203** with 2-hydroxy aromatic aldehydes (Schemes 31 and 32).[173]

The cytotoxic activities were evaluated and screened *in vitro* against cancer cell lines (SK-N-SH, NCI-H226, HT29, MDA-MB-231, and MKN45). Compounds **206** (procaspase-3 $EC_{50}$ = 1.42 μM) and **207** (procaspase-3 $EC_{50}$ = 0.25 μM) showed anti-tumor potency with $IC_{50}$ values in the rang of 0.14 μM to 0.98 μM on a panel of cancer cell lines (Fig. 19).[173]

These compounds cause increased apoptosis in cancer cells, which explains the observed cytotoxicity. Procaspase-3, a pro-

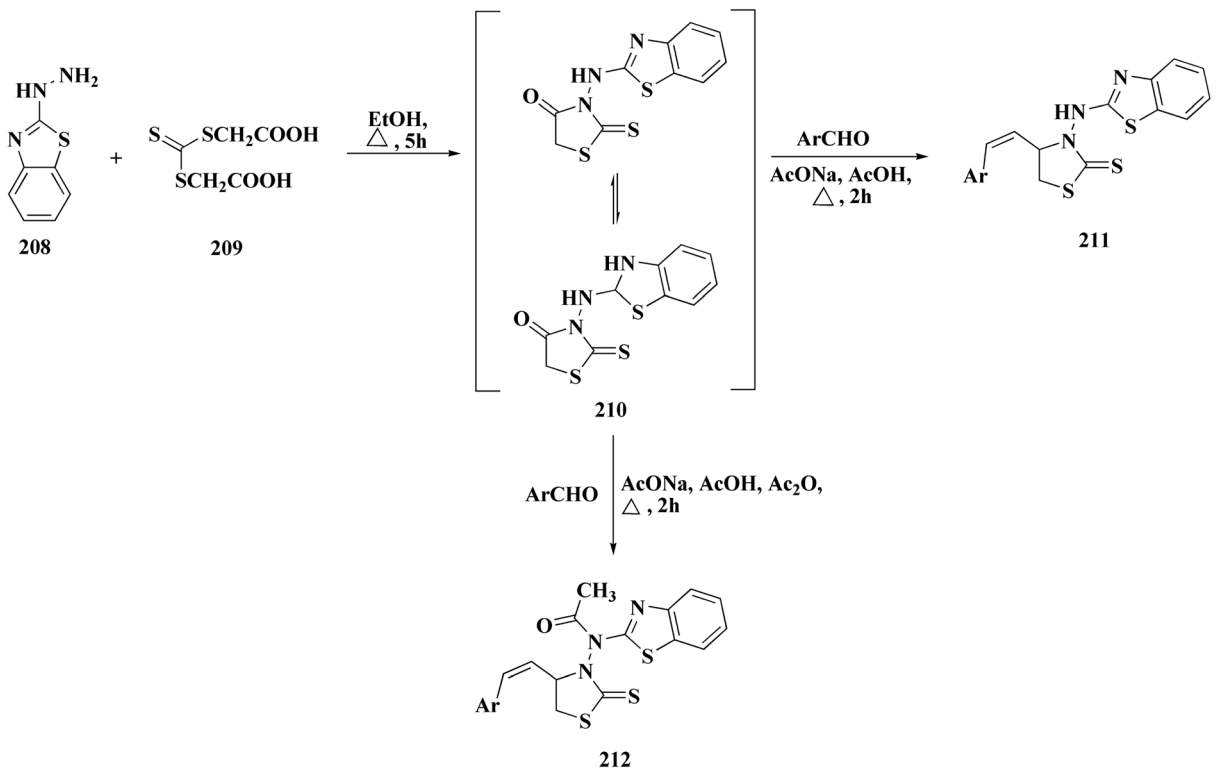


Scheme 33 Synthesis of benzothiazole substituted 4-thiazolidinones derivatives.

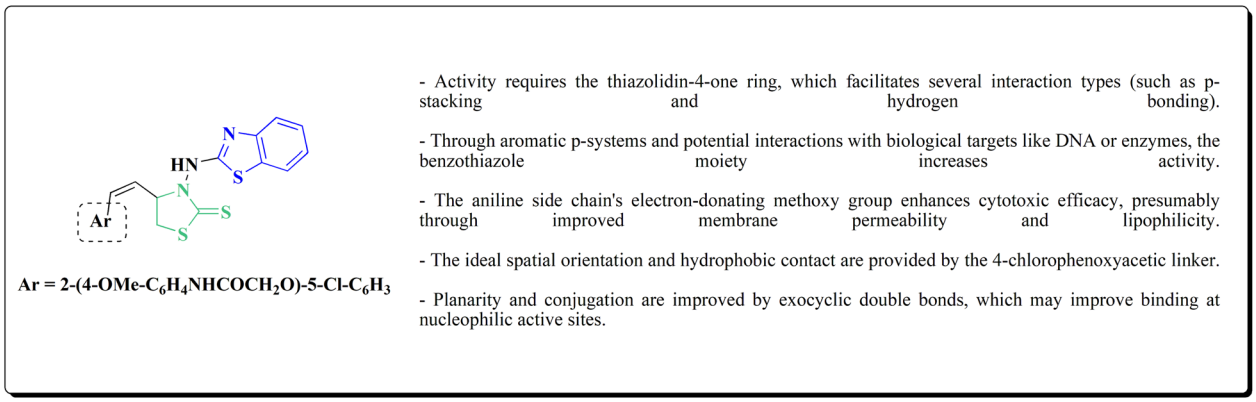


Fig. 20 Structure–activity relationship of compound **211**.

enzyme version of caspase-3, is a crucial apoptotic executioner. Although the novel compounds have noticeably more potency, this mechanism is identical to that of PAC-1.

Strong procaspase-3 activating properties are provided by the study's powerful and structurally unique anticancer agents. SAR analysis provides precise guidelines for further optimization, emphasizing steric tuning, charge distribution, and lipophilicity.[173]

In continuation, the synthesis of benzothiazole substituted 4-thiazolidinones derivatives were accomplished in Scheme 33. The thiazolidone **210** was synthesized from 2-hydrazino-1,3-benzothiazole and trithiocarbonyldiglycolic acid in ethyl alchol under reflux. Compound **210** was allowed to react with the aromatic aldehydes to yield 5-arylidene derivatives **211** *via* a knoevenagel condensation's reaction. The acetylation of exocyclic nitrogen was observed **212** following acetanhydride addition to reactive mixture.

*In vitro* anti-cancer potency of the compounds was evaluated. The compounds have showed the anticancer activity on cancers cell lines. Among examined compounds, the acetamide **211** was the most potent candidate with average logTGI and logGI50 values −4.45 and −5.38 (Fig. 20).[176]

The cell cycle arrest and apoptosis induction are likely the mechanism, albeit precise enzyme targets have not been established. The possible DNA intercalation or interaction with cysteine-rich enzymatic pockets (such as kinases or reductases) is suggested by structural characteristics.

Strong cytotoxicity was demonstrated by compound **211** against a panel of human carcinoma cell lines.

**8.1.6. Indole–benzothiazole based analogues.** By combining two active scaffolds, a novel series of benzothiazole–indole hybrid compounds was designed to target important cancer pathways: • benzothiazole, which interacts with kinase domains, tubulin, and DNA. • Indole, a heterocycle compound frequently found in antiproliferative medications and bioactive natural compounds.

Compounds **214** were prepared *via* nucleophilic substitution of different α-chlorotoluene with 3-formylindole **213**. The substituted isatins **217** were synthesized through condensation of phenylamine with trichloroacetaldehyde followed by cyclization in dihydrogen sulfate (Scheme 34).

The desired compounds **218**, **219** and **220** were obtained through the reaction of **203** with indole-3-carbaldehyde analogs **213** & **214** or 5-substituted isatins **217** (Scheme 35). The compounds were then screened for *in vitro* antitumor potency on a panel of cancer cell lines. Compounds **219** displayed good selectivity against HT29 cancer cell line. Compound **219** showed

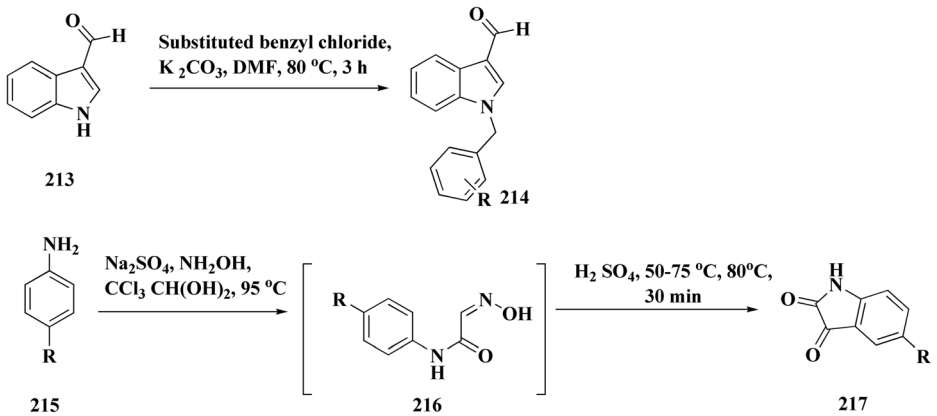


Scheme 34 Synthesis of substituted indoles and isatins.

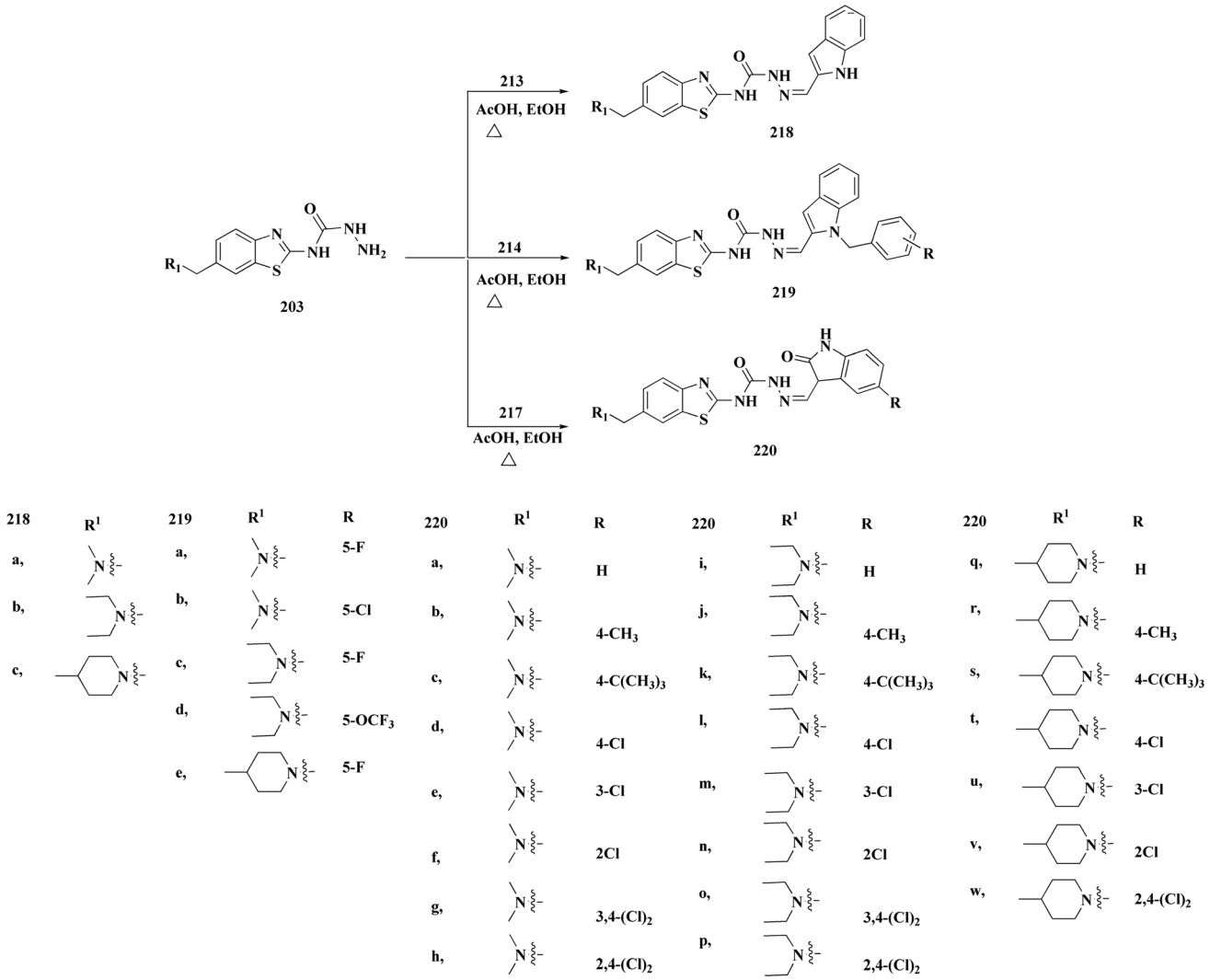


Scheme 35 Synthesis of benzothiazole-isatin & benothiazole–indole conjugates.

high antitumor potency against H460, A549, HT29, and MDA-MB-231.[177]

Strong anticancer potency was demonstrated by the newly synthesized benzothiazole–indole hybrids, especially compound **219** (Fig. 21), which activated caspase and disrupted tubulin to cause mitotic arrest and apoptosis. A prospective lead chemical for more preclinical research and mechanistic investigation is compound **219**.[177]

Following this line of the research of conjugating the indoles with benothiaoles, the isoindolines substituted with amidino-

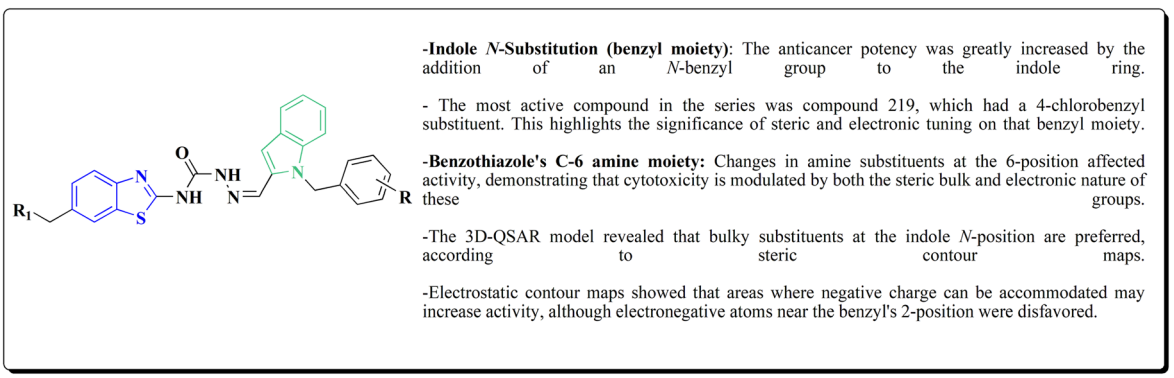


Fig. 21 Structure–activity relationship of compound **219**.

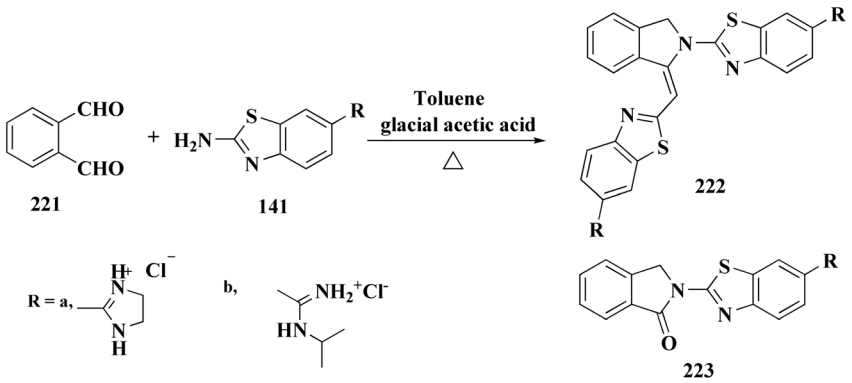


Scheme 36 Synthesis of iminoindolines and isoindolin-1-ones-benzothiazoles conjugates.

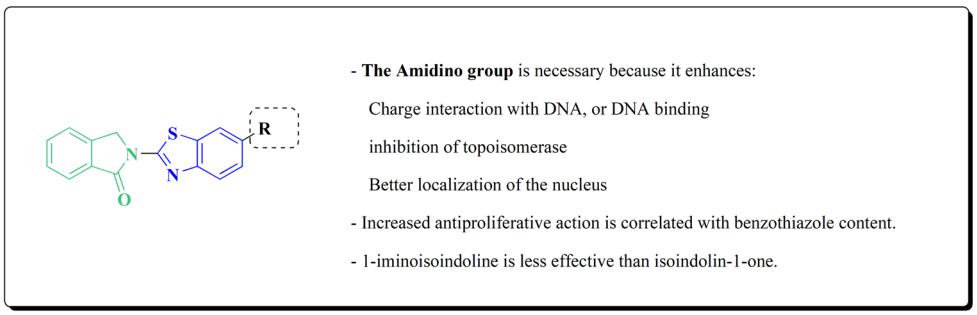


Fig. 22 Structure–activity relationship of compound **223**.

and cyano-benzothiazoles were prepared as novel anticancer agents. Amidino substituted benzo[*d*]thiazol-2-amine **141a–b** was synthesized from 6-cyano-1,3-benzothiazol-2-amine as outlined in Scheme 27. The reaction of compounds **141** with *o*-phthalaldehyde **221** afforded the 1-iminoindolines **222** and isoindolin-1-ones **223** (Scheme 36, Fig. 22).[178]

The isatin-benzothiazole analogs were synthesized as outlined in scheme. Compounds **225** were synthesized through condensing the isatain with formaldehyde and secondary amino function of amino component. The paraformaldehyde (PFA) and an amino component were dissolved in ethylalchol and iminium ion yielded *in situ* was then reacted with 1*H*-indole-2,3-dione derivatives to generate compounds **225**. The intermediate compound 2-amino-6-methylbenzothiazole was prepared from 4-toluidine, in which the substituted aniline was reacted with potassium thiocyanate and bromine in ethanoic acid. Compounds **226** were produced *via* condensation of compound **225** with 6-methyl-benzothiazol-2-ylamine (Scheme 37).

The cytotoxicity of these compounds was exhibited using three human breast tumor cell lines, and two non-cancer breast epithelial cell lines. Compound **226** is considered as the most potent compounds of this series.[179]

Among the most effective compounds against the three examined cell lines of breast cancer was compound **226,** $GI_{50}$ values: MDA-MB231: 17.61 μM, MDA-MB468: 19.76 μM, &

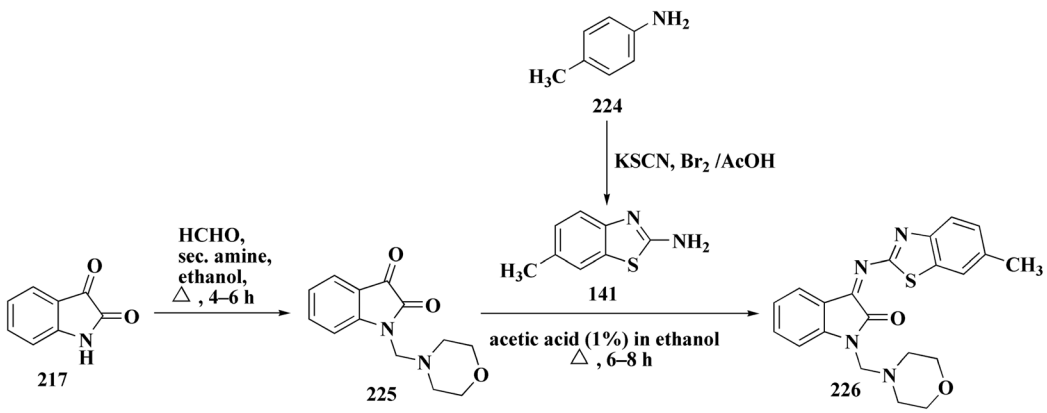


Scheme 37 Synthesis of isatin-benothiaole analogs.

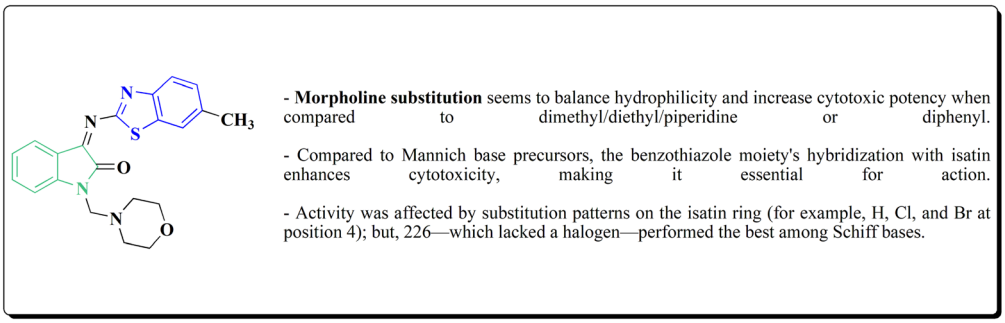


Fig. 23 Structure–activity relationship of compound **226**.

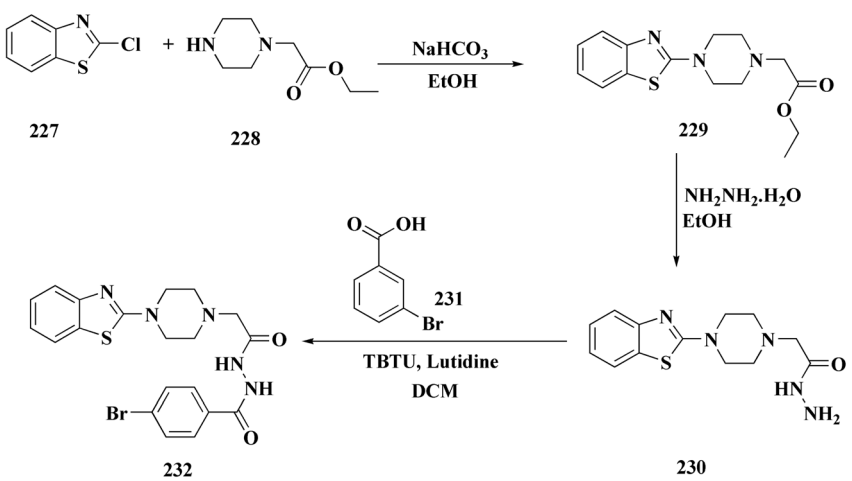


Scheme 38 Synthesis of piprazine–benzothiazoe analogs.

MCF7: 14.56 μM. $GI_{50}$ for MCF7 is 25.77 μM, which is higher than cisplatin. Compared to non-cancerous breast cells, compound **226** (Fig. 23) exhibited more cytotoxicity toward cancer cells.

There is little correlation between cell cycle arrest and **5e**'s cytotoxic impact. In MCF7 or MCF10A cells, **226** did not stop the cell cycle at 20 μM. Only MCF7 cells showed a little accumulation in the $G_2$/M phase at 40 μM. This implies that **226** causes cytotoxicity by a mechanism other than cell cycle arrest, potentially involving: oxidative stress, dysfunction of mitochondria, and non-cell-cycle mechanisms leading to apoptosis (not verified in this study).[179]

**8.1.7. Piprazine–benzothiazole based analogues.** 2-Chlorobenzo[*d*]thiazole **227** was reacted with the piperazinyl acetate **228** to afford compound **229**. The latter compound **229** was reacted with hydrazine hydrate to afford the hydrazide **230**. Further treatment of compound **230** with benzoic acids **231** in the presence of TBTU and 2,6-dimethyl pyridine (lutidine), yielded the targeted compounds **232** (Scheme 38).

The cell viability assay and *in vitro* cytotoxicity of compounds **232** were tested against Dalton's lymphoma ascites (DLA) cells. Compound **232** indicated promising antiproliferative efficacy (Fig. 24). Subsequent investigation of compound **232** on *in vivo*

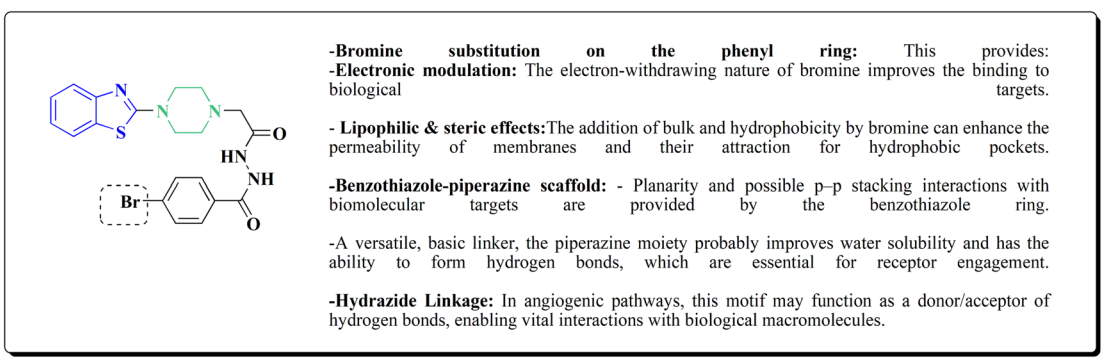


Fig. 24 Structure–activity relationship of compound **232**.

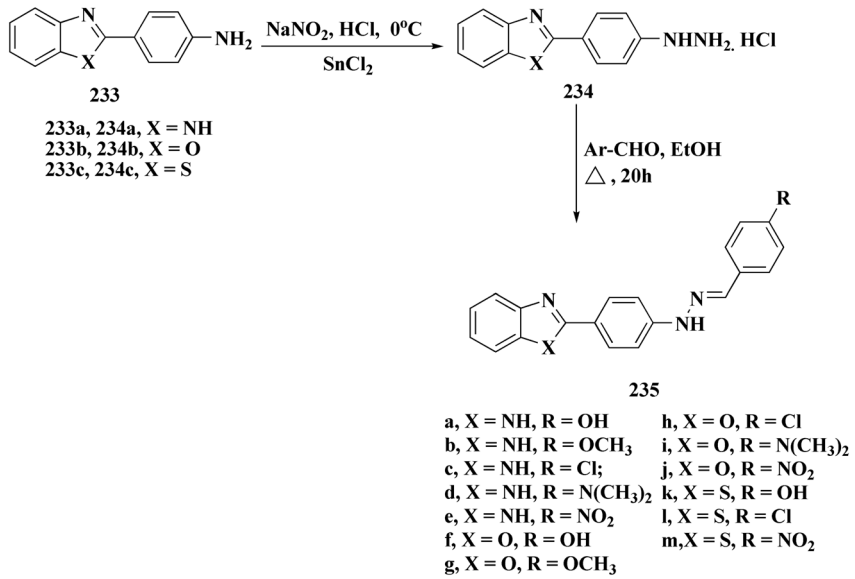


Scheme 39 Synthesis of 2-substituted benzothiazoles 235k–m.

treatment model indicated increased tumor suppression through inhibition of angiogenesis.[180]

### 8.2. Benzothiazoles linked with substituted aromatics

The phenyl hydrazine hydrochlorides **234a–c** were synthesized *via* the diazotization of aromatic amines of the benzothiazoles **233a–c** followed by their reduction. Condensation of compound **2a–c** with various aromatic aldehydes yielded the desired compounds **235a–m** (Scheme 39).

The novel compounds were examined *in vitro* against both human hepatic adenocarcinoma (HepG2) and human breast adenocarcinoma (MCF-7) cell lines. The most potent compounds **235h** ($IC_{50}$ = 0.067 μm against MCF-7) and **235l** ($IC_{50}$ = 0.027 μM against HepG2) were tested subsequently for EGFR inhibitory activity (Fig. 25).[181]

Novel resveratrol (RES) analogs were developed. The amide **237** was afforded through condensing of 3,5-dimethoxybenzoyl chloride **236** with *p*-anisidine. Treating this amide with the Lawesson's reagent (LR) afforded the thioamide **238**, which was then exposed to an oxidative cyclization (Scheme 40).

The acid chloride **236** was reacted with *m*-anisidine to afford amide **240**. Treating the latter with Lawesson's reagent furnished the thioamide **241**. The oxidative cyclization step produced, a mixture of the isomeric compounds **242** & **243**. The $BBr_3$-promoted *O*-demethylation of **243** led to compound **250**. The synthesis of benzothiazoles **250** and **251** was accomplished in Scheme 41. Condensation of 3,5-dimethoxyaniline with 4-methoxybenzoyl chloride **245** generated the amide **206**. The thioamide **248** was generated using Lawesson's reagent then the latter compound was submitted to the ferricyanide-promoted cyclization. Compound **248** was then deprotected to generate compound **250**. Compound **251** was accessed subsequent an indistinguishable synthetic approach, with the only modification consisting in condensing **245** with 2,4-dimethoxyphenylamine (Scheme 42).

The resulting analogs were estimated for their antiproliferative and vasorelaxing effect.

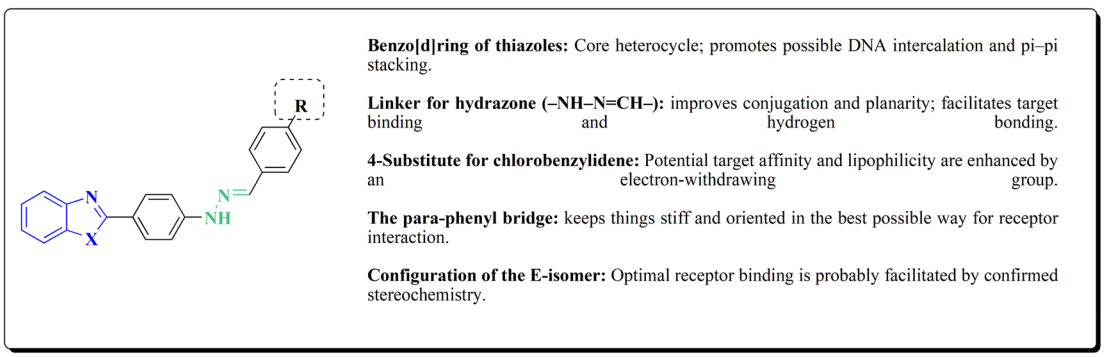


Fig. 25 Structure–activity relationship of compound 235.

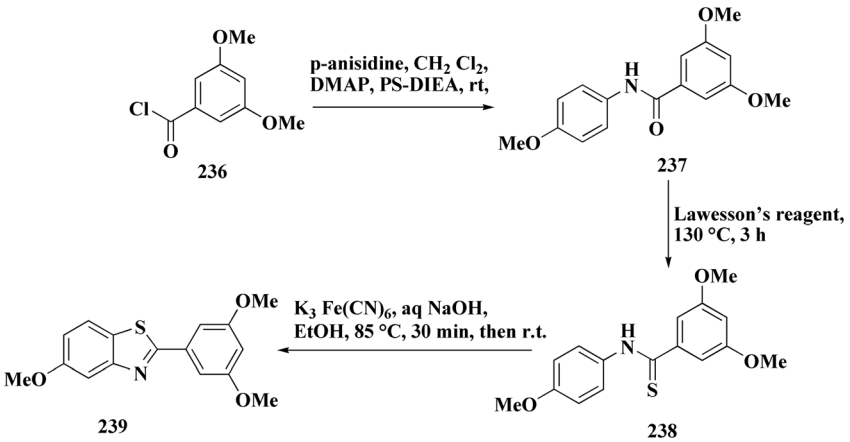


Scheme 40 Synthesis of resveratrol (RES) analogs.

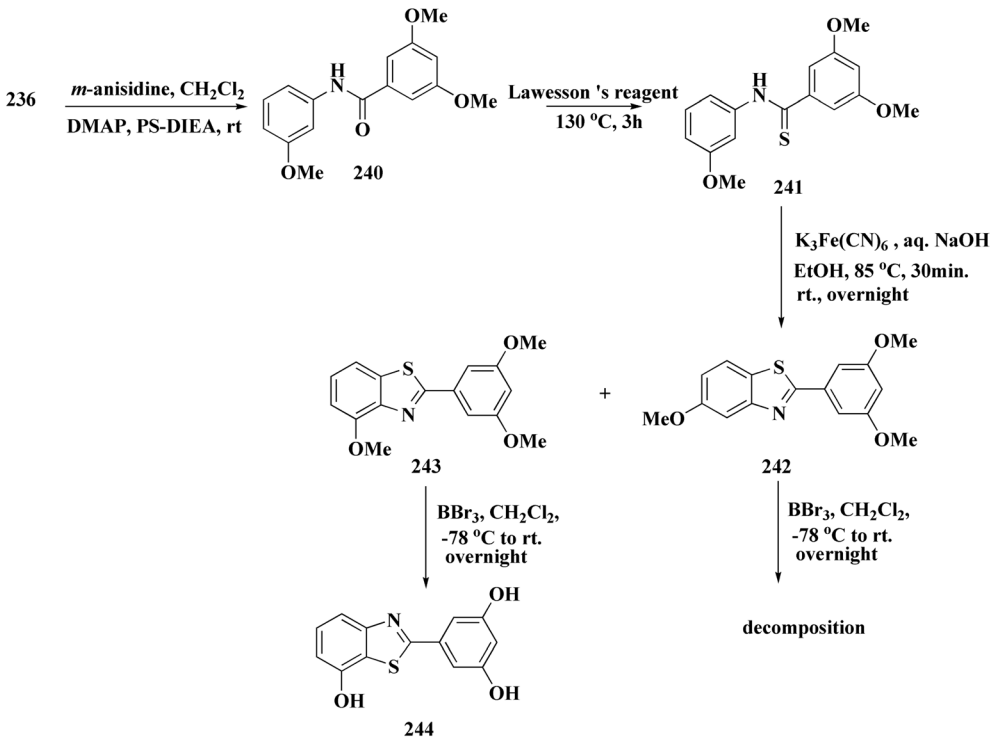


Scheme 41 Synthesis of resveratrol (RES) analogs.

2-(3,5-Dihydroxyphenyl)-6-hydroxybenzothiazole had the highest levels of potency (pIC 50 = 4.92) and efficacy ($E_{max}$ = 88.2%) in vascular testing (Fig. 26).[182]

Compound **256a** with best anti-tumor potencies was selected as a lead structure. The desired compounds were prepared *via* a multi-step substitution reaction using the benzothiazole **141**. On the amide side, phenyl replacements were inserted while the thioether with benzyl substitution was remained. Compounds **256** were afforded in good yield. Compounds **257** were generated by substitution with compound **255** (Scheme 43).

Compounds **256b**, **257a**, **257b** showed antitumor potencies. **257b** indicated high anticancer potency against HCT116 colon cancer cells.[183]

The non-sulfamide NEDD8-activating enzyme (NAE) is inhibited by compound **257b** (Fig. 27). The mechanism can be summed up as follows: inhibition of the NEDD8 pathway-NAE plays a critical role in triggering the NEDD8 cascade, a ubiquitin-like post-translational modification that is necessary for controlling cullin-RING ligases (CRLs), which determine how important cell cycle proteins degrade.

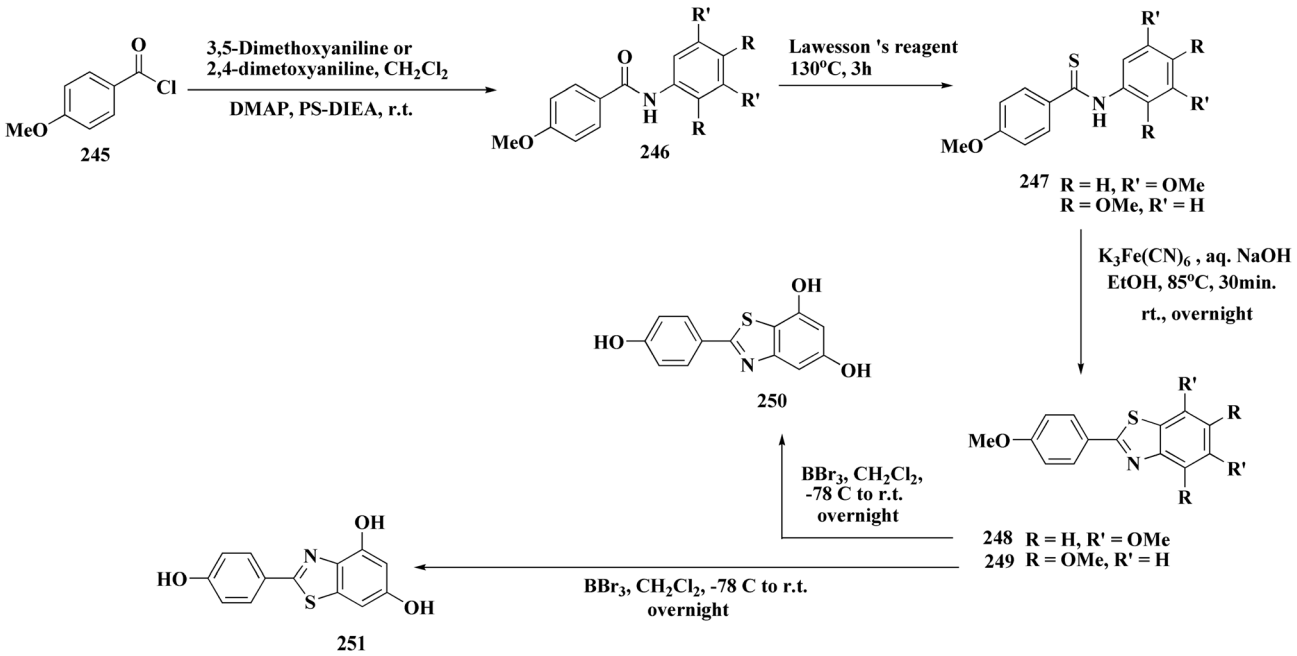


Scheme 42 Synthesis of resveratrol (RES) analogs.

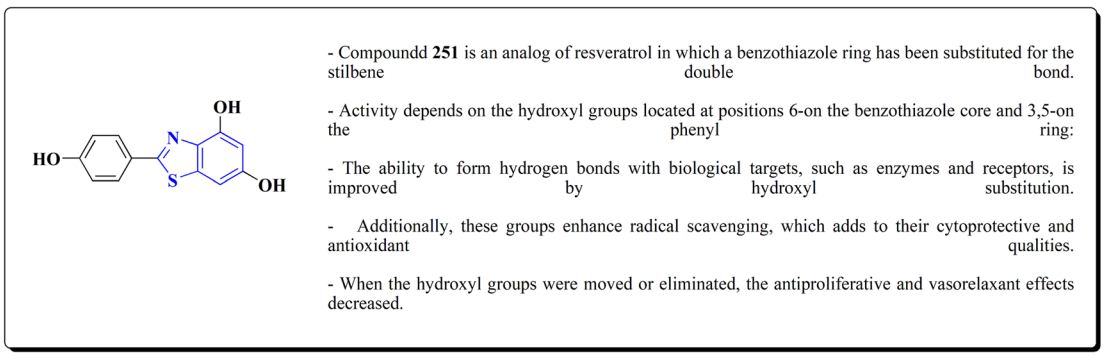


Fig. 26 Structure–activity relationship of compound **251**.

Compound **257b** forms three hydrogen bonds (Asp100, Ile148, and Gln149) and one extra H-bond with Asp167 by binding non-covalently to NAE and imitating the main hydrogen-bonding interactions observed with the natural AMP substrate. This binding effectively blocks the NEDD8 pathway, causing cancer cells to undergo apoptosis by lowering cellular levels of NEDD8 and accumulating UBC12, a downstream target. The mechanism at the molecular level was validated by a dose-dependent drop in NEDD8 levels and a matching increase in UBC12 levels.[183]

Hydrazine derivatives have several biological potencies.[184–186] 2-Amino-6-fluorobenzothiazole **141** was allowed to react with hydrazine hydrate to give the hydrazine derivative **258**. Reacting compound **258** with aromatic aldehyde using microwave irradiation afforded compounds **259** (Scheme 44).

The antitumor potency of compounds **259** (Fig. 28) against kidney fibroblast cancer (COS-7) and cervical cancer (HeLa) cell lines was tested. Compound **259** revealed excellent potency against COS-7 cell line ($IC_{50}$ value = 4.31 μmol $L^{-1}$) as compared to doxorubicin ($IC_{50}$ value = 3.04 μmol $L^{-1}$).[187]

The preparation of the compound **264** was started from compound. Then compound **264** was reduced to reduced to the amino analog which was transformed in the compound **263**. Cyano compound **263** in the Pinner reaction was transformed into the amidino compound **264**. Similarily, compound **266** was synthesized from 6-cyano-2-aminobenzothiazole. Amidino compounds **265** were obtained as outlined in Schemes 45 & 46.

*N*-Methyl iodide salts of the substituted benzothiazole **267** were synthesized *via* quaternization of the corresponding benzothiazole followed by condensation (Scheme 47).

Amidino substituted styryl benzothiazoles **270** were furnished from the corresponding benzothiazole through the condensation with benzaldehyde and subsequent Pinner reaction (Scheme 48).

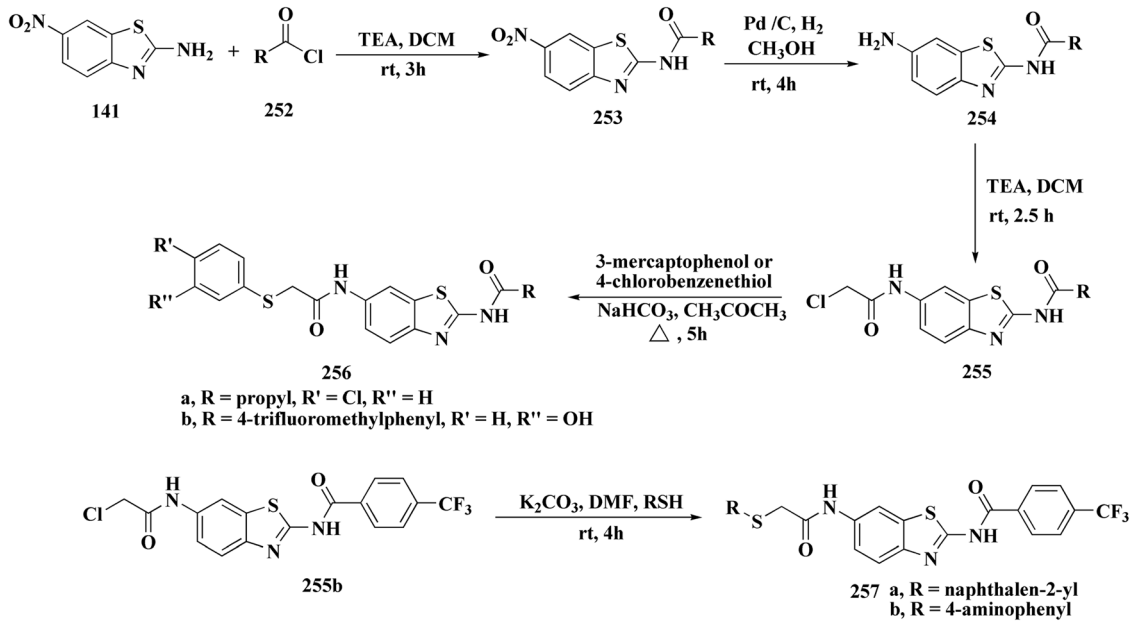


Scheme 43 Synthesis of heterocycle-based analogs of resveratrol.

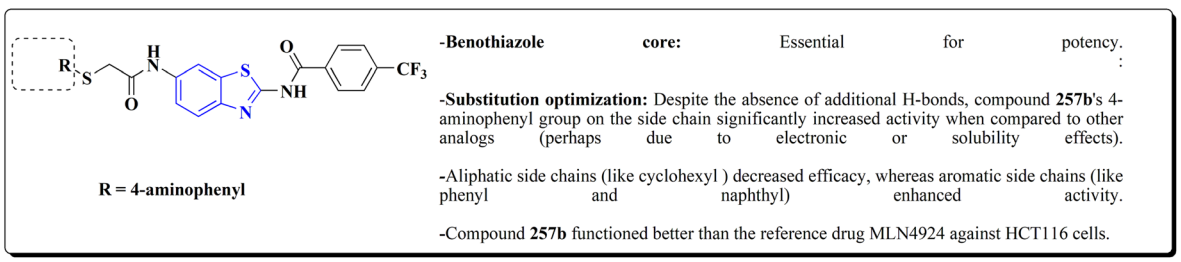


Fig. 27 Structure–activity relationship of compound 257.

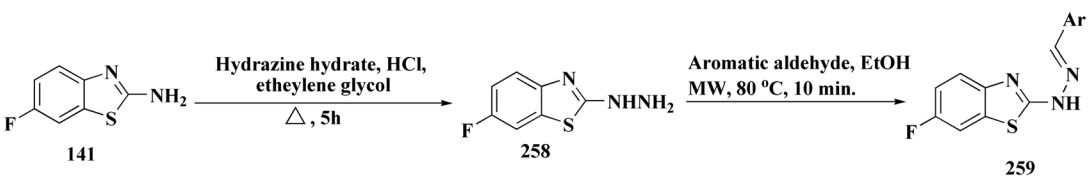


Scheme 44 Synthesis of substituted fluorobenzothiazole.

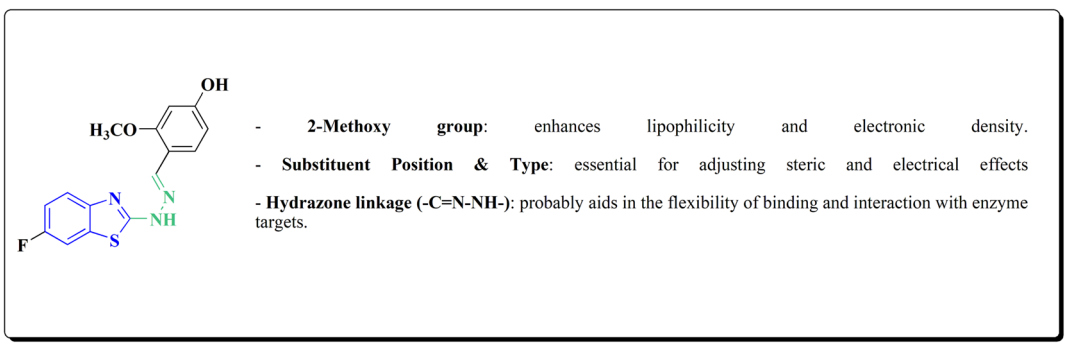


Fig. 28 Structure–activity relationship of compound 259.

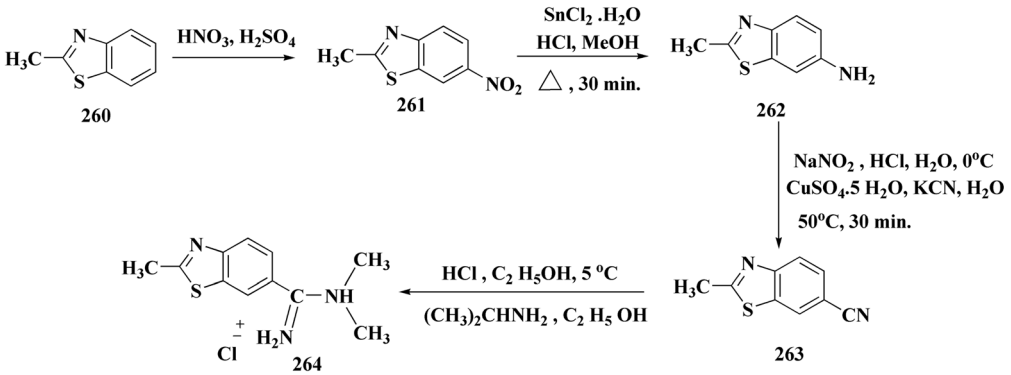


Scheme 45 Synthesis of substituted benzothiazole derivatives.

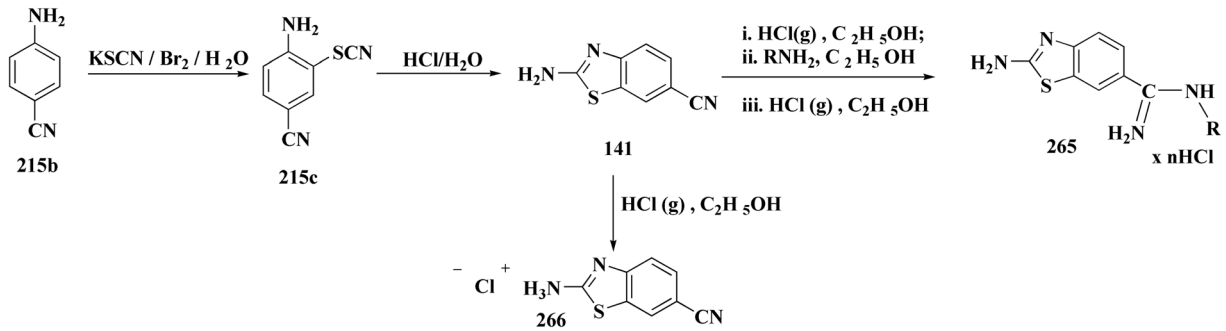


Scheme 46 Synthesis of substituted benzothiazole derivatives.

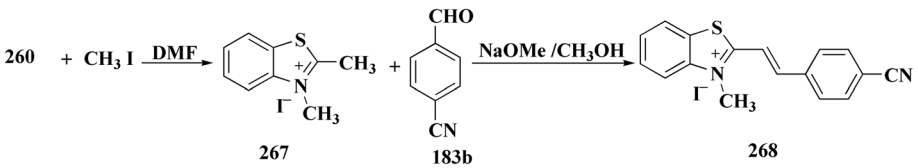


Scheme 47 Synthesis of *N*-methyl iodide salts of the substituted benzothiazole.

The compounds were examined on the cytostatic potencies against malignant cell lines. The best inhibitory effect was obtained with compounds **270** (Fig. 29). All of them inhibited the growth of the tested tumor cell lines and similarly normal fibroblasts. Other tested compounds displayed a moderate inhibitory activity, reliant on the type of the cells. Most of them inhibited the growth of WI38 and HeLa cells.[188]

The intermediate **271** could be converted into urea derivative **273**, directly be acylated or sulfonylated to access the amide **272** or sulfonamide **274**. Additionally, a reductive alkylation was carried out to afford secondary amine **275** (Scheme 49).

The screening of the compounds for their antitumor potency against 60 human cancer cell lines was performed. Compounds **273**, **275a** and **275b**, indicating high activity (Fig. 30). The compound **273** afford its average 50% growth inhibition ($GI_{50}$) at 0.38 μM.[189]

The synthesis of benzothiazole-based derivatives **279** is accomplished in Scheme 50. Compounds **277** were synthesized from phenylamine or benzylamine derivatives, and 2-chloroacetyl chloride. Compound **277** were reacted with 6-aminobenzothiazole-2-thiol to afford the amines **278.** Compounds **279** were furnished through the reaction of compound **278** with the corresponding acyl chloride.[190]

Sulfonamide moiety is considered as a key element in synthesizing a wide variety of significant heterocyles.[191–195] Benzothiazoles containing sulfonamides were reported as shown in Scheme 56. The synthesis of the benzothiazole-amine fragments **281** from the corresponding amino acid (or ester) and *o*-aminothiophenol using the polyphosphoric acid.[196] The arylsulfonamide analogues **282** were synthesized *via* coupling of the arylsulfonyl chloride with the BTA-amines. These sulfonamides were then allowed to react with bromoacetic acid *tert*-butyl ester to afford compounds **283a**; their *tert*-butyl deprotection generated the carboxylic analogues **283b**. Coupling the latter compounds with various amine-bearing derivatives. These reactions furnished the hydroxamic acids *O*-protected with 2,4-dimethoxybenzyl group (Dmb) **284**, the hydrazides protected with the arylsulfonylhydrazide or *tert*-

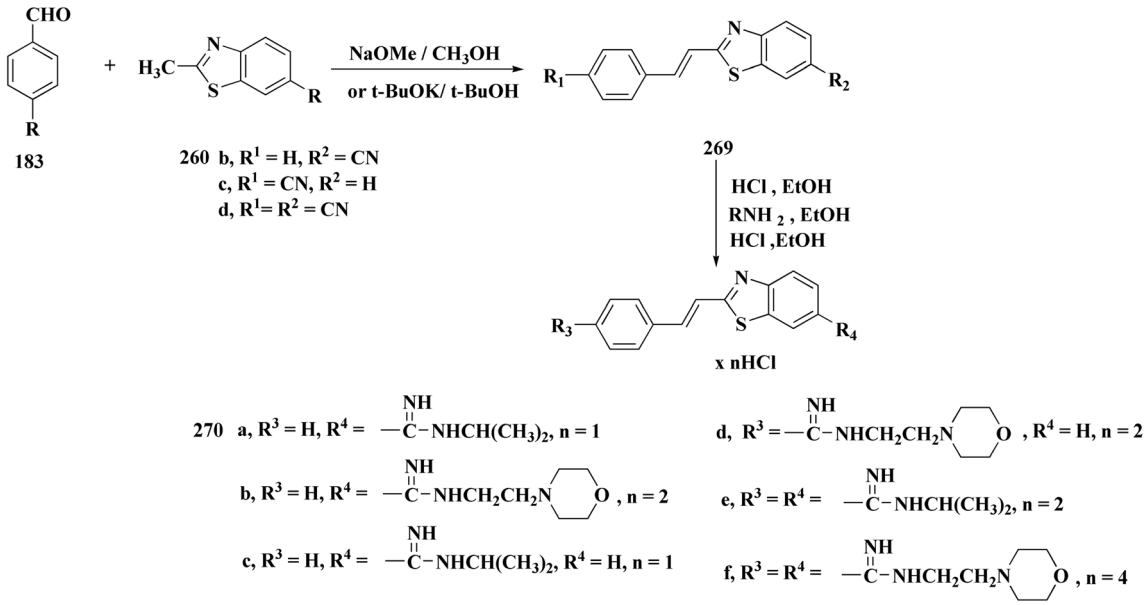


Scheme 48 Synthesis of amidino substituted styryl benzothiazoles.

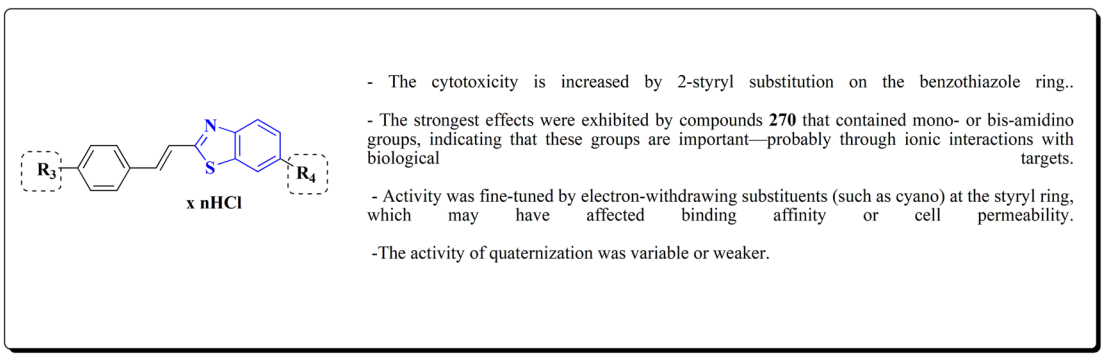


Fig. 29 Structure–activity relationship of compound 270.

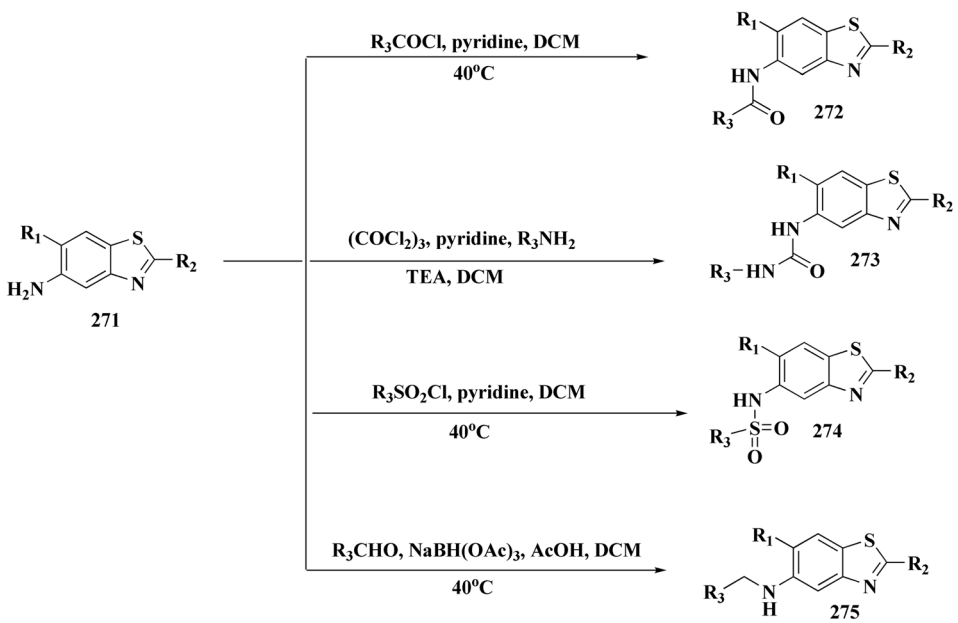


Scheme 49 Synthesis of 2-substituted benzothiazole derivatives.

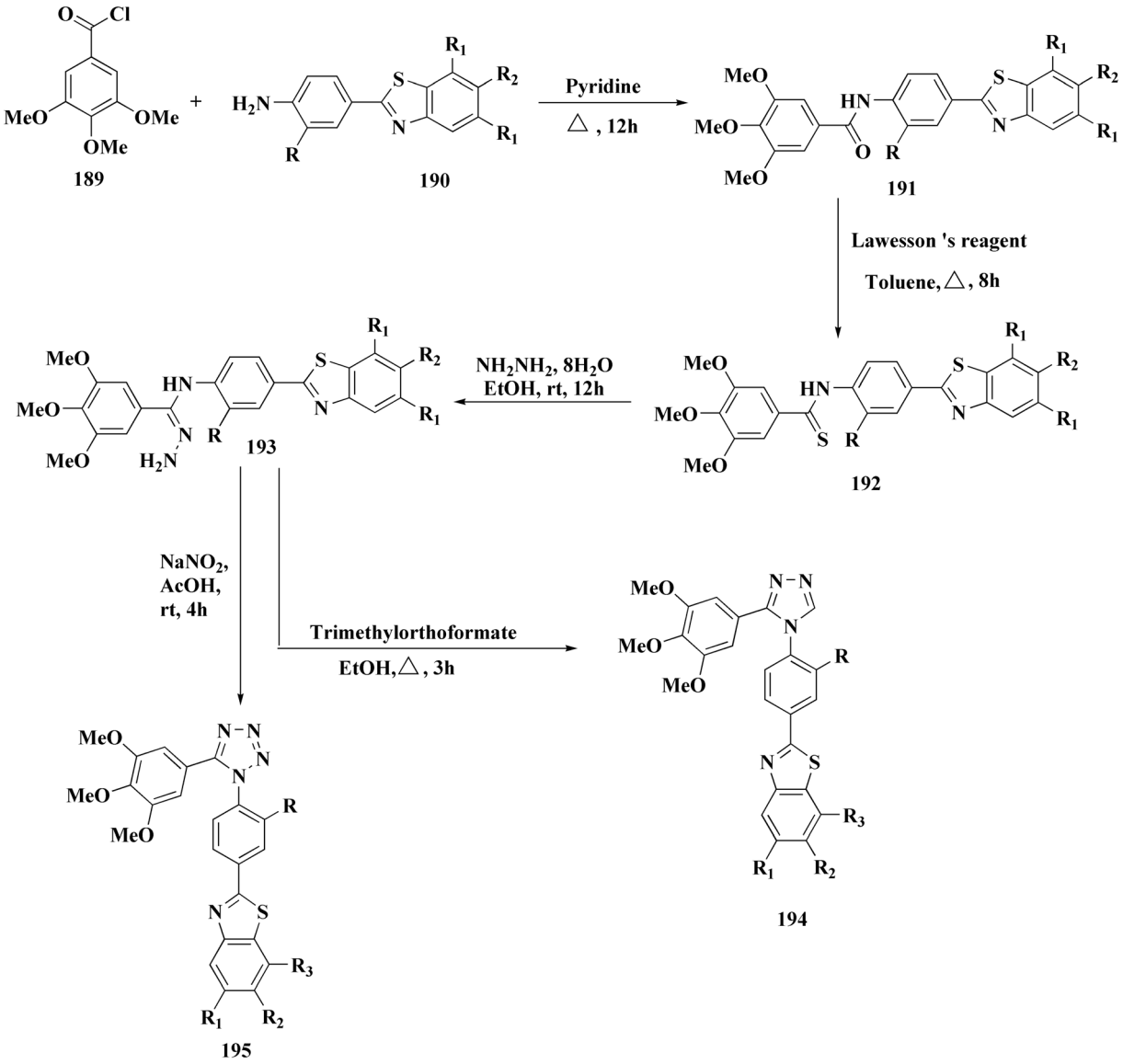


Fig. 30 Structure–activity relationship of compound 273 & 275.

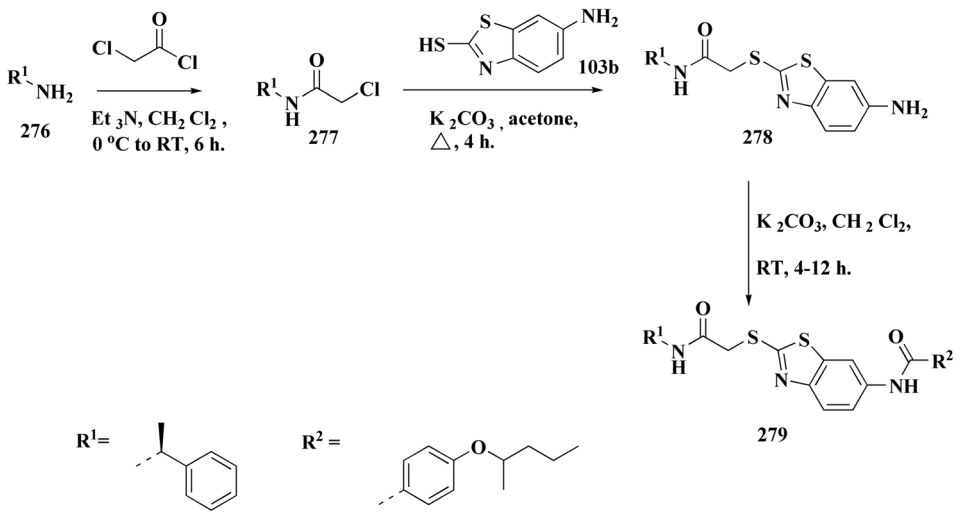


Scheme 50 Synthesis of substituted (benzo[*d*]thiazol-6-yl)benzamides.

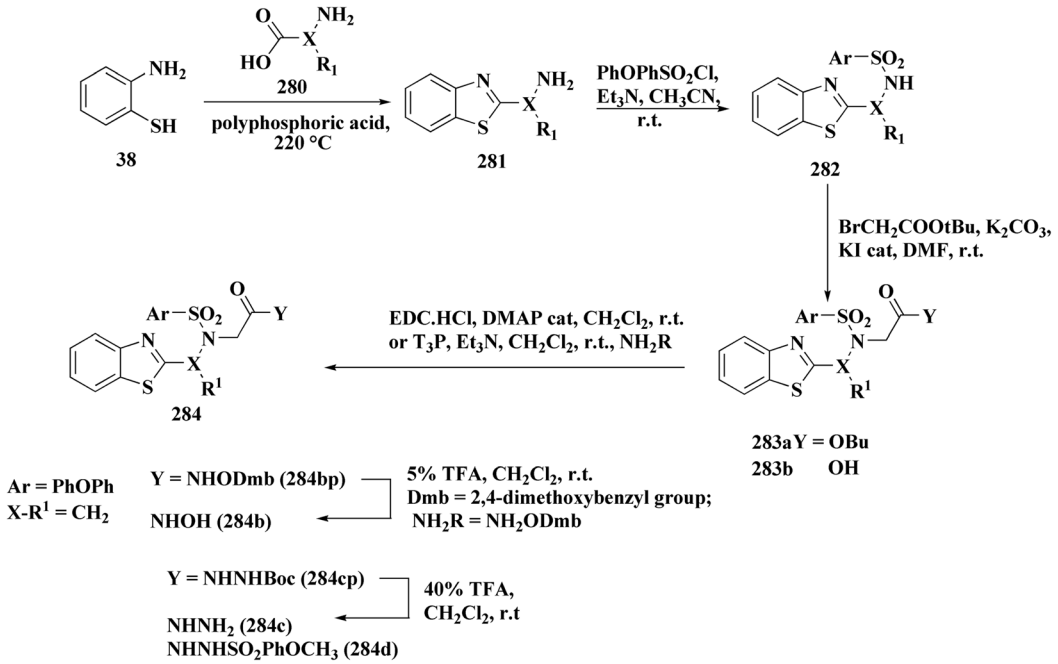


Scheme 51 Synthesis of benzothiazole carboxylic acid analogs.

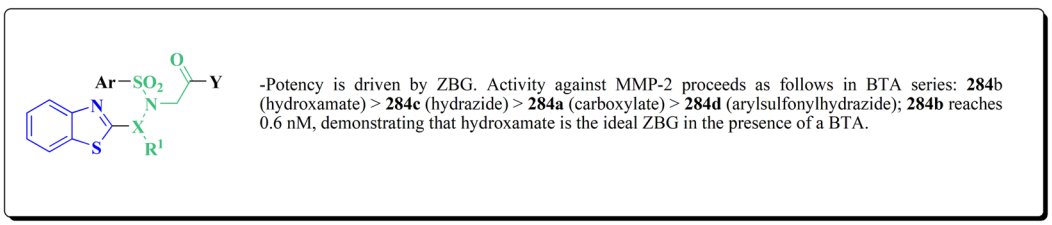


Fig. 31 Structure–activity relationship of compound 284.

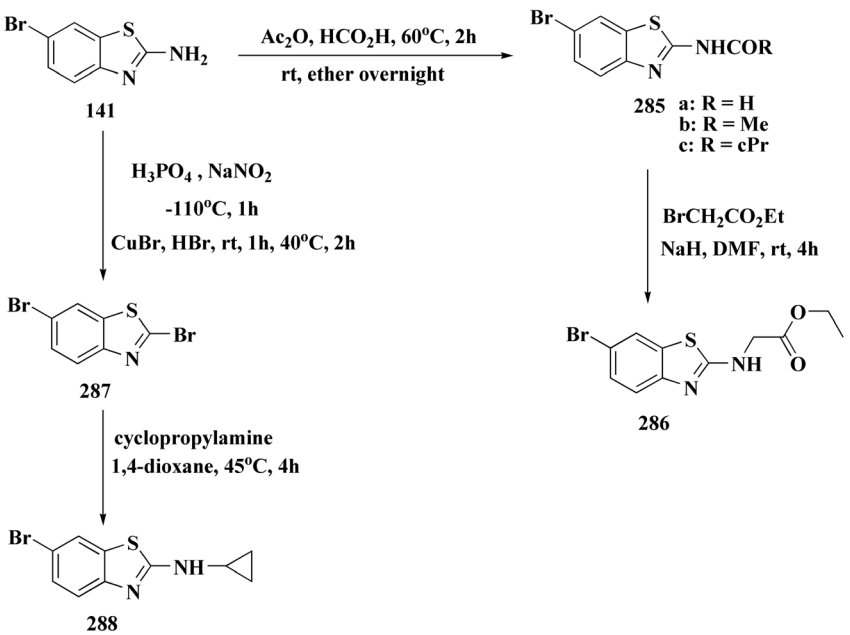


Scheme 52 Synthesis of substituted 2-amino-benzothiazole.

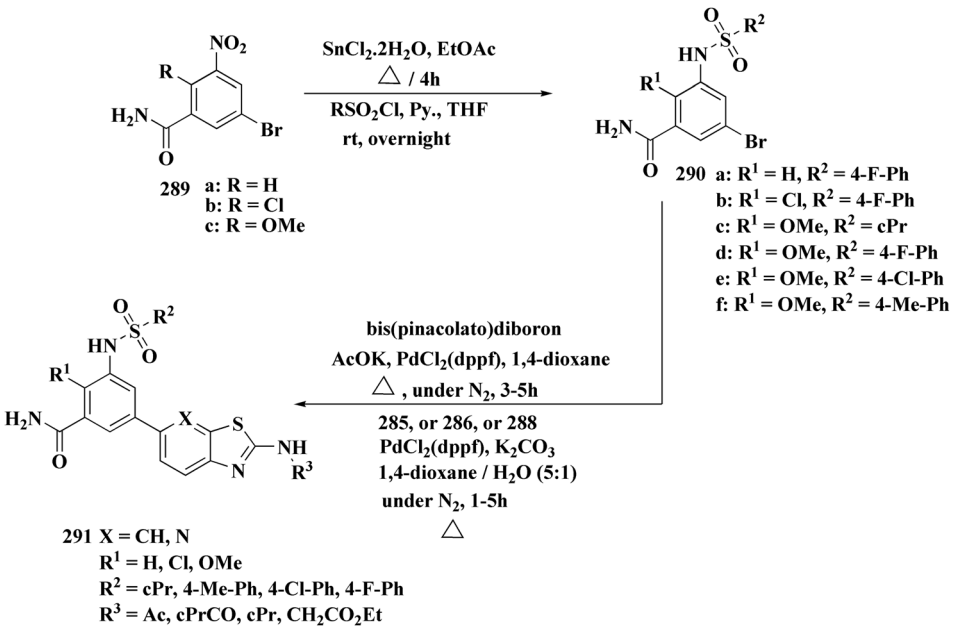


Scheme 53 Synthesis of substituted 2-amino-benzothiazole.

butyloxycarbonyl group (Boc). Deprotection of the latter afforded the hydroxamic acids or hydrazides (Scheme 51).[196]

The evidenced BTA-associated potency improvements on cell antiproliferactivity and enzyme inhibition in addition to the hydrolytic stability showed by the hydrazide group, propose that these novel bifunctional BTA-hydrazides could be utilized for developing novel categories of MMPIs with anticancer potency.[196]

Since the trend hydroxamate > carboxylate > hydrazide > arylhydrazide indicates that the zinc-binding group (ZBG) is the main factor determining efficacy, the strongest inhibitors are hydroxamate derivatives. Although it cannot completely make up for a lower ZBG, the addition of a benzothiazole (BTA) moiety enhances enzyme binding and antiproliferative activities, especially in non-hydroxamate scaffolds (Fig. 31). Strong MMP inhibition is supported throughout the series by the arylsulfonyl (4-phenoxyphenylsulfonyl) motif, which fits into the S1′ pocket and forms stabilizing H-bonds with Leu191 and Ala192.

The most efficient zinc-binding moiety in this series was the hydroxamate group; compound **284b** (Fig. 31), a benzothiazole–hydroxamate derivative, had significant antiproliferative action (A2780 $IC_{50} \approx 10.5$ μM) in addition to sub-nanomolar inhibition of MMP-2 ($IC_{50} = 0.6$ nM). Even though the parent hydroxamate, *N*-hydroxy-2-(4-phenoxyphenylsulfonamido) acetamide, was still marginally more effective (0.46 nM) because of an additional stabilizing H-bond with Pro423, the benzothiazole substituent improved binding by generating more hydrophobic and π–π interactions inside the active site. Overall, the SAR shows that arylsulfonyl anchor and hydroxamate ZBG are essential for potency, while benzothiazole scaffold enhances the biological profile even more.[196]

The synthetic pathway of generating compounds **291** is accomplished in Schemes 52 and 53. In the presence of triethylamine or DMAP, compound **141** was acylated to afford intermediates **285**. The reaction of the substituted benzothiazole **285** with ethyl 2-bromoacetate yielded compound **286** in the presence of hydridosodium. Conversion of **141** to **287** was

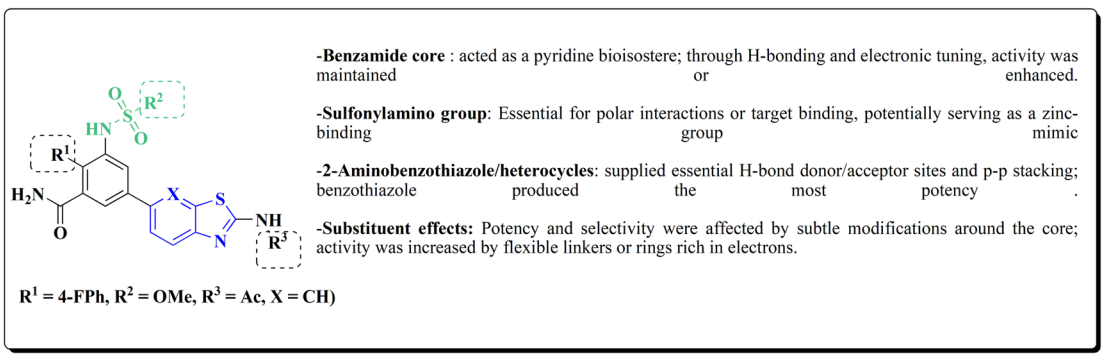


Fig. 32 Structure–activity relationship of compound **291**.

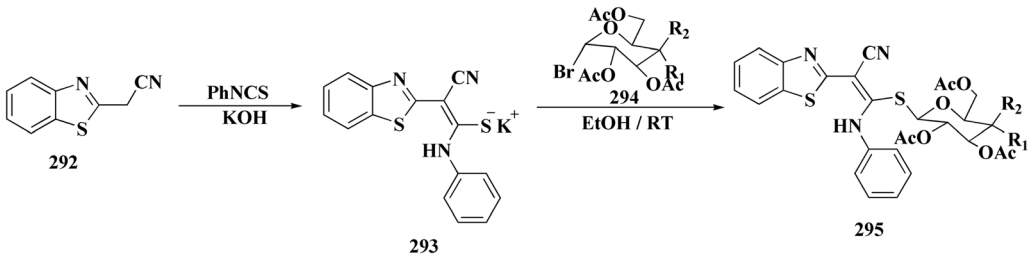


Scheme 54 Synthesis of the *S*-glucosides **295a** or *S*-galactosides **295b**.

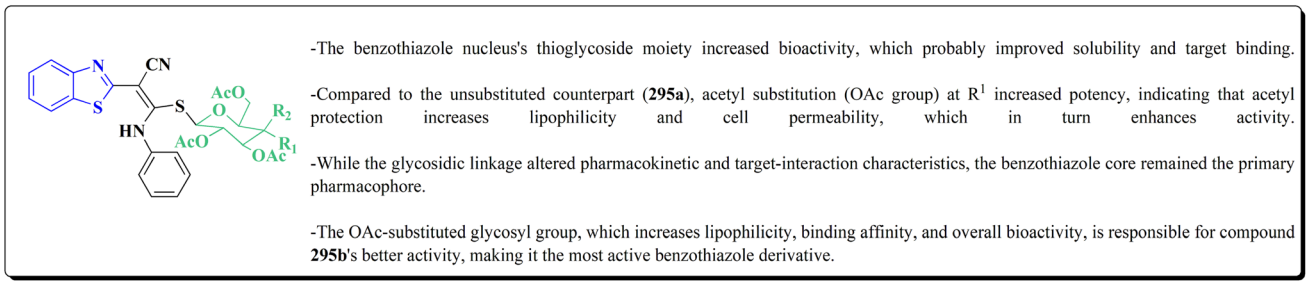


Fig. 33 Structure–activity relationship of compound **295**.

performed through diazo-reaction and bromo-substitution. Compound **287** was transformed to **288** *via* nucleophilic substitution of **287** with aminocyclopropane. The sulfonamide **290** were furnished from 5-bromobenzoic acid derivatives. Catalyzed using $PdCl_2$(dppf), intermediate **290** was allowed to react with pinacol diborane to give the arylboronic esters. Without isolating the arylboronic esters, the intermediate **285**, or **286**, or **288**, were added to the reaction mixture. The latter mixture was allowed to reflux to afford compounds **291.**

Their antiproliferative potencies were examined *in vitro via* MTT assay against human cancer cell lines comprising HCT-116, A549, U-87 MG & MCF-7. Compound **291** ($R^1$ = 4-FPh, $R^2$

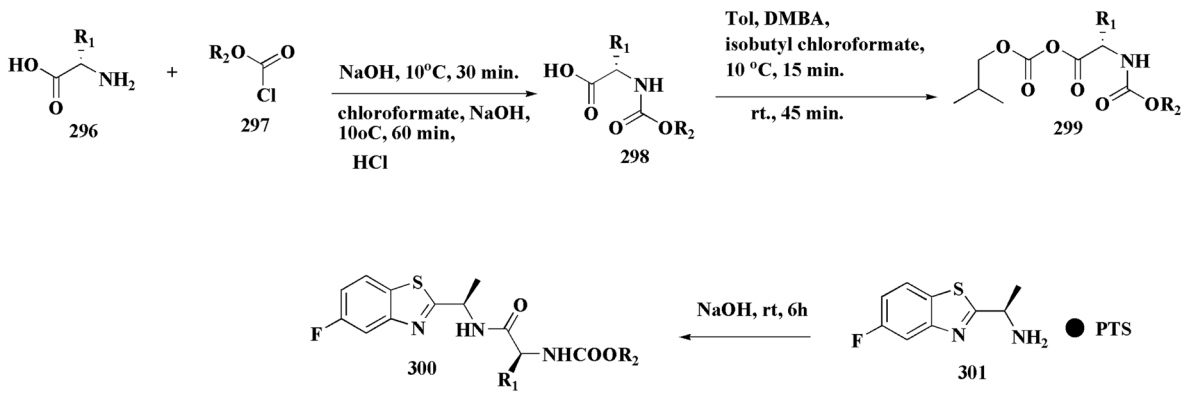


a $R^1$ = (S)-$(CH_2)_2CH_3$, $R^2$ = –$CH_3$
b $R^1$ =(S)-$(CH_2)_2CH_3$, $R^2$ = –$C_2H_5$
c $R^1$ =(S)-$(CH_2)_2CH_3$, $R^2$ = –$(CH_2)_2CH_3$
d $R^1$ = (S)-$(CH_2)_2CH_3$ , $R^2$ =–$CH(CH_3)_2$
e $R^1$ =(S)-$(CH_2)_2CH_3$ , $R^2$ =–$(CH_2)_3CH_3$
f $R^1$ =(S)-$(CH_2)_2CH_3$, $R^2$ = –$CH_2$ $CH(CH_3)_2$
g $R^1$ =(S)-$(CH_2)_2CH_3$ , $R^2$ =–$CH_2$ $CH_2Cl$
h $R^1$ =(S)-$(CH_2)_2CH_3$, $R^2$ = –$CH_2$ $CCl_3$
i $R^1$ =(S)-$(CH_2)_2CH_3$ , $R^2$ =–$CH_2$ $CF_3$
j $R^1$ =(S)-$(CH_2)_2CH_3$ , $R^2$ =–$CH_2$ $CF_2$ $CHF_2$
k $R^1$ =(S)-$(CH_2)_2CH_3$ , $R^2$ =–$CH_2$ $CF_2$ $CF_2CF$
l $R^1$ =(S)-$CH(CH_3)_2$, $R^2$ = –$CH_3$

m $R^1$ = (S)-$CH(CH_3)_2$ , $R^2$ =–$C_2H_5$
n $R^1$ =(S)-$CH(CH_3)_2$, $R^2$ = –$(CH_2)_2CH$
o $R^1$ =(S)-$CH(CH_3)_2$ , $R^2$ =–$CH(CH_3)_2$
p $R^1$ =(S)-$CH(CH_3)_2$, $R^2$ = –$(CH_2)_3CH$
q $R^1$ =(S)-$CH(CH_3)_2$ , $R^2$ =–$CH_2$ $CH(CH_3)_2$
r $R^1$ =(S)-$CH(CH_3)_2$ , $R^2$ =–$CH_2$ $CH_2Cl$
s $R^1$ =(S)-$CH(CH_3)_2$ , $R^2$ =–$CH_2$ $CH_2Br$
t $R^1$ = (S)-$CH(CH_3)_2$ , $R^2$ =–$CH_2$ $CCl_3$
u $R^1$ =(S)-$CH(CH_3)_2$ , $R^2$ =–$CH_2$ $CF_3$
v $R^1$ =(S)-$CH(CH_3)_2$ , $R^2$ =–$CH_2$ $CF_2$ $CHF_2$
w $R^1$ = (S)-$CH(CH_3)_2$ , $R^2$ =–$CH_2$ $CF_2$ $CF_2CF$

Scheme 55 Synthesis of substituted fluorobenzothiazoles.

= OMe, $R^3$ = Ac, X = CH) (Fig. 32) with active anti-proliferative potency was tested for its effect on the AKT and *p*-AKT473.[197]

As dual PI3K/mTOR inhibitors, 2-substituted-3-sulfonylaminobenzamide is an effective bioisosteric substitute for pyridine. One promising lead is compound **291** ($R^1$ = 4-FPh, $R^2$ = OMe, $R^3$ = Ac, X = CH), which has strong cytotoxicity *in vitro*, effectiveness *in vivo*, and unambiguous mechanistic confirmation. Compound **291** targets the PI3K/AKT/mTOR pathway, which is often upregulated in cancer. Western blot analysis revealed: phosphorylated AKT at Ser473 was down-regulated, indicating that PI3K activation and downstream mTOR signaling should be blocked. This leads to decreased tumor cell growth, survival, and proliferation.[197]

The benzothiazole acetonitrile **292** was reacted with phenylisothiocyanate to afford the corresponding thiolate salts **293**. The latters was reacted with α-bromosugar **294** to yield the *S*-glucosides **295a** or *S*-galactosides **295b** (Scheme 54, Fig. 33).[198]

The cytotoxic activity of the compounds were assessed against MCF-7 cell lines (breast carcinoma cell lines) and demonstrated high to moderate anti-tumor activities. In addition, molecular modeling of these compounds showed that they have moderate selectivity through hydrogen bond interaction with the atypical nucleotide binding pocket in the amino terminus of HSP90 and high binding affinity through hydrophobic–hydrophobic interaction.

### 8.3. Benzothiazoles linked with amino acids

The synthesis of cholinesterase inhibitors based on fluorobenzothiazole is outlined in Scheme 55. The amino acid is reacted with chloroformate, and the obtained acid is then converted to a reactive derivate. This reactive intermediate reacts with the substituted ethanamine, which is released from its *p*-toluene sulphonate salt *in situ*. The targeted compound **300a–w** were generated by vacuum concentration or filtration of the organic phase. The carbamates were evaluated for their ability to inhibit BChE and AChE.[199]

By comparing the compounds to the reference drugs galanthamine and rivastigmine, their inhibitory action against acetylcholinesterase (AChE) and butyrylcholinesterase (BChE)

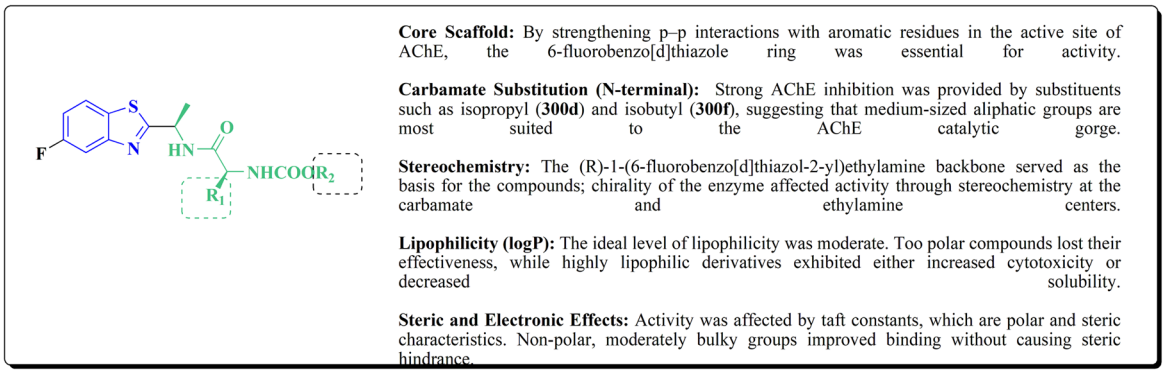


Fig. 34 Structure–activity relationship of compound 300.

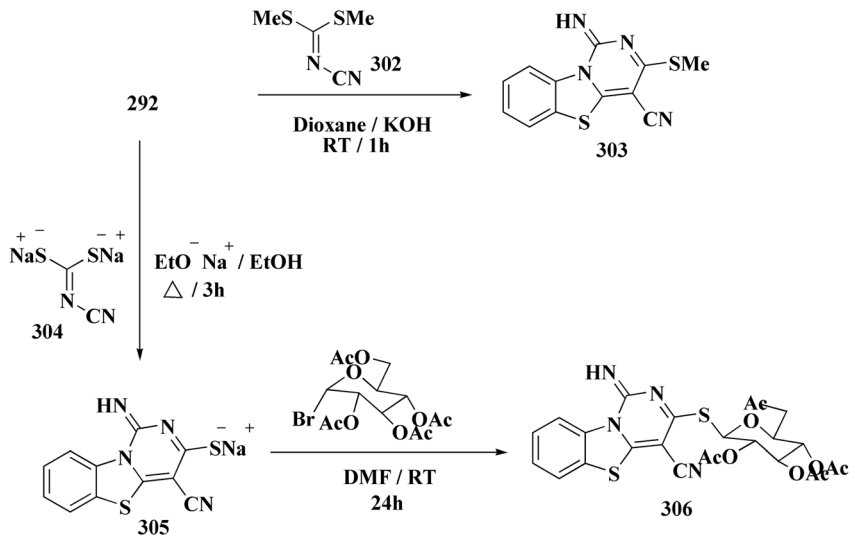


Scheme 56 Synthesis of pyrimidobenzothiazole derivatives.

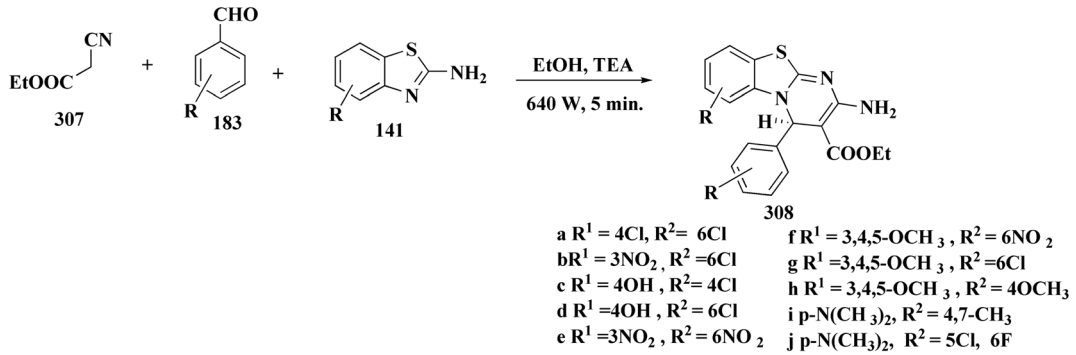


Scheme 57 Synthesis of substituted pyrimidobenzothiazole derivatives.

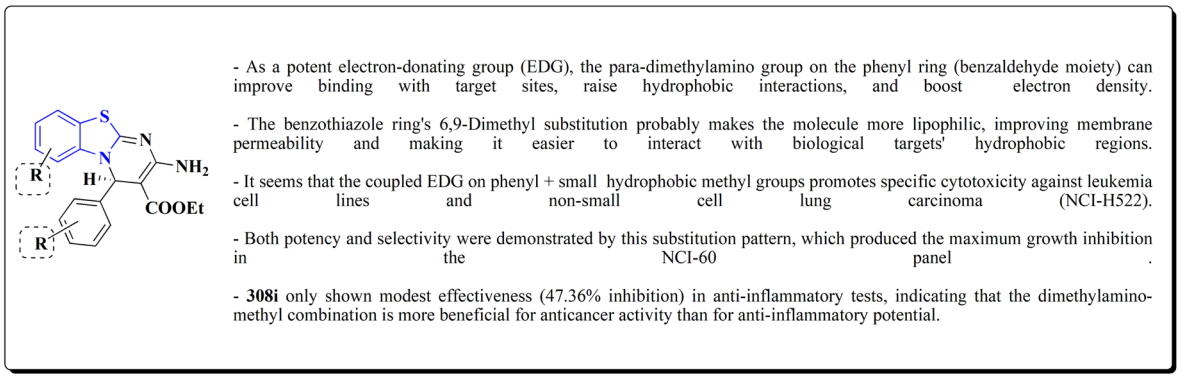


Fig. 35 Structure–activity relationship of compound **308**.

was assessed. Against AChE, two compounds, **300d** and **300f**, showed especially high potency (Fig. 34). Molecular docking studies of the most active compounds showed good π–π stacking with critical aromatic residues and appropriate orientation inside the catalytic region of AChE. Additionally, selected compounds showed acceptable cytotoxicity profiles in HepG2 and MCF-7 cell lines, indicating that they may be developed further in preclinical research.[199]

### 8.4. Benzothiazoles fused with heterocyclic compounds

**8.4.1. Benzothiazoles fused with six-membered ring heterocycles.** The pyrimidobenzothiazole derivative **303** was synthesized through reacting 2-cyanomethylbenzo[1,2-*b*]thiazole **292** with *S*,*S*-dimethyl *N*-cyanodithioimidocarbonate **302** (ref. 200) which is considered as a reactive reagent that we have recently used to synthesize various heterocycles.[201–205] Sodium cyanocarbonimidodithioate salt **304** was reacted with compound **292** in the presence of sodium ethoxide to afford compound **305**, and further reaction of **305** with α-bromosugar afforded compound **306** (Scheme 56).[200]

Substituted pyrimidobenzothiazole derivative was synthesized *via* condensation of substituted benzothiazole, substituted benzaldehyde and ethyl cyanoacetate *via* microwave multi-component reaction (Scheme 57).

Compounds examined for *in vitro* against various human tumor cell lines, and for the *in vitro* anti-inflammatory activity. Compound **308i** was found to have good antiproliferative activity and compound **308g** was found to have high anti-inflammatory potency and compounds **308a**, **308b**, **308h** also found to be effective anti-inflammatory potency.[206]

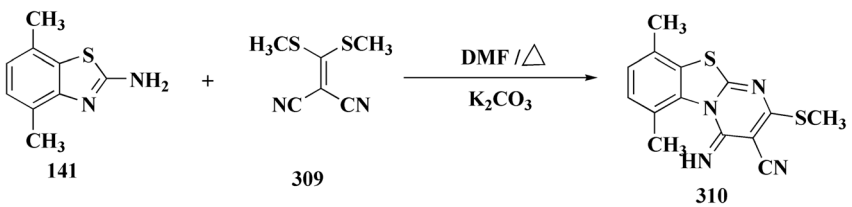


Scheme 58 Synthesis of substituted pyrimido[2,1-*b*][1,3] benzothiazole.

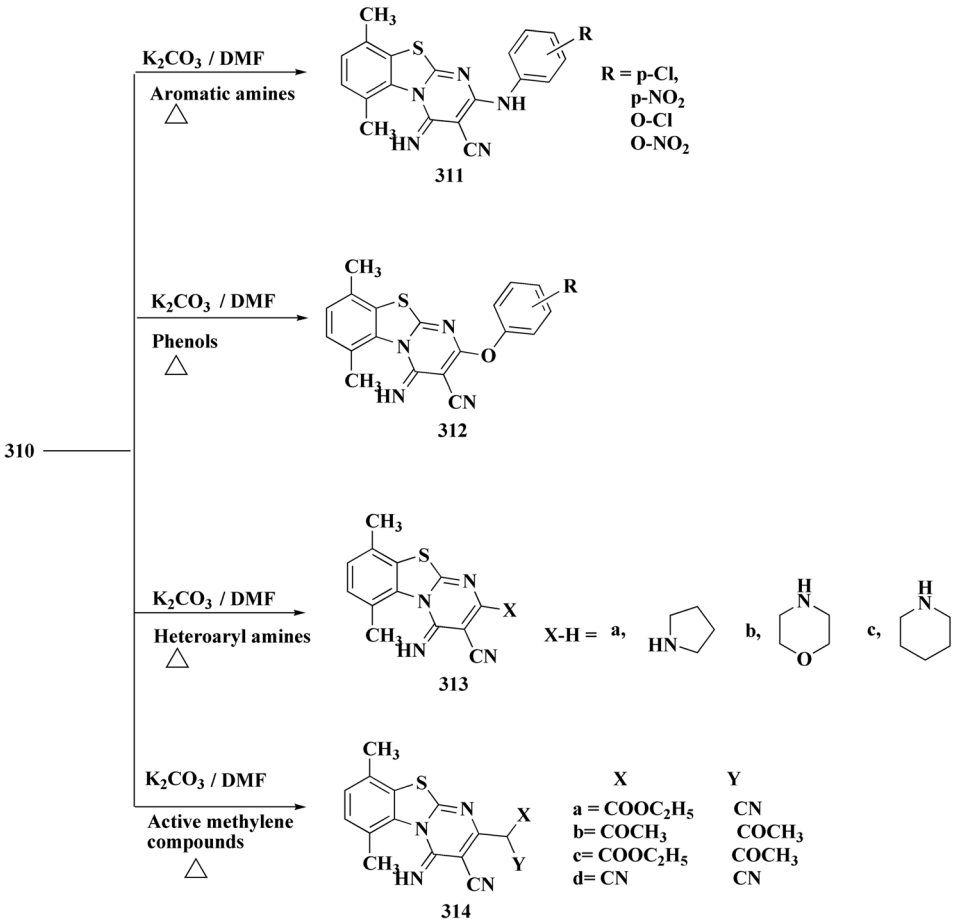


Scheme 59 Synthesis of ssynthesis of substituted pyrimido[2,1-*b*][1,3]benzothiazole.

-Compound **310**: Two methyl groups (6,9-positions) and an electron-donating $SCH_3$ group at the 2-position are responsible for the compound's high activity against lung, kidney, and breast cancer lines.

-Strong inhibition against HOP-92 (lung) and UACC-62 (melanoma) is demonstrated by **311a** (p-$CH_3$anilino derivative), suggesting that p-methyl substitution on anilino improves activity by increasing lipophilicity and membrane penetration.

- p-methoxy, an electron-donating group that improves contact with the target, gives **311d** (p-$OCH_3$ anilino derivative) strong activity against lung and melanoma lines, comparable to that of **311a**.

-**312a** (p-Cl phenoxy derivative): Excellent efficacy against K-562, RPMI-8226 (leukemia), HOP-92 (lung), and UO-31 (renal); indicates that cytotoxicity and binding affinity are enhanced by electron-withdrawing halogen (Cl) at para-position on the phenoxy ring.

-Good inhibition against breast cancer (MCF-7) and renal tumors (CAKI-1, UO-31) is demonstrated by **313a** (pyrrolidino derivative), suggesting that heterocyclic amines at the 2-position enhance hydrophilicity and potential H-bond interactions with biological targets.

- **313b** (morpholino derivative): Strong against prostate cancer (PC-3), kidney cancer, and leukemia (K-562); the oxygen in morpholine's heterocycle may improve polarity and target specificity.

Fig. 36 Structure–activity relationship of compounds **310–313**.

The synergistic action of electron-donating *para*-dimethylamino substitution on benzaldehyde and lipophilic methyl groups on the benzothiazole ring, which enhance potency and selectivity against NCI-H522 and leukemia cell lines, is responsible for **308i**'s strong anticancer activity (Fig. 35).

Along similar lines, the compound **310** has been synthesized by utilizing 2-amino 4,7-dimethyl benzothiazole **141** and by using bis-methylthio methylene malononitrile **309**[207] as reactive reagents. Its worthy to note that ketene dithioacetals have a cruial role in synthesizing a wide varity of bioactive heterocycles.[208–210] Compound **310** synthesized from 2-amino

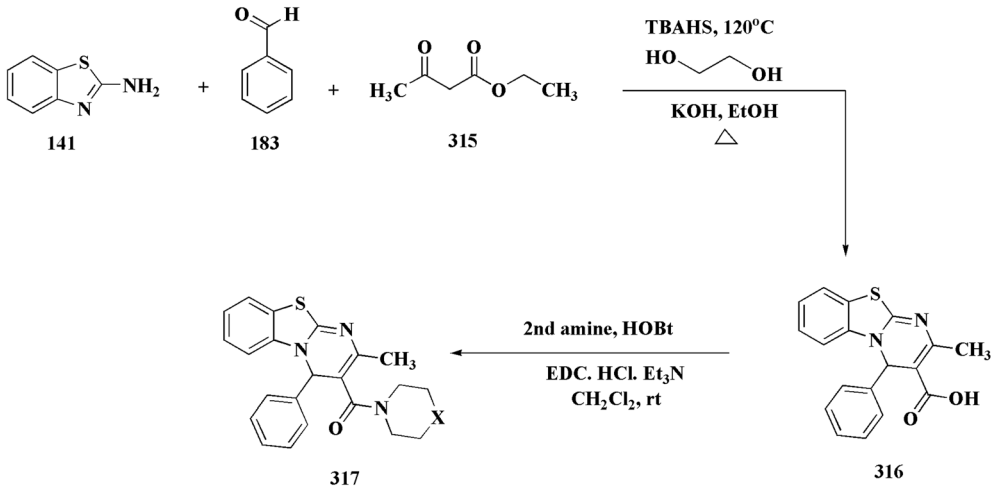


Scheme 60 Synthesis of benzo[4,5]thiazolo[1,2-*a*]pyrimidines.

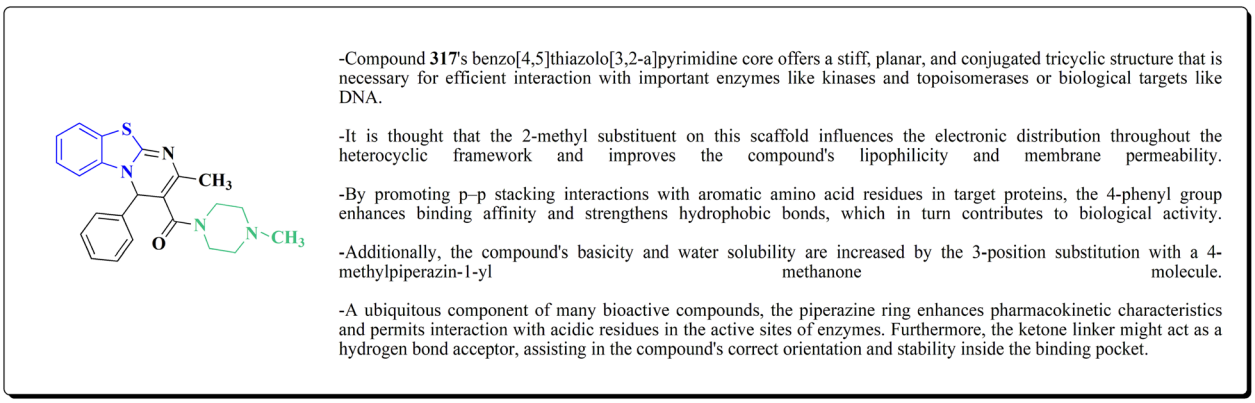


Fig. 37 Structure–activity relationship of compound 317.

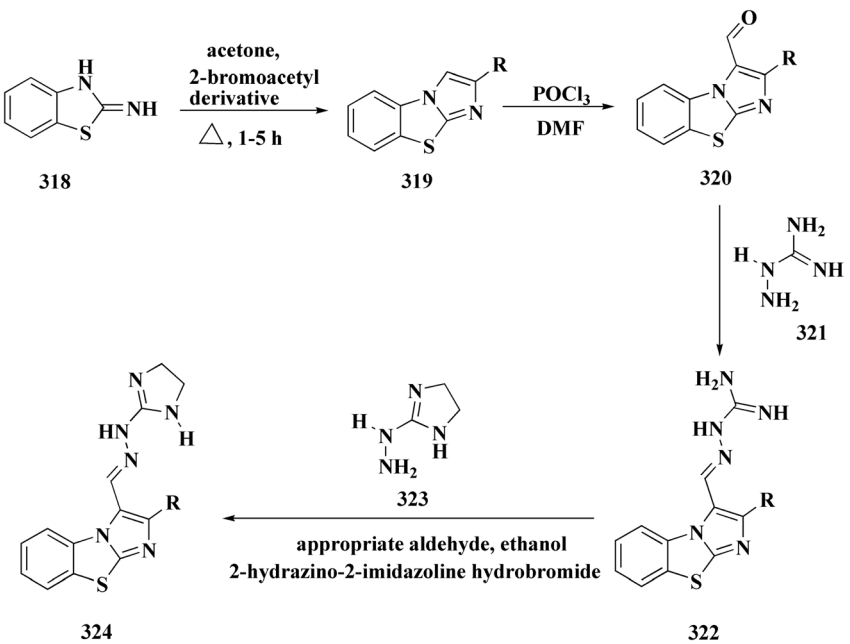


Scheme 61 Synthesis of imidazo[2,1-*b*]thiazole guanylhydrazones.

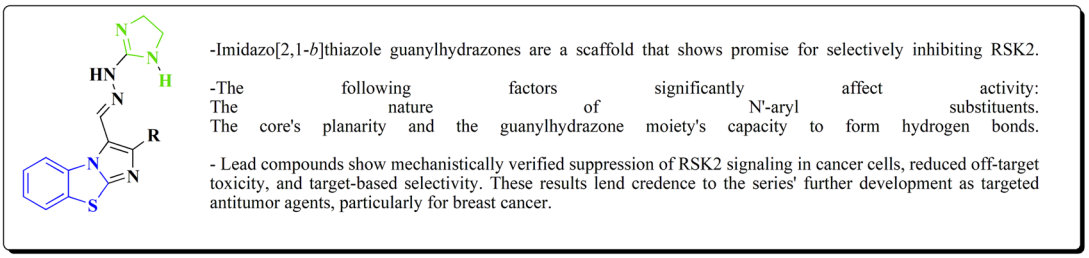


Fig. 38 Structure–activity relationship of compound **324**.

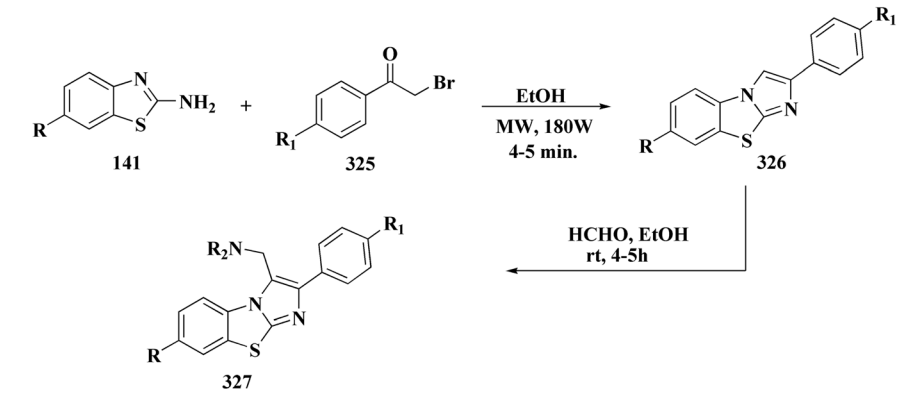


Scheme 62 Synthesis of substituted imidazobenzothiazoles.

4,7-dimethyl benzothiazole **141** was reacted with bis-methylthio methylene malononitrile **309**. The substituted derivatives **311–314** were furnished starting from compound **310** (Schemes 58 & 59).

Compound **310** and its selected derivatives **311–314** were screened for their *in vitro* anticancer potency. Compounds **310**, **311-a**, **311-d**, **312-a**, **313-a**, **314-b** displayed maximum *in vitro* anticancer activity against various cancers lines (Fig. 36).[207]

In continuation, the benzo[4,5]thiazolo[1,2-*a*]pyrimidine-3-carboxylate have been prepared as potent anti-cancer compounds. These compounds were synthesized from benzenecarboxaldehyde, 2-aminobenzothiazole and ethyl 3-oxobutanoate to afford compound **316** followed by the formation of amide through the reaction with different sec. amines (Scheme 60).

The cytotoxicity of these compounds was tested on a panel of human cancer cell lines *in vitro*. Compound **317b** indicated promising cytotoxicity particularly against human breast adenocarcinoma cell lines, MDA-MB-231 & MCF-7, while compound **317a** revealed promising cytotoxicity against MDA-MB-231 (Fig. 37).[211]

**8.4.2. Benzothiazoles fused with five-membered ring heterocycles.** The hydrazones **322a,b**, **324a** were synthesized by reaction between aminoguanidine or 2-hydrazino-2-imidazoline and an aldehyde. The aldehydes **320a,b** were yielded by Vilsmeier reaction on compounds **319a,b** synthesized from the bromoketones and the 2-amino-derivative (Scheme 61).

A determination is established regarding the imidazo[2,1-*b*] thiazole guanylhydrazones' potency to inhibit p90 ribosomal S6 kinase 2 (RSK2). It was found that subset of compounds shows

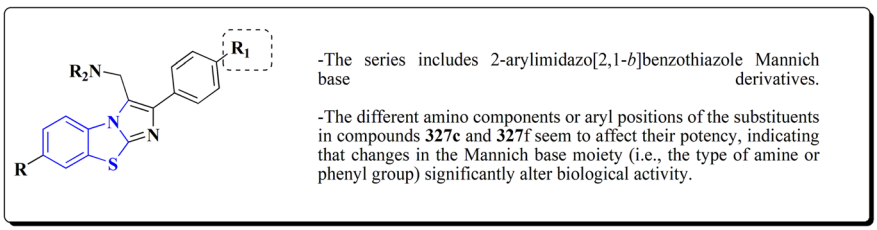


Fig. 39 Structure–activity relationship of compound **327**.

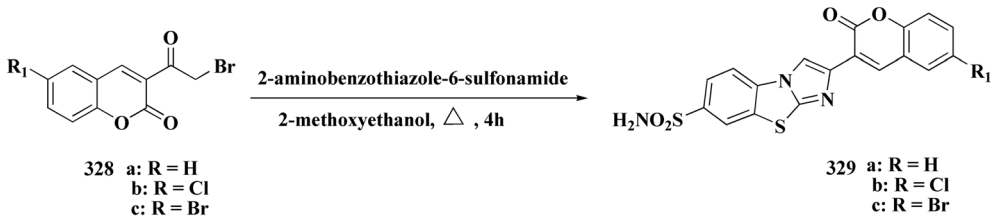


Scheme 63 Synthesis of benothiaole–coumarin conjugates.

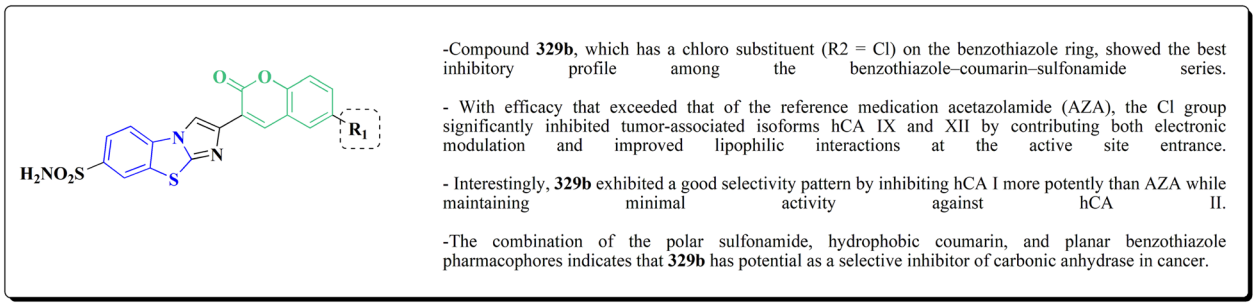


Fig. 40 Structure–activity relationship of compound 329.

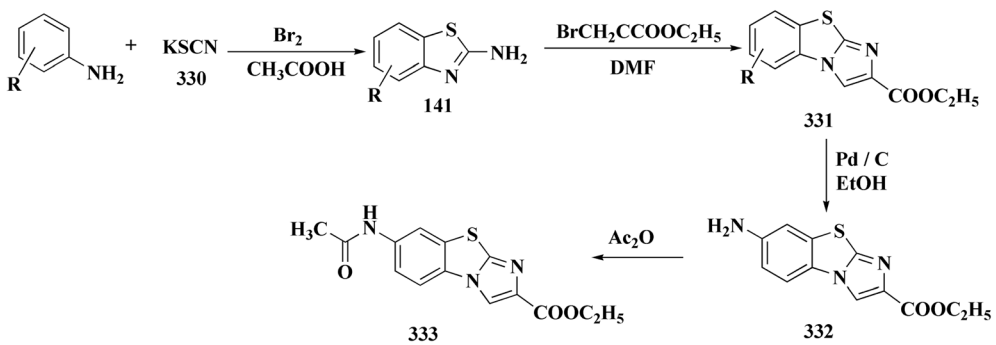


Scheme 64 Synthesis of imidazobenzothiazoles.

both efficient *invitro* inhibition of tumor cell growth and RSK2 kinase activity. The compounds can affect the RSK2 target in cells (Fig. 38).[212]

Substituted imidazobenzothiazole **327a–e** were synthesized through the reaction of compound **141** with 2-bromo-acetophenone **325** under microwave irradiations. Alkylation of compounds **326a–e** through reacting with formic aldehyde and cyclic secondary amines afforded compounds **327a–h** (Scheme 62).

The compounds were estimated for their anticancer potency. These compounds indicated better cytotoxic activity in MCF-7, HepG2, and HeLa cell lines. Additional mechanism aspects

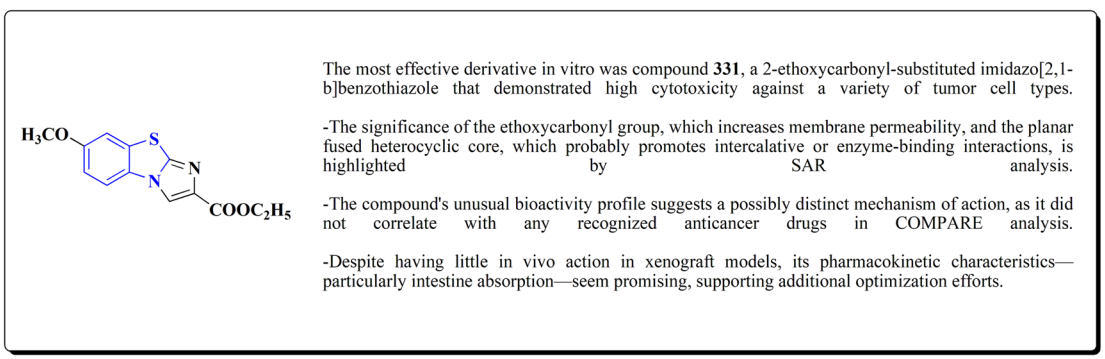


Fig. 41 Structure–activity relationship of compound 331.

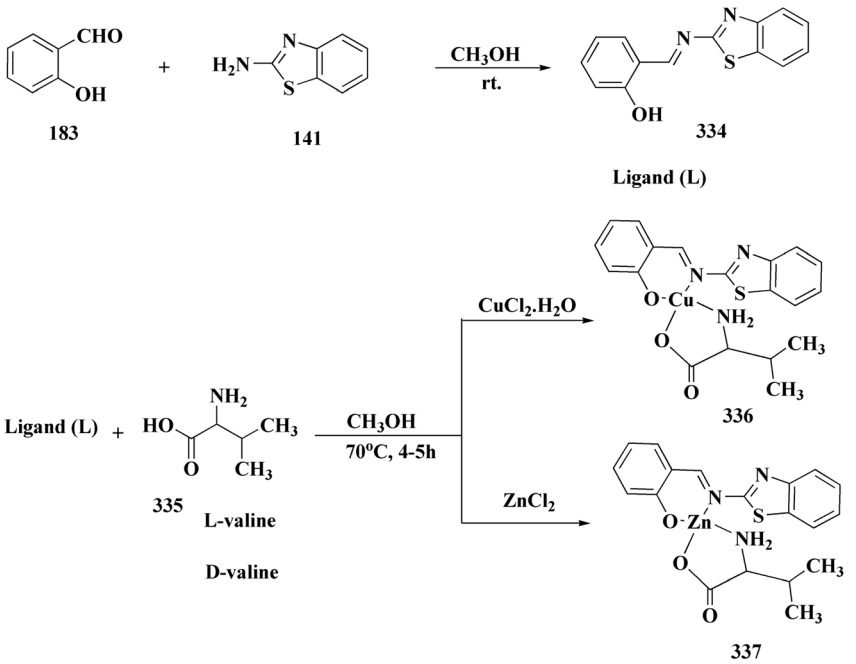


Scheme 65 Synthesis of benzothiazole–valine complexes.

accountable for the anticancer activity of compounds **327c** & **327f** in HepG2 cell line were reported.[213]

Both **327c** and **327f** in the HepG2 cell line cause cell cycle arrest at the $G_2$/M phase, which is accompanied by an upregulation of Chk2 and a downregulation of cyclin B, suggesting that the cell cycle is being interfered with. They cause apoptosis, which is the execution of programmed cell death, as shown by increased Caspase-3 levels.

In addition, those compounds inhibit important signaling proteins linked to proliferation, including p38 MAPK, *p*-JNK, C-Jun, JunB (AP-1 factors), and PKC$\alpha$, which inhibits growth and survival pathways. These findings emphasize **327f** as a potent lead candidate for additional anti-cancer research (Fig. 39).[213]

Heterocyclic series **329** consisting of three IBTs were prepared through the formation of 2-amino-benzothiazole-6-sulfonic acid amide from sulfanilamide and the subsequent reaction with 6-substituted-3-bromoacetylcoumarins (Scheme 63).

The inhibition potential of the compounds against the isoforms Hca I, II, IX & XII as selected human carbonic anhydrases was evaluated (Fig. 40). Results were compared with acetazolamide.[214]

Concurrently, the synthesis of the imidazobenzothiazoles **331** is outlined in Scheme 64. The 2-aminobenzothiazole was refluxed with ethyl bromopyruvate to afford hydrobromide as an intermediate which was subsequently cyclized to the targeted compounds. The thiocyanation reaction of 3,4-dichloroaniline allowed the synthesis of 5,6- and 6,7-dichloro-2-aminobenzothiazole. The amine **332** was acheived *via* catalytic hydrogenation of the nitrobenzothiazole. Treatment of **332** with acetic anhydride afforded the amide **333**.

The imidazobenzothiazole compounds **331** were synthesized and their cytotoxic activity estimated for testing against tumor cell lines (Fig. 41). The most potent imidazobenzothiazole derivative was subsequently estimated as a cytotoxic agent using the hollow fiber assay.[215]

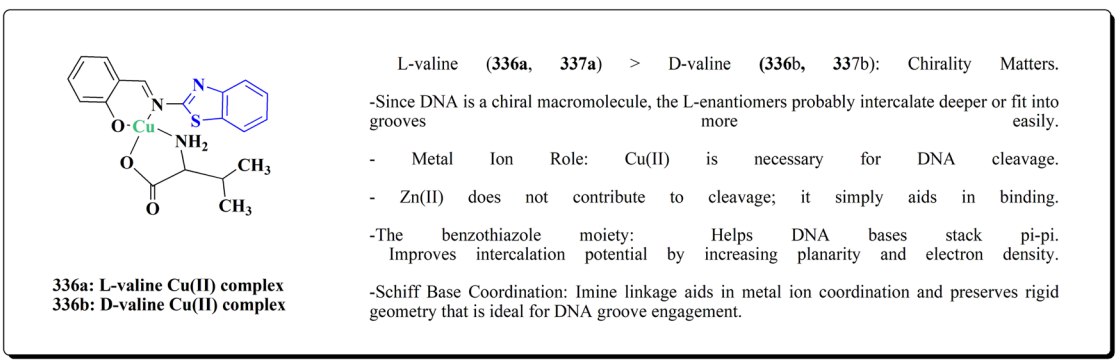


Fig. 42 Structure–activity relationship of compound **336**.

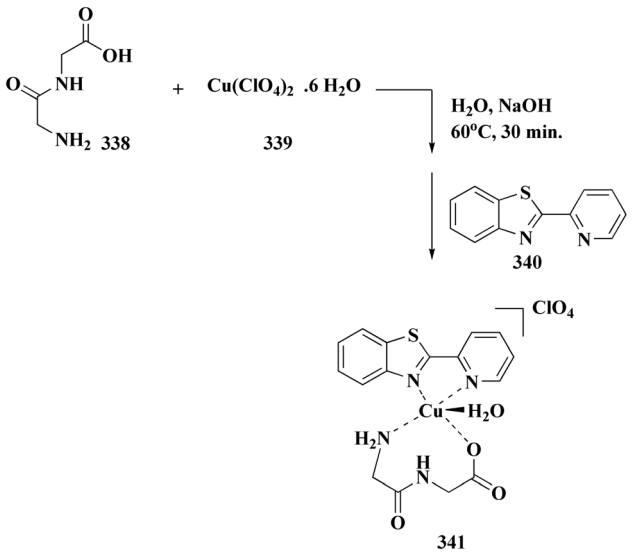


Scheme 66 Synthesis of Cu(II) complex **341**.

### 8.5. Benzothiazole complexes

The synthesis of chiral antitumor chemotherapeutic agents of the benzothiazole Schiff base–valine complexes **336a** & **b** and **337a** & **b** were performed through reacting the stoichiometric amounts of the Schiff base ligand (L), Cu(II)/Zn(II) chloride & L-/D-valine (Scheme 65).[216]

Towards DNA, the most effective and selective is **336a** (Cu–L-valine complex). L-Forms are preferable, and chirality at the valine residue has a significant impact on biological behavior. Regarding DNA binding and cleavage efficacy, the SAR trend is **336a** > **336b** > **337a** > **337b** (Fig. 42). These findings encourage the development of chiral benzothiazole–metal complexes as DNA-targeted antitumor drugs, with a focus on metal redox characteristics and stereochemistry.[216]

In continuation, the Cu(II) complex was synthesized as outlined in Scheme 66 through the reaction of diglycine with copper(II) perchlorate with pbt as a secondary ligand. The complex was exposed to cytotoxicity tests *in vitro* utilizing human cancer cells lines and indicated prominent and selective cytotoxicity against HepG2 cell lines with $IC_{50}$ value 17.78 μm.[217]

Interaction of Human Serum Albumin (HSA) parameters is reported; UV-vis shifts and fluorescence quenching demonstrate the complex's strong noncovalent bond with HSA. In biological systems, this interaction might have an impact on bioavailability and transport. The complex's quantifiable cytotoxicity is attributed to its capacity for DNA binding and cleavage (Fig. 43).[217]

## 9. Synthetic strategies for novel antimicrobial benzothiazoles

### 9.1. Benzothiazoles linked with heterocyclic compounds

**9.1.1. Pyrimidine–benzothiazole based analogues.** The synthesis of compounds **344** in which a pyrimidine ring was linked to the benzothiazole moieties through an acrylonitrile bridge, was performed as outlined in Scheme 67. The synthesis of benzazole pyrimidine acrylonitriles **344** were reported. The condensation of 2-benzazole acrylonitriles **292** and pyrimidine aldehydes **343** yielded compounds **344**.

The antibacterial activity of the novel compounds was tested against bacterial strains. Compound **344** was found to display the high potency against both *Pseudomonas aeruginosa* and *Escherichia coli* as comparable to amoxicillin (Fig. 44).[218]

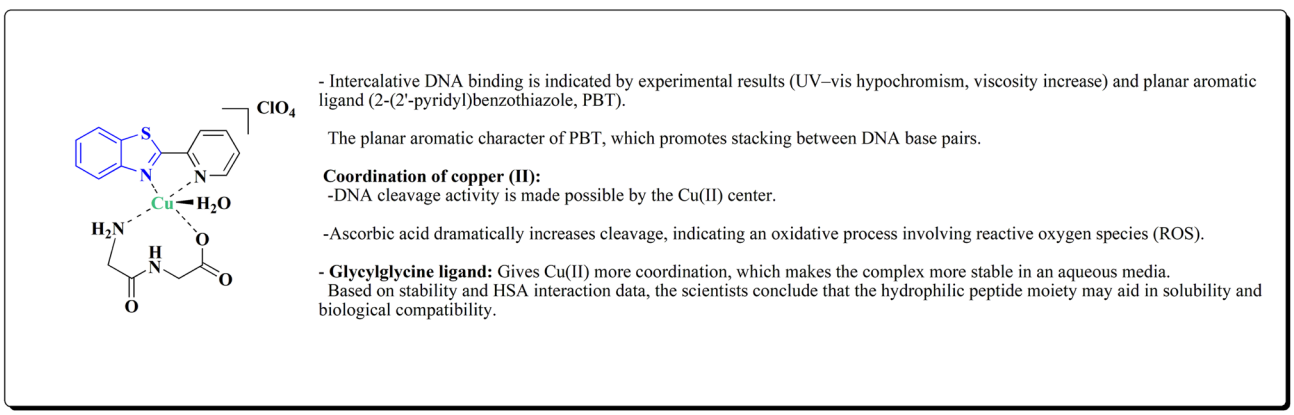


Fig. 43 Structure–activity relationship of compound **341**.

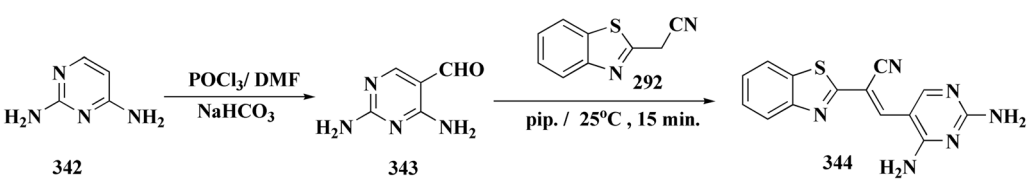


Scheme 67 Synthesis of pyrimidine–benzothiazole conjugates.

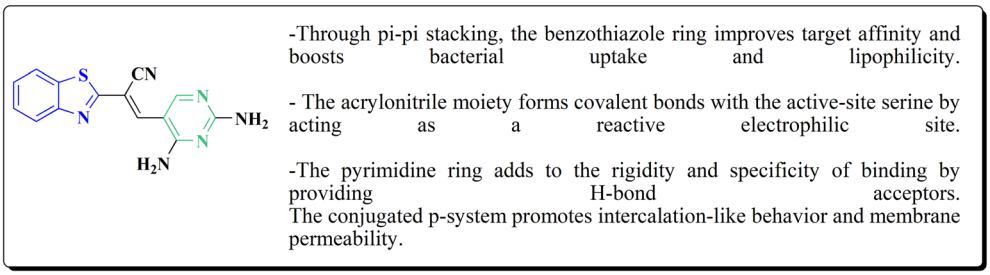


Fig. 44 Structure–activity relationship of compound **344**.

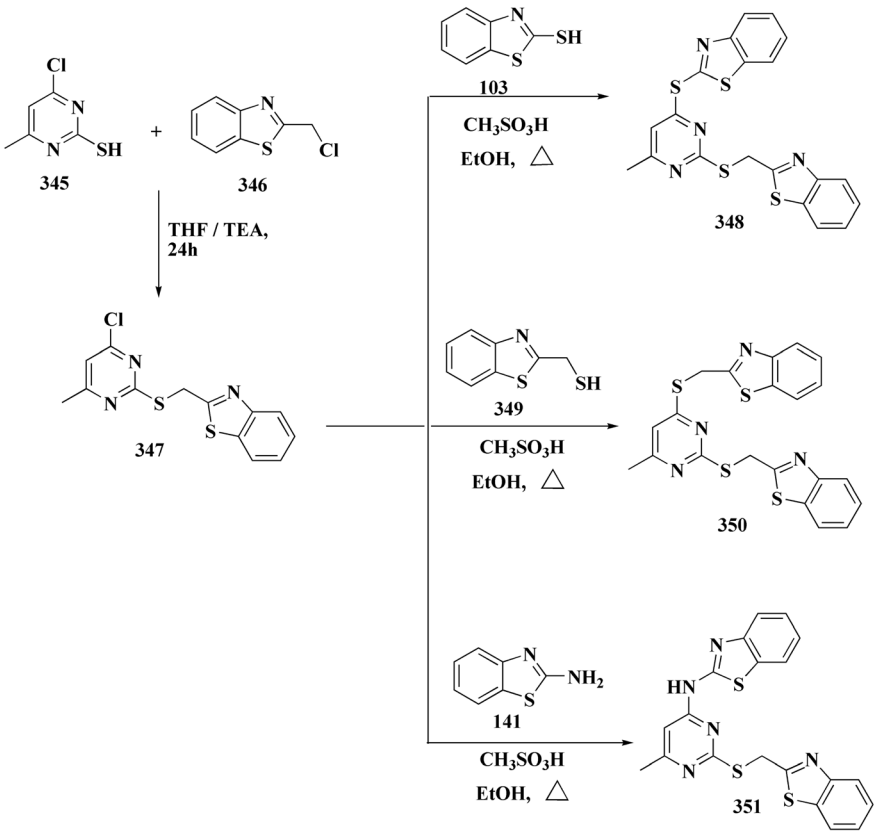


Scheme 68 Synthesis of pyrimidine–benzothiazole conjugates.

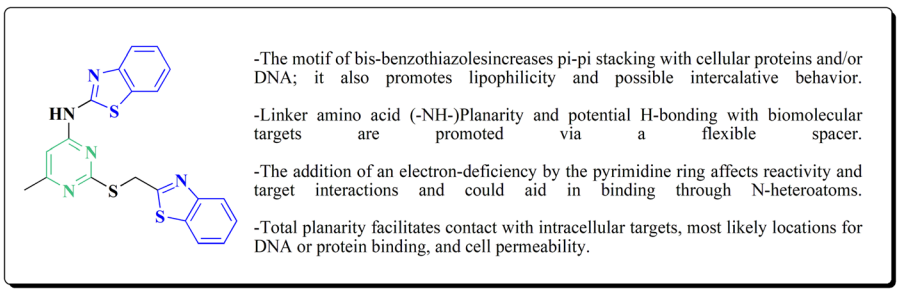


Fig. 45 Structure–activity relationship of compound **351**.

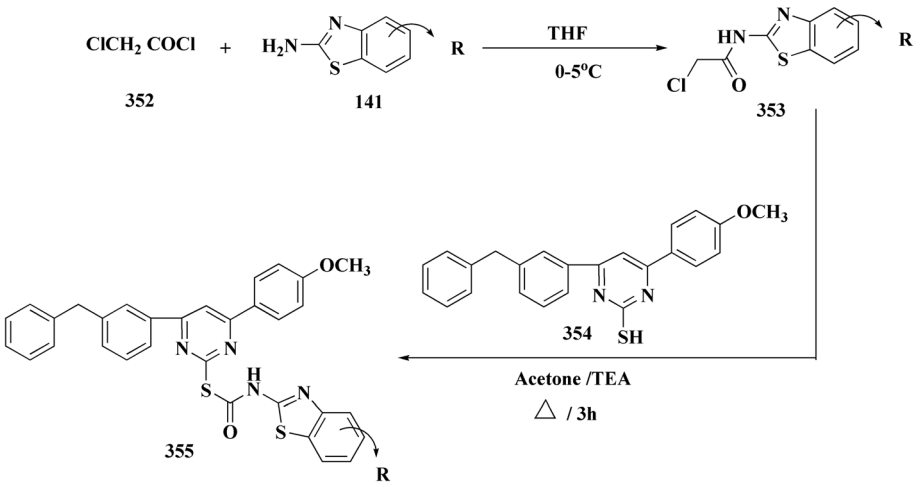


Scheme 69 Synthesis of pyrimidine based benzothiazole derivatives.

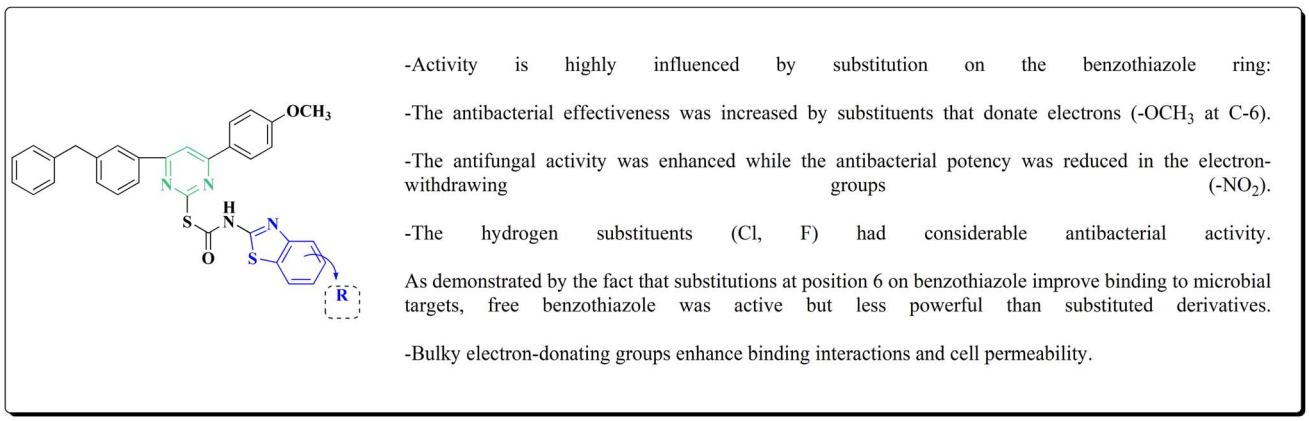


Fig. 46 Structure–activity relationship of compound **355**.

Compound **344** is structurally suitable for covalent inhibition and high affinity binding; it is able to target two enzymes (PBP and β-lactamase); and able to overcome resistance through a synergistic mechanism with amoxicillin 218.

Compounds **347** were synthesized by treating **345** with **346.** Similarly, the compounds **348** were synthesized by performing the reaction of **347** with **103.** Compounds **350** were synthesized by treating **347** with **349**. Compound **351** were furnished from the reaction of **347** with **141** (Scheme 68). The amino linked pyrimidinyl bis benzothiazole **351** displayed cytotoxic potency on A549 cells ($IC_{50}$ value = 10.5 Mm) (Fig. 45).[219]

Pyrimidines are crucial core in synthesizing numerous heterocycles with wide applications.[220–223] Pyrimidine based benzothiazole derivatives were synthesized as shown in Scheme 69. The Chalcone is generated by an aldol, condensation of *m*-phenoxy benzaldehydes with 4-methoxy acetophenone using a catalyst that is treated with thiocarbamide to furnish substituted pyrimidine. The pyrimidine treated with substituted *N*-1,3-benzothiazole-2-yl-2-chloroamide affords compound **355** (Fig. 46).[224]

The synthesized compounds screened against two Gram +ve bacteria and two Gram −ve bacteria, analyzed with chloramphenicol, ampicillin, ciprofloxacin, and norfloxacin. The synthesized compounds were screened against the anti-fungal strains *Aspergillus niger* and *Candida albicans* organisms, and were compared with griseofulvin and nystatin as standard drugs.[224]

*N*-(6-Methoxybenzo[*d*]thiazol-2-yl)-2-(4-(4-methoxyphenyl)-6-(3-phenoxyphenyl)pyrimidin-2-ylthio)acetamide indicated excellent anti-microbial potency against both Gram-positive and Gram-negative bacteria. It is comparable to ciprofloxacin for Gram-(−ve) strains. It showed less activity in anti-fungal screening, but still moderate against *Aspergillus niger*.

**9.1.2. Deazapyrimidine–benzothiazole based analogues.** Novel benzothiazole sulfonylhydrazide was reacted with ketene dithioacetal derivatives to synthesize a new series of *N*-sulfonamide 2-pyridone derivatives (Scheme 70). These substances were tested for their *in vitro* antimicrobial efficiency and capacity to concurrently inhibit both targets. They were synthesized to combine dual inhibitory action against both DHPS and DHFR enzymes within a single molecule.

Five compounds – **356b**, **357a**, **357b**, **358a**, and **358b**—of the synthesized *N*-sulfonamide 2-pyridone derivatives showed significant antibacterial activity against the tested strains of

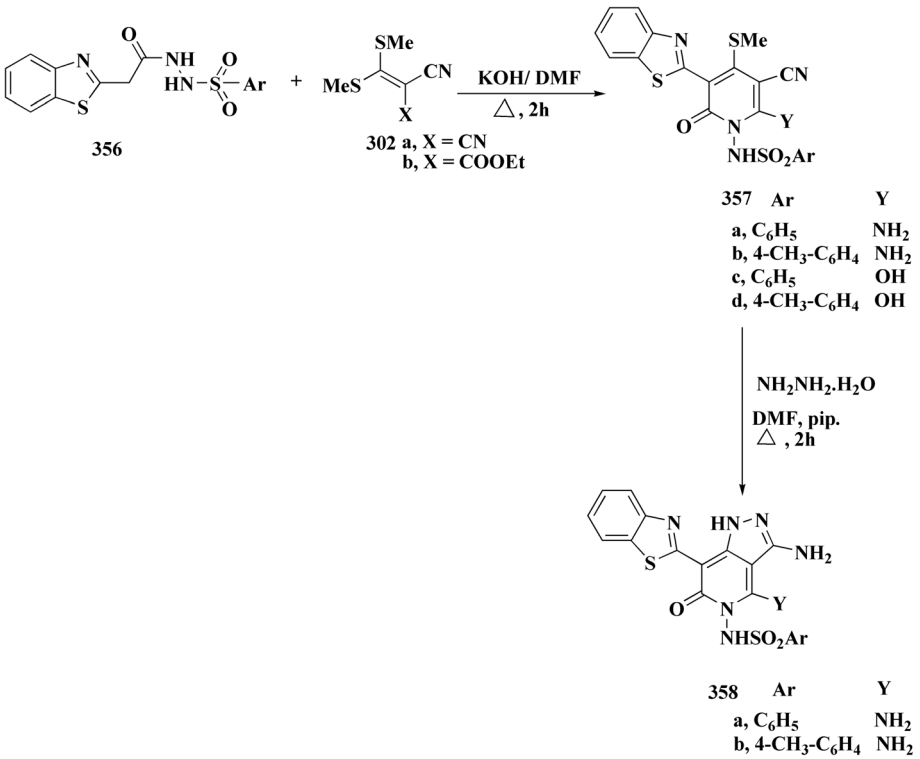


Scheme 70 Synthesis of *N*-sulfonamide 2-pyridone derivatives.

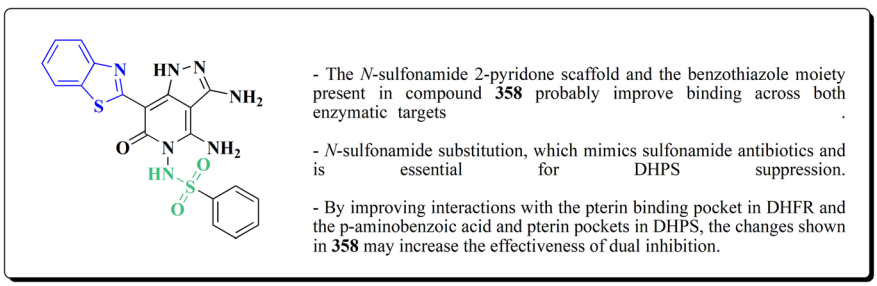


Fig. 47 Structure–activity relationship of compound **358**.

bacteria and fungi. The MTT assay was used to further assess these compounds' cytotoxicity on the human dermal fibroblast cell line HFB4. With $IC_{50}$ values of 2.76 and 0.20 μg $mL^{-1}$, respectively, compound **358a** was shown to be the most potent dual inhibitor of DHPS and DHFR in *in vitro* enzyme inhibition tests. According to molecular docking studies, **358a** efficiently resides in the pterin binding pocket of DHFR as well as the *p*-aminobenzoic acid and pterin binding sites of DHPS. These results validate that the most effective dual DHPS/DHFR inhibitor in this series is **358a** (Fig. 47). By reacting newly synthesized benzothiazole sulfonylhydrazide compounds with ketene dithioacetal derivatives, the novel *N*-sulfonamide 2-pyridone derivatives containing a benzothiazole moiety were synthesized.[225]

The most effective dual inhibitor of both the DHPS and DHFR enzymes among these was compound **358**, which had unusually low $IC_{50}$ values of 2.76 μg $mL^{-1}$ for DHPS and 0.20 μg $mL^{-1}$ for DHFR.

Compound **358** efficiently occupies crucial binding sites, according to docking analyses: DHPS – it interacts with the binding pockets of pterin and *p*-aminobenzoic acid. The pterin binding pocket is where DHFR binds. Dual-site occupancy is suggested by these interactions, improving inhibitory efficacy and specificity. From a structural standpoint, the benzothiazole and *N*-sulfonamide 2-pyridone core probably provide for flexible fitting in the enzyme active sites, promoting robust binding interactions.[225]

2-Chloropyridine-3-carboxylic acid **359** and the anilines **215a–g** were reacted under reflux in ethane-1,2-diol to yield compound **360a–g**. Further treatment of the latter with sodium hydroxide solution give the 2-anilino nicotinic acids **361a–g**. The synthesis of compounds **362a–n** was performed by reacting

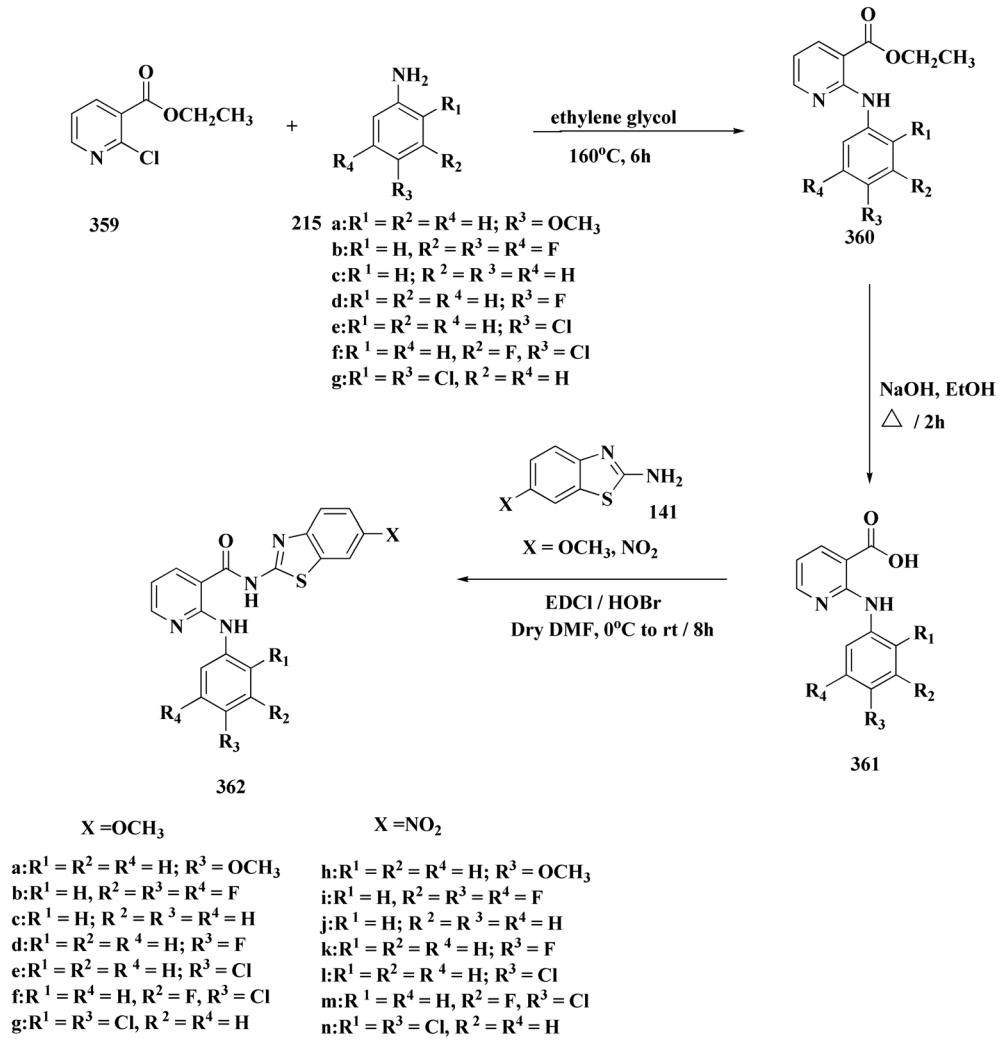


Scheme 71 Synthesis of Synthesis of pyridine based benzothiazole derivatives.

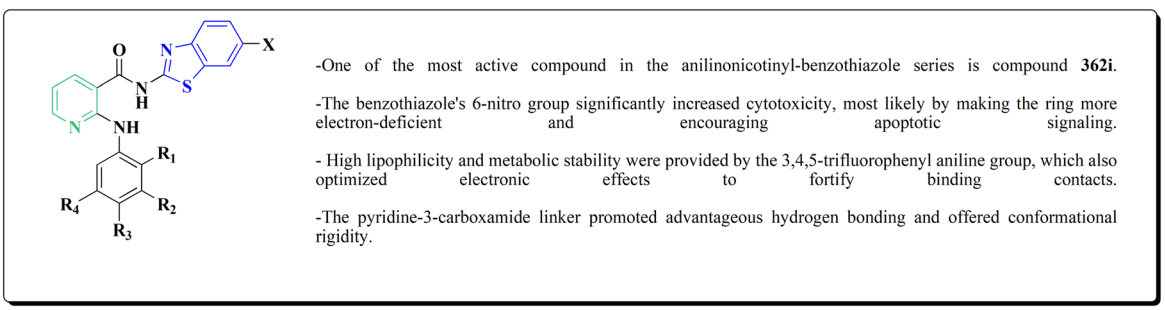


Fig. 48 Structure–activity relationship of compound 362.

6-substituted 2-amino benzothiazoles with 2-anilino nicotinic acids (Scheme 71).[226]

The compounds were estimated for their antiproliferative activity. Compounds (**362h–k** & **362n**) have displayed potent cytotoxicity against human leukemia HL-60 cell lines. All these compounds were examined for their effects on the cell cycle perturbations and induction of apoptosis. Subsequently, the mechanism of cell death was analysed. The cytotoxicity of **362i** (Fig. 48) correlated with induction of apoptosis, caspases activation and DNA damage and thus showing the apoptotic pathway of anticancer effect of these compounds.[226]

In terms of mechanism, **362i** caused apoptosis through the extrinsic and intrinsic (mitochondrial) pathways. Nuclear DNA damage was the main driver for the dose-dependent activation

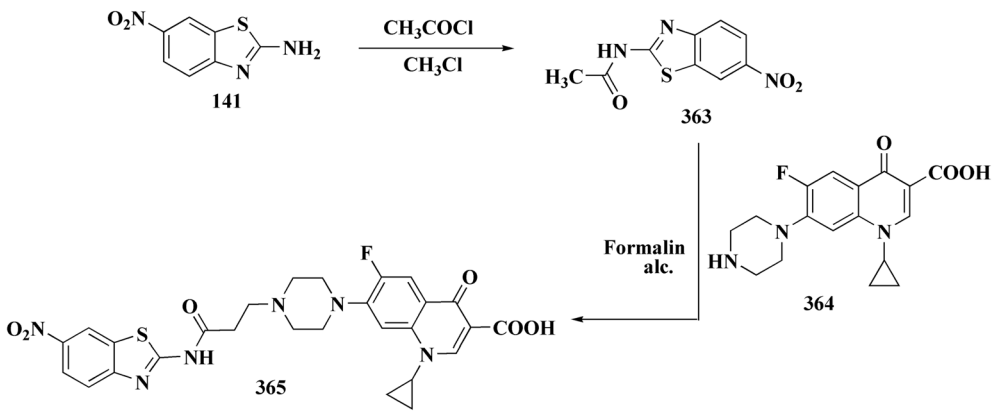


Scheme 72 Synthesis of *N*-Mannich base pro-drugs of norfloxacin.

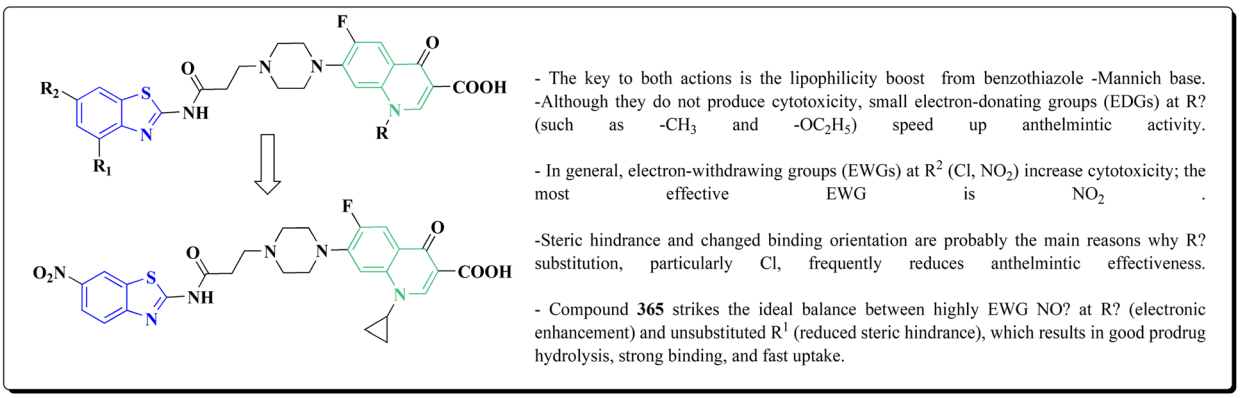


Fig. 49 Structure–activity relationship of compound **365**.

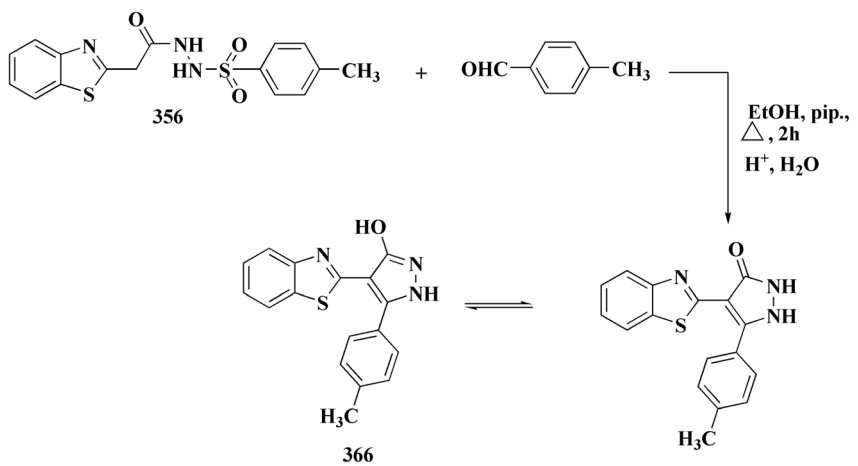


Scheme 73 Synthesis of substituted 4-(benzo[*d*]thiazole-2-yl)-1*H*-pyrazol-3(2*H*)-one.

of caspases-3, -8, and -9, which suggested dual apoptotic pathway engagement. Additionally, without influencing Bcl-2 expression, the drug increased loss of mitochondrial membrane potential, ruling out direct Bcl-2 regulation as a mechanism. Crucially, there was no rise in nitric oxide levels, indicating different processes that trigger apoptosis. Fluorescence microscopy morphological study verified the characteristic apoptotic alterations, such as decreased cell size, smoothing of the plasma membrane, and widespread blebbing.[226]

In another approach, the benzothiazoles **334** were acetylated *via* refluxing them with acetyl chloride to afford acetylated

benzothiazoles **335**. *N*-Mannich bases of the anti-bacterial agents **337** were prepared through refluxing compound **335**, antibacterial agents **336**, and formalin (Scheme 72). The compounds have been screened for antihelmintic activity and cytotoxic activity against human lung cancer cell lines A-549. Prodrug **337** ($GI_{50}$ value 28.8) has been proved most potent among all the synthesized prodrugs.[227]

Compound **365** is a derivative of benzothiazole and norfloxacin *N*-Mannich base. The benzothiazole ring in **365** (Fig. 49) has a strong electron-withdrawing $NO_2$ group at position 6 ($R_2$) and is unsubstituted at $R_1$.

The norfloxacin amine and the benzothiazole carrier are joined by the *N*-Mannich base. This raises the amine's lipophilicity and makes passive diffusion across membranes easier by lowering its p$K_a$ by about three units. Under physiological conditions, the parent drug (norfloxacin) and the benzothiazole moiety are released when the Mannich base hydrolyzes (pH-dependent).

Prior to hydrolysis, the intact benzothiazole–fluoroquinolone combination may interact with targets such as cancer cells or parasites. The benzothiazole fragment can offer further bioactivity (benzothiazoles are known anticancer/antimicrobial scaffolds), while hydrolysis releases norfloxacin, which maintains antimicrobial/anthelmintic activity.

In terms of cytotoxicity, the enhanced lipophilicity improves cellular absorption in A-549 cells; the strong growth inhibition may be explained by the $NO_2$ group increasing enzyme inhibition or DNA intercalation potential.[227]

The ability of a number of recently synthesized benzothiazole derivatives to inhibit the dihydropteroate synthase (DHPS) enzyme and exhibit antibacterial activity was assessed. Benzothiazole *N*-arylsulfonylhydrazones were synthesized by reacting

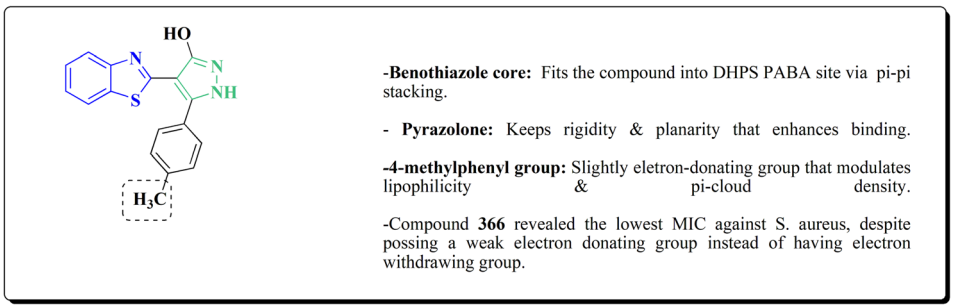


Fig. 50 Structure–activity relationship of compound **366**.

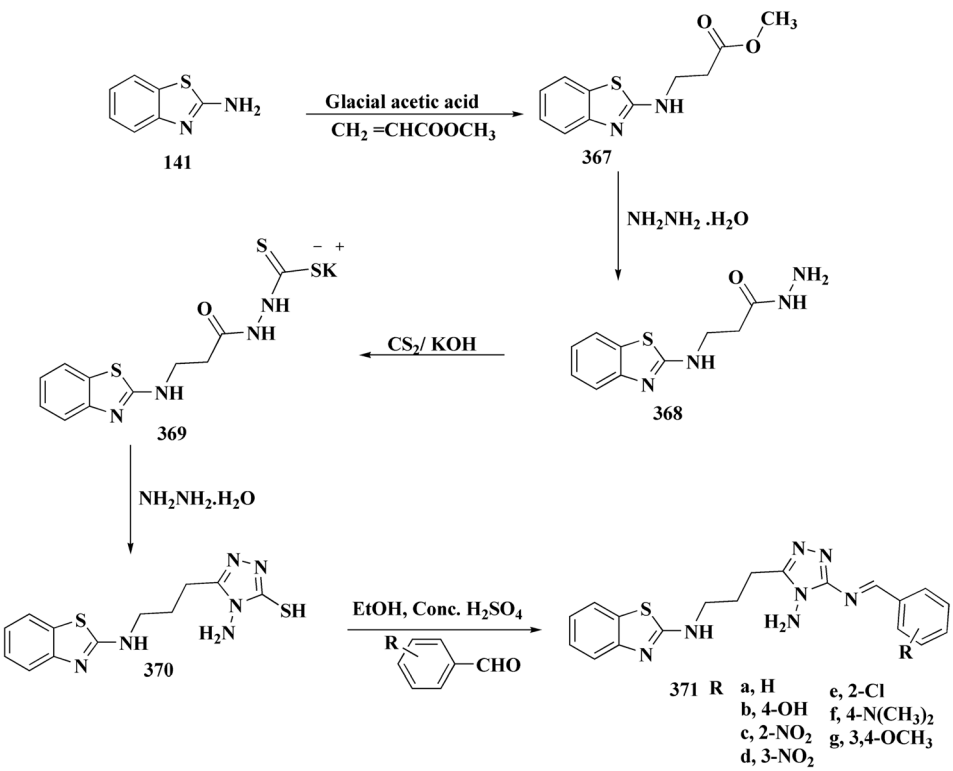


Scheme 74 Synthesis of 1,2,4-triazoles benothiazole conjugates.

with a variety of partners, such as arylaldehydes, diazonium salts of arylamine derivatives, *N*-aryl-2-cyano-3-(dimethylamino) acrylamide, and *N*-aryl-3-(dimethylamino)prop-2-en-1-one (Scheme 73). With minimum inhibitory concentrations (MICs) ranging from 0.025 to 2.609 mM, antimicrobial screening showed that many of the synthesized compounds demonstrated substantial action, especially against *Staphylococcus aureus*. With a MIC of 0.025 mM, compound **366** was the most potent of them all, outperforming common antibiotics like ampicillin and sulfadiazine.[228]

The benzothiazole–pyrazolone hybrids exert their antibacterial activity primarily through inhibition of the dihydropteroate synthase (DHPS) enzyme, a key player in the folate biosynthesis pathway in bacteria. These compounds mimic the natural substrate *para*-aminobenzoic acid (PABA) and competitively bind to the PABA-binding pocket of DHPS, thereby blocking the formation of dihydropteroate and ultimately halting DNA synthesis. The planar benzothiazole and pyrazolone moieties facilitate strong π–π stacking interactions with aromatic residues within the active site, while the sulfonylhydrazone linker provides critical hydrogen bonding interactions. Specifically, compound **366** (Fig. 50), which features a *para*-methyl-substituted phenyl group, benefits from optimal hydrophobic interactions and enhanced membrane permeability. Despite lacking a strong electron-withdrawing group, its structural balance allows efficient binding within the DHPS active site, leading to superior antibacterial potency compared to standard drugs.

**9.1.3. Triazole–benzothiazole based analogues.** The reaction of compound **370** with aromatic aldehydes yielded the 1,2,4-triazoles **371a–g** (Scheme 74).[231] Triazoles showed potency in a variety of synthesized compounds.[229,230] The synthesized compounds were screened for their antimicrobial activity.[231]

It was suggested that the *para*-substitution increases π-delocalization by enabling better electrical conjugation between the aromatic ring and the azomethine (–CH═N–) connection. Stronger π–π stacking or hydrophobic interactions with microbial enzymes or DNA may be made possible by this increased planarity. The arylidene ring was twisted out of plane by *o*-substitution (**371c**: 2-$NO_2$; **371e**: 2-Cl), which decreased conjugation and binding affinity.

By increasing the electron density on the aromatic ring, electron-donating groups (EDGs) like –OH (**371b**), –$NMe_2$ (**371f**), and –$OCH_3$ (**371g**) can: –strengthen donor/acceptor hydrogen-bond interactions with microbial biomolecules. –May increase lipophilicity, which would facilitate penetration of cell walls and membranes. –Nitro (**371c**, **371d**) and other electron-withdrawing groups (EWGs) reduce electron density and typically diminish activity, potentially as a result of less interaction with π-rich or nucleophilic sites in the microbial target (Fig. 51).

In addition, the benzothiazole–triazole scaffold has key role: the benzothiazole moiety is recognized for its ability to

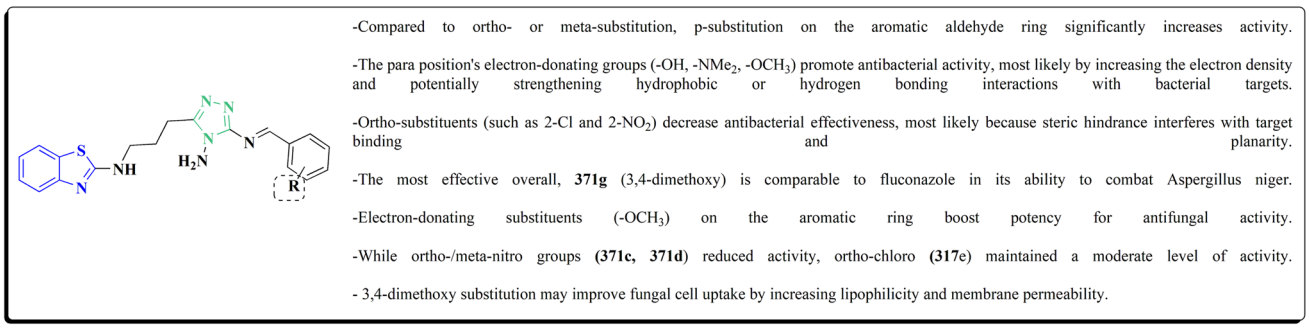


Fig. 51 Structure–activity relationship of compound **371**.

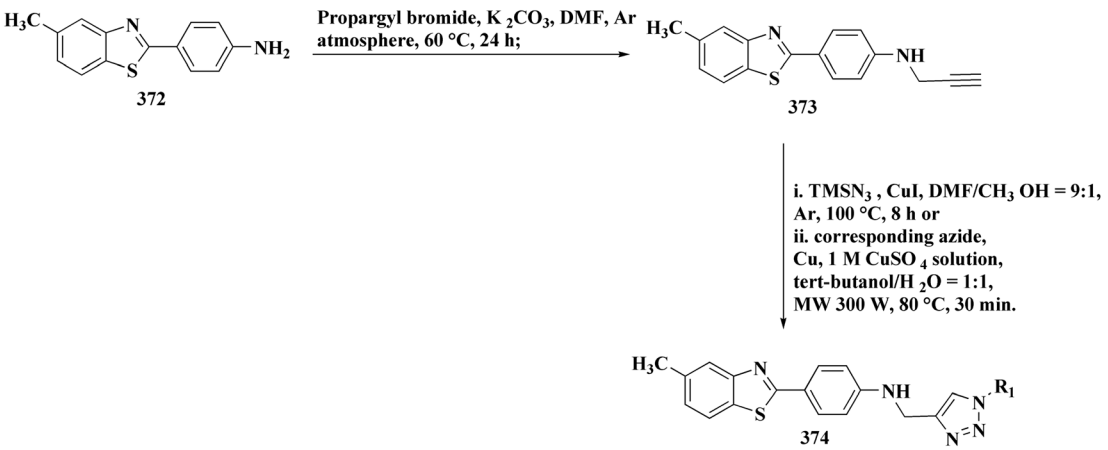


Scheme 75 Synthesis of 1,2,3-triazole based bis-heterocycles.

intercalate DNA or attach to grooves in microorganisms. It facilitates hydrogen bonding and π-interactions for enzyme inhibition.

On the other hand the ring 1,2,4-triazole has the ability to bind with cytochrome P450 enzymes' heme iron, which is crucial for antifungal action. Also it promotes hydrogen bonding and could help microbial metalloenzyme chelation. Compound **371g** has most potency against the anti-fungal activity. Possibly as a result of the methoxy groups' improved lipophilicity, which facilitates the penetration through fungal cell membranes, 3,4-dimethoxy substitution enhanced efficacy against Candida albicans and *A. niger*. Additionally, they might line up to better fit the hydrophobic regions of fungal enzyme targets, such as sterol biosynthesis enzymes.

- The presence of *para*-electron-donating substituents in the arylidene ring maximizes activity by maintaining conjugation and planarity with the benzothiazole–triazole core, which improves target binding and microbial penetration. This is disrupted by *ortho*-substitution, and the interaction potential is decreased by electron-withdrawing groups.[231]

The halogen-substituted aromatic azide precursors essential for the synthesis of 1,2,3-triazole based bis-heterocycles **374** were prepared from the corresponding arylamines. 1,2,3-Triazole-benzofused heterocycle conjugates **374** were accessed by copper(I)-catalyzed click chemistry using microwave irradiation. The 1,2,3-triazole-tethered benzofused heterocycle–coumarin chimeras were synthesized from terminal alkynes and coumarin azides (Schemes 75).

The antibacterial activities of the compounds were evaluated against selected Gram (+ve) and Gram (−ve) bacteria. Hybridization aspect utilizing Cu(I)-catalyzed click reaction using microwave irradiation was assumed in synthesizing the triazole tethered heterocycles **374**.[232]

Benzothiazole, triazole, and the coumarin motifs were fused to generate a unique design (compound **374**; Fig. 52) with specific anti-*M. catarrhalis* activity; the combined scaffold provides a distinct interaction profile than single motifs. This is why hybridization was important.

The active substances in this block were 7-substituted coumarins; the coumarin substitution pattern had a significant impact on both biological activity and fluorescence. The coumarin fragment's function was reported to affect the antibacterial potency. Rather than having broad Gram-negative/Gram-positive coverage, the activity was selective for the picky Gram-negative *M. catarrhalis*, indicating a particular target or uptake/penetration characteristic unique to this species.[232]

Bis-heterocycles were accessed *via* the cycloaddition reaction of compound **376** with various azides. 2-Mercaptobenzothiazole was reacted under reflux with propargyl bromide in dry THF to afford compound **376**. The azides were allowed to react with propargylated 2-mercaptobenzothiazole (**376**) under click chemistry conditions to afford compound **377**. Aromatic azides with different substituents were reacted with compound **376** (Scheme 76).

The synthesized compounds have been examined for their anti-inflammatory potency *via* the utilization biochemical

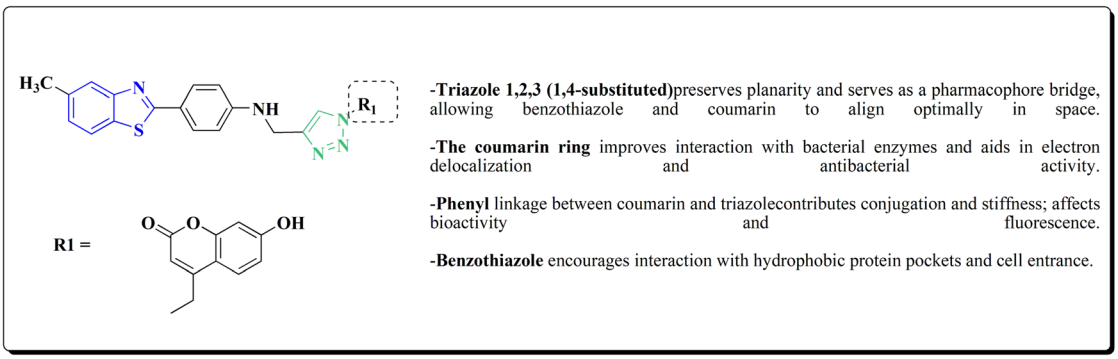


Fig. 52 Structure–activity relationship of compound **374**.

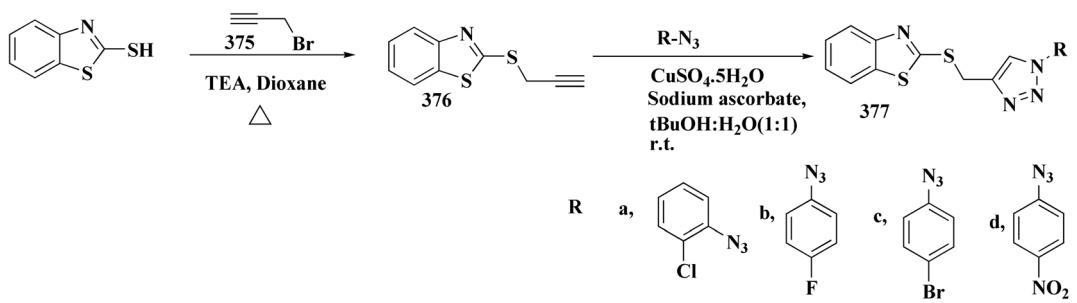


Scheme 76 Synthesis of 1,2,3-triazole based benzothiazoles.

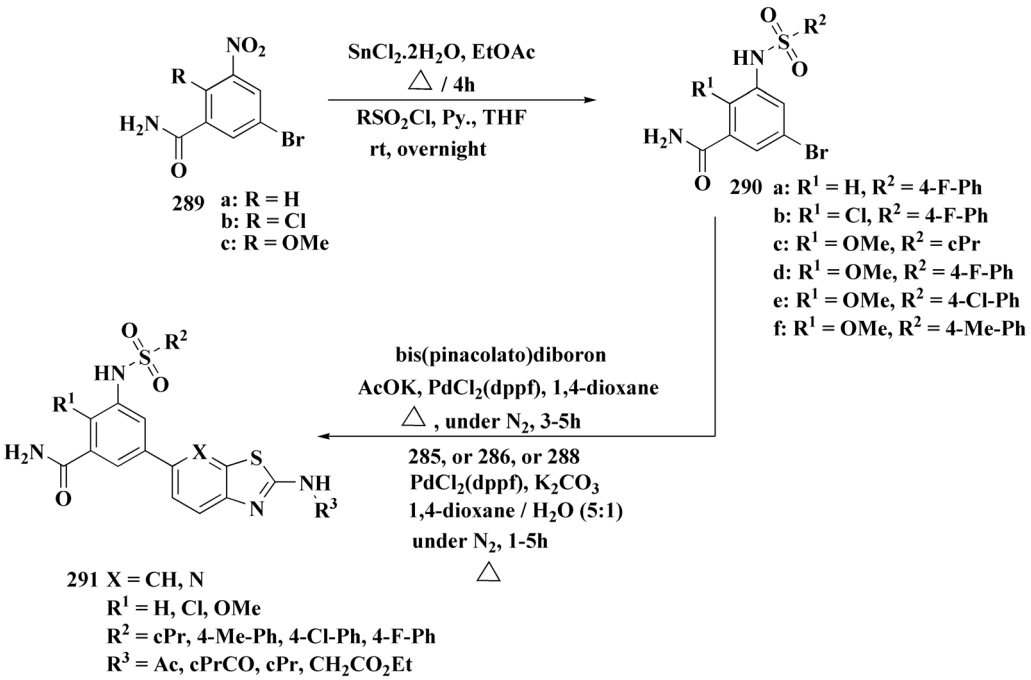


Fig. 53 Structure–activity relationship of compound 377.

cyclooxygenase (COX) activity assays and carrageen an-induced hind paw edema. Compound **377d** (Fig. 53) displayed a potent selective COX-2 inhibition with COX-2/COX-1 ratio of 0.44. Results from carrageenan-induced hind paw edema indicated that compounds **377a**, **377b**, **377c** and **377d** have significant anti-inflammatory activity comparable to Ibuprofen. Crucially,

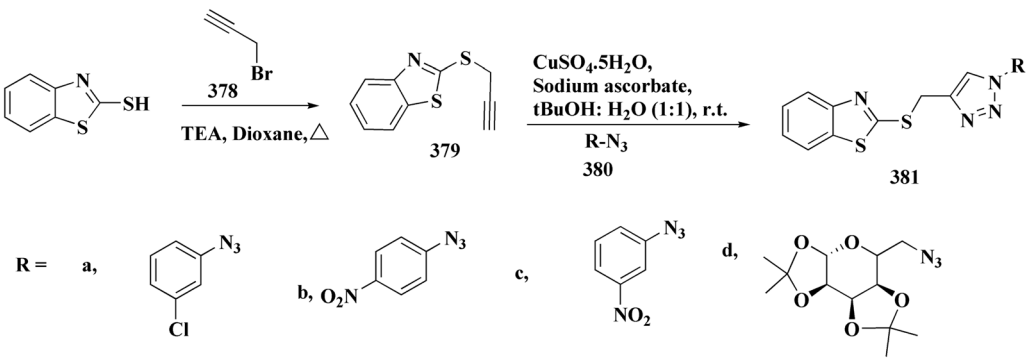


Scheme 77 Synthesis of benzothiazole-1,2,3-triazole conjugates.

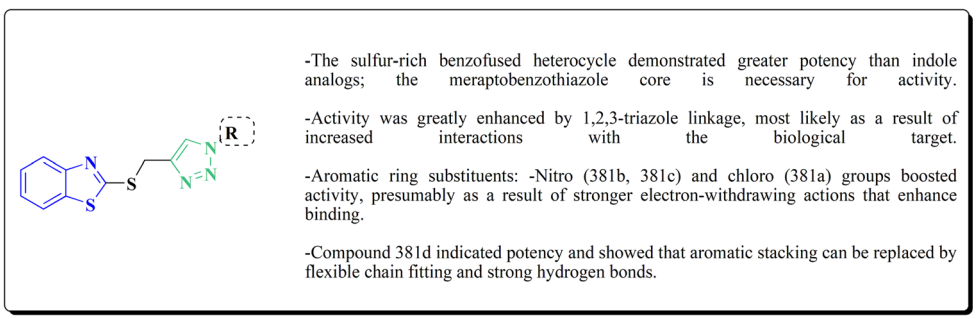


Fig. 54 Structure–activity relationship of compound 381.

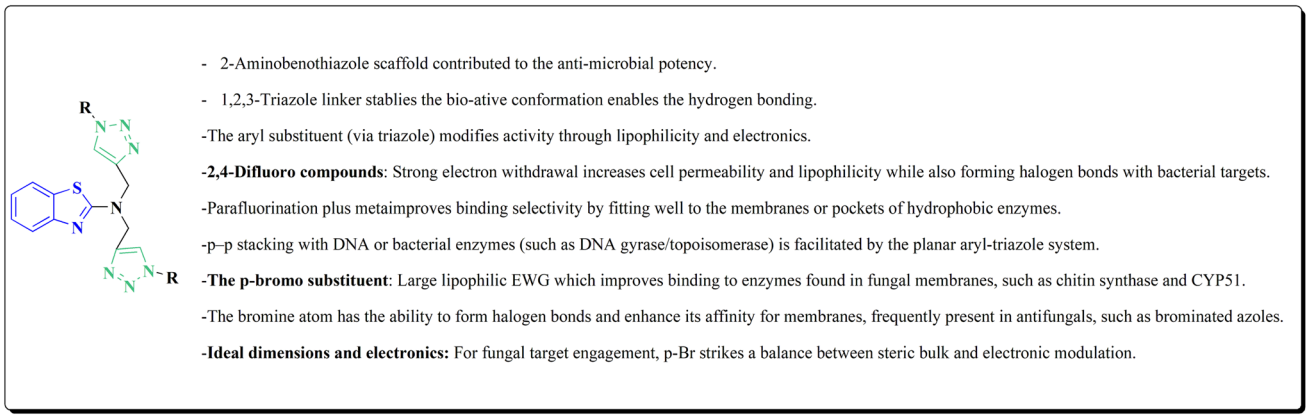


Fig. 55 Structure–activity relationship of compound 384.

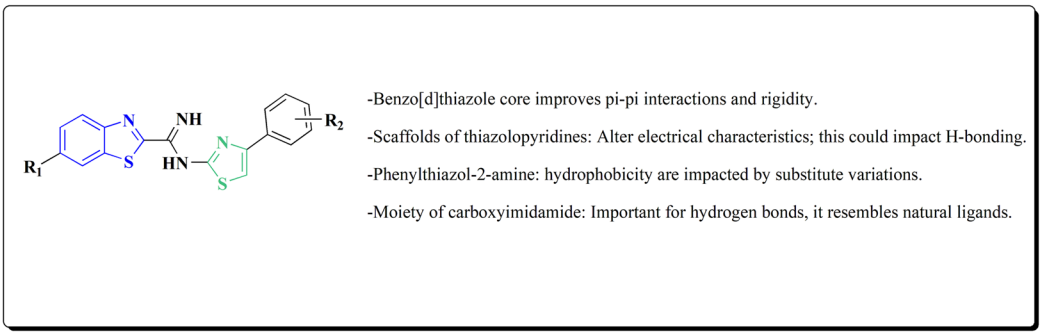


Fig. 56 Structure–activity relationship of compound 387.

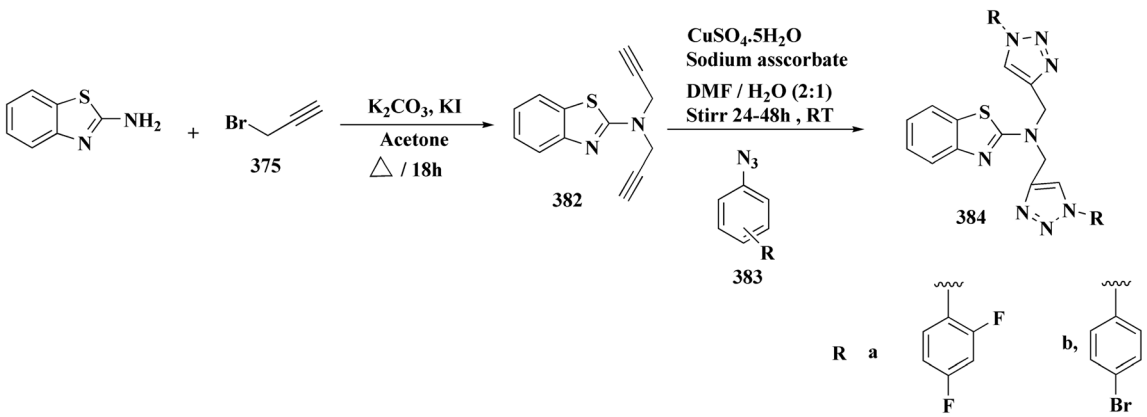


Scheme 78 Synthesis of substituted aryl azides.

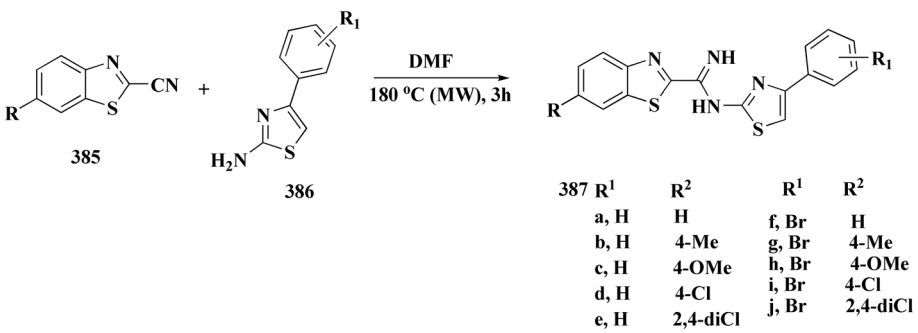


Scheme 79 Synthesis of benzothiazole–thiazole conjugates.

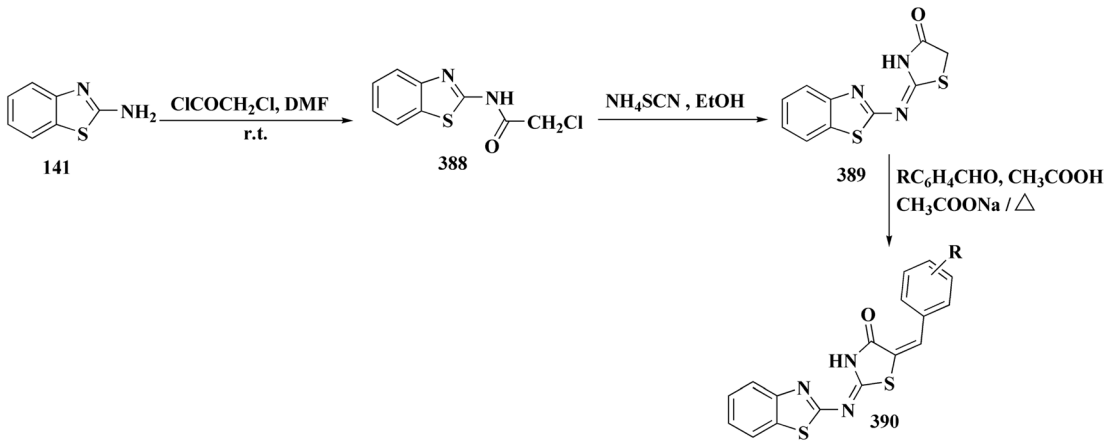


Scheme 80 Synthesis of 2-(benzothiazolylimino) thiazolidin-4-ones.

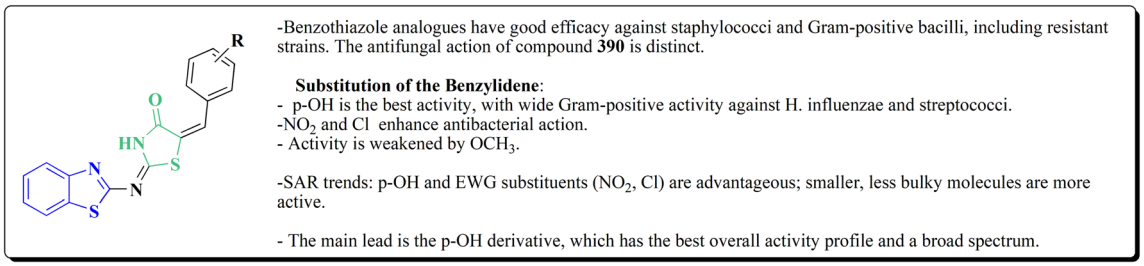


Fig. 57 Structure–activity relationship of compound 390.

none developed stomach ulcers, indicating perhaps better gastro-safety in comparison to standard NSAIDs.[233]

The 1,2,3-triazole conjugates of 2-mercaptobenzothiazole was synthesized by an azide–alkyne cycloaddition catalyzed by copper(I) (also known as "click chemistry") as depicted in Scheme 84. First, in the presence of triethylamine in dioxane under reflux, 2-mercaptobenzothiazole was alkylated with propargyl bromide to get the propargyl derivative **379**. Separately, other substituted benzyl halides or similar precursors reacted with sodium azide to yield the respective azides **380**. In order to synthesize the 1,4-disubstituted 1,2,3-triazole ring that connects the benzothiazole core and the substituted side chain, the alkyne intermediate **379** and the azides **380** were subsequently exposed to click conditions, which included $CuSO_4 \cdot 5H_2O$ and sodium ascorbate in a *t*-BuOH/$H_2O$ (1 : 1) combination at room temperature. The target bis-heterocyclic

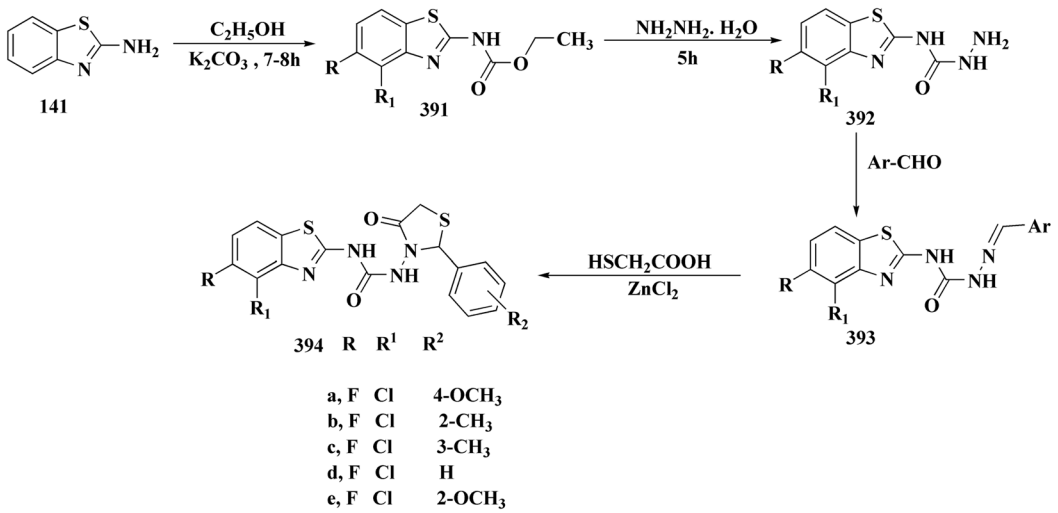


Scheme 81 Synthesis of benzothiazolyl ureas.

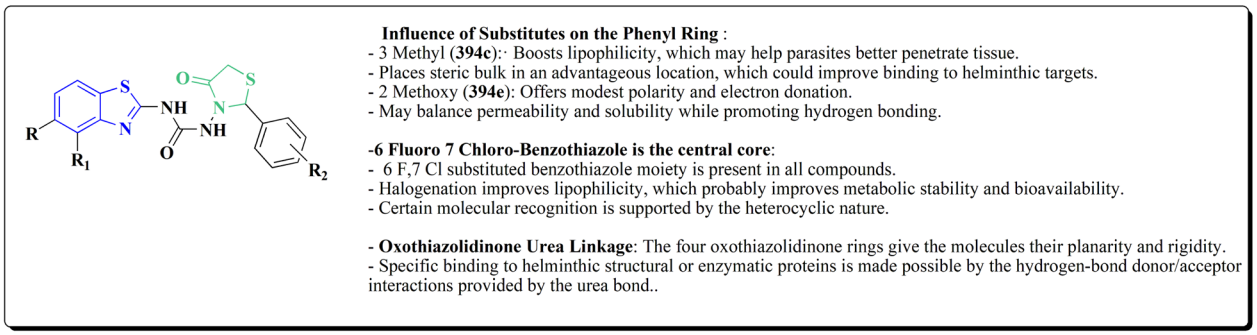


Fig. 58 Structure–activity relationship of compound **394**.

compounds **381** were obtained in high isolated yields (87–97%) using this one-pot, regioselective method (Scheme 77; Fig. 54).

The compounds were screened against *Mycobacterium tuberculosis* H37Rv strain for their antitubercular activity.[234]

Dialkyne substituted benzo[*d*]thiazol-2-amine was reacted with different substituted aryl azides to furnish compounds **384** by click chemistry (Scheme 78). These compounds were screened for their antibacterial activity. The compound **384a** indicated maximum activity against all Gram (+ve)/Gram (−ve) bacterial strains with MIC value 3.12 mg $mL^{-1}$, which is two-fold more potent comparable to ciprofloxacin (MIC 6.25 mg $mL^{-1}$). Compound **384b** was found to be the most potent against all fungal strains with MIC value ranging from 1.56 mg $mL^{-1}$ to 12.5 mg $mL^{-1}$.[235]

Fluorine atoms may interact favorably with the active regions of enzymes and enhance membrane penetration. The difluoroaryl group's hydrophobic and polar interactions are probably what give compound **384a** its enhanced activity (Fig. 55). Compound **384b** most likely interacts with biosynthetic enzymes or fungal membrane proteins, and because of its size and polarizability, the bromine improves binding and selectivity.

Because of its fluorine atoms, **384a** probably targets bacterial enzymes like DNA gyrase and MurB and more easily passes through Gram(−) membranes. Bromine increases the binding affinity and selectivity of **384b**, which most likely binds to fungal cytochrome enzymes or cell wall synthesis machinery.[235]

**9.1.4. Thiazole–benzothiazole based analogues.** The reaction of 4,5-dichloro-1,2,3-dithiazolium chloride (Appel's salt) with *ortho*-halogenated anilines, aminophenols, and aminopyridines afforded the aryliminodithiazoles. Copper(I)-mediated or nucleophilic-assisted cyclization of aryliminodithiazoles generated cyano-functionalized benzothiazoles. The latter were reacted with substituted thiazol-2-amines to afford novel polyaromatic carboximidamides.

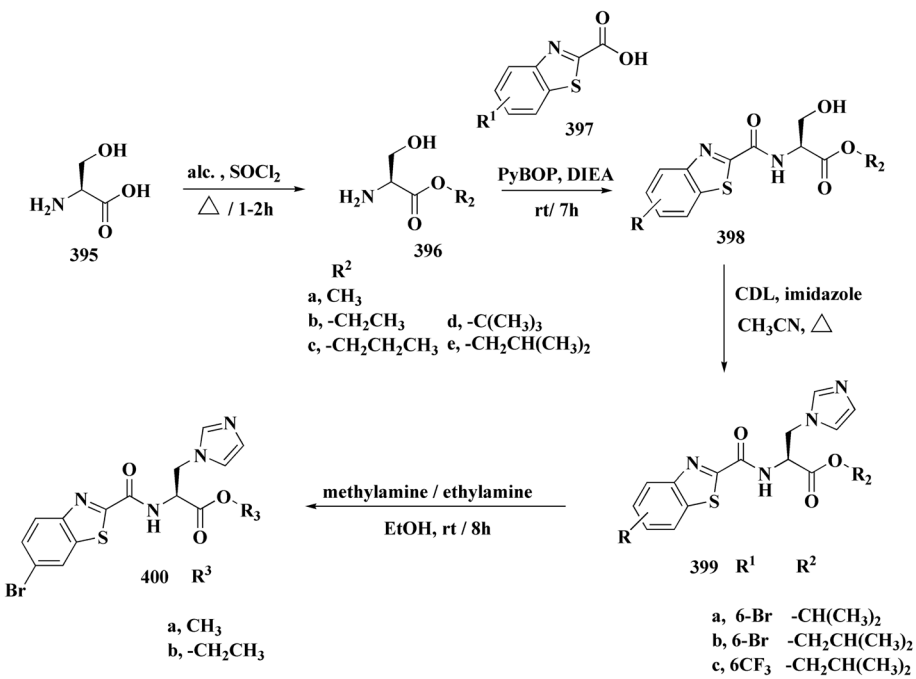


Scheme 82 Synthesis of substituted benzo[*d*]thiazole-2-carboxamide.

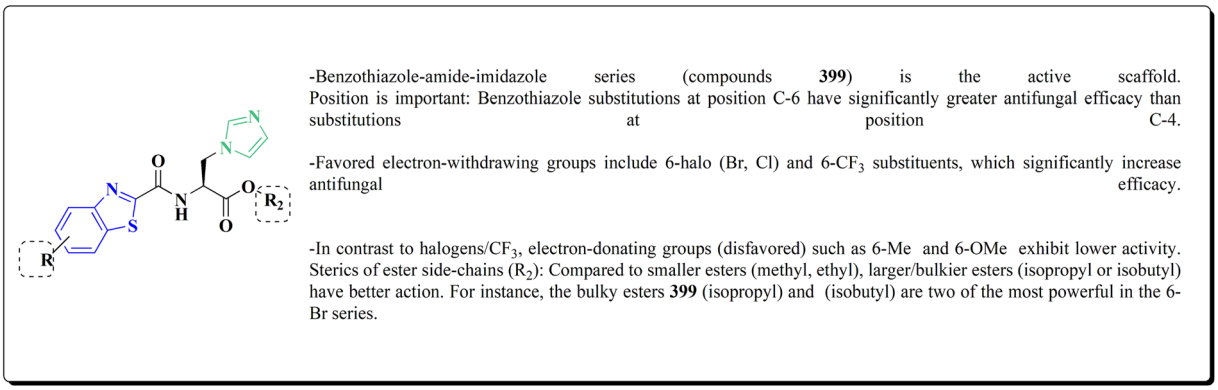


Fig. 59 Structure–activity relationship of compound **399**.

Microwave irradiation of the carbonitrile and the amine in dimethylformamide afforded the substituted benzo[*d*]thiazole-2-carboximidamides **387** (Scheme 79; Fig. 56).[236]

The 2-(benzothiazolylimino) thiazolidin-4-one **390** was achieved in Scheme 87. The synthetic procedures were preformed by reacting chloroacetylchloride with the appropriate amine. Cyclisation of 2-chloro-*N*-(etheroaryl)acetamide, yielded the 2-(heteroarylimino)thiazolidin-4-ones **389.** Compounds **390** were accessed by refluxing the latter intermediates with aldehydes (Scheme 80; Fig. 57).

The compounds were assayed *in vitro* for their antimicrobial potency. Most of the benzothiazole analogues exhibit good inhibition of the growth of Gram (+ve) staphylococci and bacilli. Among the synthesized analogues a few derivatives indicate a selective and strong activity against bacilli.[237]

The preparation of the benzothiazolyl ureas **394** were accessed by reaction with the semicarbazon **393** with DMF, thioglycolic acid and zinc chloride (Scheme 81).

The synthesized compounds indicated good to moderate anthelmintic potency against *Perituma posthuma*. The results of the ureas derivatives revealed anthelmintic activity against Albendazole.[238]

Analogues **394c** and **394e** (Fig. 58) were the most effective anthelmintic compounds against Perituma posthuma, outperforming other compounds in the series when compared to albendazole.

The uptake of parasite tissue is improved by lipophilicity, which is boosted by F, Cl, and methyl. Methoxy and other substituents that provide electrons may improve interactions with helminth targets. Planar arrangement and structural rigidity facilitate efficient target engagement in worm metabolic pathways.The most effective anthelmintic analogue is TH18, which has a 3 methyl phenyl group. Better hydrophilic balance and virtually equal activity are provided by TH20 (with a 2 methoxy substituent).These emphasizes how crucial strategically positioned lipophilic or H-bonding substituents are for this scaffold's best performance.[238]

**9.1.5. Imidazole–benzothiazole based analogues.** L-Serine **395** was dissolved in alcohol and refluxed with thionyl chloride to yield the serine esters **396a–e**. Compounds **396** were then treated with the intermediates **397** to afford compounds **398.** The desired compounds **399** were accessed through the introduction of an imidazole group. Compounds **400a–b** were prepared from **399** *via* an aminolysis reaction (Scheme 82).

The antifungal activity of these compounds was tested *in vitro*, and their SARs were estimated. The synthesized compounds indicated excellent inhibitory activity against *Cryptococcus neoformans* and *Candida albicans*. The most active compounds **399a, b**, and **c** (Fig. 59) revealed potent activity, with MIC values ranging from 0.125 to 2 μg $mL^{-1}$.[239]

The experimental CYP51 inhibition was performed and a significant drop in ergosterol and an accumulation of lanosterol and eburicol, the same sterol-pattern generated by fluconazole (a known CYP51 inhibitor), were observed in GC-MS sterol profiling following *C. albicans* treatment with **399b** ($R^1$ =

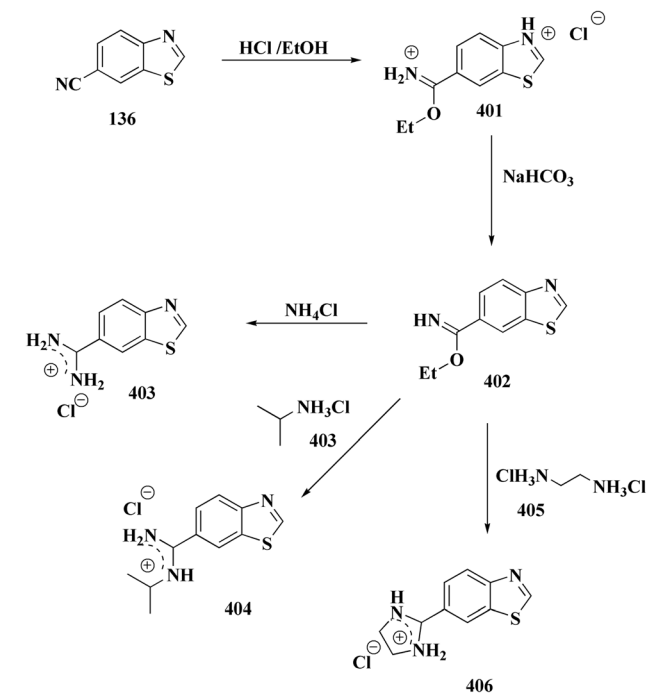


Scheme 83 Synthesis of substituted benzothiazoles.

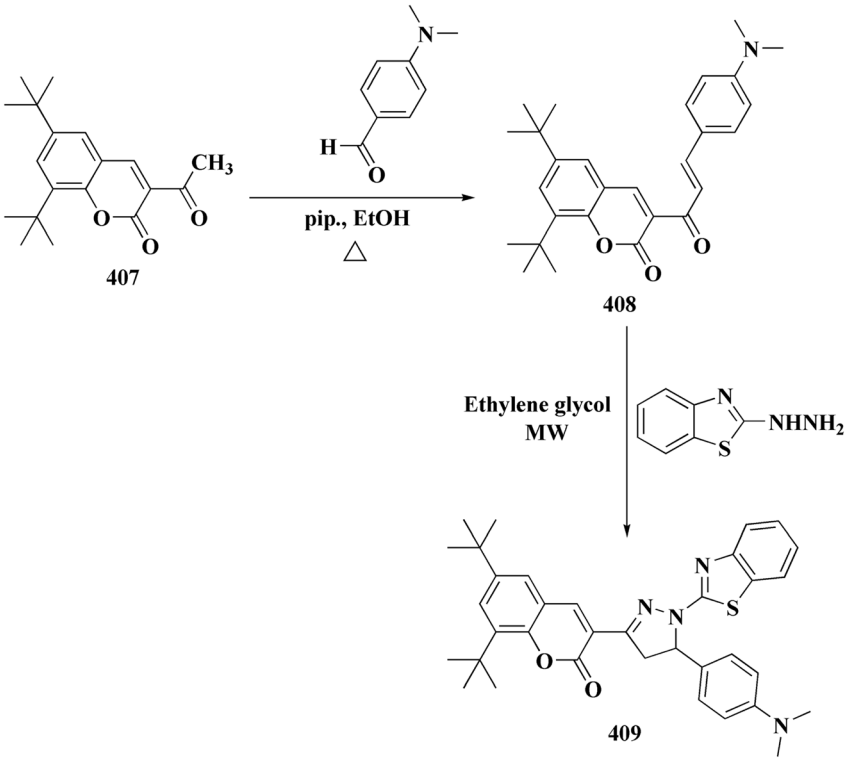


407 408 409

Scheme 84 Synthesis of substituted benzothizole **409**.

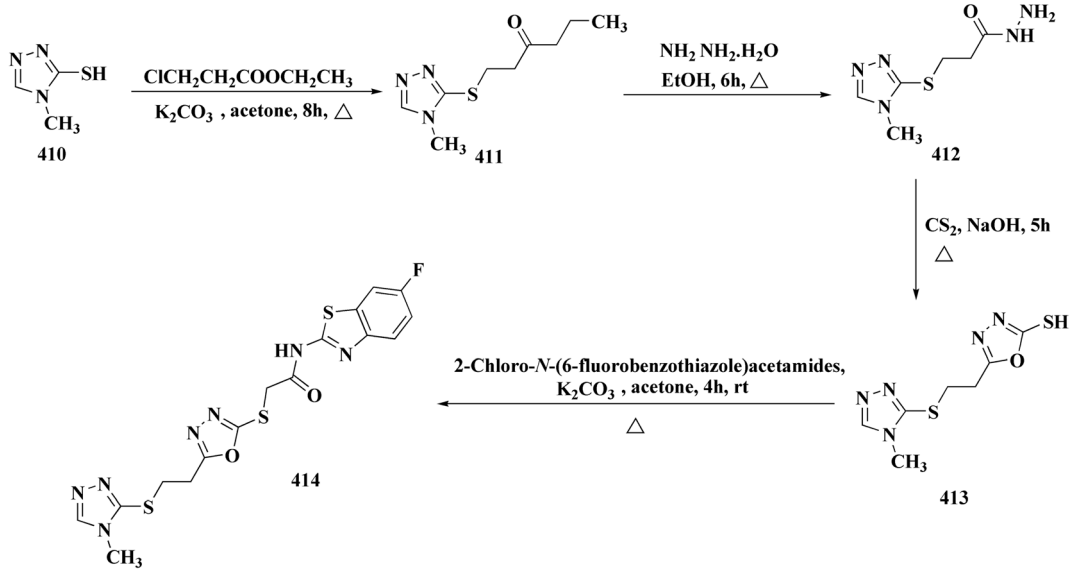


410 411 412 413 414

Scheme 85 Synthesis of triazole-oxadiazole benzothiazole conjugates.

6-Br; $R^2 = (-CH_2CH(CH_3)_2)$. This study clearly shows that fungal lanosterol 14$\alpha$-demethylase (CYP51) is inhibited by **399b.**

*In silico* docking/binding hypothesis shows that fungal CYP51 docking (CDOCKER) reveals: –(azole-like coordination) the heme iron is coordinated by the imidazole. –A hydrophobic pocket accommodates the alkyl ester (isobutyl) (contacts Ile139, Met313), and hydrophobic/vdW interactions are formed when the benzothiazole tail extends into the enzyme channel (His381, Phe241, Pro238, Leu95, Ala69). These interactions explain (a) why an imidazole is necessary, (b) why large hydrophobic ester groups are advantageous, and (c) why potency is increased by lipophilic electron-withdrawing C-6 substituents.

Activity against fluconazole-resistant strains: fluconazole is inert (>64 μg $mL^{-1}$), whereas **399b** maintains modest activity against two fluconazole-resistant *C. albicans* strains (MICs 8–16 μg $mL^{-1}$). This suggests that **399b** may overcome some

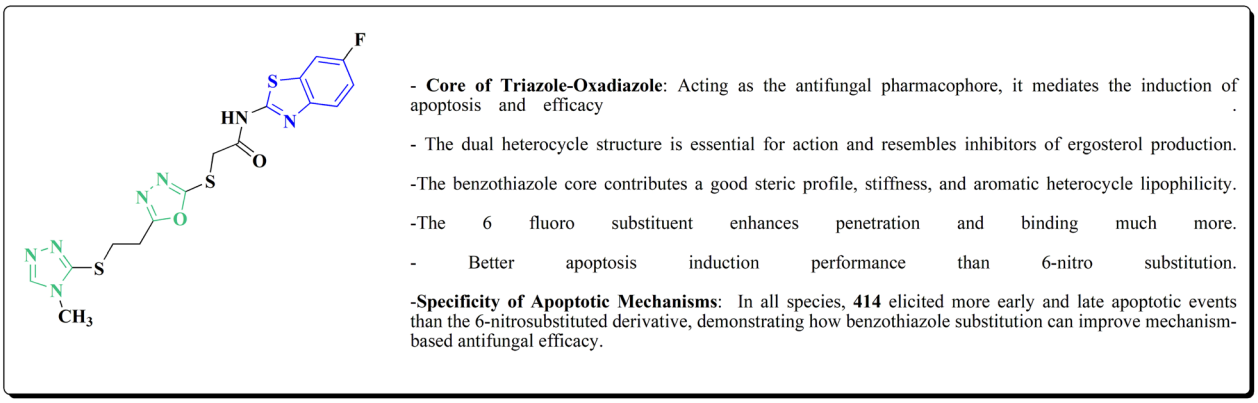


Fig. 60 Structure–activity relationship of compound **414**.

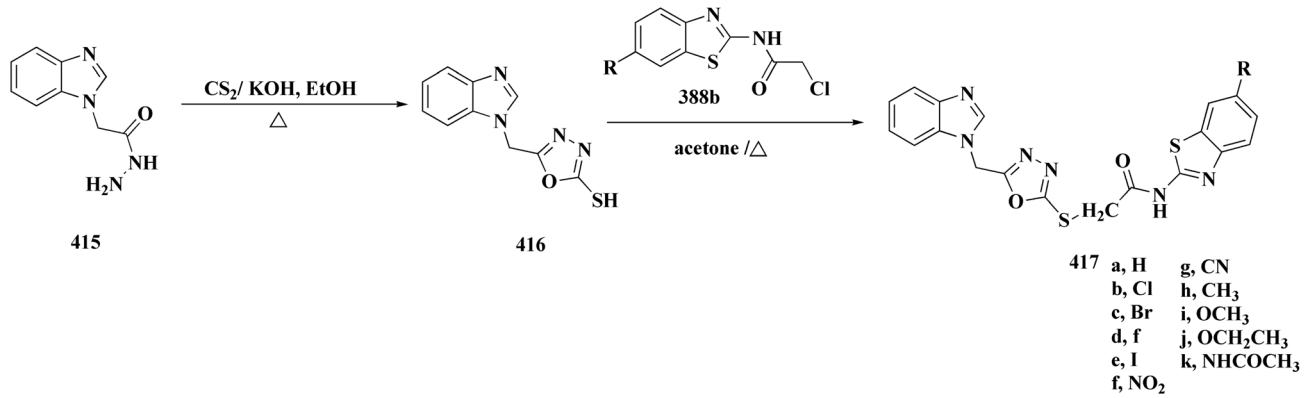


Scheme 86 Synthesis of 2-amino-6-substituted benzothiazoles.

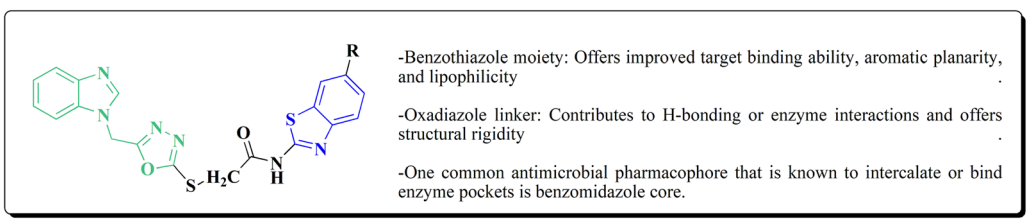


Fig. 61 Structure–activity relationship of compound **417**.

resistance mechanisms and indicates partial (not full) cross-resistance.[239]

New amidino, 2-imidazolinyl, *N*-isopropylamidino-substituted benzothiazoles and 2-aminothiophenoles were synthesized *via* the Pinner reaction is shown in Scheme 83. The new ring opening of benzothiazole with ethylenediamine and ammonia was occurred. The ring opening with ethylenediamine is appropriate to compounds having amonolytically and hydrolytically unstable substituents.[240]

Heterocycle-based chromophores comprising pyrazoline scaflods were synthesized using microwave irradiation (Scheme 84). The heterocyclic chromophores were fluorescent, with some examples emitting blue light (410–460 nm) whilst others emitted green light (529 nm). The absorption maxima of the chromophores were found to vary from 349 to 463 nm conditional on the degree of conjugation.[241]

These compounds' emission and absorption spectra were recorded in a solution of chloroform. New heterocyclic chromophores were discovered to have fluorescene in solution. Green light was emitted by compounds 409 (529 nm). These heterocyclic chromophores may be used as optical materials in a variety of applications, including biosensors, fluorescent probes in biological applications, OLED materials, and two-photon absorption materials.

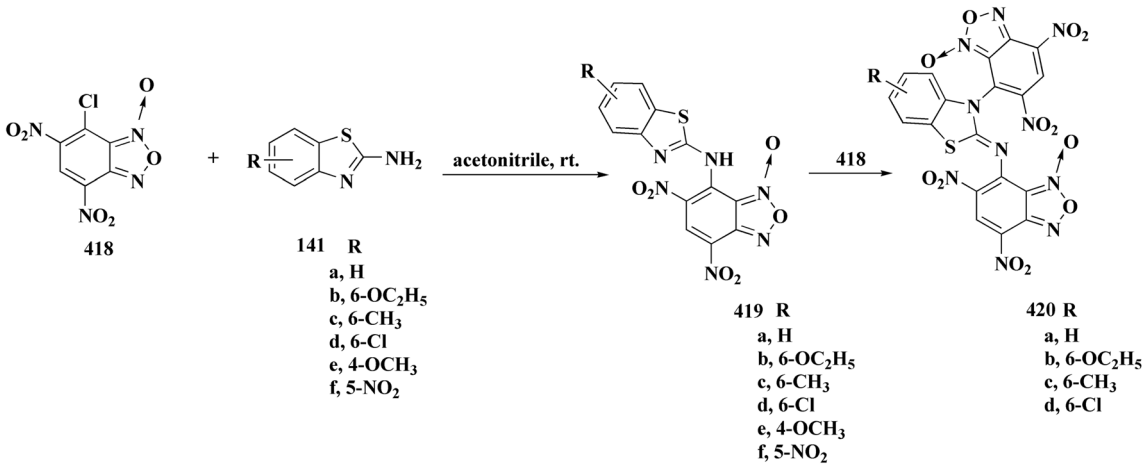


Scheme 87 Synthesis of 2-aminobenzothiazole-benzofuroxan conjugates.

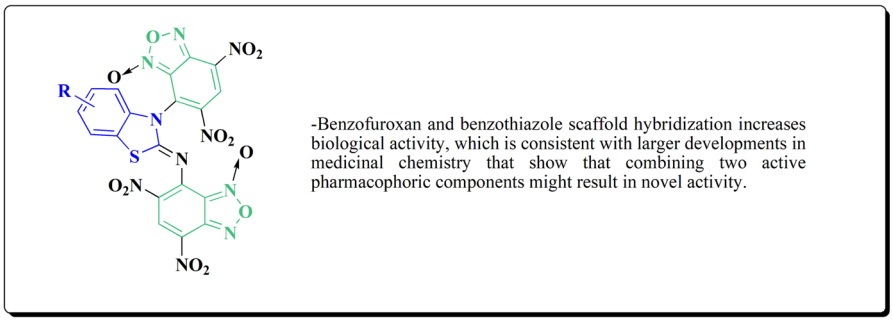


Fig. 62 Structure–activity relationship of compound **420**.

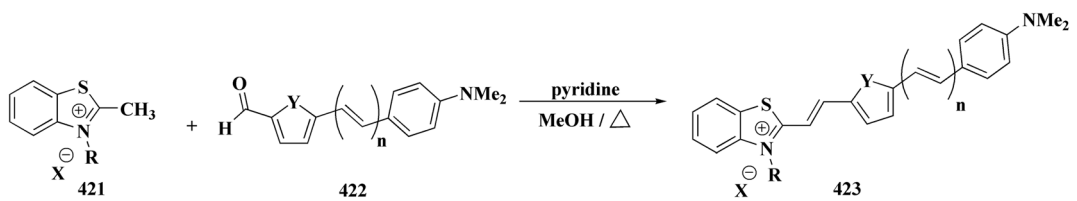


Scheme 88 Synthesis of benzothiazolium derivatives.

**9.1.6. Oxadiazole–benzothiazole based analogues.** Novel triazole–oxadiazole compounds were prepared as shown in scheme. 4-Methyl-4*H*-1,2,4-triazole-3-thiol was reacted with 3-chloropropionic acid ethyl ester to afford ethyl 3-[(4-methyl-4*H*-1,2,4-triazol)thio]propionate **411.** The ester group of compound **411** was hydrazinated to afford the hydrazide **412.** The

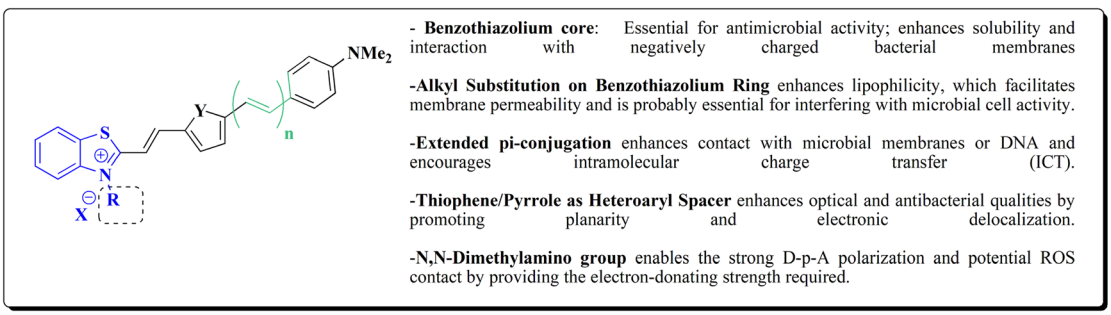


Fig. 63 Structure–activity relationship of compound **423**.

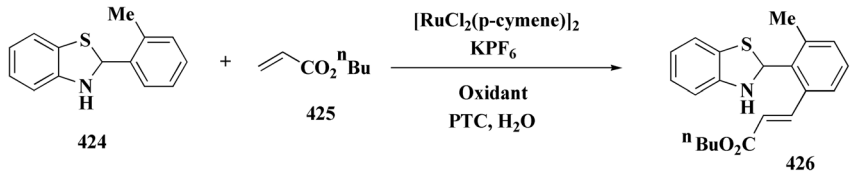


Scheme 89 Synthesis of 2-arylbenzo[*d*]thiazoles.

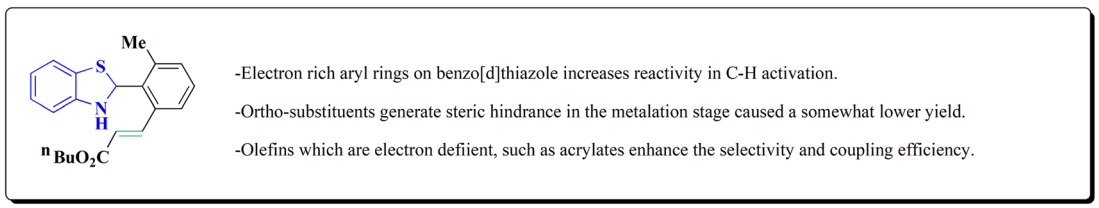


Fig. 64 Structure–activity relationship of compound **426**.

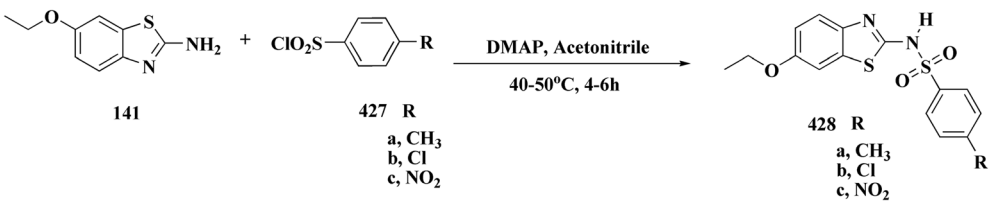


Scheme 90 Synthesis of benzothiazole sulfonamides.

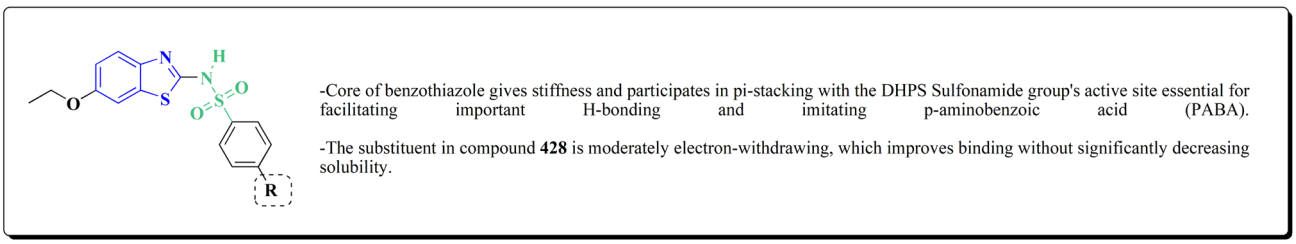


Fig. 65 Structure–activity relationship of compound **428**.

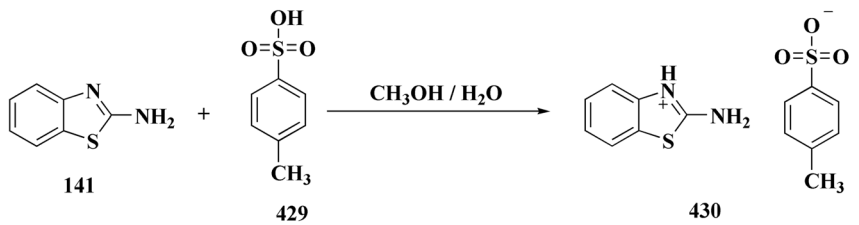


Scheme 91 Synthesis of 2-aminobenzothiazolium-4-methylbenzenesulphonate.

intermediate **413** was acheived *via* ring-closure reaction of compound **412** with carbon disulfide (Scheme 85).

The *in vitro* apoptotic and antifungal activity were tested. The compounds **414** (Fig. 60) were detected as the most potent compounds against *C. glabrata* and *C. albicans*.[242]

The 2-amino-6-substituted benzothiazoles were transformed to the chloroacetamides **412** using chloroacetyl chloride. The acetamide derivatives **412** were then condensed to the oxadiazole-2-thiol **416** to yield **417** (Scheme 86; Fig. 61).

Upon biological screening, it was detected that the majority of the compounds were found to have a remarkable broad spectrum antitubercular (6.25–25 mg $mL^{-1}$ of MIC) and antimicrobial (3.12–25 mg $mL^{-1}$ of MIC) potential.[243]

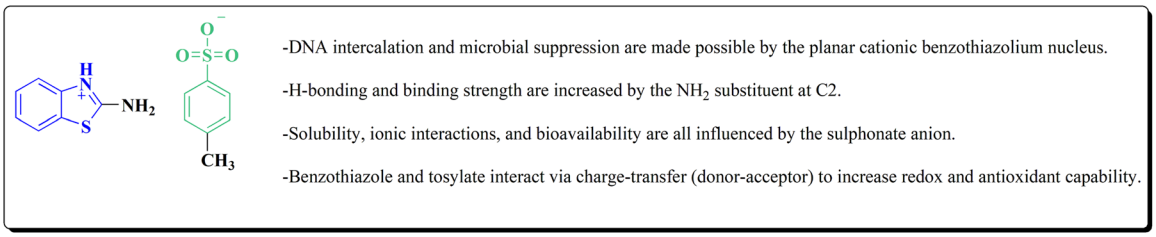


Fig. 66 Structure–activity relationship of compound **430**.

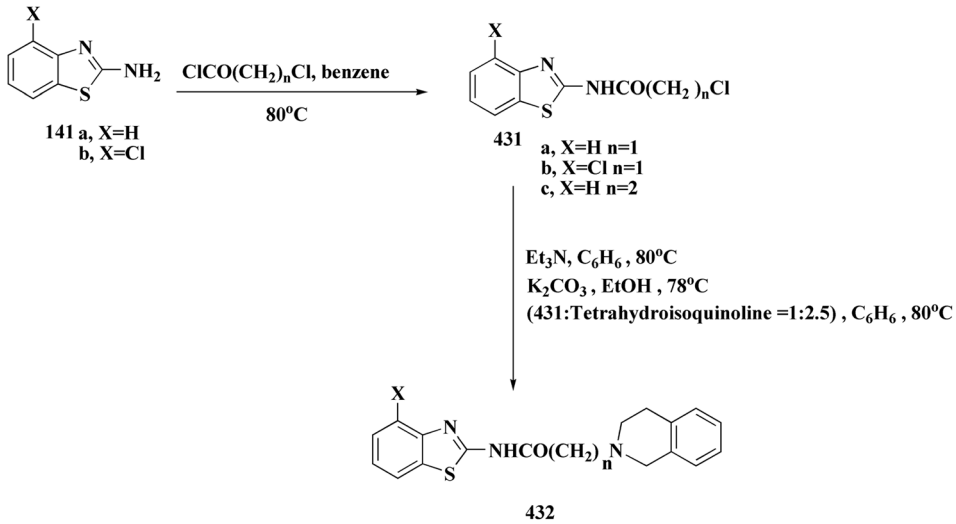


Scheme 92 Synthesis of dihydroisoquinolin-2(1*H*)-yl]alkanamides.

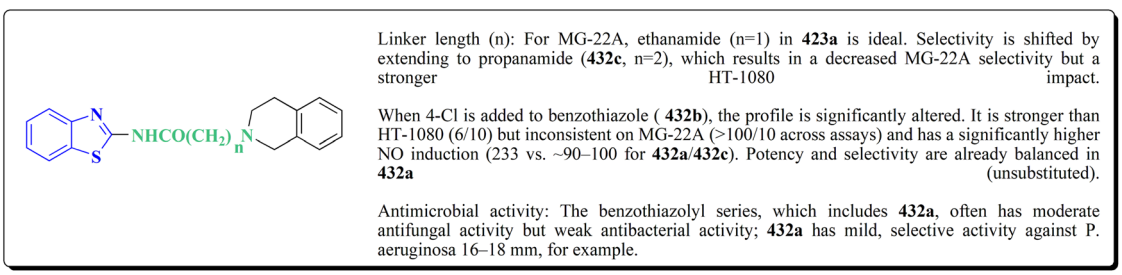


Fig. 67 Structure–activity relationship of compound **432**.

A mixture of mono-adducts **419a–d** and di-adducts **420a–d** were accessed from the reaction of benzofuroxan **418** and 2-aminobenzothiazole derivatives (Scheme 87; Fig. 62).[244]

**9.1.7. Pyrrole–benzothiazole based analogues.** New derivatives containing an electron-donating *N*,*N*-dimethylaminophenyl ring connected to an electron-withdrawing benzothiazole or benzothiazolium moiety *via* a heteroaryl system and up to two ethenylene groups have been prepared. Benzothiazolium derivatives **423** were acheived from carbaldehydes **322** and compounds **421** (Scheme 88).

The antimicrobial activities of the compounds were estimated against unicellular organisms. The 3-alkylbenzothiazolium salts exhibited high toxicity against different tested microbes.[245]

The antimicrobial potency is due to the cationic charge of the benzothiazolium core that disrupts the cell membranes of the bacteria. Also, the lipophilic alkyl chain enhances cellular uptake. The D–π–A conjugation facilitates the charge transfer, and cause interference with the microbial redox systems (Fig. 63).

## 9.2. Benzothiazoles linked with substituted aromatics

An effective Ru-catalyzed *ortho*-oxidative alkenylation of 2-arylbenzo[*d*]thiazoles *via* twofold C–H bond functionalization in

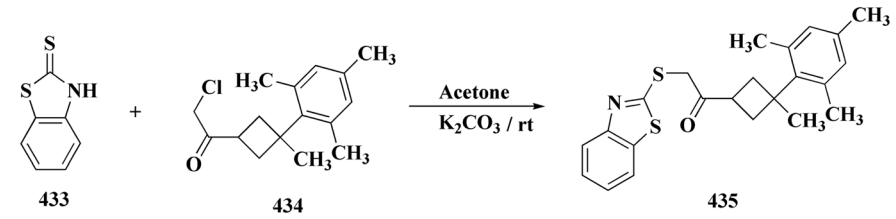


433 434 435

Scheme 93 Synthesis of 2-(benzo[*d*]thiazol-2-ylthio)-1-((1*S*,3*S*)-3-mesityl-3-methylcyclobutyl) ethan-1-one.

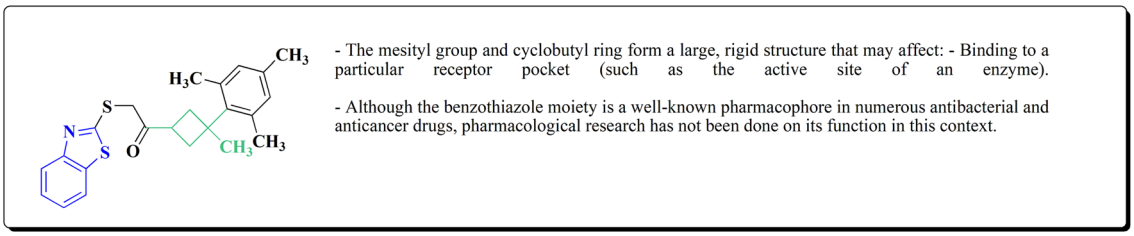


Fig. 68 Structure–activity relationship of compound **435**.

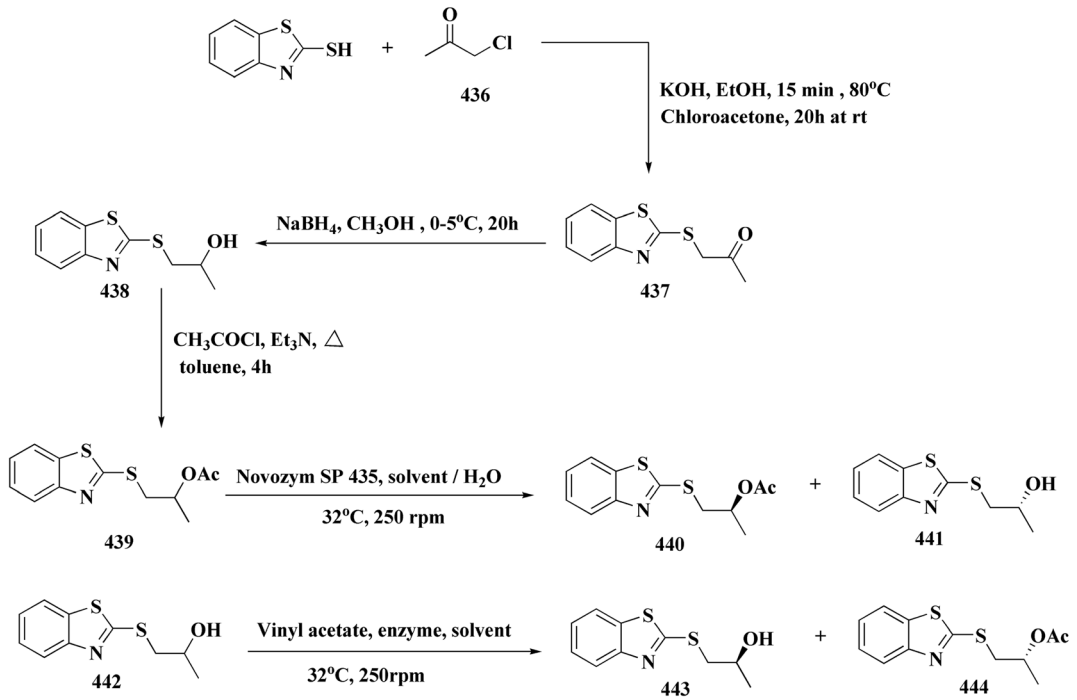


Scheme 94 Synthesis of 1-(1,3-benzothiazol-2-ylsulfanyl)propan-2-ol.

aqueous solution of anionic surfactant sodium dodecylbenzenesulfonate (SDBS) has been developed using activated olefins as coupling partner (Scheme 89; Fig. 64).[246]

The sulfonamide has been prepared (Scheme 90; Fig. 65) and screened for antibacterial activity. It was found to be highly potent (MIC value 50–3.1 μg $mL^{-1}$) against various human pathogens, and most effective against *E. coli*.[247]

Compound **428** exhibits broad-spectrum antibacterial activity, particularly against Gram-negative bacteria. Compound **428**'s SAR pattern demonstrates support for enhancing binding by using electron-withdrawing *para*-substituents on the sulfonyl phenyl group while maintaining the benzothiazole ring.[247]

2-Aminobenzothiazolium-4-methylbenzenesulphonate (ABPTS) was synthesized as accomplished in Scheme 91. The antifungal and antibacterial activities of synthesized complex were examined against different fungi and bacteria strains. The free radical scavenging activity of the complex has been identified against ABTS, DPPH, and OH radicals (Fig. 66).[248]

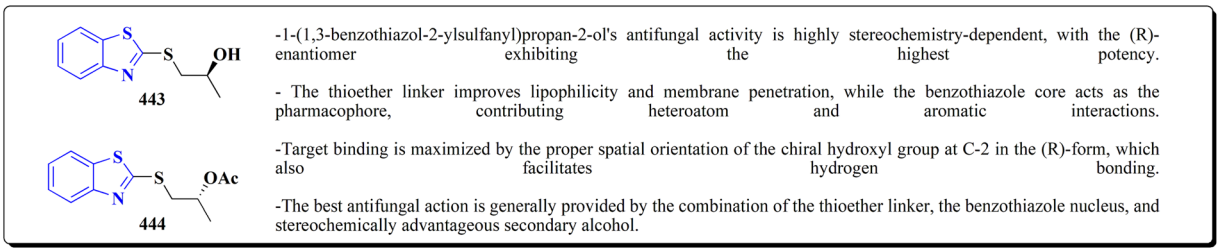


Fig. 69 Structure–activity relationship of compound 443 & 444.

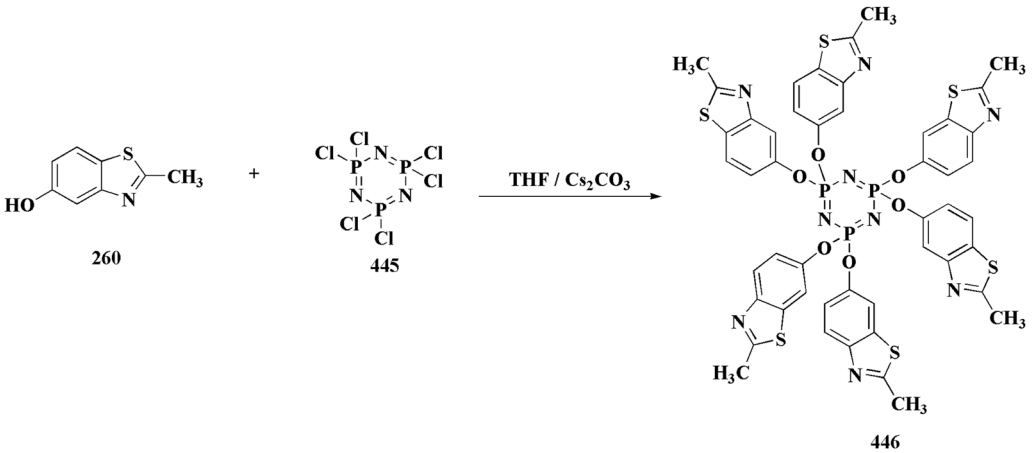


Scheme 95 Synthesis of cyclotriphosphazene derivatives.

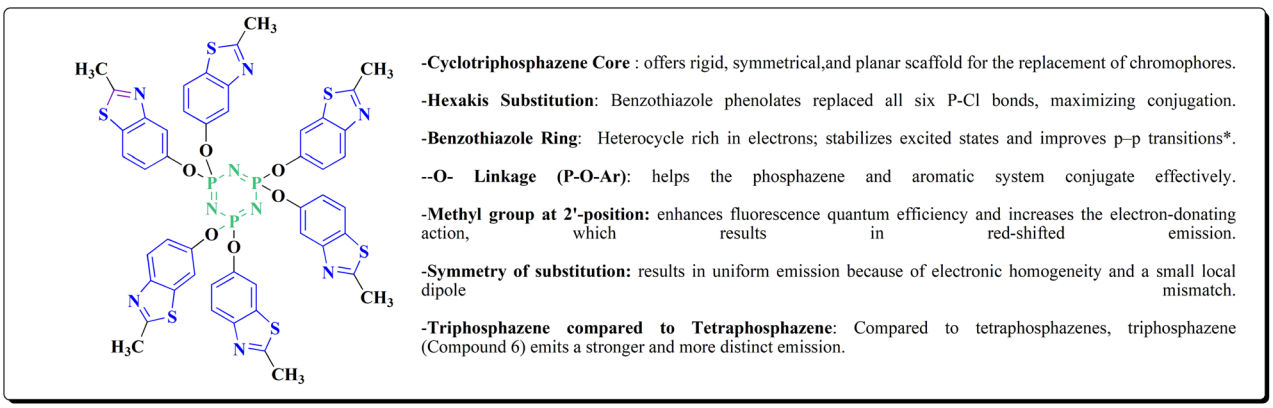


Fig. 70 Structure–activity relationship of compound 446.

Proteus sp., *P. aeruginosa*, *S. aureus*, *Aspergillus flavus*, *A. fumigatus*, and other bacteria are significantly inhibited by ABPTS.

Regarding the binding of DNA, the hypochromism was evident in the absorption titration using CT-DNA; the binding constant, $K_b = 3.6 \times 10^4\ M^{-1}$ as intercalative binding.

Dose-dependent cleavage of supercoiled pBR322 DNA into linear and nicked forms was demonstrated by agarose gel electrophoresis, which is compatible with intercalative/oxidative DNA disruption. Concerning the activity of antioxidants: ABPTS efficiently scavenged DPPH, hydroxyl, and ABTS radicals; its redox activity was confirmed by published $IC_{50}$ values and comparison to ascorbic acid.[248]

The synthesis of compounds **432** is accomplished in Scheme 85. The strategy for the synthesis of dihydroisoquinolin-2(1*H*)-yl]alkanamides **432** involved the synthesis of the propanamido intermediates **431a–c**, which were utilized as alkylating agents in reaction with 1,2,3,4-tetrahydroisoquinoline to give the targeted compounds (Scheme 92). The compounds were found to be potent in psychotropic, anti-inflammatory and cytotoxicity *in vitro* screening. They have obvious sedative action, show high antiinflammatory potency, have selective cytotoxic effects and



 

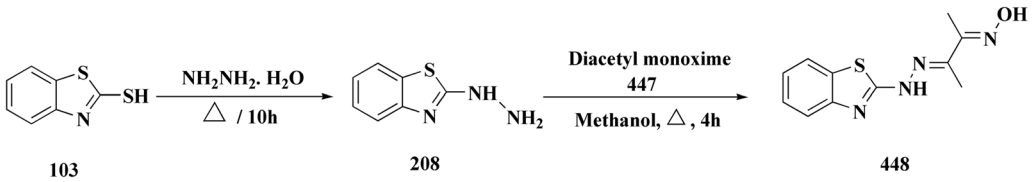


Scheme 96 Synthesis substituted benzothiazol-2-yl hydrazine **448**.

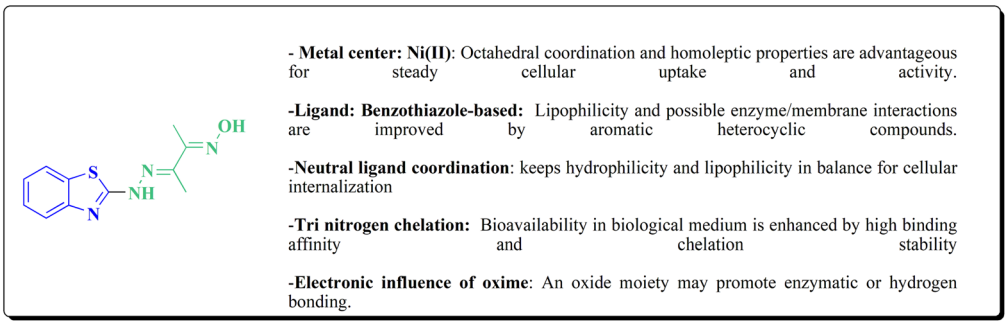


Fig. 71 Structure–activity relationship of compound **448**.

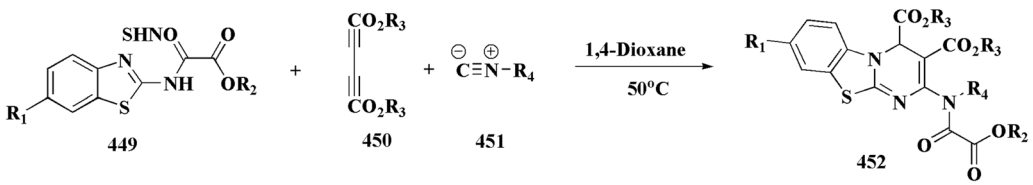


Scheme 97 Synthesis of functionalized benzo[4,5]thiazolo[1,2-*a*]pyrimidines **452**.

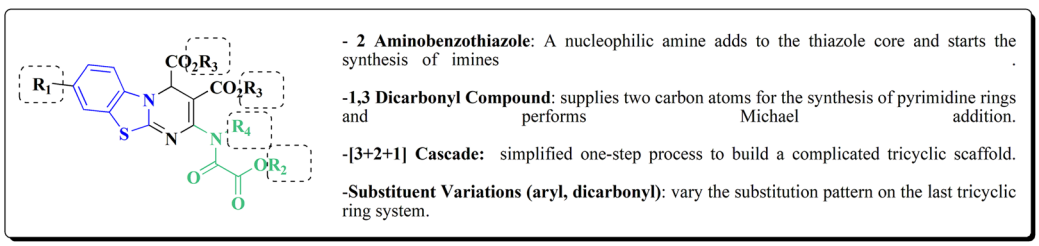


Fig. 72 Structure of compound **452**.

nitric oxide (NO) induction ability regarding tumour cell lines. Some of the compounds synthesized exhibit antimicrobial activity.[249]

The compounds was synthesized by using an amide spacer to join a 3,4-dihydroisoquinoline fragment, which is present in a number of biologically active alkaloids, with a 1,3-benzothiazole moiety, which is known for its anticancer and antibacterial properties. The goal of this design was to generate a single structure that combined the pharmacological potential of both heterocyclic systems (Fig. 67).

The most effective motif for MG-22A in terms of tumor cytotoxicity is benzothiazole linked to a short linker (**432a**); ring substituents (**432b**) change selectivity and NO signaling, while lengthening the linker (**432c**) changes potency toward HT-1080 and antifungal properties (Fig. 66).[249]

2-(Benzo[*d*]thiazol-2-ylthio)-1-((1*S*,3*S*)-3-mesityl-3-methylcyclobutyl) ethan-1-one was synthesized as shown in Scheme 93 (Fig. 68).[250]

The reaction of chloroacetone **436** with potassium hydroxide activated 1,3-benzothiazol-2-thiolate afforded the ketone **437**. The reduction of the latter generated 1-(1,3-benzothiazol-2-ylsulfanyl)propan-2-ol. In order to synthesize an analytical standard of racemic resolution product, racemic alcohol was esterified with acetylchloride. This procedure yielded racemic acetyl ester (Scheme 94).

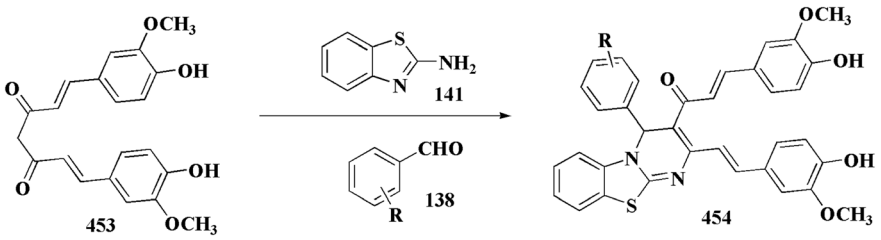


Scheme 98 Synthesis of pyrimido[2,1-*b*]benzothiazole derivatives.

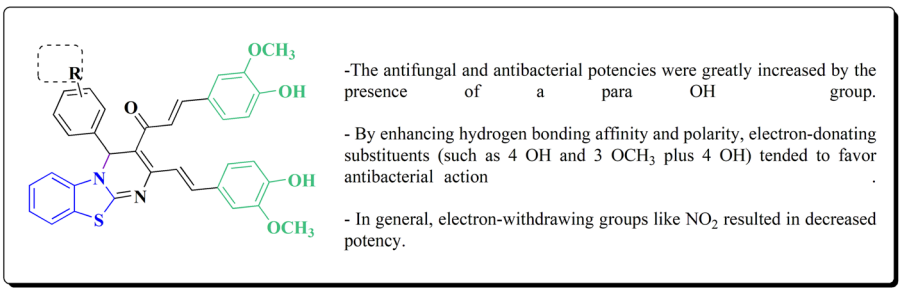


Fig. 73 Structure–activity relationship of compound **454**.

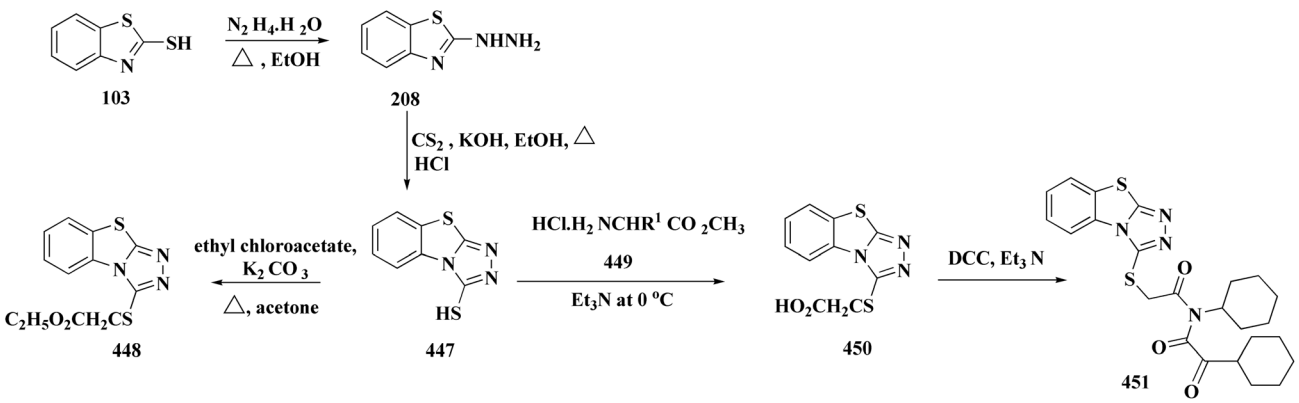


Scheme 99 Synthesis of *s*-triazolobenzothiazolylthioacetyl/propionyl amino acid derivatives.

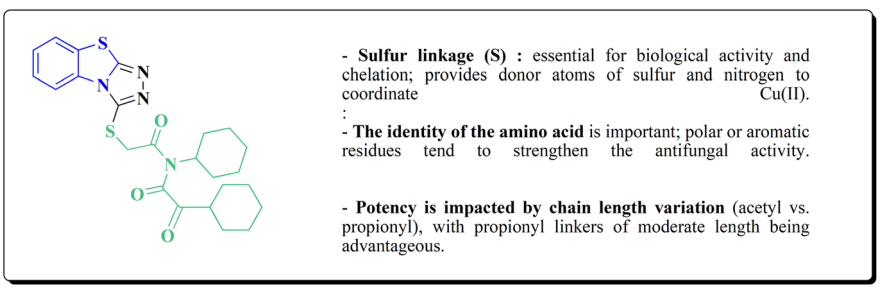


Fig. 74 Structure–activity relationship of compound **451**.

Chemoenzymatic synthesis of the two enantiomers of 1-(1,3-benzothiazol-2-ylsulfanyl)propan-2-ol was performed (Fig. 69). Different lipase preparations were examined as bio-catalysts in the kinetic resolution process of desired compound *via* enantioselective transesterification and/or hydrolysis. It was discovered that CAL-B (Novozym 435) was the ideal catalyst. It seemed that the lipase-mediated hydrolysis method was better than the transesterification procedure.[251]

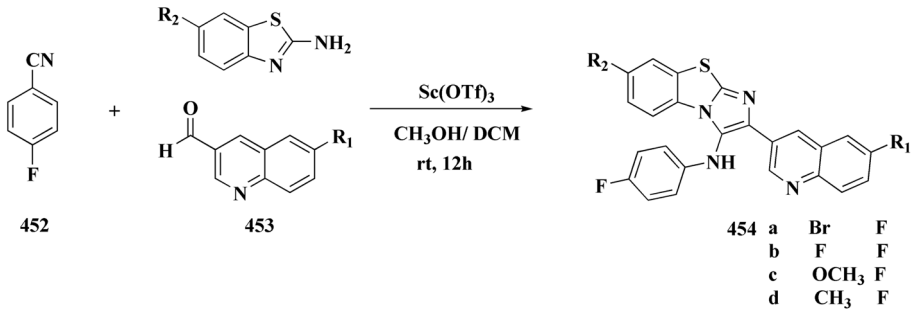


Scheme 100 Synthesis of imidazobenzothiazole–quinoline conjugates.

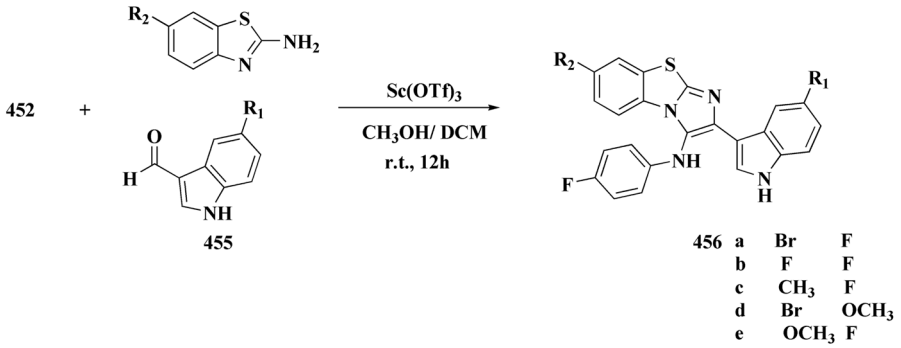


Scheme 101 Synthesis of synthesis of imidazobenzothiazole–indole conjugates.

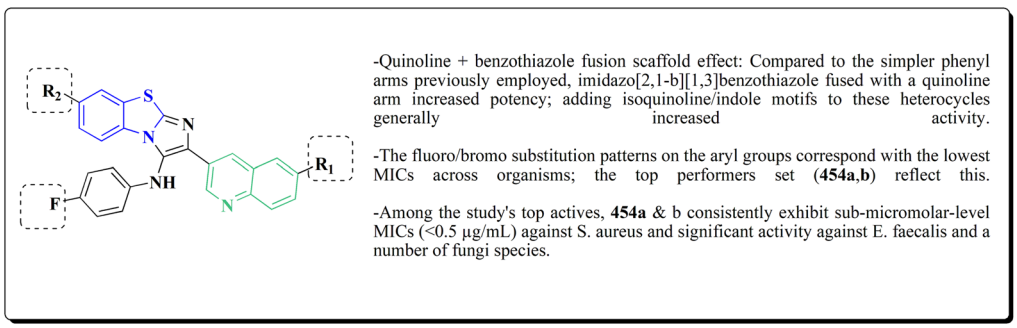


Fig. 75 Structure–activity relationship of compound 454.

### 9.3. Cyclotriphosphazene–benzothiazole based analogues

The cyclotriphosphazene derivatives **446** were prepared from the reactions of hexachlorocyclotriphosphazatriene **445** with 5-hydroxy-2-methylbenzothiazole **260** (Scheme 95). The fluorescence assets of these cyclophosphazene analogs **446** were evaluated in tetrahydrofuran solution.[252]

In comparison to the thiadiazole analogues, the benzothiazole-substituted cyclotriphosphazene based on triphosphazene core showed a noteworthy emission maximum and increased intensity of fluorescence emission. This implies that benzothiazole rings' π-rich aromaticity and advantageous electronicle interactions boost photoluminescence (Fig. 70).

Benzothiazole scaffold reduces non-radiative decay and produced a stronger emission, probably as a result of improved π-conjugation. Compared to tetraphosphazene analogues, triphosphazene cores tended to produce more distinct emission peaks, maybe as a result of tighter, symmetrical replacement that improved photophysical uniformity.

All results are measured in THF; aggregation or solvent–solute interactions may cause emission behavior to change in polar *versus* nonpolar solvents.[252]

The 3-(hydroxyimino)-2-butanone-2-(1*H*-benzimidazol-2-yl) hydrazone and 3-(hydroxyimino)-2-butanone-2-(1*H*-benzothiazol-2-yl)hydrazine are synthesized *via* condensing 2-hydrazino-benzothiazole/benzimidazole with diacetyl monoxime (Scheme 96). The complexes have been investigated for their NCI-60 Human Cancer Cell Line anticancer screening. Sequently, the nickel complex of benzothiazole core is utilized for one dose growth inhibition screening. The complex has

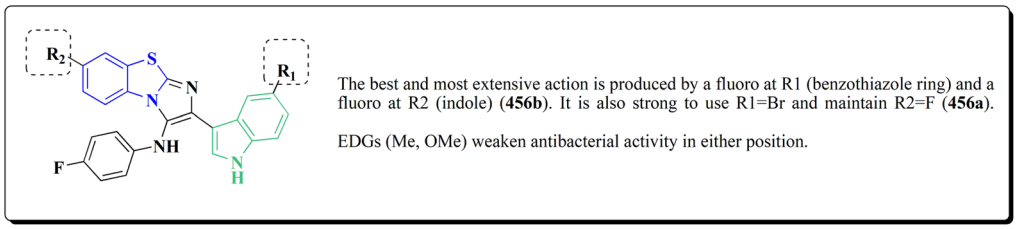


Fig. 76 Structure–activity relationship of compound 456.



indicated highest growth inhibition over a Non-Small Cell Lung Cancer cell line EKVX. Additionally, the compounds were screened for their antifungal and antibacterial activities. The complexes have indicated promising antimicrobial activities (Fig. 71).[253]

### 9.4. Benzothiazoles fused with heterocyclic compounds

**9.4.1. Benzothiazoles fused with six-membered ring heterocycles.** The synthesis of the tricyclic fused pyrimidine derivatives was shown in Scheme 90. A three-component cyclization using *N*-(benzothiazol-2-yl)amide, isocyanides and dialkyl acetylenedicarboxylates generating functionalized benzo[4,5]thiazolo[1,2-*a*]pyrimidine was reported (Scheme 97).[254]

The choice of aryl glyoxal or 1,3 dicarbonyl components results in structural variation; replacement affects the final tricycle's yield and electronic nature. The structural insights provide helpful SAR-style reasoning for synthetic application, notwithstanding the lack of bioactivity reported (Fig. 72).[254]

Pyrimido[2,1-*b*]benzothiazole **454** derivatives of curcumin have been prepared under solvent and solvent free conditions in microwave (Scheme 98). The synthesized compounds were tested for their anti-fungal activity against fungi and anti-bacterial activity against gram (+ve) and gram (−ve) bacteria.[255]

In microbial cells, membrane insertion and potential enzyme target binding are most likely caused by the benzothiazole–pyrimidine tricyclic core. The planar heterocycle and electronic distribution of the scaffold may facilitate interactions with nucleic acids or active site pockets in bacteria or fungi; the *para* OH substituent may allow for improved hydrogen bonding to microbial enzymes or cell wall/membrane components (Fig. 73).

**9.4.2. Benzothiazoles fused with five-membered ring heterocycles.** *s*-Triazolobenzothiazolylthioacetyl/propionyl

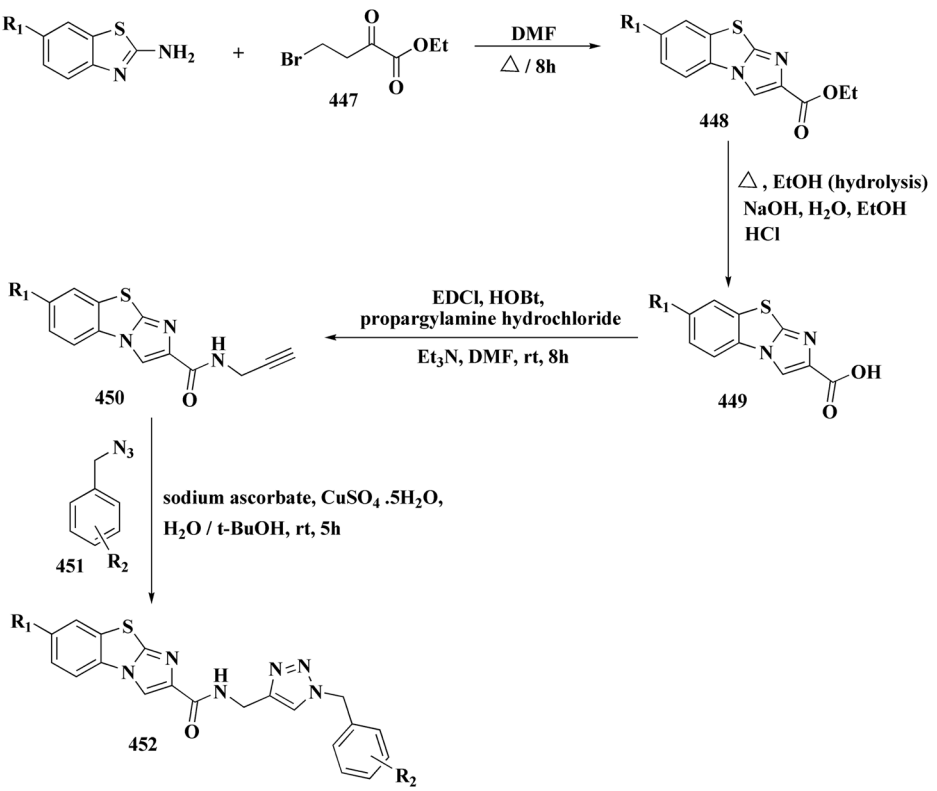


Scheme 102 Synthesis of 1,2,3-triazolo linked benzo-imidazothiazole conjugates.

amino acid derivatives were prepared as outlined in Scheme 99. The synthesized compounds were screened for their anti-fungal activity against *Candida albicans* and *Aspergillus flavus*. Compounds **447** were found to have high activity against *C. albicans* as compared to fluconazole at 100 mg $mL^{-1}$.[256]

The triazolobenzothiazole scaffold targets fungal melanin production or membrane integrity by imitating the well-known fungicide tricyclazole. The amino acid moiety and S Linker may improve target selectivity and cellular absorption. Selective binding to fungal enzymes or cell wall constituents may be facilitated by fluorency or polar side chains. These compounds present possible triazole-drug analogs for the development of antifungal agents (Fig. 74).[256]

Compound were reacted with quinoline carboxaldehyde derivatives **453** followed by reaction with the fluorophenyl isocyanide **452** to afford the polycyclic compounds **454**. The reaction of aminobenzothiazole with indole carbaldehyde **445** followed by the addition of isocyanide **452**, afforded compounds **456** (Schemes 100 & 101).

Their anti-microbial potencies were estimated against several Gram (+ve), Gram (−ve) bacteria and fungi. Compounds **454a**, **454b**, **456a** and **456b** showed strong inhibition of the estimated fungal and bacterial strains comparable to control antibiotics cefixime and amoxicillin and the anti-fungal agent fluconazole (Fig. 75 and 76).[257]

The 1,2,3-triazolo linked benzo-imidazothiazole conjugates **452** were prepared as outlined in Scheme 102.[258] Refluxing 2-aminobenzothiazoles derivatives with the ethylbromopyruvate **447** in DMF generated compound **448**, which upon sodium hydroxide mediated ester hydrolysis afforded compound **449**. These were reacted with propargylamine hydrochloride under nitrogen atmosphere to access the terminal alkynes **450**. The targeted compound **452** was afforded by exposing benzo-imidazothiazole terminal alkynes **450** to the benzyl azides **451**.

Compounds **452** tested for their cytotoxic potency against some human cancer cell lines. Preliminary results showed that compounds **452** ($R^1$ = H, $R^2$ = 4-F) and **452** ($R^1$ = Me, $R^2$ = 4-F) displayed effective antiproliferative effect against human breast cancer cells (MCF-7) with $IC_{50}$ values of 0.60 and 0.78 μM.[258]

The assessed cytotoxic activity of a novel class of 1,2,3-triazolo linked benzo[*d*]imidazo[2,1-*b*]thiazole conjugates was reported. The human breast cancer cell line (MCF-7) was significantly cytotoxically affected by conjugates **452** ($R^1$ = H, $R^2$ = 4-F) and **452** ($R^1$ = Me, $R^2$ = 4-F) (Fig. 77). Based on these scaffolds, the SAR offered a useful insight for generating better leads. These conjugates result in cell cycle arrest at the $G_2$/M phase, according to the flow cytometric study. The existence of elevated tubulin and cyclin B1 protein levels in the soluble portion of cells is in good agreement with the suppression of tubulin polymerization. Additionally, they successfully prevent

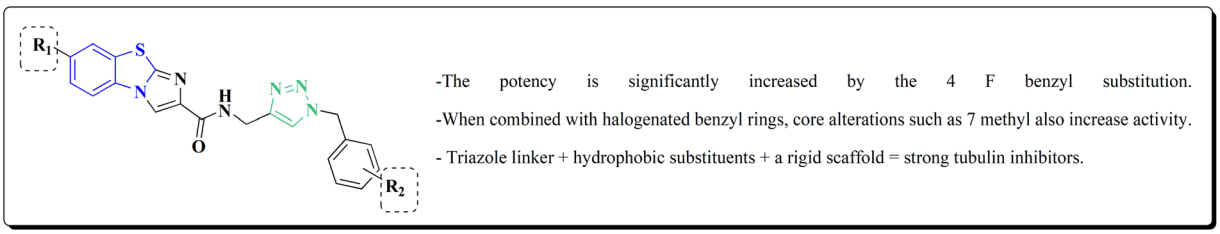


Fig. 77 Structure–activity relationship of compound **452**.

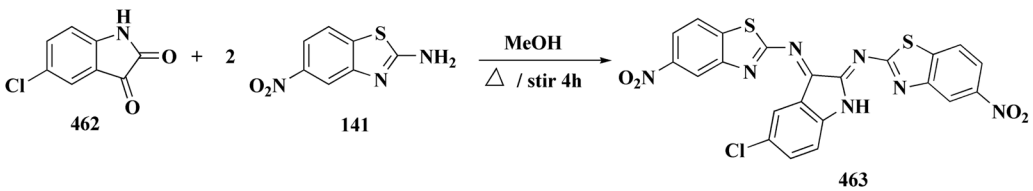


Scheme 103 Synthesis of indoline-2,3-diylidene-benzothiazole conjugates.

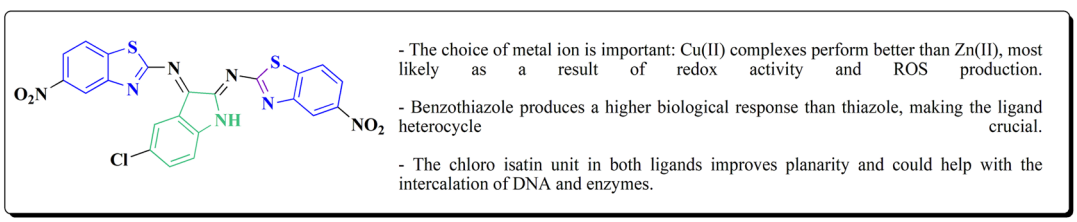


Fig. 78 Structure–activity relationship of compound **463**.

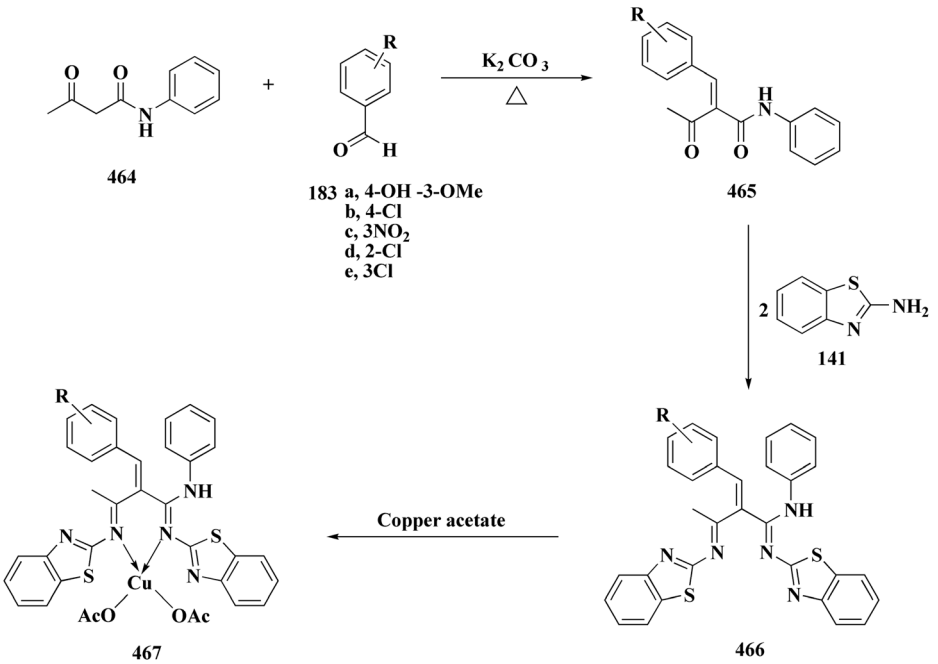


Scheme 104 Synthesis of copper complexes of 2-aminobenzothiazole derivatives.

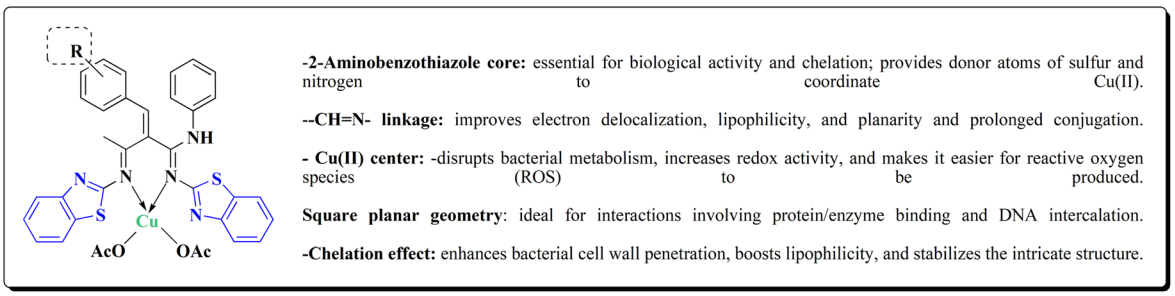


Fig. 79 Structure–activity relationship of compound 467.

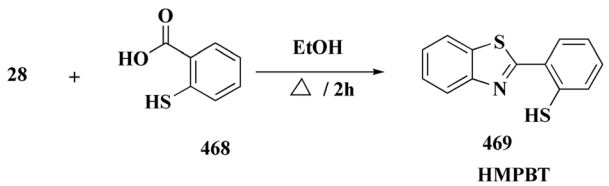


Scheme 105 Synthesis of (HMPBT) ligand.

microtubule assembly and interfere with the architecture of microtubules in breast cancer cells. These conjugates bind at the tubulin's colchicine site, according to molecular docking studies. Annexin V FITC test and mitochondrial membrane potential are linked to the induction of apoptosis. These conjugates may therefore be regarded as promising scaffolds that aid in the discovery of novel leads for breast cancer chemotherapy.[258]

### 9.5. Benzothiazole complexes

New bioactive 5-chloro isatin based Schiff base ligands **463** derived from 5-nitrobenzo[*d*]thiazol-2-amine and 5-nitrothiazol-2-amine and their metal complexes have been prepared (Scheme 103).

*In vitro* antibacterial investigations were performed against various bacterial strains and scavenging activity against standard control at several concenterations unfolded pronounced anti-bacterial and radical scavenging activities of the metal complexes comparable to free ligands. Additionaly, *in vitro* cytotoxicity of ligands and its metal complexes was screened on MCF7, HepG2, and HeLa cell lines and normal cells (peripheral blood mononuclear cells, PBMC). The antiproliferative outcomes showed that metal complexes display superior activity comparable to free ligands **463** where metal complexes of 5-chloro isatin-linked benzothiazole motif **463** are showed potency as chemotherapeutic agents (Fig. 78).[259]

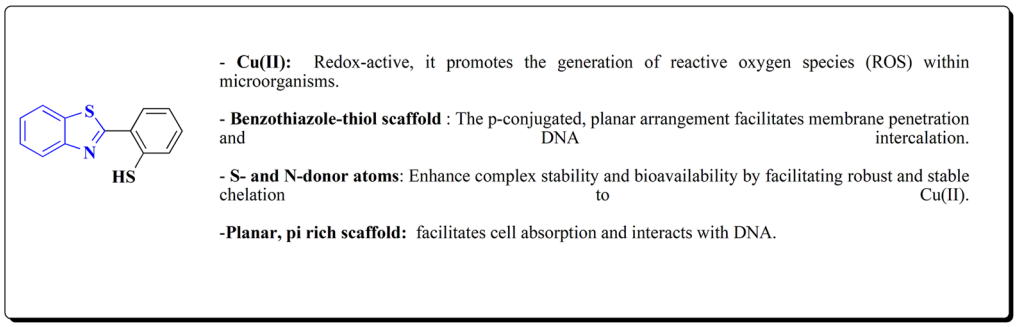


Fig. 80 Structure–activity relationship of compound 469.

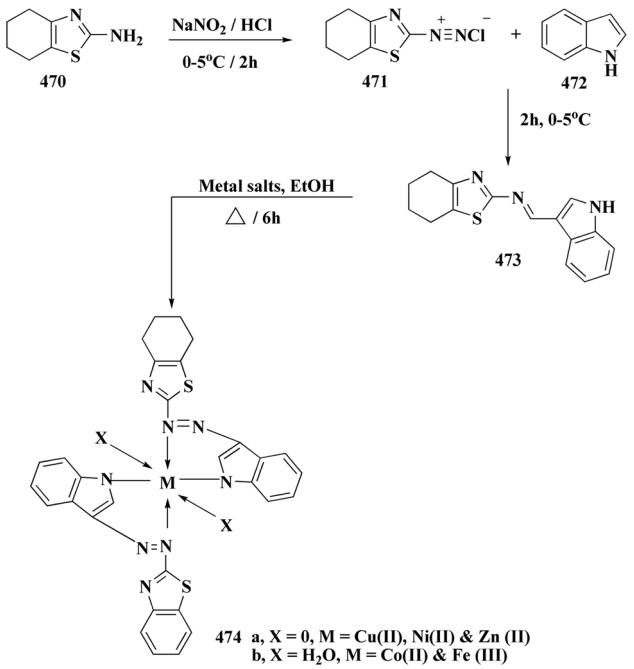


Scheme 106 Synthesis of 2-(1*H*-indol-3-yldiazenyl)-4,5,6,7-tetrahydro-1,3-benzothiazole complexes.

The Cu(II) core and the benzothiazole-containing Schiff-ligand, supported by planar isatin architecture, are necessary for optimal activity.[259]

New copper complexes of 2-aminobenzothiazole derivatives were prepared *via* the condensation of 2-aminobenzothiazole and knoevenagal condensate acetoacetanilide (Scheme 104).[260]

By condensation of the Knoevenagel products with two aminobenzothiazole, followed by a reaction with Cu(II) ions, a series of copper(II) complexes were synthesized.

A variety of Gram-positive and Gram-negative microorganisms were screened for using antibacterial agents. When compared to their free ligands, all Cu complexes demonstrated increased antibacterial activity. For bioactivity, Cu(II)–ligand chelation is essential (Fig. 79). The *para*-position of a methyl group improves electron delocalization throughout the π-system, ligand basicity, and Cu(II) binding.[260]

Novel ligand (HMPBT) ligand is synthesized through the reaction of 2-mercaptoaniline with 2-mercaptobenzoic acid (Scheme 105). The estimated metal complexes and ligand were screened for their *in vitro* anti-microbial potencies against various kinds of bacterial and fungal strains. The results assert on the examined compounds as a highly promising fungicides and bactericides.[261]

Direct DNA interference and oxidative stress are probably both involved in the mechanism. The 2-(2′-mercaptophenyl) benzothiazole copper(II) complex had the most potent antibacterial action against *B. subtilis*, *C. albicans*, *S. aureus*, and *E. coli* (Fig. 80). Viscosity, gel electrophoresis, and UV-Vis titration studies demonstrated a significant DNA-binding affinity.

Several processes are responsible for these complexes' antimirobial action. While the Cu(II) center contributes to oxidative stress by producing reactive oxygen species (ROS), which causes

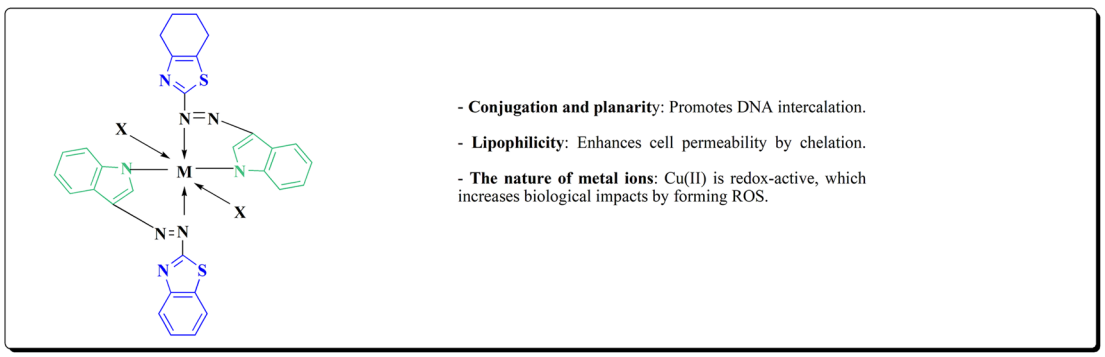


Fig. 81 Structure–activity relationship of compound 474.

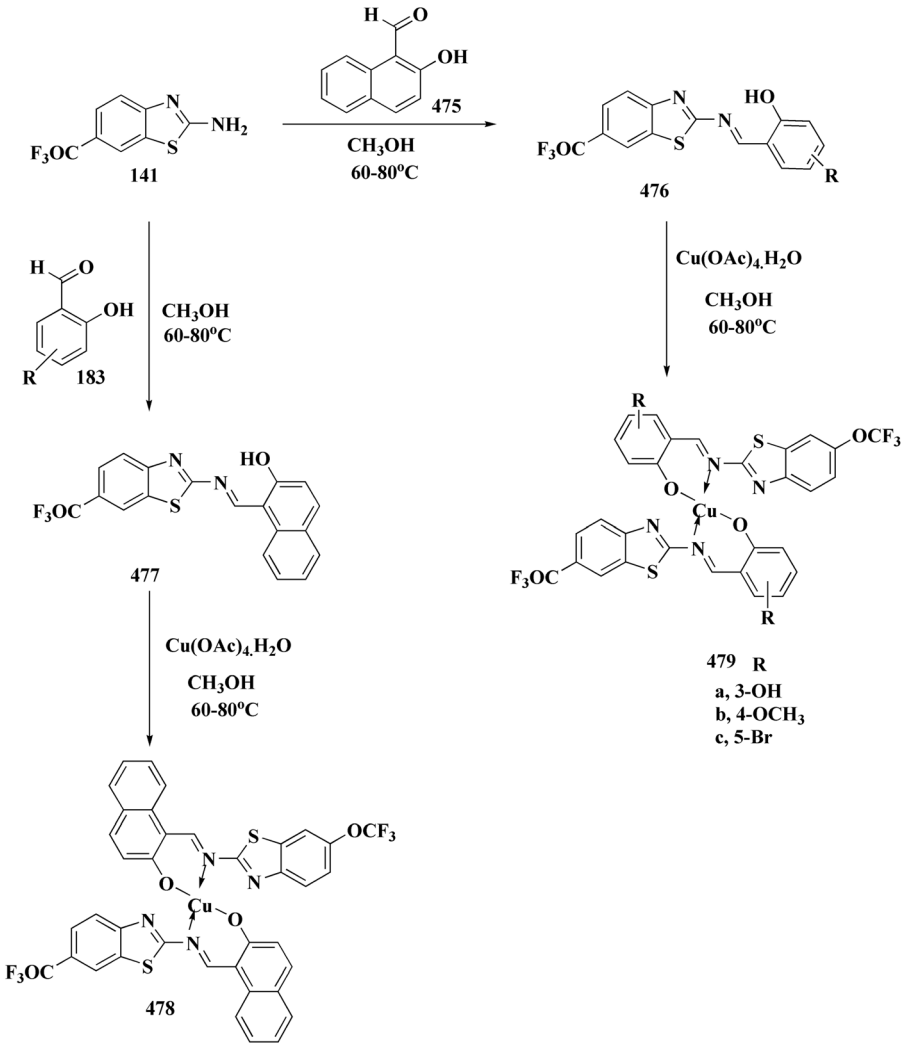


Scheme 107 Synthesis of benzothiazole-based phthalonitrile analogs & tetra substituted metal free phthalocyanines.

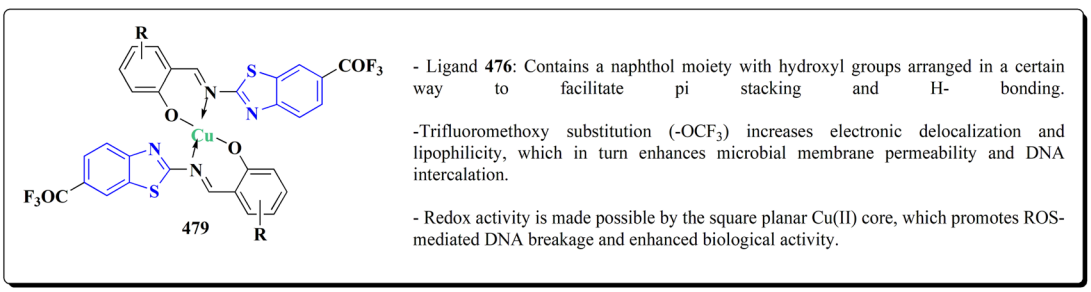


Fig. 82 Structure–activity relationship of compound 479.

oxidative damage of proteins, lipids, and DNA, the lipophilic aspect of the ligand structure encourages rupture of microbial membranes. Additionally, increased cellular uptake and improved bioavailability are made possible by a synergistic interaction between the metal ion and the ligand.

An intercalative binding mode was suggested by the hypochromic effect and minor red shift observed upon DNA addition in the UV-Vis absorption titration. Viscosity experiments, which showed that a rise in DNA viscosity verified base pair insertion, provided more evidence for this. DNA cleavage was directly demonstrated by gel electrophoresis, with Cu(II)-complex showing especially strong action.[261]

The bioactive metal complexes were prepared from the tetrahydro-1,3-benzothiazole (Scheme 106). The synthesized

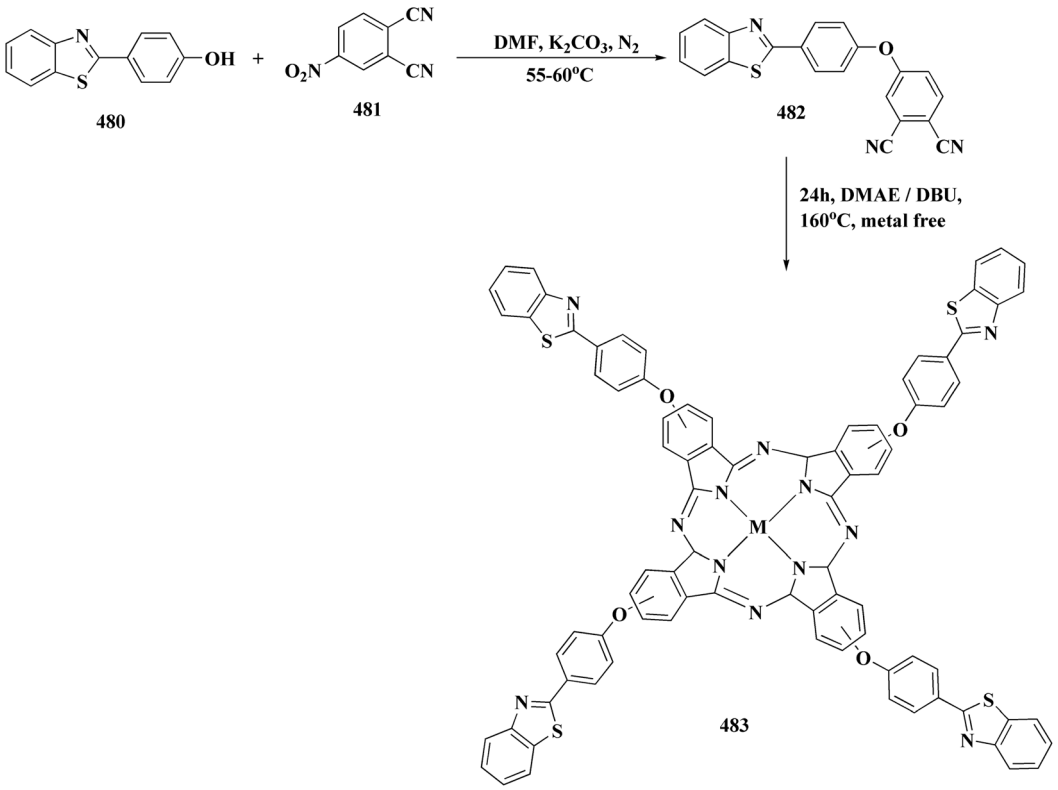


Scheme 108 Synthesis of metal-free & metallophthalocyanines.

compounds displayed antimicrobial potency against tested pathogens. The antimycobacterial potency of the synthesized compounds was studied and all the metal chelates showed higher activity than the free ligand.[262]

The azo-linked indole–benzothiazoline ligand and its metal(II) complexes (Co(II), Ni(II), Cu(II), and Zn(II)) are the main subjects of the investigation. Important mechanistic details and findings: including the mode of ligand binding in which the ligand forms a bidentate chelate ring with the metal ions by coordinating with azo nitrogen (–N=N–) and thiazole nitrogen. Coordination was indicated by FTIR spectra, which verified shifts in $\nu$(N=N) and the disappearance/shift of NH and C=N peaks (Fig. 81).

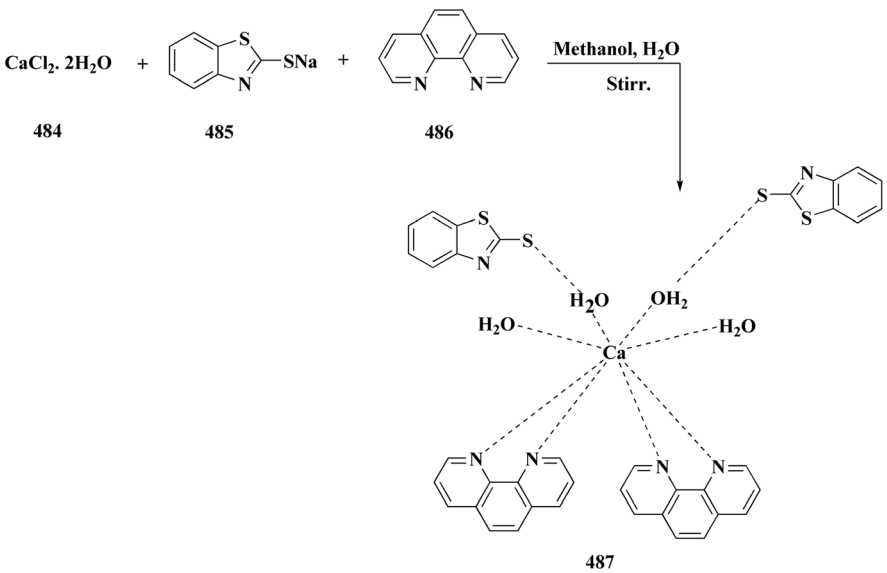


Scheme 109 Synthesis of Ca-complex 487.

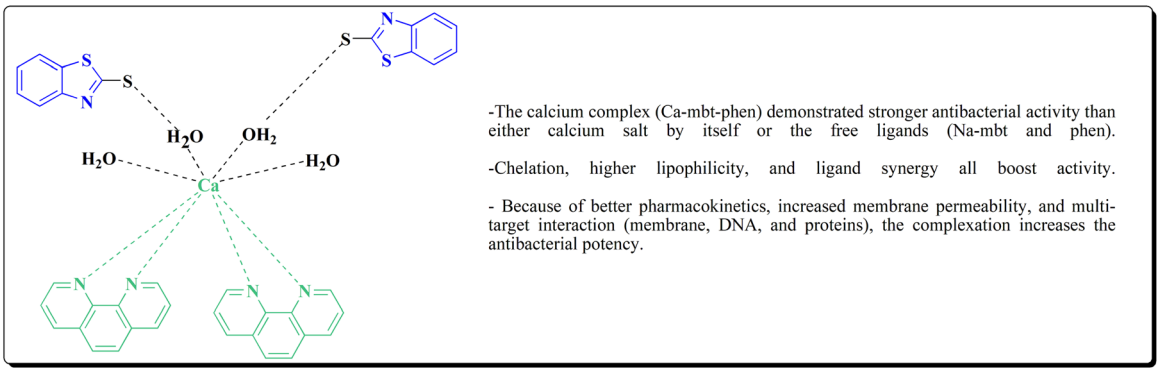


Fig. 83 Structure–activity relationship of compound **487**.

The Cu(II) complex's capacity to produce reactive oxygen species (ROS) through redox cycling ($Cu^{2+}/Cu^{+}$) was responsible for the whole DNA cleavage. The mechanism most likely uses superoxide or hydroxyl radicals to cause oxidative DNA scission.

The antimicrobial mechanism can be explained by the chelation theory, often known as Tweedy's theory, provided an explanation for the metal complexes' increased activity in comparison to the free ligand: chelation increases lipophilicity by decreasing metal ion polarity, which improves complexes' membrane permeability and provides improved intracellular access to biological targets like enzymes or DNA.[262]

The Schiff base ligands, and their binary copper(II) complexes **478** & **479** have been prepared (Scheme 107). After screening the ligands and their Cu(II) complexes against bacterial strains for anti-microbial potency and it was observed that all Cu(II) complexes are more active than corresponding ligands (Fig. 82).[263]

The most active complex in terms of DNA binding and cleavage, as well as antibacterial activity, was complex **479** ($Cu(L^2)_2$). Viscosity measurements, fluorescence titration, and UV-Vis all confirm intercalative binding to CT-DNA, while ifs strongest π–π stacking interactions with base pairs, as evidenced by the highest binding constant and cleavage efficiency among the four complexes. Compared to the ligand and the other complexes, complex **479** shown higher potency against bacterial (*e.g.*, *E. coli*, *P. aeruginosa*, *B.*

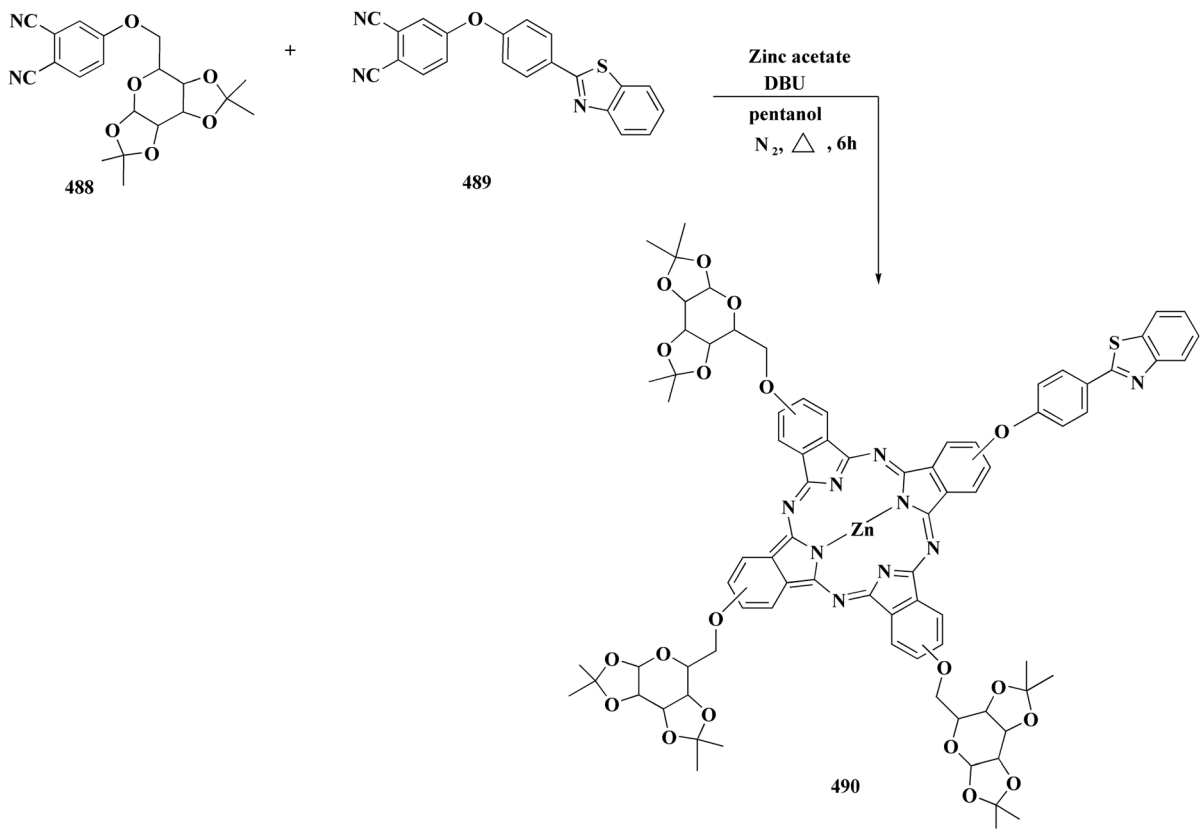


Scheme 110 Synthesis of the complex **490**.

*amyloliquefaciens*, *S. aureus*) and fungal (*S. rolfsii*, *M. phaseolina*) strains.[263]

Benzothiazole-based phthalonitrile analog and its peripherally tetra substituted metal free phthalocyanines have been prepared (Scheme 108). Their fluorescence quenching properties by the addition of 1,4-benzoquinone was also investigated.

The synthesis of 4-(1,3-benzothiazol-2-yl)phenoxy substituted phthalonitrile **482** and its target metal-free and metallophthalocyanines is indicated.[264]

Each tetrakis substituted phthalocyanine had a rigid benzothiazole moiety connected by a 1,4 benzene spacer. This design reduces aggregation and promotes orderly self-assembly behavior by providing steric impediment while maintaining adequate stiffness. The benzothiazole units have two functions: they are directing groups for supramolecular organization and electronic modulators (*via* S and N atoms).

The compounds' red/near-IR fluorescence emissions ranged from mild to strong; the benzothiazole substituents' steric blocking results in less π stacking, which improves the fluorescence quantum yield. The Zn(II) complex was the most appropriate for optical and photophysical applications due to its intense fluorescence, high quantum yield, and decreased aggregation. The Cu(II) complex was not the best for fluorescence-based applications, but it probably showed the strongest photochemical quenching (because of paramagnetism).

By preventing planar π–π stacking, the benzothiazole arms preserve monomeric absorption bands and molecular

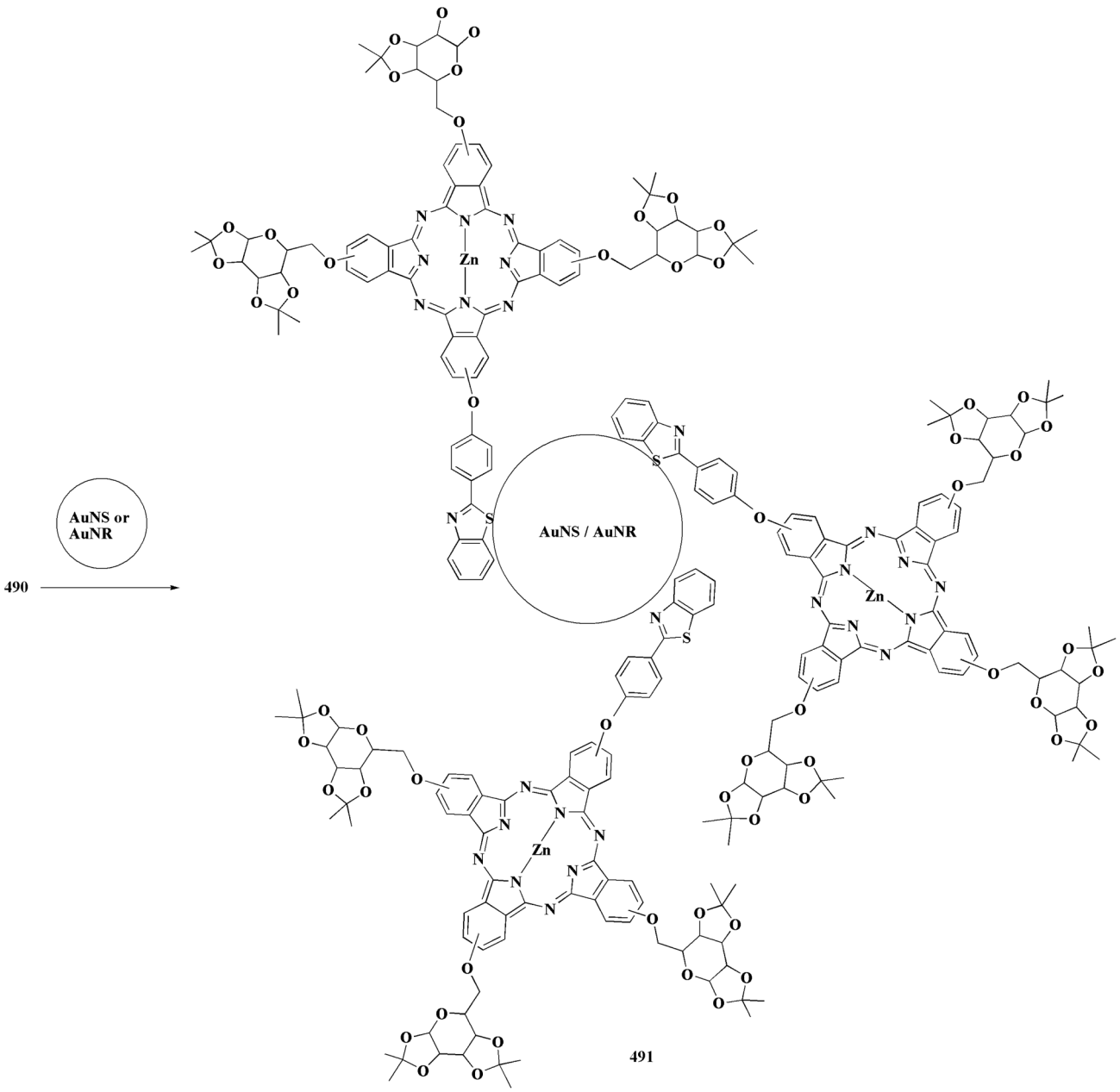


Scheme 111 Synthesis of gold nanospheres (AuNS) and nanorods (AuNR).

- S-Au/N-Au self-assembly was used to generate a glycosylated zinc phthalocyanine (complex **491**) and its conjugated form into gold nanorods (AuNR) and gold nanospheres (AuNS).

-In comparison to free complex **491**, both conjugates (**491**-AuNR and **491**-AuNS) had increased triplet and singlet oxygen quantum yields but decreased fluorescence quantum yield. Crucially, the **491**-AuNR conjugate shown better photophysical characteristics than the **491**-AuNS.

Fig. 84 Structure–activity relationship of compound **491**.



separation. The benzothiazole spacer modifies electron distribution, improving photophysical characteristics including excited-state lifetime and absorption cross-section *via* prolonged conjugation. Self-assembly took place in thin films or aggregates, enabling ordered nano-systems with desired optical properties.

Benzothiazole–phthalocyanine hybrids show promise for photonic applications such as optical limiting and nonlinear absorbers; thin-film optoelectronics, where performance is improved by ordered stacking; and possible scaffolds for supramolecular structures or nanoparticle conjugation.[264]

A novel Ca-complex has been prepared through the reaction of sodium 2-mercaptobenzothiazole, 1,10-phenanthroline and calcium chloride (Scheme 109). The complex was evaluated against various bacterial strains. The complex exhibited good anti-bacterial activity against *Acinetobacter baumanni* and remarkable anti-bacterial activity against *Pseudomonas aeruginosa* as compared to levofloxacin 265.

The synthesis of a new calcium(II) compound and its biological assessment was acccomplished using the sodium 2-mercaptobenzothiazole (Na-mbt), is a bidentate ligand that coordinates *via* nitrogen and sulfur, and 1,10-phenanthroline (phen) which is a planar aromatic bi-dentate ligand with the ability to intercalate DNA and promote biological activity. Mechanism of action most likely comprises enzyme inhibition (mbt ligand), membrane rupture, and DNA binding (phen). The [Ca(mbt)(phen)] complex is the most active molecule because of its optimal metal–ligand geometry and dual ligand effects (Fig. 83).

In order to examine the impact of nanoparticle morphology on photodynamic treatment (PDT) performance, a study presents the synthesis of glycosylated zinc phthalocyanine (ZnPc) coupled to gold nanoparticles (AuNPs) with a variety of geometries (spherical, rod-shaped, and star-shaped).

The synthesis of complex **490** and its linkage to gold nanoparticles (AuNPs) of various shapes *via* S–Au/N–Au self-assembly was accomplished in Schemes 110 & 111. The conjugates of complex **490** with both gold nanospheres (AuNS) and nanorods (AuNR), exhibited decreased fluorescence quantum yield with corresponding enhanced singlet and triplet quantum yields comparable to complex **490** alone, however **491**-AuNR indicated enhanced behavior than **491**-AuNS. Complex **491** revealed comparatively low *in vitro* dark cytotoxicity against the epithelial breast cancer cells with cell survival greater than eightyfive percent at conc. $\leq$160 μg mL$^{-1}$ (Fig. 84).[266]

Cell survival >85% at doses <160 μg mL$^{-1}$ indicated that free complex **491** exhibited comparatively low dark cytotoxicity toward epithelial breast cancer cells. However, its PDT efficacy was decreased, most likely as a result of aggregation. In contrast, at doses $\geq$40 μg mL$^{-1}$, **491**-AuNR reached 50% cell viability. For **491**-AuNS to have the same impact, larger amounts ($\geq$80 μg mL$^{-1}$) were needed. Since nanorods absorb more light at 680 nm than nanospheres do, photothermal effects have

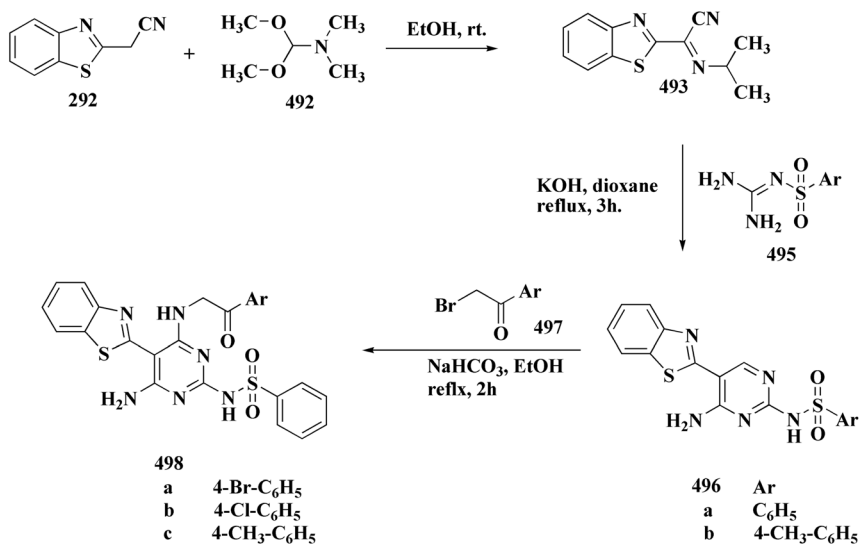


Scheme 112 Synthesis of substituted (pyrimidin-2-yl)benzenesulfonamide.

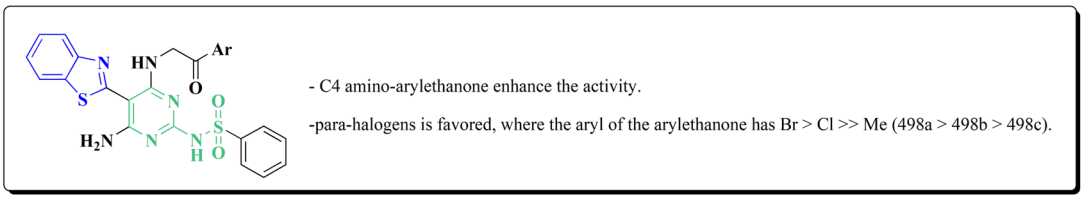


Fig. 85 Structure–activity relationship of compound 498.



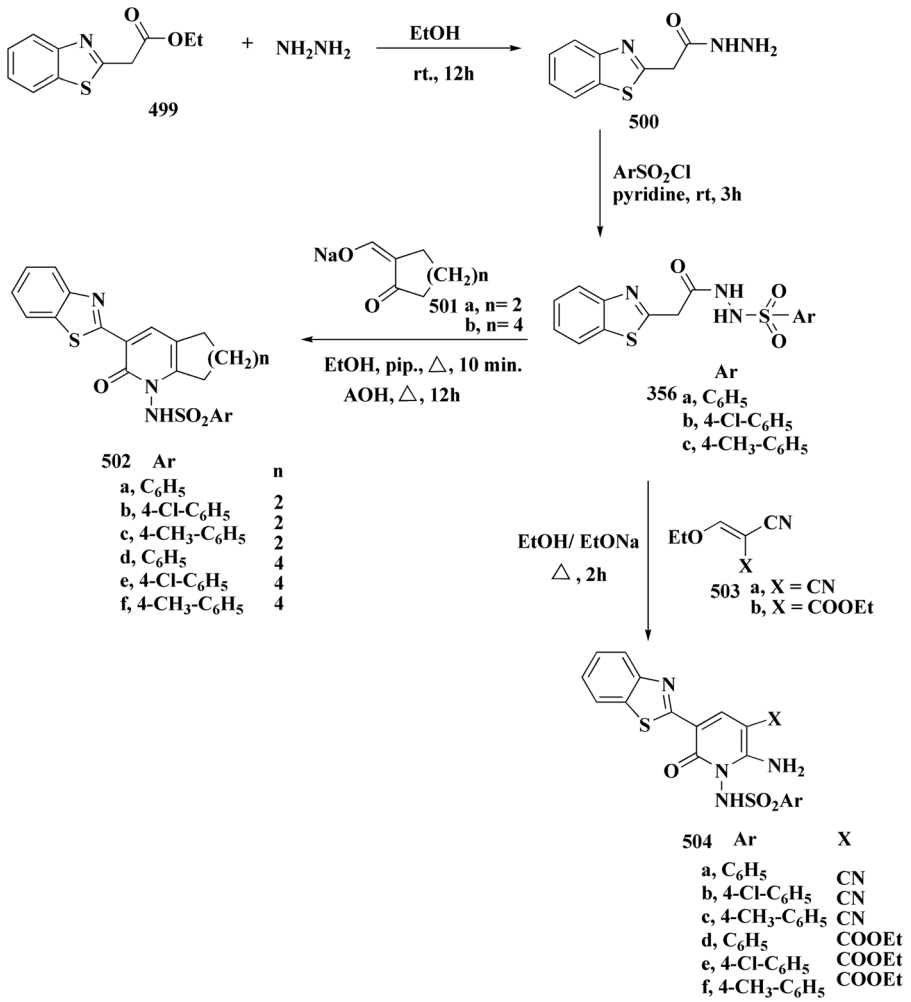


Scheme 113 Synthesis of arylsulfonamides.

been identified as the reason for the higher activity of 491-AuNR.[266]

## 10. Synthetic strategies for novel anti-viral benzothiazoles

### 10.1. Benzothiazoles linked with heterocyclic compounds

The antiviral activity of a novel series of substituted 2-pyrimidylbenzothiazoles with either sulfonamide groups or an amino substituent at the C2 position of the pyrimidine ring was assessed. The core ring system was synthesized by reacting guanidine or *N*-arylsulfonated guanidine with different ylidene benzothiazole derivatives by a Michael addition process (Scheme 112).

A plaque reduction assay against a panel of viruses, including HSV-1, CBV4, HAV (HM175 strain), HCVcc (genotype 4), and HAdV7, was used to evaluate the synthetic compounds' antiviral activity. Notably, compounds **498a** & **498b** showed considerable action against HSV-1, with selectivity index (SI), $IC_{50}$, and $CC_{50}$ values higher than those of acyclovir, and viral inhibition rates ranging from 70% to 90%.

The promise of compound **498a** as a prospective lead anti-viral drug was highlighted by its remarkable broad-spectrum antiviral efficacy against all five tested viruses. Additionally,

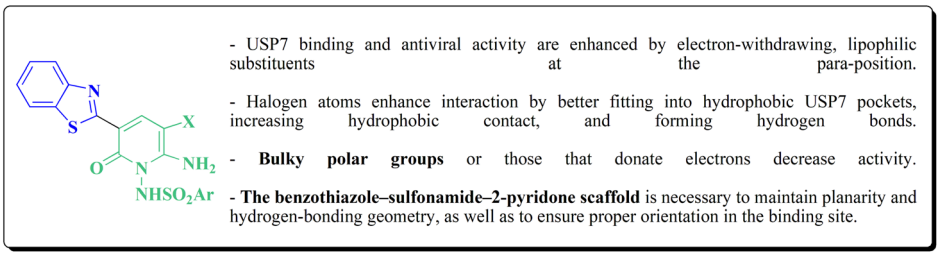


Fig. 86 Structure–activity relationship of compound **504**.

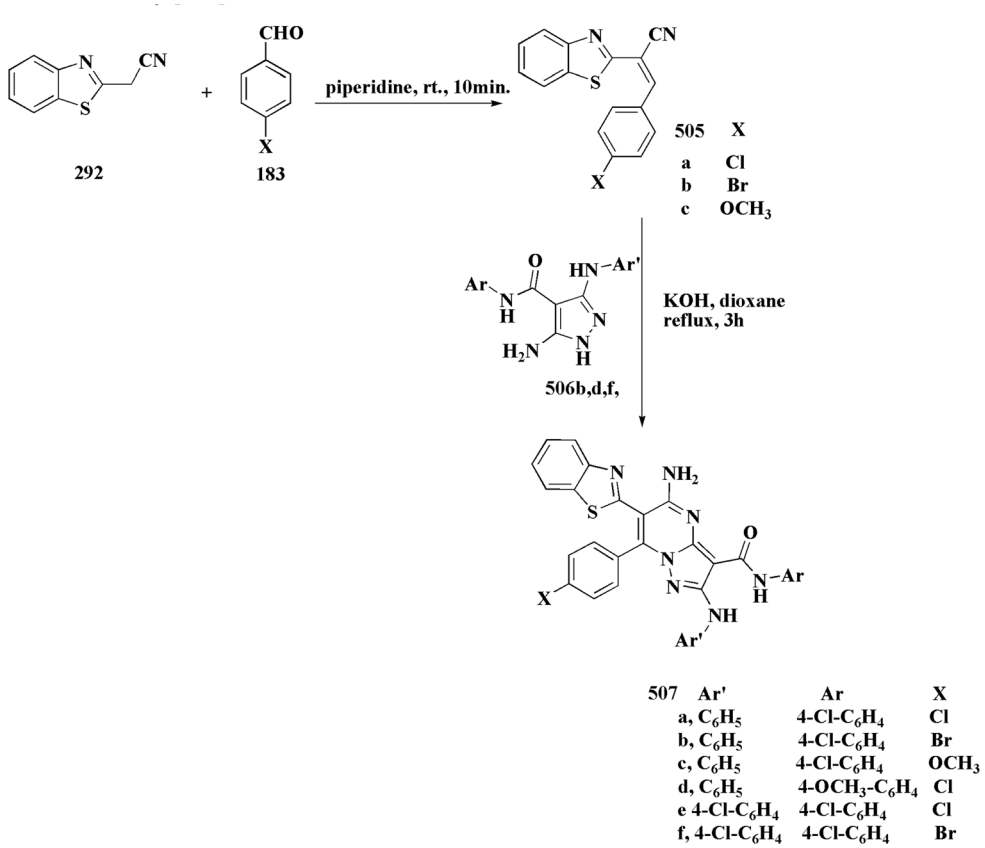


Scheme 114 Synthesis of substituted pyrazolopyrimidines.

with $IC_{50}$ values ranging from 4.87 to 10.47 μg $mL^{-1}$, the strongest anti-HSV-1 compounds—**498a**, & **498b** also inhibited Hsp90α. Curiously, these compounds increased antiviral potency when combined with acyclovir, lowering $IC_{50}$ values compared to acyclovir alone. Molecular docking studies demonstrated that compounds **498a** & **498b** have favorable binding interactions within the Hsp90α active site, confirming their dual function as Hsp90α inhibitors and antiviral agents (Fig. 85).[267]

By reacting benzothiazole sulfonylhydrazide with the sodium salts of hydroxymethylene cycloalkanones, unsaturated ketones, and ethoxymethylene analogues, a new series of benzothiazole-linked *N* sulfonamide 2-pyridone derivatives was synthesized (Scheme 113). Five compounds—**502a**, **502c**, **502e**, **502f**, and **504a**—achieved above 50% viral suppression in *in vitro* antiviral studies against HSV 1, HAV HM175, HCVcc genotype **4a**, CBV4, and HAdV7. The selectivity indices and $CC_{50}$ and $IC_{50}$ values for these lead compounds were computed.

According to an *in silico* assessment of physicochemical properties, all five candidates had plausible cell-permeability and good oral bioavailability. The most effective HSV 1 inhibitors among them were **502e** and **504a**, which also showed detectable inhibition of the USP7 enzyme. Both **502e** and **504a** occupy the USP7 binding pocket and interact strongly with important active-site residues, as further demonstrated by molecular docking (Fig. 86).[268]

Regarding the enzyme inhibition of USP7, the USP7 contributes to the stabilization of viral proteins and the inhibition of p53. Reactivation of host antiviral defenses (*via* p53 reactivation), decreased viral protein stability, and impaired viral DNA replication in infected cells are the results of its inhibition. The compounds form hydrogen bonds and π–π

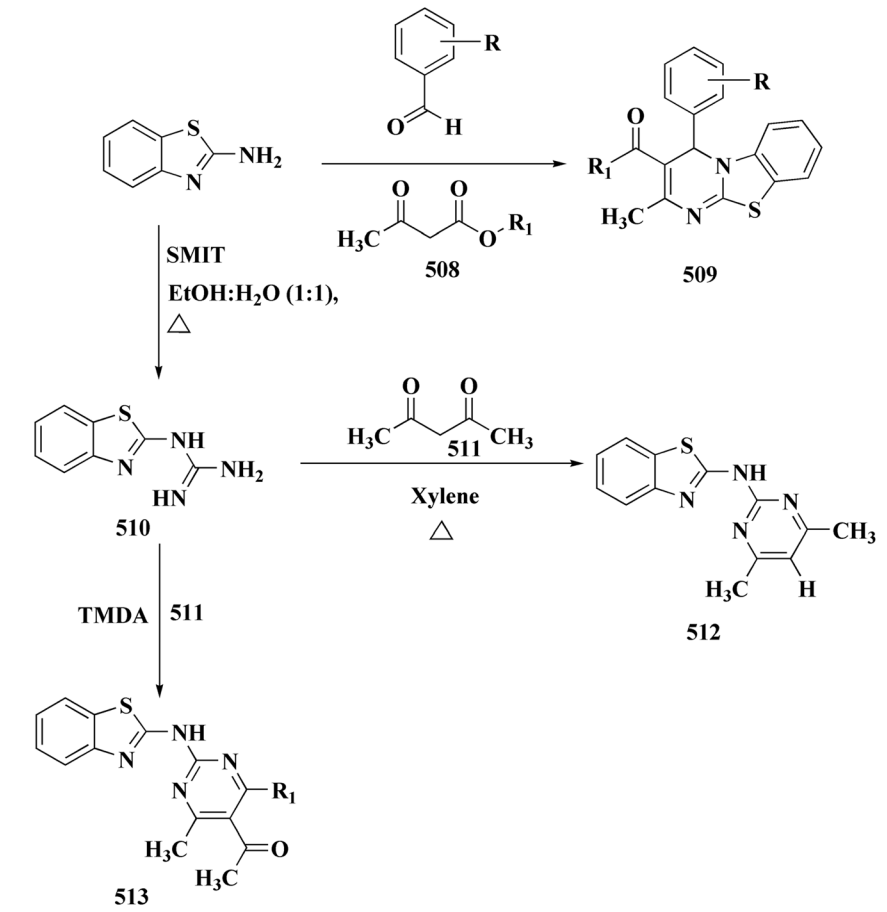


Scheme 115 Synthesis of pyrimidobenzothiazole-3-carboxylate derivatives and substituted aminobenzothiazole.

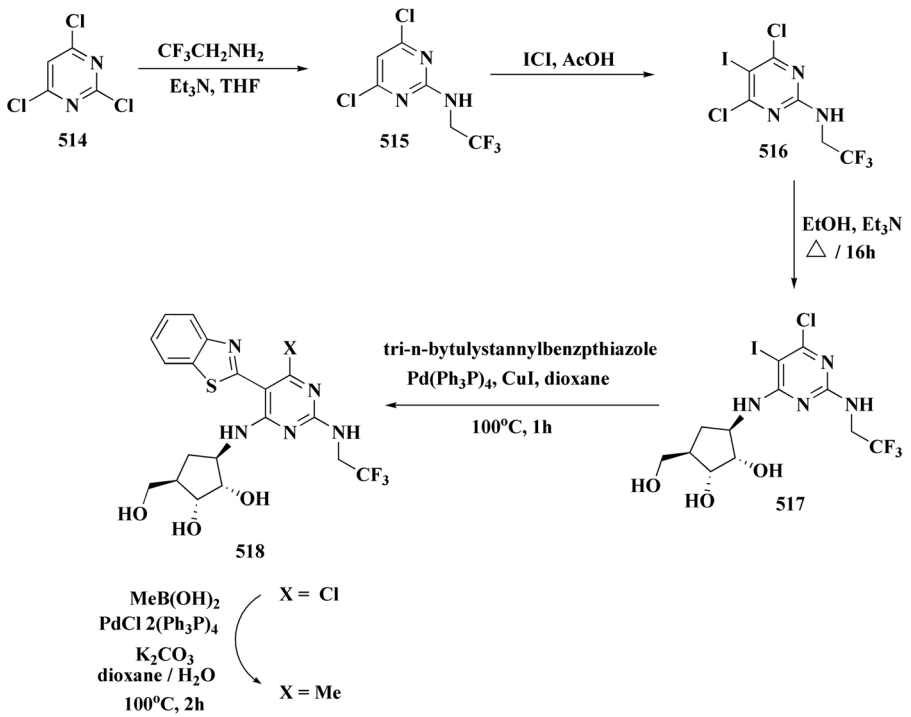


Scheme 116 Synthesis of benzothiazole substituted pyrimidines.

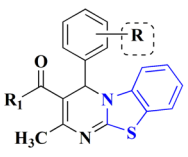


-The meta-nitro (3-$NO_2$) substituent gave the maximum activity among the aryl-substituted derivatives, while compound **509** (ethyl ester, 3-$NO_2$ phenyl) was shown to be the most effective counterpart.

-In the post-QSAR, the fused pyrimidobenzothiazole nucleus with a 2-methyl substituent contributes positively in terms of sterics and electrostatics (as indicated by the S_229 and H_654 descriptors).

-The MLCK/Ca-channel modulation theory is supported by the docking mode, which consists of several van der Waals contacts along with important H-bonds with Lys144, Glu181, and Asp183 (Glide score/energy given).

-Crystallography: **509** supports the designated solid-state conformation by crystallizing in a triclinic lattice with polymeric chain packing.

Fig. 87 Structure–activity relationship of compound **509**.

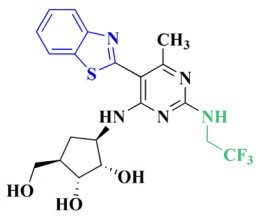


-Compound **518b** has a C-2 trifluoroethylamino group and a C-4 methyl group, making it a 5-benzothiazolyl-substituted pyrimidine derivative.
- Unlike alkynyl or other aryl groups, a benzothiazole moiety at the pyrimidine 5-position is ideal for high anti-HCV potency and good selectivity.
- Small alkoxy and methylamino groups are tolerated, while halo groups at benzothiazole sites lessen efficacy. Potency and metabolic stability are maintained by the unsubstituted benzothiazole, as in **518b**.
- C-4 position: Despite having good PK, larger or bulkier groups (like cyclopropyl) reduce efficacy; small size of the methyl group is ideal. Potency is negatively altered by removing the C-4 substituent or replacing it with Cl.
- C-2 position: Rat plasma exposure and liver concentration are significantly increased by adding a trifluoroethylamino group here without sacrificing efficacy. The effects of other polar or alkyl substituents vary; ether-containing chains are strong but not always PK-favorable, while dimethylamino decreases potency.

Fig. 88 Structure–activity relationship of compound **518**.

stacking with key residues (*e.g.*, Asp295, Gly277, Tyr465) when they bind to the catalytic domain of USP7. Preventing the deubiquitination process, which causes important proteins that support the virus to be broken down by proteases.[268]

By reacting pyrazole carboxamide intermediates with different benzothiazole derivatives, new benzothiazolyl–pyrazopyrimidine carboxamide compounds were synthesized (Scheme 114). The antiviral activity of these compounds against the H5N1 virus that causes avian influenza was then assessed. Although compound **507f** had the most CDK9 inhibitory activity (0.062 μmol $\mu L^{-1}$) of all of them, its antiviral efficacy was rather modest, only attaining 40% virus suppression. On the other hand, compound **507b** showed the largest antiviral efficacy with 71.6% inhibition, although having the least CDK9 inhibition (0.955 μmol $\mu L^{-1}$). This suggests that while **507b** most likely uses a mechanism that is independent of CDK9 to produce its antiviral effects, **507f** may predominantly function as a CDK9 inhibitor with negligible antiviral qualities. With similar CDK9 inhibitory activity (0.143 and 0.144 μmol $\mu L^{-1}$, respectively), compounds **507a** and **507d** demonstrated moderate antiviral effects of 71.67% and 61.67%. All of these results point to the possibility that the investigated compounds' antiviral effects are mediated by other routes or mechanisms of action, as there is no discernible relationship between CDK9 inhibition and antiviral activity.[269]

2-Aminobenzothiazole was reacted with acetoacetic acid methyl ester or ethyl 3-oxobutyrate **508** and several substituted arylcarbaldehydes to furnish the benzothiazole-3-carboxylates **509** (Scheme 115).

Benzothiazolyl guanidine was treated with **511** to provide compound **512**. The benzothiazolamine was also furnished from compound **510** as depicted in Scheme 116.

The benzothiazole-3-carboxylate **509** (R = 3-$NO_2$, $R^1 = C_2H_5$) (Fig. 87) displayed $IC_{50}$ on MLCK assay of 2.1 ± 1.7 lM with selectivity of L-type calcium channels and comparable to nifedipine.[270]

The primary drivers of compound **509**'s activity are (1) an ethyl carboxylate arm (the ethyl ester at C-3), which increases lipophilicity and provides a favorable PK profile, and (2) a 3-nitro (*meta*-$NO_2$) substituent on the phenyl ring, which the authors determined to be the most advantageous aryl substitution. These characteristics, along with the 2-methyl pyrimidobenzothiazole core (positive steric/electrostatic contributions in the 3D-QSAR), allow for selective L-type $Ca^{2+}$-channel modulation and MLCK inhibition ($IC_{50} = 2.1 \pm 1.7$ μM) that is comparable to nifedipine.[270]

It was discovered that the best substituent at the pyrimidine 5-position was a benzothiazole moiety. As a result of potential reactivity concern, the 4-chloro residue was replaced by a methyl group with roughly loss in activity and improved rat *in vivo* profile. Wide-ranging estimations at the C-2 position leads to identification of compound **518b** (Scheme 116; Fig. 88) that indicated very good replicon activity, rodent plasma/target organ concentration and selectivity. Inhibitor **518b** also showed oral bioavailability and good plasma levels in dogs, whereas monkey exposure was relatively low.[271]

The hepatitis C virus (HCV) replication complex, generally known as the replicase, may be inhibited by the

carbanucleoside-like pyrimidines, according to previous target engagement studies. RT-PCR was used to detect the suppression of viral RNA replication in HCV genotype 1b subgenomic replicon tests, which showed the antiviral activity. Although no specific enzymatic target was identified in this study, previous research suggests that the replicase complex is the site of action.[271]

The sulfonamide inhibitors **522** was synthesized as depicted in Scheme 117.

The synthesis and SAR of aryl uracil series for HCV NS5B inhibition is reported. Various analogs exhibit replicon cell culture activities along with excellent rat pharmacokinetic values (Fig. 89).[272]

(*E*)-(4-(2-(Benzo[*d*]thiazol-2yl)hydrazono)methyl-2,6-diphenylpiperidin-1-yl)(phenyl)methanone [EPHDPM] and its derivatives were prepared (Scheme 118). The reported EPHDPM molecule utilized as an active NLO material since it has high $\mu B_0$ value.[273]

A set of novel 3-(benzo[*d*]thiazol-2-yl)-2*H*-chromen-2-one derivatives (**529a–h**) were designed and synthesized (Scheme 119). The emission efficiency gradually decreased as electron-withdrawing substituents were added from the parent molecule **529a** to the dibromo derivative **529h**, according to fluorescence measurements. Positive binding interactions were predicted for each molecule using molecular docking and virtual screening against the human coronavirus NL63 nucleocapsid protein (PDB ID: 5epw). The most effective anti-COVID-19 candidate among the series was **529h**, which formed five important interactions inside the binding pocket. It was determined that the two bromine atoms in **529h** were essential to its increased activity (Fig. 90).[274]

By reacting novel 5-mercaptothiophen compounds replaced with the benzothiazole moiety and then coupling with different halo sugar derivatives, new benzothiazole-2-thiophene *S*-glycoside derivatives were synthesized (Scheme 120). The antiviral activity of the novel compounds was evaluated against HSV-1, HAV HM 175, COB4, HAdV7, and the ED-43/SG-Feo (VYG) replicon of HCV genotype **4a**. With a viral reduction of over 50%, two compounds showed significant antiviral effectiveness against the CBV4, HSV-1, and HCVcc viruses. The most effective compounds against HCVcc viruses, compounds **533c**, was evaluated against the NS3/4A protease and their actions were contrasted with those of the reference medication, sovaldi. The compound was been shown to be the most effective against HSV-1. Further analysis of the produced compounds' anticancer properties revealed that two of them, **533a** and **533c**, inhibit the

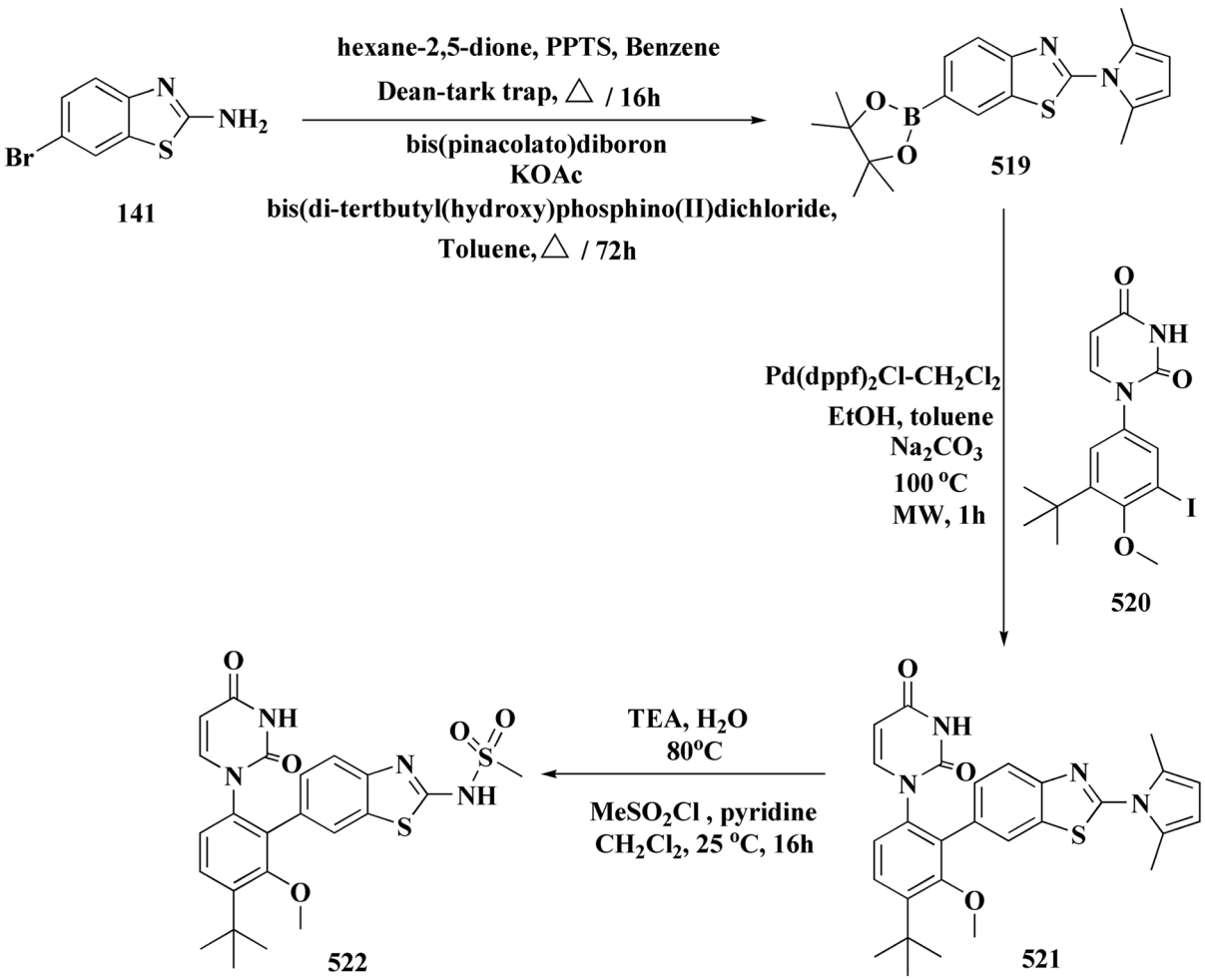


Scheme 117 Synthesis of uracil–benzothiazole conjugates.

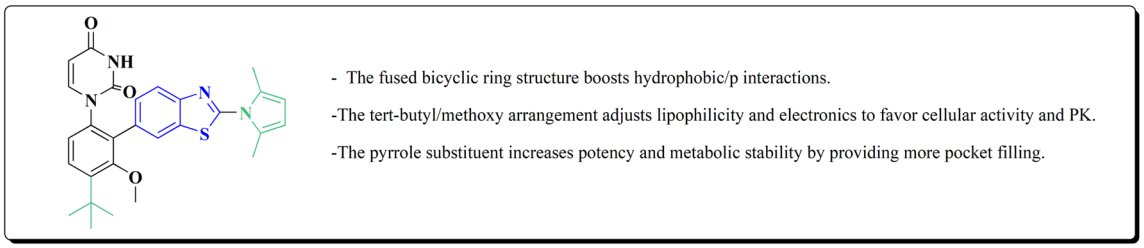


Fig. 89 Structure–activity relationship of compound **521**.

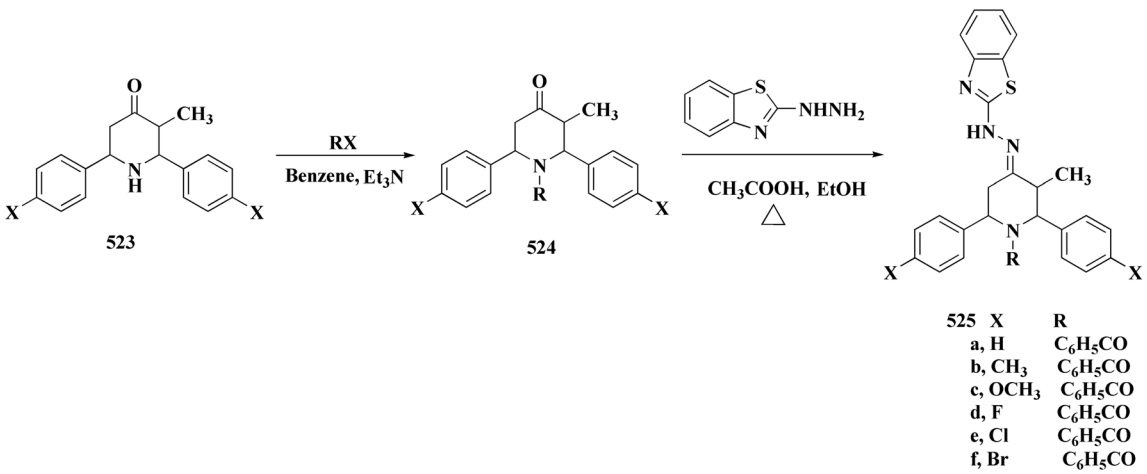


Scheme 118 Synthesis of (*E*)-(4-(2-(benzo[*d*]thiazol-2yl)hydrazono)methyl-2,6-diphenylpiperidin-1-yl)(phenyl)methanone.

majority of cancer kinds, but **533d** and **533f** only inhibited three and two cell lines, respectively.[275]

In comparison to their fully acetylated counterparts (**533f**) or other substitution patterns, compounds having $R_1$ = H and $R_2$ = OAc (*e.g.*, **533c**) consistently performed better. This trend implies that the equilibrium between solubility and lipophilicity is optimized by a free anomeric OH ($R_1$ = H) with per-*O*-acetylation elsewhere, improving bioactivity (Fig. 91).

Comparing series **533** compounds with intact acetates (**533a–f**) to their deacetylated counterparts in series 9, the former were noticeably more active. This emphasizes how crucial acetyl groups are for both cell permeability and antiviral activity.

In terms of NS3 protease inhibition and anti-HCV activity, 533c stood out. Additionally, it demonstrated a high level of inhibition against USP7, making it the series' dual-active lead. The SAR is extremely substitution-sensitive, as seen by the low activity of other 533-series analogs.[275]

The L-glutamic acid ester **534** was transformed to the *g*-lactam-acid **535** through treating with cyanomethyl bromide, followed by reduction with $PtO_2$, cyclization, and then hydrolysis (Scheme 121). Subsequent coupling of **535** to *N*-methoxymethylamine utilizing the EDC–HOBt procedure yielded the Weinreb amide **536**. The latter compound was then reacted with benzothiazole to give compound **537**, which was then followed by deprotection and then coupling to the peptides **534** in the existence of HBTU and DIPEA to yield compounds **538**.

The synthesis of dipeptide-type inhibitors with new P3 scaffolds that exhibit inhibitory potency against SARS-CoV 3CLpro was reported. Compound **538** exhibited the most active inhibitory potency, with a $K_i$ value of 0.006 mM (Fig. 92).[276]

By closely resembling the substrate P1′ side chain and slipping into the S1′ pocket, the benzothiazole at the P1′ location increases binding affinity. The S1 pocket's hydrogen bonding is mediated by the γ lactam at P1. The hydrophobic S2 subsite contains the Leu or hydrophobic residue at P2. The stiff indole 2 carbonyl at P3 (in compound **538**) helps to achieve the ideal stiffness and binding geometry by forming a stable H bond with Glu166.[276]

The preparation of benzothiazole-6-sulfonic acid was developed starting from sulfanilamide as depicted in Scheme 122 (Fig. 93). The replacement of *t*-butylurea scaffold by benzothiazolesulfonamide afforded HIV inhibitors with enhanced activity and antiviral potencies. Some of the compounds have indicated good oral bioavailability and half-life in rats.[277]

In order to successfully simulate the transition-state hydroxyl, the sulfonamide nitrogen and nearby oxygen atoms establish crucial hydrogen interactions with the catalytic Asp25/Asp25′ residues in the protease active site. With flap areas and

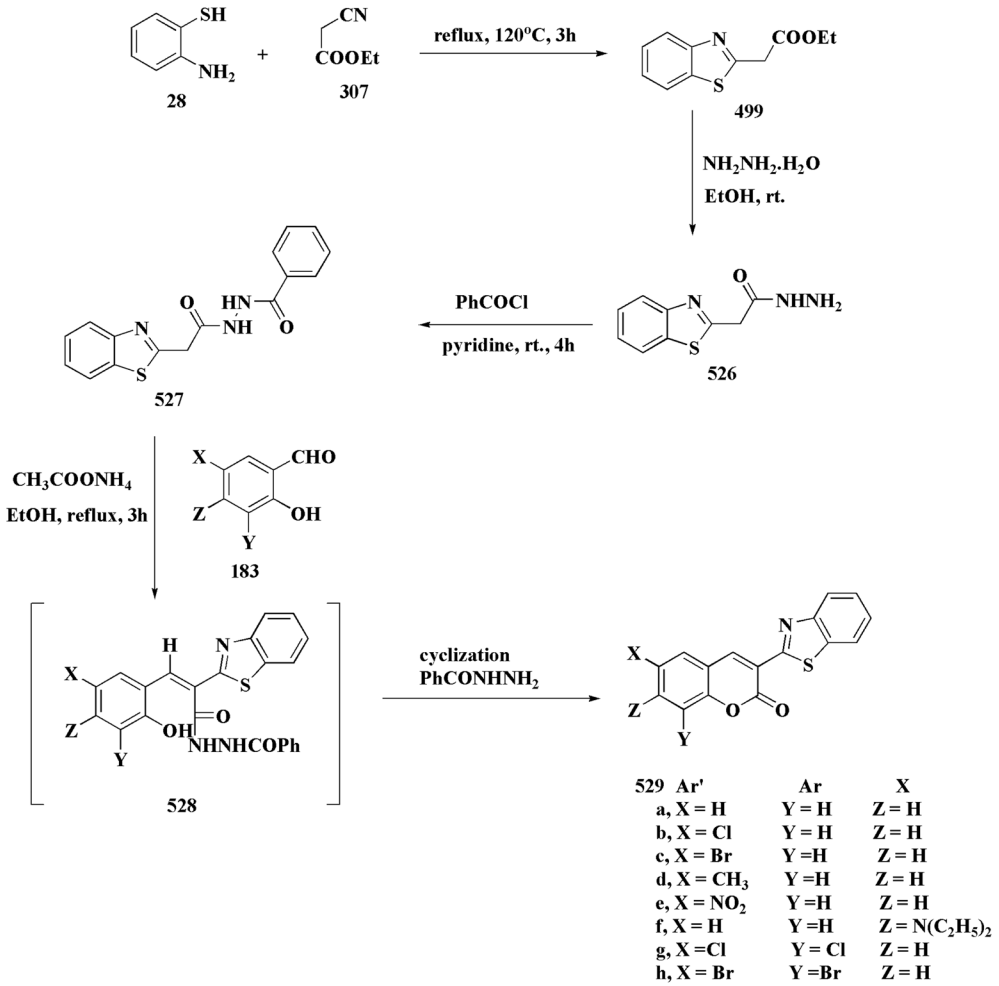


Scheme 119 Synthesis of 3-(benzo[*d*]thiazol-2-yl)-2*H*-chromen-2-one derivatives.

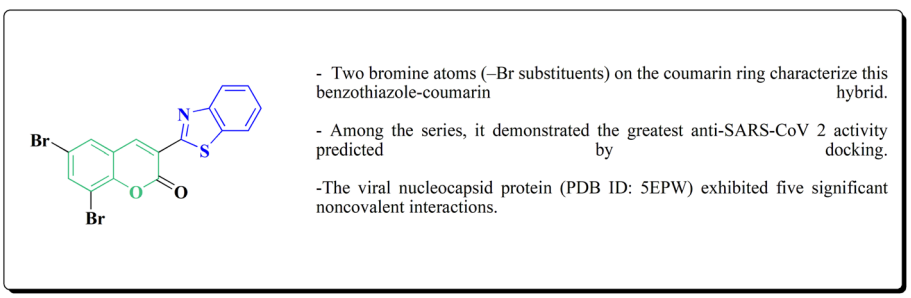


Fig. 90 Structure–activity relationship of compound **529**.

side chains such as Ile50 and Pro81, the benzothiazole ring improves hydrophobic and aromatic interactions. The whole scaffold effectively prevents the proteolytic cleavage of Gag-Pol precursors by supporting tight, reversible occupancy of the active site. These compounds bind directly to the catalytic aspartyl residues of HIV-1 protease to function as competitive active-site inhibitors.

Hydrogen bonding with the catalytic Asp25/Asp25′ dyad is one of the key interactions. The interactions with S1/S2 subsites that are hydrophobic. Through π–π stacking and dipole interactions, the benzothiazolesulfonamide moiety improves binding affinity and produces a stiff scaffold.

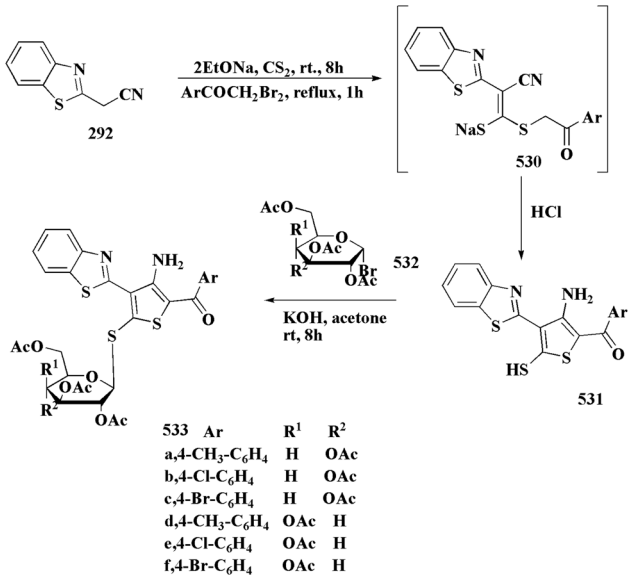


Scheme 120 Synthesis of benzothiazole-2-thiophene *S*-glycosides.

### 10.2. Benzothiazoles fused with heterocyclic compounds

The synthesis and in cellulo anti-HCV & *in vitro* anti-NS5B evaluation of pyridobenzothiazole-4-carboxylate derivatives are reported (Scheme 123; Fig. 94).[278]

These compounds attach to the HCV NS5B polymerase thumb domain allosteric location. The four carboxylate derivatives (as ester, amide, or sulfonamide) point toward solvent-exposed regions, affecting solubility and binding orientation; the pyridobenzothiazole core offers a rigid, planar scaffold that fits into the hydrophobic thumb pocket; potential π–π and hydrophobic interactions with residues in the thumb region.

The NS5B polymerase is inhibited by these non-nucleoside allosteric pyrido[2,1-*b*][1,3]benzothiazole 4 carboxylate derivatives. They don't bind at the active site or mimic nucleotides. Rather, they attach to an allosteric site in the thumb domain, changing the structure of the enzyme and preventing it from functioning.

According to molecular modeling and pharmacological research, the substances bind to the thumb domain and disrupt the conformational dynamics necessary for RNA elongation.[278]

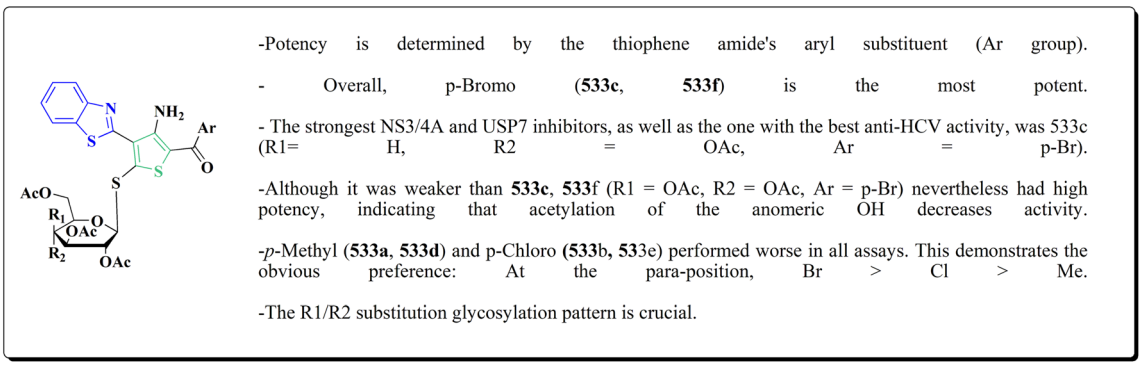


Fig. 91 Structure–activity relationship of compound 533.

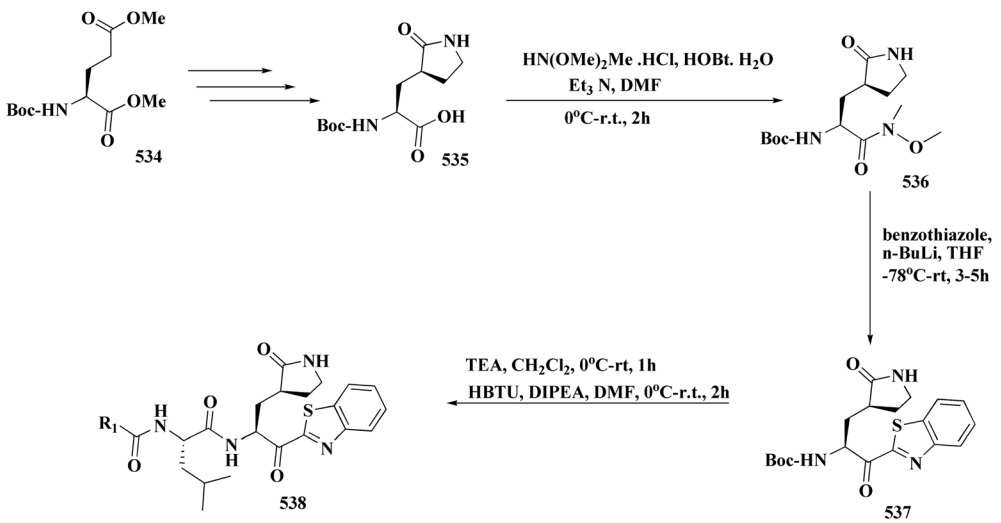


Scheme 121 Synthesis of 2-substituted benzothiazole.

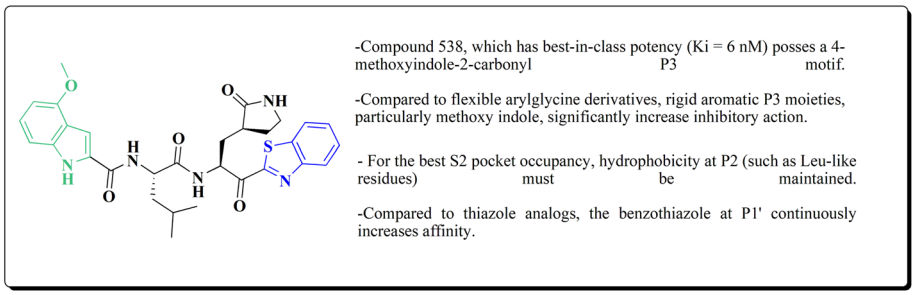


Fig. 92 Structure–activity relationship of compound **538**.

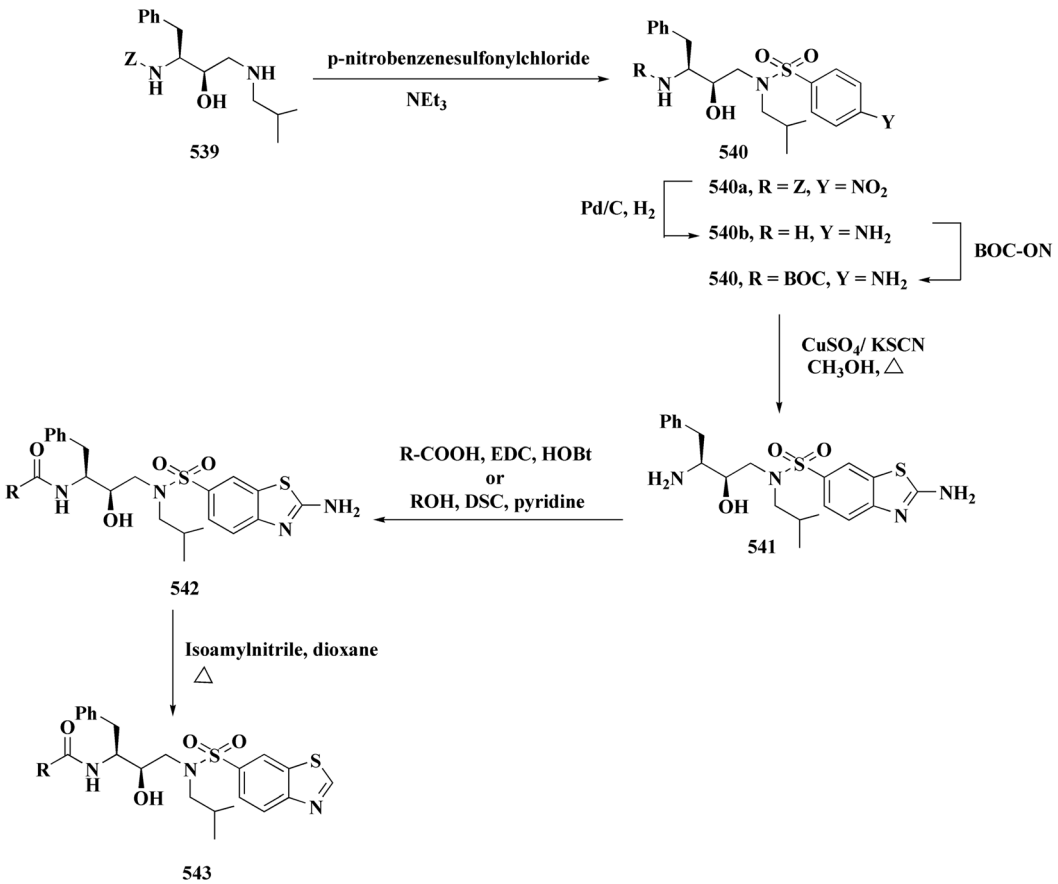


Scheme 122 Synthesis of benzothiazole-6-sulfonic acid derivatives.

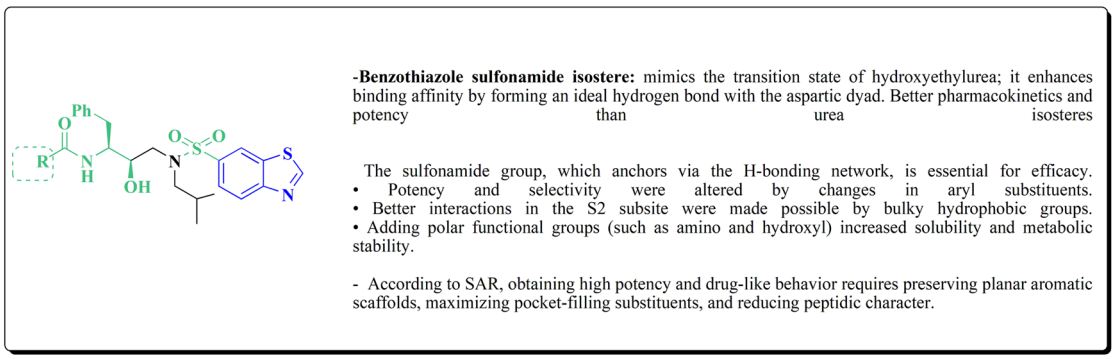


Fig. 93 Structure–activity relationship of compound **543**.

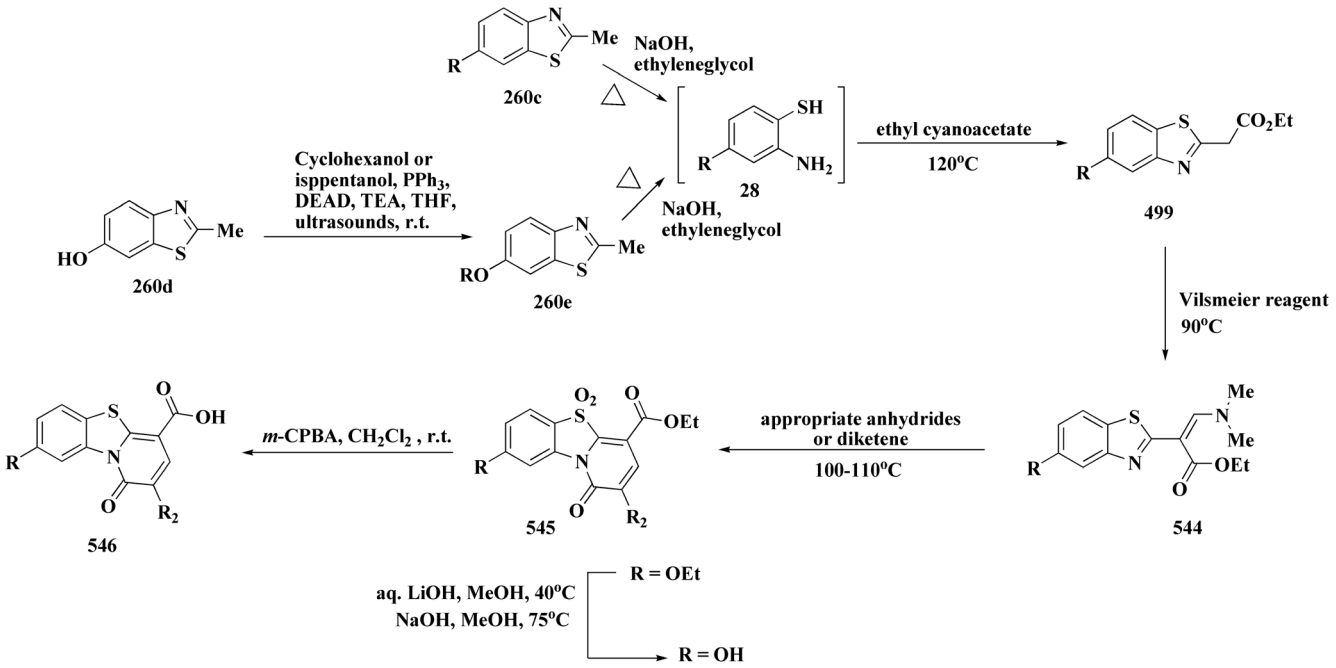


Scheme 123 Synthesis of pyridobenzothiazole-4-carboxylate derivatives.

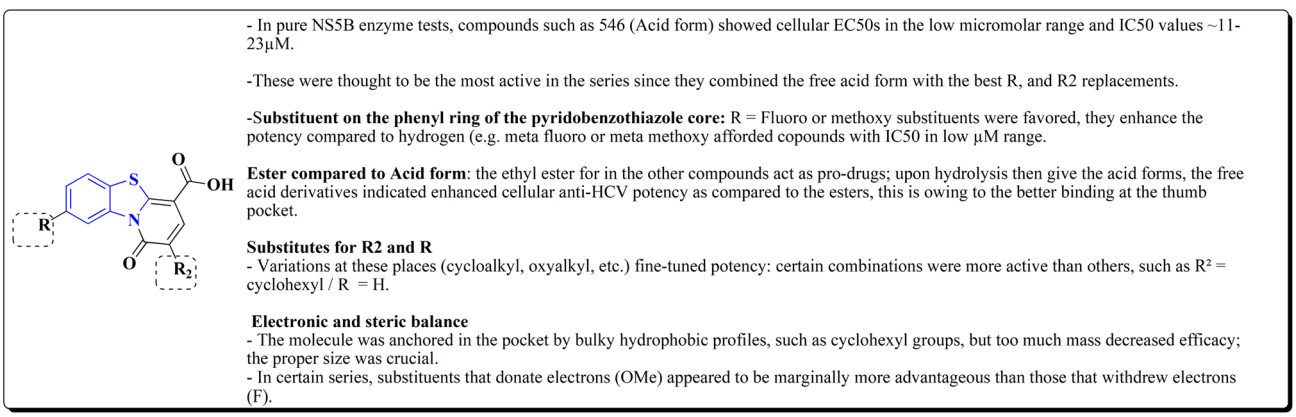


Fig. 94 Structure–activity relationship of compound.

## 11. Conclusion

Synthetic approaches of novel targeting therapeutical benzothiazoles were provided. Various benzothiazole-based compounds have emerged as significant structures, they are viable bioactive agents that are interested in advancing the research of the therapeutic arena. Several benzothiazole-based drugs were accomplished. Up-to-date synthetic strategies of anti-neurodegenerative, anti-inflammatory, antitumor, antimicrobial, and anti-viral benzothiazoles are depicted. The biological evaluation of the new synthesized compounds is also emphasized. The pharmacological potency and selectivity of benzothiazoles have been further improved by structural alterations and hybridization with other pharmacophores. Numerous medications, both licensed and under research, as well as novel molecules, have shown encouraging preclinical and clinical results. To effectively transform these heterocycles into medicinal medicines, more research is needed to understand their structure–activity correlations (SAR), molecular processes, and *in vivo* efficacy. The synthesis of safer and more effective benzothiazole-based medications will be further accelerated by the combination of computational tools, tailored delivery methods, and green synthesis methodologies.

## Conflicts of interest

There are no conflicts to declare.

## Data availability

No primary research results, software or code have been included and no new data were generated or analysed as part of this review.

## References

1 R. A. Mohamed-Ezzat, M. A. Omar, A. Temirak, A. S. Abdelsamie, M. M. Abdel-Aziz, S. A. Galal, G. H. Elgemeie, H. I. El Diwani, K. J. Flanagan and M. O. Senge, Synthesis, biological evaluation, and docking studies of pyrazole-linked benzothiazole hybrids as promising anti-TB agents, *J. Mol. Struct.*, 2024, **1311**, 138415, DOI: **10.1016/j.molstruc.2024.138415**.

2 X. Peng, G. Xie, Z. Wang, H. Lin, T. Zhou, P. Xiang, Y. Jiang, S. Yang, Y. Wei, L. Yu and Y. Zhao, SKLB-163, a new benzothiazole-2-thiol derivative, exhibits potent anticancer activity by affecting RhoGDI/JNK-1 signaling pathway, *Cell Death Dis.*, 2014, **5**(3), e1143, DOI: **10.1038/cddis.2014.107**.

3 G. H. Elgemeie and R. A. Mohamed-Ezzat, *New Strategies Targeting Cancer Metabolism*, Elsevier, Amsterdam, 2022, pp. 1–619, DOI: **10.1016/B978-0-12-821783-2.00010-8**.

4 X. Zhang, W. Jiang, J. M. Richter, J. A. Bates, S. K. Reznik, S. Stachura, R. Rampulla, D. Doddalingappa, S. Ulaganathan, J. Hua, J. S. Bostwick, C. Sum, S. Posy, S. Malmstrom, J. Dickey, D. Harden, R. M. Lawrence, V. R. Guarino, W. A. Schumacher, P. Wong, J. Yang, D. A. Gordon, R. R. Wexler and E. S. Priestley, Discovery of Potent and Selective Quinoxaline-Based Protease-Activated Receptor 4 (PAR4) Antagonists for the Prevention of Arterial Thrombosis, *J. Med. Chem.*, 2024, **67**(5), 3571–3589, DOI: **10.1021/acs.jmedchem.3c01986**.

5 T. Kato, K. Fukao, T. Ohara, N. Naya, R. Tokuyama, S. Muto, H. Fukasawa, A. Itai and K. I. Matsumura, Design, Synthesis, and Anti-Inflammatory Evaluation of a Novel PPARδ Agonist with a 4-(1-Pyrrolidinyl)piperidine Structure, *J. Med. Chem.*, 2023, **66**(16), 11428–11446, DOI: **10.1021/acs.jmedchem.3c00932**.

6 R. Zeng, M. Fang, A. Shen, X. Chai, Y. Zhao, M. Liu, L. Zhu, W. Rui, B. Feng, L. Hong, C. Ding, Z. Song, W. Lu and A. Zhang, Discovery of a Highly Potent Oxysterol Receptor GPR183 Antagonist Bearing the Benzo[*d*]thiazole Structural Motif for the Treatment of Inflammatory Bowel Disease (IBD), *J. Med. Chem.*, 2024, **67**(5), 3520–3541, DOI: **10.1021/acs.jmedchem.3c01905**.

7 U. K. Bandarage, A. M. Aronov, J. Cao, J. H. Come, K. M. Cottrell, R. J. Davies, S. Giroux, M. Jacobs, S. Mahajan, D. Messersmith, C. S. Moody, R. Swett and J. Xu, Discovery of a Novel Series of Potent and Selective Alkynylthiazole-Derived PI3Kγ Inhibitors, *ACS Med. Chem. Lett.*, 2020, **12**(1), 129–135, DOI: **10.1021/acsmedchemlett.0c00573**.

8 L. Zhang, Y. Li, C. Tian, R. Yang, Y. Wang, H. Xu, Q. Zhu, S. Chen, L. Li and S. Yang, From Hit to Lead: Structure-Based Optimization of Novel Selective Inhibitors of Receptor-Interacting Protein Kinase 1 (RIPK1) for the Treatment of Inflammatory Diseases, *J. Med. Chem.*, 2024, **67**(1), 754–773, DOI: **10.1021/acs.jmedchem.3c02102**.

9 W. Zhu, W. Zhang, J. Chen, Y. Tong, F. Xu and J. Pang, Discovery of Effective Dual PROTAC Degraders for Neurodegenerative Disease-Associated Aggregates, *J. Med. Chem.*, 2024, **67**(5), 3448–3466, DOI: **10.1021/acs.jmedchem.3c01719**.

10 S. Mourtas, B. Mavroidi, A. Marazioti, M. Kannavou, M. Sagnou, M. Pelecanou and S. G. Antimisiaris, Liposomes Decorated with 2-(4'-Aminophenyl) benzothiazole Effectively Inhibit $A\beta_{1-42}$ Fibril Formation and Exhibit in Vitro Brain-Targeting Potential, *Biomacromolecules*, 2020, **21**(12), 4685–4698, DOI: **10.1021/acs.biomac.0c00811**.

11 Y. Sun, L. Xu, H. Shao, D. Quan, Z. Mo, J. Wang, W. Zhang, J. Yu, C. Zhuang and K. Xu, Discovery of a Trifluoromethoxy Cyclopentanone Benzothiazole Receptor-Interacting Protein Kinase 1 Inhibitor as the Treatment for Alzheimer's Disease, *J. Med. Chem.*, 2022, **65**(21), 14957–14969, DOI: **10.1021/acs.jmedchem.2c01478**.

12 R. Mallesh, J. Khan, K. Pradhan, R. Roy, N. R. Jana, P. Jaisankar and S. Ghosh, Design and Development of Benzothiazole-Based Fluorescent Probes for Selective Detection of Aβ Aggregates in Alzheimer's Disease, *ACS Chem. Neurosci.*, 2022, **13**(16), 2503–2516, DOI: **10.1021/acschemneuro.2c00361**.

13 M. F. Lindberg, E. Deau, F. Miege, M. Greverie, D. Roche, N. George, P. George, L. Merlet, J. Gavard, S. J. T. Brugman, E. Aret, P. Tinnemans, R. de Gelder, J. Sadownik, E. Verhofstad, D. Sleegers, S. Santangelo, J. Dairou, A. Fernandez-Blanco, M. Dierssen, A. Krämer, S. Knapp and L. Meijer, Chemical, Biochemical, Cellular, and Physiological Characterization of Leucettinib-21, a Down Syndrome and Alzheimer's Disease Drug Candidate, *J. Med. Chem.*, 2023, **66**(23), 15648–15670, DOI: **10.1021/acs.jmedchem.3c01888**.

14 K. Terpstra, Y. Wang, T. T. Huynh, N. Bandara, H. J. Cho, B. E. Rogers and L. M. Mirica, Divalent 2-(4-Hydroxyphenyl)benzothiazole Bifunctional Chelators for $^{64}$Cu Positron Emission Tomography Imaging in Alzheimer's Disease, *Inorg. Chem.*, 2022, **61**(50), 20326–20336, DOI: **10.1021/acs.inorgchem.2c02740**.

15 R. W. Sabnis, Novel Substituted Benzothiazole Compounds for Treating Huntington's Disease, *ACS Med. Chem. Lett.*, 2021, **12**(4), 534–535, DOI: **10.1021/acsmedchemlett.1c00148**.

16 K. Anand, F. I. Khan, T. Singh, P. Elumalai, C. Balakumar, D. Premnath, D. Lai, A. A. Chuturgoon and M. Saravanan, Green Synthesis, Experimental and Theoretical Studies to Discover Novel Binders of Exosomal Tetraspanin CD81 Protein, *ACS Omega*, 2020, **5**(29), 17973–17982, DOI: **10.1021/acsomega.0c01166**.

17 R. A. Azzam, R. E. Elsayed and G. H. Elgemeie, Design and Synthesis of a New Class of Pyridine-Based *N*-Sulfonamides Exhibiting Antiviral, Antimicrobial, and Enzyme Inhibition Characteristics, *ACS Omega*, 2020, **5**(40), 26182–26194, DOI: **10.1021/acsomega.0c03773**.

18 K. W. Pugh, Z. Zhang, J. Wang, X. Xu, V. Munthali, A. Zuo and B. S. J. Blagg, From Bacteria to Cancer: A Benzothiazole-Based DNA Gyrase B Inhibitor Redesigned for Hsp90 C-Terminal Inhibition, *ACS Med. Chem. Lett.*,

2020, **11**(8), 1535–1538, DOI: 10.1021/acsmedchemlett.0c00100.

19 Y. Wei, M. Zhang, Z. Lyu, G. Yang, T. Tian, M. Ding, X. Zeng, F. Xu, P. Wang, F. Li, Y. Liu, Z. Cao, J. Lu, X. Hong and H. Wang, Benzothiazole Amides as TRPC3/6 Inhibitors for Gastric Cancer Treatment, *ACS Omega*, 2021, **6**(13), 9196–9203, DOI: 10.1021/acsomega.1c00514.

20 Z. Tang, J. Li, L. Peng, F. Xu, Y. Tan, X. He, C. Zhu, Z. M. Zhang, Z. Zhang, P. Sun, K. Ding and Z. Li, Novel Covalent Probe Selectively Targeting Glutathione Peroxidase 4 In Vivo: Potential Applications in Pancreatic Cancer Therapy, *J. Med. Chem.*, 2024, **67**(3), 1872–1887, DOI: 10.1021/acs.jmedchem.3c01608.

21 N. C. Kuznik, V. Solozobova, N. Jung, S. Gräßle, Q. Lei, E. M. Lewandowski, R. Munuganti, A. Zoubeidi, Y. Chen, S. Bräse and A. C. B. Cato, Development of a Benzothiazole Scaffold-Based Androgen Receptor N-Terminal Inhibitor for Treating Androgen-Responsive Prostate Cancer, *ACS Chem. Biol.*, 2021, **16**(11), 2103–2108, DOI: 10.1021/acschembio.1c00390.

22 K. Yuan, F. Xia, Q. Li, M. Zheng, H. Shen, W. Chen, H. Yang, X. Zhuang, X. Y. Zhang, Y. Xiao and P. Yang, Discovery of Potent, Selective, and Orally Bioavailable DYRK2 Inhibitors for the Treatment of Prostate Cancer, *J. Med. Chem.*, 2023, **66**(23), 16235–16256, DOI: 10.1021/acs.jmedchem.3c01626.

23 N. S. Williams, S. Gonzales, J. Naidoo, G. Rivera-Cancel, S. Voruganti, P. Mallipeddi, P. C. Theodoropoulos, S. Geboers, H. Chen, F. Ortiz, B. Posner, D. Nijhawan and J. M. Ready, Tumor-Activated Benzothiazole Inhibitors of Stearoyl-CoA Desaturase, *J. Med. Chem.*, 2020, **63**(17), 9773–9786, DOI: 10.1021/acs.jmedchem.0c00899.

24 E. Deau, M. F. Lindberg, F. Miege, D. Roche, N. George, P. George, A. Krämer, S. Knapp and L. Meijer, A Class of DYRK/CLK Kinase Inhibitors Inspired by the Marine Sponge Natural Product Leucettamine B, *J. Med. Chem.*, 2023, **66**(15), 10694–10714, DOI: 10.1021/acs.jmedchem.3c00884.

25 R. A. Azzam, N. M. Gad and G. H. Elgemeie, Novel Thiophene Thioglycosides Substituted with the Benzothiazole Moiety: Synthesis, Characterization, Antiviral and Anticancer Evaluations, and NS3/4A and USP7 Enzyme Inhibitions, *ACS Omega*, 2022, **7**(40), 35656–35667, DOI: 10.1021/acsomega.2c03444.

26 R. A. Azzam, H. A. Elboshi and G. H. Elgemeie, Novel Synthesis and Antiviral Evaluation of New Benzothiazole-Bearing N-Sulfonamide 2-Pyridone Derivatives as USP7 Enzyme Inhibitors, *ACS Omega*, 2020, **5**(46), 30023–30036, DOI: 10.1021/acsomega.0c04424.

27 R. A. Azzam, R. R. Osman and G. H. Elgemeie, Efficient Synthesis and Docking Studies of Novel Benzothiazole-Based Pyrimidinesulfonamide Scaffolds as New Antiviral Agents and Hsp90α Inhibitors, *ACS Omega*, 2020, **5**(3), 1640–1655, DOI: 10.1021/acsomega.9b03706.

28 K. Tsuji, T. Ishii, T. Kobayakawa, N. Higashi-Kuwata, K. Shinohara, C. Azuma, Y. Miura, H. Nakano, N. Wada, S. I. Hattori, H. Bulut, H. Mitsuya and H. Tamamura, Structure-Activity Relationship Studies of SARS-CoV-2 Main Protease Inhibitors Containing 4-Fluorobenzothiazole-2-carbonyl Moieties, *J. Med. Chem.*, 2023, **66**(19), 13516–13529, DOI: 10.1021/acs.jmedchem.3c00777.

29 M. Li, S. Castro Lingl and J. Yang, Reduction of Hemagglutination Induced by a SARS-CoV-2 Spike Protein Fragment Using an Amyloid-Binding Benzothiazole Amphiphile, *Sci. Rep.*, 2024, **14**, 12317, DOI: 10.1038/s41598-024-59585-4.

30 Z. Zhu, C. Chen, J. Zhang, F. Lai, J. Feng, G. Wu, J. Xia, W. Zhang, Z. Han, C. Zhang, Q. Yang, Y. Wang, B. Liu, T. Li and S. Wu, Exploration and Biological Evaluation of 1,3-Diamino-7H-pyrrol[3,2-f]quinazoline Derivatives as Dihydrofolate Reductase Inhibitors, *J. Med. Chem.*, 2023, **66**(20), 13946–13967, DOI: 10.1021/acs.jmedchem.3c00891.

31 S. Cascioferro, B. Parrino, D. Carbone, D. Schillaci, E. Giovannetti, G. Cirrincione and P. Diana, Thiazoles, Their Benzofused Systems, and Thiazolidinone Derivatives: Versatile and Promising Tools to Combat Antibiotic Resistance, *J. Med. Chem.*, 2020, **63**(15), 7923–7956, DOI: 10.1021/acs.jmedchem.9b01245.

32 Q. W. Lin, J. Q. Lu, Y. S. Huang, J. J. Liu, W. M. Chen and J. Lin, Cyclic Diguanylate G-Quadruplex Inducer-Nitric Oxide Donor Conjugate as a Bifunctional Antibiofilm Agent and Antibacterial Synergist against Pseudomonas aeruginosa with a Hyperbiofilm Phenotype, *J. Med. Chem.*, 2023, **66**(17), 11927–11939, DOI: 10.1021/acs.jmedchem.3c00516.

33 A. K. Carrillo, T. M. Kadayat, J. Y. Hwang, Y. Chen, F. Zhu, G. Holbrook, K. Gillingwater, M. C. Connelly, L. Yang, M. Kaiser and R. K. Guy, Antitrypanosomal Chloronitrobenzamides, *J. Med. Chem.*, 2024, **67**(5), 3437–3447, DOI: 10.1021/acs.jmedchem.3c01680.

34 S. Martínez-Cerón, N. A. Gutiérrez-Nágera, E. Mirzaeicheshmeh, R. I. Cuevas-Hernández and J. G. Trujillo-Ferrara, Phenylbenzothiazole Derivatives: Effects against a Trypanosoma cruzi Infection and Toxicological Profiles, *Parasitol. Res.*, 2021, **120**(8), 2905–2918, DOI: 10.1007/s00436-021-07137-4.

35 R. I. Cuevas-Hernández, R. M. B. M. Girard, S. Martínez-Cerón, M. Santos da Silva, M. C. Elias, M. Crispim, J. G. Trujillo-Ferrara and A. M. Silber, A Fluorinated Phenylbenzothiazole Arrests the Trypanosoma cruzi Cell Cycle and Diminishes the Infection of Mammalian Host Cells, *Antimicrob. Agents Chemother.*, 2020, **64**(2), e01742–19, DOI: 10.1128/AAC.01742-19.

36 P. Linciano, C. Pozzi, L. D. Iacono, F. di Pisa, G. Landi, A. Bonucci, S. Gul, M. Kuzikov, B. Ellinger, G. Witt, N. Santarem, C. Baptista, C. Franco, C. B. Moraes, W. Müller, U. Wittig, R. Luciani, A. Sesenna, A. Quotadamo, S. Ferrari, I. Pöhner, A. Cordeiro-da-Silva, S. Mangani, L. Costantino and M. P. Costi, Enhancement of Benzothiazoles as Pteridine Reductase-1 Inhibitors for the Treatment of Trypanosomatidic Infections, *J. Med. Chem.*, 2019, **62**(8), 3989–4012, DOI: 10.1021/acs.jmedchem.8b02021.

37 A. Avila-Sorrosa, J. D. Tapia-Alvarado, B. Nogueda-Torres, K. F. Chacón-Vargas, F. Díaz-Cedillo, M. E. Vargas-Díaz and D. Morales-Morales, Facile Synthesis of a Series of Non-Symmetric Thioethers Including a Benzothiazole Moiety and Their Use as Efficient In Vitro Anti-Trypanosoma cruzi Agents, *Molecules*, 2019, **24**(17), 3077, DOI: **10.3390/molecules24173077**.

38 C. Fleau, A. Padilla, J. Miguel-Siles, M. T. Quesada-Campos, I. Saiz-Nicolas, I. Cotillo, J. Cantizani Perez, R. L. Tarleton, M. Marco and G. Courtemanche, Chagas Disease Drug Discovery: Multiparametric Lead Optimization against Trypanosoma cruzi in Acylaminobenzothiazole Series, *J. Med. Chem.*, 2019, **62**(22), 10362–10375, DOI: **10.1021/acs.jmedchem.9b01429**.

39 L. Racané, V. Rep, S. Kraljević Pavelić, P. Grbčić, I. Zonjić, M. Radić Stojković, M. C. Taylor, J. M. Kelly and S. Raić-Malić, Synthesis, antiproliferative and antitrypanosomal activities, and DNA binding of novel 6-amidino-2-arylbenzothiazoles, *J. Enzyme Inhib. Med. Chem.*, 2021, **36**, 1952–1967, DOI: **10.1080/14756366.2021.1959572**.

40 L. Racané, L. Ptiček, S. Kostrun, S. Raić-Malić, M. C. Taylor, M. Delves, S. Alsford, F. Olmo, A. F. Francisco and J. M. Kelly, Bis-6-amidino-benzothiazole derivative that cures experimental stage 1 African trypanosomiasis with a single dose, *J. Med. Chem.*, 2023, **66**, 13043–13057, DOI: **10.1021/acs.jmedchem.3c01051**.

41 O. Sadek, L. A. Galán, F. Gendron, B. Baguenard, S. Guy, A. Bensalah-Ledoux, B. Le Guennic, O. Maury, D. M. Perrin and E. Gras, Chiral benzothiazole monofluoroborate featuring chiroptical and oxygen-sensitizing properties: synthesis and photophysical studies, *J. Org. Chem.*, 2021, **86**, 11482–11491, DOI: **10.1021/acs.joc.1c00995**.

42 J. Kasparkova, A. Hernández-García, H. Kostrhunova, M. Goicuría, V. Novohradsky, D. Bautista, L. Markova, M. D. Santana, V. Brabec and J. Ruiz, Novel 2-(5-arylthiophen-2-yl)-benzoazole cyclometalated iridium(III) dppz complexes exhibit selective phototoxicity in cancer cells by lysosomal damage and oncosis, *J. Med. Chem.*, 2024, **67**, 691–708, DOI: **10.1021/acs.jmedchem.3c01978**.

43 J. U. Yang, S. Kim, K. C. Lee, Y. J. Lee, J. Y. Kim and J. A. Park, Development of brain-tumor-targeted benzothiazole-based boron complex for boron neutron capture therapy, *ACS Med. Chem. Lett.*, 2022, **13**, 1615–1620, DOI: **10.1021/acsmedchemlett.2c00284**.

44 T. T. Huynh, Y. Wang, K. Terpstra, H. J. Cho, L. M. Mirica and B. E. Rogers, 68Ga-labeled benzothiazole derivatives for imaging Aβ plaques in cerebral amyloid angiopathy, *ACS Omega*, 2022, **7**, 20339–20346, DOI: **10.1021/acsomega.2c02369**.

45 H. E. Chia, K. J. Koebke, A. A. Rangarajan, N. M. Koropatkin, E. N. G. Marsh and J. S. Biteen, New orange ligand-dependent fluorescent reporter for anaerobic imaging, *ACS Chem. Biol.*, 2021, **16**, 2109–2115, DOI: **10.1021/acschembio.1c00391**.

46 R. Roychaudhuri, M. M. Gadalla, T. West and S. H. Snyder, A novel stereospecific bioluminescent assay for detection of endogenous d-cysteine, *ACS Chem. Neurosci.*, 2022, **13**, 3257–3262, DOI: **10.1021/acschemneuro.2c00528**.

47 Y. Sato, S. Sobu, K. Nakabayashi, S. Samitsu and H. Mori, Highly transparent benzothiazole-based block and random copolymers with high refractive indices by RAFT polymerization, *ACS Appl. Polym. Mater.*, 2020, **8**, 3205–3214, DOI: **10.1021/acsapm.0c00365**.

48 Y. Long, J. Liu, D. Tian, F. Dai, S. Zhang and B. Zhou, Cooperation of ESIPT and ICT processes in the designed 2-(2′-hydroxyphenyl)benzothiazole derivative: a near-infrared two-photon fluorescent probe with a large Stokes shift for the detection of cysteine and its application in biological environments, *Anal. Chem.*, 2020, **92**, 14236–14243, DOI: **10.1021/acs.analchem.0c03490**.

49 M. Fakis, V. Petropoulos, P. Hrobárik, J. Nociarová, P. Osuský, M. Maiuri and G. Cerullo, Exploring solvent and substituent effects on the excited state dynamics and symmetry breaking of quadrupolar triarylamine end-capped benzothiazole chromophores by femtosecond spectroscopy, *J. Phys. Chem. B*, 2022, **126**, 8532–8543, DOI: **10.1021/acs.jpcb.2c03103**.

50 W. J. Shi, R. Chen, J. Yang, Y. F. Wei, Y. Guo, Z. Z. Wang, J. W. Yan and L. Niu, Novel meso-benzothiazole-substituted BODIPY-based AIE fluorescent rotor for imaging lysosomal viscosity and monitoring autophagy, *Anal. Chem.*, 2022, **94**, 14707–14715, DOI: **10.1021/acs.analchem.2c03094**.

51 H. Li, F. Han, L. Jiang, T. Yang, L. Du and J. Zhu, Continuous synthesis of N-cyclohexyl-2-benzothiazole sulfenamide with microfluidics and its kinetic study, *Ind. Eng. Chem. Res.*, 2021, **39**, 14134–14142, DOI: **10.1021/acs.iecr.1c02881**.

52 **https://go.drugbank.com/**.

53 M. Delanne-Cuménal, S. Lamoine, M. Meleine, Y. Aissouni, L. Prival, M. Fereyrolles, J. Barbier, C. Cercy, L. Boudieu, J. Schopp, M. Lazdunski, A. Eschalier, S. Lolignier and J. Busserolles, The TREK-1 potassium channel is involved in both the analgesic and anti-proliferative effects of riluzole in bone cancer pain, *Biomed. Pharmacother.*, 2024, **176**, 116887, DOI: **10.1016/j.biopha.2024.116887**.

54 P. R. Padi, M. R. Ganta, S. Bollikonda, S. R. Chaganti, R. Akula and L. M. P. Dommati, Process for preparing riluzole, *US Pat.*, 20080108827A1.

55 R. Singh and M. Parmar, *Pramipexole, StatPearls*, StatPearls Publishing, Treasure Island (FL), 2024, **https://www.ncbi.nlm.nih.gov/books/NBK557539/**, updated 2023 Apr. 17.

56 H. Huan, Q. Huang, K. Li and Y. Shi, Preparation method of pramipexole dihydrochloride, *Chinese Patent*, CN109232471B, 2022.

57 E. S. Luckett, J. Schaeverbeke, S. De Meyer, K. Adamczuk, K. Van Laere, P. Dupont and R. Vandenberghe, Longitudinal changes in 18F-Flutemetamol amyloid load in cognitively intact APOE4 carriers versus noncarriers: methodological considerations, *NeuroImage Clin.*, 2023, **37**, 103321, DOI: **10.1016/j.nicl.2023.103321**.

58 H. P. Erba, P. Montesinos, H. J. Kim, E. Patkowska, R. Vrhovac, P. Žák, P. N. Wang, T. Mitov, J. Hanyok, Y. M. Kamel, J. E. C. Rohrbach, L. Liu, A. Benzohra, A. Lesegretain, J. Cortes, A. E. Perl, M. A. Sekeres, H. Dombret, S. Amadori, J. Wang, M. J. Levis and R. F. Schlenk, QuANTUM-First Study Group, Quizartinib plus chemotherapy in newly diagnosed patients with FLT3-internal-tandem-duplication-positive acute myeloid leukaemia (QuANTUM-First): a randomised, double-blind, placebo-controlled, phase 3 trial, *Lancet*, 2023, **401**, 1571–1583, DOI: 10.1016/S0140-6736(23)00464-6.

59 IAEA, *Production and Quality Control of Fluorine-18 Labelled Radiopharmaceuticals*, IAEA, 1st edn, 2021.

60 G. Montalban-Bravo, E. Jabbour, K. Chien, D. Hammond, N. Short, F. Ravandi, M. Konopleva, G. Borthakur, N. Daver, R. Kanagal-Shammana, S. Loghavi, W. Qiao, X. Huang, H. Schneider, M. Meyer, H. Kantarjian and G. Garcia-Manero, Phase 1 study of azacitidine in combination with quizartinib in patients with FLT3 or CBL mutated MDS and MDS/MPN, *Leuk. Res.*, 2024, **142**, 107518, DOI: 10.1016/j.leukres.2024.107518.

61 https://www.atamanchemicals.com/2–morpholinothio–benzothiazole_u30480/.

62 L. Zhou, B. Zhang, M. Wang and Z. Wang, Method for preparing 2,2'-dibenzothiazyl disulfide by catalyzing oxidation through molecular oxygen, *Chinese Patent*, CN102167686A, 2011.

63 M. J. C. Alicot and A. P. N. Tignol, Process for the preparation of dibenzothiazyl disulfide, *US Pat.*, US4337344A, 1982.

64 D. Simon and H. U. Simon, Therapeutic strategies for eosinophilic dermatoses, *Curr. Opin. Pharmacol.*, 2019, **46**, 29–33, DOI: 10.1016/j.coph.2019.01.002.

65 S. Mignani, J.-P. Majoral, J.-F. Desaphy and G. Lentini, From Riluzole to Dexpramipexole via Substituted-Benzothiazole Derivatives for Amyotrophic Lateral Sclerosis Disease Treatment: Case Studies, *Molecules*, 2020, **25**(15), 3320, DOI: 10.3390/molecules25153320.

66 Y. Tanaka, T. Nagoshi, H. Takahashi, Y. Oi, A. Yoshii, H. Kimura, K. Ito, Y. Kashiwagi, T. D. Tanaka and M. Yoshimura, URAT1-selective inhibition ameliorates insulin resistance by attenuating diet-induced hepatic steatosis and brown adipose tissue whitening in mice, *Mol. Metab.*, 2022, **55**, 101411, DOI: 10.1016/j.molmet.2021.101411.

67 T. Taniguchi, N. Ashizawa, K. Matsumoto, R. Saito, K. Motoki, M. Sakai, N. Chikamatsu, C. Hagihara, M. Hashiba and T. Iwanaga, Pharmacological evaluation of dotinurad, a selective urate reabsorption inhibitor, *J. Pharmacol. Exp. Ther.*, 2019, **371**(1), 162–170, DOI: 10.1124/jpet.119.259341.

68 Y. Tanaka, T. Nagoshi, H. Takahashi, Y. Oi, R. Yasutake, A. Yoshii, H. Kimura, Y. Kashiwagi, T. D. Tanaka, M. Shimoda and M. Yoshimura, URAT1 is expressed in cardiomyocytes and dotinurad attenuates the development of diet-induced metabolic heart disease, *iScience*, 2023, **26**(9), 107730, DOI: 10.1016/j.isci.2023.107730.

69 K. Omura, K. Miyata, S. Kobashi, A. Ito, M. Fushimi, J. Uda, T. Sasaki, T. Iwanaga and T. Ohashi, Ideal pharmacokinetic profile of dotinurad as a selective urate reabsorption inhibitor, *Drug Metab. Pharmacokinet.*, 2020, **35**(3), 313–320, DOI: 10.1016/j.dmpk.2020.03.002.

70 S. Lefere, T. Puengel, J. Hundertmark, C. Penners, A. K. Frank, A. Guillot, K. de Muynck, F. Heymann, V. Adarbes, E. Defrêne, C. Estivalet, A. Geerts, L. Devisscher, G. Wettstein and F. Tacke, Differential effects of selective- and pan-PPAR agonists on experimental steatohepatitis and hepatic macrophages, *J. Hepatol.*, 2020, **73**(4), 757–770, DOI: 10.1016/j.jhep.2020.04.025.

71 X. Xu, Q. Xie, F. Zhang, L. Huang and H. Wang, Preparation method of dotinurad, CN111793039A, 2020.

72 S. M. Francque, P. Bedossa, V. Ratziu, Q. M. Anstee, E. Bugianesi, A. J. Sanyal, R. Loomba, S. A. Harrison, R. Balabanska, L. Mateva, N. Lanthier, N. Alkhouri, C. Moreno, J. M. Schattenberg, D. Stefanova-Petrova, L. Vonghia, R. Rouzier, M. Guillaume, A. Hodge, M. Romero-Gómez, P. Huot-Marchand, M. Baudin, M. P. Richard, J. L. Abitbol, P. Broqua, J. L. Junien and M. F. Abdelmalek, NATIVE Study Group, A Randomized, Controlled Trial of the Pan-PPAR Agonist Lanifibranor in NASH, *N. Engl. J. Med.*, 2021, **385**(17), 1547–1558, DOI: 10.1056/NEJMoa2036205.

73 M. Yoneda, T. Kobayashi, N. Asako, M. Iwaki, S. Saito and A. Nakajima, Pan-Peroxisome Proliferator-Activated Receptor Agonist Lanifibranor as a Dominant Candidate Pharmacological Therapy for Nonalcoholic Fatty Liver Disease, *Hepatobiliary Surg. Nutr.*, 2022, **11**(3), 433–435, DOI: 10.21037/hbsn-21-579.

74 H. L. Lutsep, Repinotan, a 5-HT1A Agonist, in the Treatment of Acute Ischemic Stroke, *Curr. Drug Targets: CNS Neurol. Disord.*, 2005, **4**(2), 119–120, DOI: 10.2174/1568007053544165.

75 J. L. Gross, A Concise Stereospecific Synthesis of Repinotan (BAY×3702), *Tetrahedron Lett.*, 2003, **44**, 8563–8565.

76 A. N. Geria and N. S. Scheinfeld, Talarozole, a Selective Inhibitor of P450-Mediated All-Trans Retinoic Acid for the Treatment of Psoriasis and Acne, *Curr. Opin. Invest. Drugs*, 2008, **9**(11), 1228–1237.

77 M. Ezzo and S. Etienne-Manneville, Microtubule-Targeting Agents: Advances in tubulin binding and small molecule therapy for gliomas and neurodegenerative diseases, *Int. J. Mol. Sci.*, 2025, **26**(15), 7652, DOI: 10.3390/ijms26157652.

78 T. C. Gauler, D. C. Christoph, J. Fischer, N. Frickhofen, R. Huber, C. Gonschorek, K. Roth, M. Giurescu and W. E. Eberhardt, Phase-I Study of Sagopilone in Combination with Cisplatin in Chemotherapy-Naive Patients with Metastasized Small-Cell Lung Cancer, *Eur. J. Cancer*, 2013, **49**(11), 2461–2468, DOI: 10.1016/j.ejca.2013.03.029.

79 D. C. Tully, P. V. Rucker, D. Chianelli, J. Williams, A. Vidal, P. B. Alper, D. Mutnick, B. Bursulaya, J. Schmeits, X. Wu,

D. Bao, J. Zoll, Y. Kim, T. Groessl, P. McNamara, H. M. Seidel, V. Molteni, B. Liu, A. Phimister, S. B. Joseph and B. Laffitte, Discovery of Tropifexor (LJN452), a Highly Potent Non-Bile Acid FXR Agonist for the Treatment of Cholestatic Liver Diseases and Nonalcoholic Steatohepatitis (NASH), *J. Med. Chem.*, 2017, **60**(24), 9960–9973, DOI: 10.1021/acs.jmedchem.7b00907.

80 E. D. Hernandez, L. Zheng, Y. Kim, B. Fang, B. Liu, R. A. Valdez, W. F. Dietrich, P. V. Rucker, D. Chianelli, J. Schmeits, D. Bao, J. Zoll, C. Dubois, G. C. Federe, L. Chen, S. B. Joseph, L. B. Klickstein, J. Walker, V. Molteni, P. McNamara, S. Meeusen, D. C. Tully, M. K. Badman, J. Xu and B. Laffitte, Tropifexor-Mediated Abrogation of Steatohepatitis and Fibrosis Is Associated with the Antioxidative Gene Expression Profile in Rodents, *Hepatol. Commun.*, 2019, **3**(8), 1085–1097, DOI: 10.1002/hep4.1368.

81 B. Laffitte, K. Young, S. Joseph, B. Lui, D. Bao, J. Zoll, *et al.*, A Novel, Highly Potent, Non-Bile Acid FXR Agonist for the Treatment of NASH and Cholestasis, *Hepatol. Int.*, 2016, **10**, S97.

82 M. K. Badman, J. Chen, S. Desai, S. Vaidya, S. Neelakantham, J. Zhang, L. Gan, K. Danis, B. Laffitte and L. B. Klickstein, Safety, Tolerability, Pharmacokinetics, and Pharmacodynamics of the Novel Non-Bile Acid FXR Agonist Tropifexor (LJN452) in Healthy Volunteers, *Clin. Pharmacol. Drug Dev.*, 2020, **9**(3), 395–410, DOI: 10.1002/cpdd.762.

83 K. J. Lucas, P. Lopez, E. J. Lawitz, A. Sheikh, D. Aizenberg, S. Hsia, G. G. Boon Bee, J. Vierling, J. Frias, J. White, Y. Eguchi, D. Lazas, G. Neff, M. Yoneda, S. Augustin, W. Kim, Y. Loeffler, F. Schaefer, S. Lamle, M. Martic, C. Brass and A. Sanyal, Tropifexor, a Highly Potent FXR Agonist, Produces Robust and Dose-Dependent Reductions in Hepatic Fat and Serum Alanine Aminotransferase in Patients with Fibrotic NASH After 12 Weeks of Therapy: FLIGHT-FXR Part C Interim Results, *Hepatol*, 2019, **70**, 1479A–1480A, DOI: 10.1016/j.dld.2019.12.129.

84 A. J. Sanyal, P. M. Lopez, E. Lawitz, W. Kim, J. F. Huang, P. Andreone, *et al.*, Tropifexor (TXR), an FXR Agonist for the Treatment of NASH – Interim Results from First Two Parts of Phase 2b Study FLIGHT-FXR, *Hepatol*, 2018, **68**, 1460A–1461A.

85 M. Camilleri, S. L. Nord, D. Burton, I. Oduyebo, Y. Zhang, J. Chen, K. Im, P. Bhad, M. K. Badman, D. S. Sanders and J. R. F. Walters, Randomized Clinical Trial: Significant Biochemical and Colonic Transit Effects of the Farnesoid X Receptor Agonist Tropifexor in Patients with Primary Bile Acid Diarrhea, *Aliment. Pharmacol. Ther.*, 2020, **52**(5), 808–820, DOI: 10.1111/apt.15967.

86 C. Schramm, H. Wedemeyer, A. Mason, G. M. Hirschfield, C. Levy, K. V. Kowdley, P. Milkiewicz, E. Janczewska, E. S. Malova, J. Sanni, P. Koo, J. Chen, S. Choudhury, L. B. Klickstein, M. K. Badman and D. Jones, Farnesoid X Receptor Agonist Tropifexor Attenuates Cholestasis in a Randomized Trial in Patients with Primary Biliary Cholangitis, *JHEP Rep.*, 2022, **4**(11), 100544, DOI: 10.1016/j.jhepr.2022.100544.

87 P. Kocienski, Synthesis of tropifexor, *Synfacts*, 2018, **14**(3), 230.

88 Y. T. Lee, S. K. Fraser, S. M. Meno-Tetang, D. T. Chu, H. G. Hollis, H. E. O'Neill, Y. Zhang, Y. Li, J. L. Fadra, A. S. Geders, J. D. Swearingen, A. Q. Wang and L. A. Lesburg, Discovery of tropifexor (LJN452), a highly potent non-bile acid FXR agonist for the treatment of cholestatic liver diseases and nonalcoholic steatohepatitis (NASH), *J. Med. Chem.*, 2017, **60**(21), 9960–9973, DOI: 10.1021/acs.jmedchem.7b01147.

89 M. C. Van Zandt, M. L. Jones, D. E. Gunn, L. S. Geraci, J. H. Jones, D. R. Sawicki, J. Sredy, J. L. Jacot, A. T. Dicioccio, T. Petrova, A. Mitschler and A. D. Podjarny, Discovery of 3-[(4,5,7-trifluorobenzothiazol-2-yl)methyl]indole-*N*-acetic acid (lidorestat) and congeners as highly potent and selective inhibitors of aldose reductase for treatment of chronic diabetic complications, *J. Med. Chem.*, 2005, **48**(9), 3141–3152, DOI: 10.1021/jm0492094.

90 V. Chandrashekhar and M. Patel, Lidorestat in diabetic neuropathy: A review of pharmacodynamics and clinical outcomes, *J. Diabetes Its Complications*, 2016, **30**(4), 688–693, DOI: 10.1016/j.jdiacomp.2015.12.002.

91 M. C. Van Zandt, M. L. Jones, D. E. Gunn, L. S. Geraci, J. H. Jones, D. R. Sawicki, J. Sredy, J. Jacot, J. L. DiCioccio, A. T. Petrova, T. Mitschler, A. Podjarny and A. D. Alberto, Discovery of 3-[(4,5,7-trifluorobenzothiazol-2-yl)methyl] indole-*N*-acetic acid (lidorestat) and congeners as highly potent and selective inhibitors of aldose reductase for treatment of chronic diabetic complications, *J. Med. Chem.*, 2005, **48**(9), 3141–3154, DOI: 10.1021/jm048982u.

92 R. Krauss, F. Wagner, R. Doblhofer, B. Dietrich, J. Ehlert, M. H. G. Kubbutat, A. Lingnau, F. Totzke, C. Schachtele and B. Hentsch, 1251 POSTER: Preclinical and clinical development of 4SC-203 – a novel multi-target kinase inhibitor, *Eur. J. Cancer*, 2011, **47**(2), S160, DOI: 10.1016/S0959-8049(11)70863-2.

93 I. Dierynck, H. Van Marck, M. Van Ginderen, T. H. Jonckers, M. N. Nalam, C. A. Schiffer, A. Raoof, G. Kraus and G. Picchio, TMC310911, a novel human immunodeficiency virus type 1 protease inhibitor, shows in vitro an improved resistance profile and higher genetic barrier to resistance compared with current protease inhibitors, *Antimicrob. Agents Chemother.*, 2011, **55**(12), 5723–5731, DOI: 10.1128/AAC.00748-11.

94 R. Mishra and S. V. Dhamnaskar, Industrial process for preparing environmentally safe tricyclazole, WO2004060897A1, 2004.

95 R. C. Guy, Saccharin, in *Encyclopedia of Toxicology*, ed. P. Wexler, Academic Press, 3rd edn, 2014, pp. 193–194, ISBN 9780123864550, DOI: 10.1016/B978-0-12-386454-3.00923-4.

96 J. Tonne, P. Germain and C. Gras, Preparation of saccharin, *US Pat.*, 4464537, 1984.

97 T. Jin, L. Zhao, H. P. Wang, M. L. Huang, Y. Yue, C. Lu and Z. B. Zheng, Recent advances in the discovery and

development of glyoxalase I inhibitors, *Bioorg. Med. Chem.*, 2020, **28**(4), 115243, DOI: 10.1016/j.bmc.2019.115243.

98 M. Mohajeri, P. T. Kovanen, V. Bianconi, M. Pirro, A. F. G. Cicero and A. Sahebkar, Mast cell tryptase – Marker and maker of cardiovascular diseases, *Pharmacol. Ther.*, 2019, **199**, 91–110, DOI: 10.1016/j.pharmthera.2019.03.008.

99 F. Ruiz, I. Hazemann, A. Mitschler, A. Joachimiak, T. Schneider, M. Karplus and A. Podjarny, The crystallographic structure of the aldose reductase-IDD552 complex shows direct proton donation from tyrosine 48, *Acta Crystallogr., Sect. D: Biol. Crystallogr.*, 2004, **60**(Pt 8), 1347–1354, DOI: 10.1107/S0907444904011370.

100 M. Doble, The pharmacology and mechanism of action of riluzole, *Neurology*, 1996, **47**(6), S233–S241.

101 A. Urbani and O. Belluzzi, Involvement of presynaptic metabotropic glutamate receptors in the induction of long-term potentiation in the olfactory cortex, *Neuroscience*, 2000, **97**, 363–368, DOI: 10.1016/S0306-4522(00)00029-6.

102 A. Doble, The role of excitotoxicity in neurodegenerative disease: implications for therapy, *CNS Drugs*, 1996, **6**, 333–343, DOI: 10.2165/00023210-199606050-00004.

103 M. W. Debono, G. Le Guern, D. Canton, J. M. Kemel and F. Ben-Ari, Kainate-induced electrographic seizures and selective neuronal loss in the immature rat hippocampus, *Neurosci. Lett.*, 1993, **163**, 165–168, DOI: 10.1016/0304-3940(93)90391-3.

104 M. Carbone, L. Duty and S. Rattray, Riluzole elevates GLT-1 activity and levels in striatal astrocytes, *Neurochem. Int.*, 2012, **60**, 548–555, DOI: 10.1016/j.neuint.2012.01.016.

105 S. J. Wang, S. J. Wang, H. C. Su, Y. T. Huang and H. C. Ho, Riluzole inhibits the release of glutamate in rat cerebral cortex nerve terminals, *Br. J. Pharmacol.*, 2004, **142**, 909–916, DOI: 10.1038/sj.bjp.0705851.

106 A. V. Gourine, M. Kasymov, R. Marina, J. F. R. Spyer, M. Teschemacher, N. Deisseroth and S. Kasparov, Astrocytes control breathing through pH-dependent release of ATP, *J. Neurochem.*, 2005, **92**, 1156–1164, DOI: 10.1111/j.1471-4159.2004.02953.x.

107 M. J. Millan, L. Maiofiss, D. Cussac, V. Audinot, J. A. Boutin and A. Newman-Tancredi, Differential actions of antiparkinson agents at multiple classes of monoaminergic receptor, *Eur. J. Pharmacol.*, 2002, **442**, 13–28, DOI: 10.1016/S0014-2999(02)01527-3.

108 P. P. Zarrinkar, A. Gunawardane, C. Cramer, B. Gardner, M. Brigham, R. Belli, E. Karaman, D. Bebernitz, S. Mookhtiar and M. Patel, AC220 is a uniquely potent and selective inhibitor of FLT3 for the treatment of acute myeloid leukemia (AML), *Blood*, 2009, **114**, 2984–2992, DOI: 10.1182/blood-2009-01-199216.

109 C. C. Smith, J. Wang, R. Chin, A. Salerno, M. J. Damon, A. Levis, M. W. Perl and N. P. Shah, Validation of ITD mutations in FLT3 as a therapeutic target in human acute myeloid leukaemia, *Cancer Discov.*, 2012, **2**, 668–679, DOI: 10.1158/2159-8290.CD-12-0013.

110 H. Kantarjian, A. Erba, J. E. Claxton, G. Goldberg, R. DiNardo, M. Arellano, M. Lyons, N. Pullarkat, D. J. Deangelo and J. Fujimoto, Phase 2 study of CPX-351, a fixed-ratio liposomal formulation of daunorubicin and cytarabine, in older adults with untreated secondary acute myeloid leukaemia, *Lancet Oncol.*, 2019, **20**, 839–850, DOI: 10.1016/S1470-2045(19)30148-2.

111 H. P. Erba, J. DiNardo, G. Fathi, J. E. Cortes, M. Arellano, A. Advani, A. Douer, T. Cluzeau, A. Wei and R. Hills, CPX-351 versus 7 + 3 cytarabine and daunorubicin chemotherapy in older adults with newly diagnosed high-risk or secondary acute myeloid leukaemia: overall survival after 5 years of follow-up, *J. Clin. Oncol.*, 2023, **41**, 1740–1750, DOI: 10.1200/JCO.22.01370.

112 U.S. FDA, Approval summary for CPX-351 (Vyxeos), U.S. Food and Drug Administration, 2017, available at: https://www.fda.gov.

113 N. Nelissen, C. Vandenbulcke, K. Lemmens, J. Van Laere, K. De Vos, K. Slegers, C. Casteels, S. Morrens, B. Sabbe and P. Van Heeringen, Regional differences in 5-HT2A receptor binding potential in patients with depression: a [18F]altanserin PET study, *Eur. J. Nucl. Med. Mol. Imaging*, 2009, **36**, 708–720, DOI: 10.1007/s00259-008-1017-2.

114 M. Koole, C. Van Laere, C. Casteels, P. Boon, L. Bruyn, K. Slegers, K. Bormans and R. Vandenberghe, Whole-body biodistribution and radiation dosimetry of [18F] altanserin: a study in healthy volunteers, *J. Nucl. Med.*, 2009, **50**, 818–825, DOI: 10.2967/jnumed.108.060426.

115 A. S. Sabri, D. Rowe, S. Barthel, S. Beta, S. Reininger, C. Sheehan, C. Becker, M. Heinzel-Gutenbrunner, C. Burchner, D. Stephens, J. Mueller, L. Bennacef, S. Koglin, L. Hoffmann, J. Roth, P. De Lepeleire, M. Vandenberghe, P. Nieuweboer, C. Reininghaus, J. Hoffmann, T. Schulz-Schaeffer, J. Kupsch, F. van Berckel, T. Cselenyi, A. Wall, B. Gulyas, M. Moghbel, A. Buck, H. Zijlstra, G. Delva, G. Vaupel, R. Wagener, R. Kronenberg, J. Declerck, M. Vandenbulcke, M. Peremans, J. Denecke, M. Brendel, C. Bartenstein, A. Stephens, S. De Vos, R. Sabbagh, E. Dubois, L. Nelissen, D. Devous, J. Vlassenko, R. Coleman, F. Heurling, M. Ohlmeier, P. Matthews, E. Dyrks, R. Deleye and R. Van Laere, Evaluation of the safety, tolerability and efficacy of florbetaben (18F) PET imaging in patients with Alzheimer's disease and healthy volunteers, *NeuroImage Clin.*, 2015, **7**, 391–398, DOI: 10.1016/j.nicl.2015.01.007.

116 T. Hosoya, I. Ohno, S. Nomura, I. Hisatome and S. Uchida, Clinical efficacy and safety of dotinurad, a novel selective urate reabsorption inhibitor (SURI), in Japanese hyperuricemic patients with or without gout: A phase 2 randomized, double-blind, placebo-controlled study, *Clin. Exp. Nephrol.*, 2020, **24**, 995–1003, DOI: 10.1007/s10157-020-01857-0.

117 H. Yanai, H. Adachi, M. Hakoshima, S. Iida and H. Katsuyama, A Possible Therapeutic Application of the Selective Inhibitor of Urate Transporter 1 Dotinurad for

Metabolic Syndrome, Chronic Kidney Disease, and Cardiovascular Disease, *Cells*, 2024, **13**, 450, DOI: 10.3390/cells13050450.

118 T. Hosoya, T. Sano, T. Sasaki, M. Fushimi, T. Ohashi, *et al.*, Dose-dependent serum uric acid-lowering effect of dotinurad in hyperuricemic patients: Phase 2 randomized, multicenter, double-blind, placebo-controlled study, *Clin. Exp. Nephrol.*, 2020, **24**(1), 44–52, DOI: 10.1007/s10157-019-01802-w.

119 K. Motoki, T. Igarashi, K. Omura, *et al.*, Pharmacokinetic/pharmacodynamic modeling of dotinurad in healthy volunteers: single/multiple-dose study, *Pharmacol. Res. Perspect.*, 2019, e00533, DOI: 10.1002/prp2.533.

120 S. Francque, *et al.*, Lanifibranor is a pan-PPAR agonist that improves liver histology in NASH, *N. Engl. J. Med.*, 2021, **385**, 1548–1558, DOI: 10.1056/NEJMoa2028701.

121 B. Staels, S. Francque and B. Cariou, Lanifibranor: a first-in-class pan-PPAR agonist for the treatment of NASH, *Nat. Rev. Gastroenterol. Hepatol.*, 2023, **20**, 689–703, DOI: 10.1038/s41575-023-00791-9.

122 S. J. Roofeh, A. M. Vang, M. V. Stawski, J. E. Farber, B. Y. Chang, S. S. Agarwal and M. V. Trojanowska, The pan-PPAR agonist lanifibranor improves systemic and pulmonary vascular function in a mouse model of systemic sclerosis, *Front. Pharmacol*, 2021, **12**, 711891, DOI: 10.3389/fphar.2021.711891.

123 S. Roussel, M. Pinard and B. Seylaz, Repinotan (BAY x 3702) reduces infarct size after transient middle cerebral artery occlusion in rats, *Stroke*, 2005, **36**(3), 705–709.

124 H. C. Diener, R. Lees, A. Lyden and D. Grotta, Safety and tolerability of Repinotan HCl in acute ischemic stroke: results of the BRAINS study, *Stroke*, 2005, **36**(4), 948–954.

125 H. Van der Goot, T. T. Hooft, M. Van der Lee and A. J. Van der Laan, Identification of R115866 as a novel and potent cytochrome P450RAI (CYP26) inhibitor, *J. Pharmacol. Exp. Ther.*, 2005, **315**(1), 275–282, DOI: 10.1124/jpet.105.087452.

126 F. Dell'Accio, C. De Bari and M. E. Dakin, Talarozole restores atRA levels and suppresses injury-induced inflammatory gene expression via a PPARγ-dependent mechanism, *Osteoarthritis Cartil.*, 2022, **30**(12), 1669–1679, DOI: 10.1016/j.joca.2022.06.011.

127 U. Klar, J. Hoffmann and M. Giurescu, Sagopilone (ZK-EPO): from a natural product to a fully synthetic clinical development candidate, *Expert Opin. Invest. Drugs*, 2008, **17**(11), 1735–1748.

128 J. Hoffmann, *et al.*, Improved cellular pharmacokinetics and pharmacodynamics underlie the wide anticancer activity of sagopilone, *Cancer Res.*, 2008, **68**(13), 5301–5308.

129 S. Winsel, A. Sommer, J. Eschenbrenner, K. Mittelstaedt and J. Hoffmann, Molecular mode of action and role of TP53 in the sensitivity to the novel epothilone sagopilone (ZK-EPO) in A549 non-small cell lung cancer cells, *PLoS One*, 2011, **6**(4), e18713.

130 J. Hoffmann, I. Fichtner, M. Lemm, P. Lienau, H. Hess-Stumpp, A. Rotgeri, B. Hofmann and U. Klar, Sagopilone crosses the blood–brain barrier in vivo to inhibit brain tumor growth and metastases, *Neuro-Oncology*, 2009, **11**(2), 158–166, DOI: 10.1215/15228517-2008-072.

131 D. C. Tully, J. R. Rucker, J. A. Chianelli, C. D. Williams, G. Vidal, L. Alon, C. G. Lavey, C. V. LaSala and J. D. Hawryluk, Discovery of Tropifexor (LJN452), a potent, non–bile acid FXR agonist for the treatment of cholestatic and metabolic liver diseases, *J. Med. Chem.*, 2017, **60**(24), 9960–9973, DOI: 10.1021/acs.jmedchem.7b00841.

132 F. Haczeyni, L. Poekes, P. Wang, A. E. Mayrhofer, C. T. Teoh, M. A. Watt, R. S. Oeztuerk, J. D. Sumida, C. J. Palmer, A. J. Butcher, *et al.*, Tropifexor-mediated abrogation of steatohepatitis and fibrosis in rodent models of NASH, *Hepatol. Commun.*, 2019, **3**(8), 1085–1097, DOI: 10.1002/hep4.1372.

133 Y. Miao, L. Calabrese, M. M. Sun and S. B. Kliewer, Structural basis for tropifexor efficacy in treating cholestatic liver disease, *Nat. Commun.*, 2020, **11**, 5484, DOI: 10.1038/s41467-020-19229-9.

134 A. J. Sanyal, A. R. Loomba, A. Silvestre, K. Y. Tang, A. S. Alkhouri, J. Rinella, B. K. Shapiro, M. V. Ratziu, M. D. Caldwell, *et al.*, Effects of Tropifexor on liver fat in nonalcoholic steatohepatitis: the FLIGHT-FXR phase 2 study, *Hepatol. Commun.*, 2023, e0016, DOI: 10.1097/HC9.0000000000000016.

135 S. A. Satoh, H. Watanabe, K. Tomoda, T. Kobayashi and H. Kobayashi, Discovery and preclinical evaluation of lidorestat, a potent and selective aldose reductase inhibitor for the treatment of diabetic complications, *J. Med. Chem.*, 2020, **63**, 6387–6399, DOI: 10.1021/acs.jmedchem.9b02147.

136 https://www.technologynetworks.com/genomics/news/-4sc-announces-start-of-dosing-in-firstinman-phase-i-study-with-4sc203-184569?utm_source.

137 S. De Meyer, D. Christ, E. Debyser, M. Daelemans and S. Daelemans, Inhibition of HIV replication by newly developed non-nucleoside reverse transcriptase inhibitors, *Antimicrob. Agents Chemother.*, 2008, **52**(9), 3225–3229, DOI: 10.1128/AAC.00381-08.

138 A. Peeters, M. Van Hende, K. D'Hondt, L. De Maeyer, A. De Spiegeleer, R. Van Bambeke, P. Augustijns and P. Annaert, Intestinal absorption of the antiviral drug darunavir: Involvement of efflux transporters and influence of ritonavir, *J. Antimicrob. Chemother.*, 2010, **65**(9), 1905–1913.

139 U.S. FDA, Clinical Pharmacology and Biopharmaceutics Review: Darunavir, U.S Food and Drug Administration, 2011, https://www.accessdata.fda.gov.

140 N. Pathak, A. Singh, S. Singh, R. Vibhuti, V. Nayak, S. Dey, A. Singh, R. Pant, S. Kumar, B. Dwivedi, A. Srivastava and R. Tripathi, Computational and in-vitro assessment of TMC-310911 and its analogs as potential SARS-CoV-2 main protease inhibitors, *Front. Pharmacol*, 2021, **12**, 686501, DOI: 10.3389/fphar.2021.686501.

141 M. H. Wheeler and A. A. Bell, Melanins and their importance in pathogenic fungi, *Curr. Top. Med. Mycol.*, 1988, **2**, 338–387.

142 Y. Kubo, T. Takano, M. Endo, H. Yasuda, I. Tajima and I. Furusawa, Melanin biosynthesis in *Colletotrichum lagenarium*, *Phytopathology*, 1991, **81**, 1041–1047.

143 F. Carta, A. Maresca, M. Bua, J. T. Reid and C. T. Supuran, Discovery of saccharin and acesulfame K derivatives as selective inhibitors of carbonic anhydrase IX and XII, *Bioorg. Med. Chem.*, 2013, **21**(6), 1419–1424.

144 C. T. Supuran, Advances in structure-based drug discovery of carbonic anhydrase inhibitors, *Expert Opin. Drug Discovery*, 2020, **15**(6), 663–686.

145 P. Jiang, B. Cui, M. Zhao, D. Liu, K. A. Snyder, Y. Benard, Y. Osman, M. Margolskee, Z. Max Lu and L. Jiang, The sweet taste transduction pathway in the hT1R2–hT1R3 heterodimer involves PLCβ2 activation and $Ca^{2+}$ signaling, *Proc. Natl. Acad. Sci. U. S. A.*, 2005, **102**(36), 12900–12905.

146 P. A. Temussi, Sweet, bitter and umami receptors: a complex relationship, *Trends Biochem. Sci.*, 2009, **34**(6), 296–301.

147 V. Alterio, A. Di Fiore, F. D'Ambrosio, C. Supuran and G. De Simone, Multiple binding modes of inhibitors to carbonic anhydrases: how to design specific drugs targeting 15 different isoforms?, *J. Med. Chem.*, 2011, **54**(3), 856–861.

148 J. Suez, T. Zmora, G. Zilberman-Schapira, E. Mor, A. Dori-Bachash, D. Bashiardes, M. Zur, R. Regev-Lehavi, T. Ben-Zeev Brik, H. Federici Sivan, *et al.*, Artificial sweeteners induce glucose intolerance by altering the gut microbiota, *Nature*, 2014, **514**(7521), 181–186.

149 X. Bian, M. Chi, J. Gao, J. Tu, L. Ru, L. Lu, Y. Yang, Y. Luo, Y. Zhang, Y. Xia, *et al.*, The artificial sweetener saccharin induces gut dysbiosis and glucose intolerance by altering the gut microbiota, *Microbiome*, 2017, **5**(1), 53.

150 R. Hussain, H. Ullah, S. Khan, Y. Khan, R. Iqbal, *et al.*, A promising acetylcholinesterase and butyrylcholinesterase inhibitors: In vitro enzymatic and in silico molecular docking studies of benzothiazole-based oxadiazole containing imidazopyridine hybrid derivatives, *Results Chem.*, 2024, **7**, 101503.

151 Ş. Karaca, D. Osmaniye, B. N. Sağlık, S. Levent, S. Ilgın, Y. Özkay, A. Ç. Karaburun, Z. A. Kaplancıklı and N. Gundogdu-Karaburun, Synthesis of novel benzothiazole derivatives and investigation of their enzyme inhibitory effects against Alzheimer's disease, *RSC Adv.*, 2022, **12**(36), 23626–23636, DOI: **10.1039/d2ra03803j**.

152 D. E. Hafez, M. Dubiel, G. La Spada, M. Catto, D. Reiner-Link, Y. T. Syu, M. Abdel-Halim, T. L. Hwang, H. Stark and A. H. Abadi, Novel benzothiazole derivatives as multitargeted-directed ligands for the treatment of Alzheimer's disease, *J. Enzyme Inhib. Med. Chem.*, 2023, **38**(1), 2175821, DOI: **10.1080/14756366.2023.2175821**.

153 A. A. Elbatrawy, T. A. Ademoye, H. Alnakhala, A. Tripathi, A. Zami, R. Ostafe, U. Dettmer and J. S. Fortin, Discovery of small molecule benzothiazole and indole derivatives tackling tau 2N4R and α-synuclein fibrils, *Bioorg. Med. Chem.*, 2024, **100**, 117613, DOI: **10.1016/j.bmc.2024.117613**.

154 G. Kumar and N. P. Singh, Synthesis, anti-inflammatory and analgesic evaluation of thiazole/oxazole substituted benzothiazole derivatives, *Bioorg. Chem.*, 2021, **107**, 104608, DOI: **10.1016/j.bioorg.2020.104608**.

155 X. J. Zheng, C. S. Li, M. Y. Cui, Z. W. Song, X. Q. Bai, C. W. Liang, H. Y. Wang and T. Y. Zhang, Synthesis, biological evaluation of benzothiazole derivatives bearing a 1,3,4-oxadiazole moiety as potential anti-oxidant and anti-inflammatory agents, *Bioorg. Med. Chem. Lett.*, 2020, **30**(13), 127237, DOI: **10.1016/j.bmcl.2020.127237**.

156 A. E. Ghonim, A. Ligresti, A. Rabbito, A. M. Mahmoud, V. Di Marzo, N. A. Osman and A. H. Abadi, Structure-activity relationships of thiazole and benzothiazole derivatives as selective cannabinoid CB2 agonists with in vivo anti-inflammatory properties, *Eur. J. Med. Chem.*, 2019, **180**, 154–170, DOI: **10.1016/j.ejmech.2019.07.002**.

157 X. Xu, Z. Zhu, S. Chen, Y. Fu, J. Zhang, Y. Guo, Z. Xu, Y. Xi, X. Wang, F. Ye, H. Chen and X. Yang, Synthesis and biological evaluation of novel benzothiazole derivatives as potential anticancer and anti-inflammatory agents, *Front. Chem.*, 2024, **12**, 1384301, DOI: **10.3389/fchem.2024.1384301**.

158 I. Ivanov, S. Manolov, D. Bojilov, Y. Stremski, G. Marc, S. Statkova-Abeghe, S. Oniga, O. Oniga and P. Nedialkov, Synthesis of novel benzothiazole–profen hybrid amides as potential NSAID candidates, *Molecules*, 2025, **30**, 107, DOI: **10.3390/molecules30010107**.

159 T. B. Shaik, S. M. A. Hussaini, V. L. Nayak, M. L. Sucharitha, M. S. Malik and A. Kamal, Rational design and synthesis of 2-anilinopyridinyl-benzothiazole Schiff bases as antimitotic agents, *Bioorg. Med. Chem. Lett.*, 2017, **27**(11), 2549–2558, DOI: **10.1016/j.bmcl.2017.03.089**.

160 V. F. Pape, S. Tóth, A. Füredi, K. Szebényi, A. Lovrics, P. Szabó, M. Wiese and G. Szakács, Design, synthesis and biological evaluation of thiosemicarbazones, hydrazinobenzothiazoles and arylhydrazones as anticancer agents with a potential to overcome multidrug resistance, *Eur. J. Med. Chem.*, 2016, **117**, 335–354, DOI: **10.1016/j.ejmech.2016.03.078**.

161 N. Liu, S. Zhu, X. Zhang, X. Yin, G. Dong, J. Yao, Z. Miao, W. Zhang, X. Zhang and C. Sheng, The discovery and characterization of a novel scaffold as a potent hepatitis C virus inhibitor, *Chem. Commun.*, 2016, **52**(16), 3340–3343, DOI: **10.1039/c5cc10594c**.

162 X. X. Xie, H. Li, J. Wang, S. Mao, M. H. Xin, S. M. Lu, Q. B. Mei and S. Q. Zhang, Synthesis and anticancer effects evaluation of 1-alkyl-3-(6-(2-methoxy-3-sulfonylaminopyridin-5-yl)benzo[*d*]thiazol-2-yl)urea as anticancer agents with low toxicity, *Bioorg. Med. Chem.*, 2015, **23**(19), 6477–6485, DOI: **10.1016/j.bmc.2015.08.013**.

163 M. A. Abu-Zaied, G. H. Elgemeie and R. A. Mohamed-Ezzat, Novel acrylamide-pyrazole conjugates: Design, synthesis and antimicrobial evaluation, *Egypt. J. Chem.*, 2024, **67**(13), 529–536.

164 M. A. Abu-Zaied, G. H. Elgemeie, R. A. Mohamed-Ezzat and P. G. Jones, Crystal structure of (E)-*N*-(4-bromophenyl)-2-cyano-3-[3-(2-methylpropyl)-1-phenyl-1*H*-pyrazol-4-yl]prop-

2-enamide, *Acta Crystallogr., Sect. E: Crystallogr. Commun.*, 2024, **80**, 501–505.

165 G. H. Elgemeie, S. R. El-Ezbawy and H. A. Ali, Reactions of chlorocarbonylisocyanate with 5-aminopyrazoles and active methylene nitriles: A novel synthesis of pyrazolo [1,5-*a*]-1,3,5-triazines and barbiturates, *Synth. Commun.*, 2001, **31**(22), 3459–3467, DOI: 10.1081/SCC-100106205.

166 G. H. Elgemeie, W. A. Zaghary, T. M. Nasr and K. M. Amin, First Synthesis of Thienopyrazole Thioglycosides, *J. Carbohydr. Chem.*, 2008, **27**(6), 345–356, DOI: 10.1080/07328300802236178.

167 M. A. Abdelgawad, R. B. Bakr and H. A. Omar, Design, synthesis and biological evaluation of some novel benzothiazole/benzoxazole and/or benzimidazole derivatives incorporating a pyrazole scaffold as antiproliferative agents, *Bioorg. Chem.*, 2017, **74**, 82–90, DOI: 10.1016/j.bioorg.2017.07.007.

168 Y. Oguro, D. R. Cary, N. Miyamoto, M. Tawada, H. Iwata, H. Miki, A. Hori and S. Imamura, Design, synthesis, and evaluation of novel VEGFR2 kinase inhibitors: Discovery of [1,2,4]triazolo[1,5-*a*]pyridine derivatives with slow dissociation kinetics, *Bioorg. Med. Chem.*, 2013, **21**(15), 4714–4729, DOI: 10.1016/j.bmc.2013.04.042.

169 L. Racané, R. Stojković, V. Tralić-Kulenović, H. Cerić, M. Đaković, K. Ester, A. M. Krpan and M. R. Stojković, Interactions with polynucleotides and antitumor activity of amidino and imidazolinyl substituted 2-phenylbenzothiazole mesylates, *Eur. J. Med. Chem.*, 2014, **86**, 406–419, DOI: 10.1016/j.ejmech.2014.08.072.

170 M. Cindrić, S. Jambon, A. Harej, S. Depauw, M. H. David-Cordonnier, S. Kraljević Pavelić, G. Karminski-Zamola and M. Hranjec, Novel amidino substituted benzimidazole and benzothiazole benzo[b]thieno-2-carboxamides exert strong antiproliferative and DNA binding properties, *Eur. J. Med. Chem.*, 2017, **136**, 468–479, DOI: 10.1016/j.ejmech.2017.05.014.

171 A. Aljuhani, M. S. Nafie, N. R. Albujuq, M. Alsehli, S. K. Bardaweel, K. M. Darwish, S. Y. Alraqa, M. R. Aouad and N. Rezki, Discovery of new benzothiazole-1,2,3-triazole hybrid-based hydrazone/thiosemicarbazone derivatives as potent EGFR inhibitors with cytotoxicity against cancer, *RSC Adv.*, 2025, **15**(5), 3570–3591, DOI: 10.1039/d4ra07540d.

172 A. V. Subba Rao, K. Swapna, S. P. Shaik, V. Lakshma Nayak, T. Srinivasa Reddy, S. Sunkari, T. B. Shaik, C. Bagul and A. Kamal, Synthesis and biological evaluation of cis-restricted triazole/tetrazole mimics of combretastatin-benzothiazole hybrids as tubulin polymerization inhibitors and apoptosis inducers, *Bioorg. Med. Chem.*, 2017, **25**(3), 977–999, DOI: 10.1016/j.bmc.2016.12.010.

173 J. Ma, D. Chen, K. Lu, L. Wang, X. Han, Y. Zhao and P. Gong, Design, synthesis, and structure-activity relationships of novel benzothiazole derivatives bearing the *ortho*-hydroxy N-carbamoylhydrazone moiety as potent antitumor agents, *Eur. J. Med. Chem.*, 2014, **86**, 257–269, DOI: 10.1016/j.ejmech.2014.08.058.

174 R. A. Mohamed-Ezzat and A. M. Srour, Recent advances in benzothiazole derivatives with anticancer activity, *Adv. Anticancer Agents Med. Chem.*, 2024, **24**(7), 544–557.

175 R. A. Mohamed-Ezzat, B. M. Kariuki and A. M. Srour, Crystal structure report, *Acta Crystallogr., Sect. E: Crystallogr. Commun.*, 2023, **79**, 999–1002.

176 D. Havrylyuk, L. Mosula, B. Zimenkovsky, O. Vasylenko, A. Gzella and R. Lesyk, Synthesis and anticancer activity evaluation of 4-thiazolidinones containing benzothiazole moiety, *Eur. J. Med. Chem.*, 2010, **45**(11), 5012–5021, DOI: 10.1016/j.ejmech.2010.08.008.

177 J. Ma, G. Bao, L. Wang, W. Li, B. Xu, B. Du, J. Lv, X. Zhai and P. Gong, Design, synthesis, biological evaluation and preliminary mechanism study of novel benzothiazole derivatives bearing indole-based moiety as potent antitumor agents, *Eur. J. Med. Chem.*, 2015, **96**, 173–186, DOI: 10.1016/j.ejmech.2015.04.018.

178 I. Sović, S. Jambon, S. Kraljević Pavelić, E. Markova-Car, N. Ilić, S. Depauw, M. H. David-Cordonnier and G. Karminski-Zamola, Synthesis, antitumor activity and DNA binding features of benzothiazolyl and benzimidazolyl substituted isoindolines, *Bioorg. Med. Chem.*, 2018, **26**(8), 1950–1960, DOI: 10.1016/j.bmc.2018.02.045.

179 V. R. Solomon, C. Hu and H. Lee, Hybrid pharmacophore design and synthesis of isatin-benzothiazole analogs for their anti-breast cancer activity, *Bioorg. Med. Chem.*, 2009, **17**(21), 7585–7592, DOI: 10.1016/j.bmc.2009.08.068.

180 M. Al-Ghorbani, G. S. Pavankumar, P. Naveen, T. Thirusangu, B. T. Prabhakar and S. A. Khanum, Synthesis and an angiolytic role of novel piperazine-benzothiazole analogues on neovascularization, a chief tumoral parameter in neoplastic development, *Bioorg. Chem.*, 2016, **65**, 110–117, DOI: 10.1016/j.bioorg.2016.02.006.

181 M. B. Labib, J. N. Philoppes, P. F. Lamie and E. R. Ahmed, Azole-hydrazone derivatives: Design, synthesis, in vitro biological evaluation, dual EGFR/HER2 inhibitory activity, cell cycle analysis and molecular docking study as anticancer agents, *Bioorg. Chem.*, 2018, **76**, 67–80, DOI: 10.1016/j.bioorg.2017.10.016.

182 S. Bertini, V. Calderone, I. Carboni, R. Maffei, A. Martelli, A. Martinelli, F. Minutolo, M. Rajabi, L. Testai, T. Tuccinardi, R. Ghidoni and M. Macchia, Synthesis of heterocycle-based analogs of resveratrol and their antitumor and vasorelaxing properties, *Bioorg. Med. Chem.*, 2010, **18**(18), 6715–6724, DOI: 10.1016/j.bmc.2010.07.059.

183 H. Ma, C. Zhuang, X. Xu, J. Li, J. Wang, X. Min, W. Zhang, H. Zhang and Z. Miao, Discovery of benzothiazole derivatives as novel non-sulfamide NEDD8 activating enzyme inhibitors by target-based virtual screening, *Eur. J. Med. Chem.*, 2017, **133**, 174–183, DOI: 10.1016/j.ejmech.2017.03.076.

184 R. A. Mohamed-Ezzat, B. M. Kariuki and G. H. Elgemeie, Unexpected products of the reaction of cyanoacetylhydrazones of aryl/heteryl ketones with

hydrazine: A new route to aryl/heterylhydrazones, X-ray structure, and in vitro anti-proliferative activity against NCI 60-cell line panel, *Egypt. J. Chem.*, 2023, **66**, 225–239.

185 T. H. Abdelhafez, M. K. F. Khattab, A. Temirak, Y. M. Shaker, S. M. Abu Bakr, E. M. Abbas, S. M. H. Khairat, M. A. Abdullaziz, A. A. El Rashidi, R. A. Mohamed-Ezzat, S. A. Galal, P. E. I. Moustafa, S. A. El Awdan, H. I. Ali, W. I. El-Eraky, M. K. El Awady and H. I. El Diwani, Design and synthesis of antiviral benzimidazoles and quinoxalines, *Egypt. Pharm. J.*, 2022, **21**(2), 249–271, DOI: **10.4103/epj.epj_13_22**.

186 R. A. Mohamed-Ezzat, B. M. Kariuki, A. A. K. Al-Ashmawy and A. M. Srour, Synthesis and crystal structure of 5-{(E)-[(1*H*-indol-3-ylformamido)-imino]-meth-yl}-2-meth-oxy-phenyl propane-1-sulfonate, *Acta Crystallogr., Sect. E: Crystallogr. Commun.*, 2025, **81**, 310–313.

187 M. T. Gabr, N. S. El-Gohary, E. R. El-Bendary, M. M. El-Kerdawy and N. Ni, Synthesis, in vitro antitumor activity and molecular modeling studies of a new series of benzothiazole Schiff bases, *Chin. Chem. Lett.*, 2016, **27**(3), 380–386, DOI: **10.1016/j.cclet.2015.12.033**.

188 I. Caleta, M. Grdisa, D. Mrvos-Sermek, M. Cetina, V. Tralić-Kulenović, K. Pavelić and G. Karminski-Zamola, Synthesis, crystal structure and antiproliferative evaluation of some new substituted benzothiazoles and styrylbenzothiazoles, *Farmaco*, 2004, **59**(4), 297–305, DOI: **10.1016/j.farmac.2004.01.008**.

189 X. Xie, Y. Yan, N. Zhu and G. Liu, Benzothiazoles exhibit broad-spectrum antitumor activity: their potency, structure–activity and structure–metabolism relationships, *Eur. J. Med. Chem.*, 2014, **76**, 67–78, DOI: **10.1016/j.ejmech.2014.02.007**.

190 M. Zhang, W. Zhu and Y. Li, Discovery of novel inhibitors of signal transducer and activator of transcription 3 (STAT3) signaling pathway by virtual screening, *Eur. J. Med. Chem.*, 2013, **62**, 301–310, DOI: **10.1016/j.ejmech.2013.01.009**.

191 R. A. Mohamed-Ezzat, B. M. Kariuki and G. H. Elgemeie, Synthesis and crystal structure of N-phenyl-2(phenylsulfanyl)acetamide, *Acta Crystallogr., Sect. E: Crystallogr. Commun.*, 2023, **80**(Pt 4), 392–395.

192 G. H. Elgemeie, R. A. Mohamed, H. A. Hussein and P. G. Jones, Crystal structure of N-(2-amino-5-cyano-4-methylsulfanyl-6-oxo-1,6-dihydropyrimidin-1-yl)-4-bromobenzenesulfonamide dimethylformamidemonosolvate, *Acta Crystallogr., Sect. E: Crystallogr. Commun.*, 2015, **71**, 1322–1324.

193 R. A. Mohamed-Ezzat, B. M. Kariuki and R. A. Azzam, Discovery of promising sulfadiazine derivatives with anti-proliferative activity against tumor cell lines, *Egypt. J. Chem.*, 2024, **61**(12), 1980–1998.

194 R. A. Mohamed-Ezzat, B. M. Kariuki and R. A. Azzam, Synthesis and crystal structure of N-(5-acetyl-4-methyl-pyrimidin-2-yl)benzenesulfonamide, *Acta Crystallogr., Sect. E: Crystallogr. Commun.*, 2023, **79**(Pt 4), 331–334.

195 R. A. Mohamed-Ezzat, B. M. Kariuki and R. A. Azzam, Morpholin-4-ium 5-cyano-6-(4-methylphenyl)-4-(morpholin-4-yl)pyrimidin-2-ylamide, *IUCrData*, 2022, **7**(11), x221033.

196 S. M. Marques, C. C. Abate, S. Chaves, F. Marques, I. Santos, E. Nuti, A. Rossello and M. A. Santos, New bifunctional metalloproteinase inhibitors: an integrated approach towards biological improvements and cancer therapy, *J. Inorg. Biochem.*, 2013, **127**, 188–202, DOI: **10.1016/j.jinorgbio.2013.03.003**.

197 H. Li, X. M. Wang, J. Wang, T. Shao, Y. P. Li, Q. B. Mei, S. M. Lu and S. Q. Zhang, Combination of 2-methoxy-3-phenylsulfonylaminobenzamide and 2-aminobenzothiazole to discover novel anticancer agents, *Bioorg. Med. Chem.*, 2014, **22**(14), 3739–3748, DOI: **10.1016/j.bmc.2014.04.064**.

198 G. H. Elgemeie, A. B. Farag, K. M. Amin, O. M. El-Badry and G. S. Hassan, Design, synthesis and cytotoxic evaluation of novel heterocyclic thioglycosides, *Med. Chem.*, 2014, **4**, 814–820, DOI: **10.4172/2161-0444.1000234**.

199 A. Imramovský, V. Pejchal, Š. Štěpánková, K. Vorčáková, J. Jampílek, J. Vančo, P. Šimůnek, K. Královec, L. Brůčková, J. Mandíková and F. Trejtnar, Synthesis and in vitro evaluation of new derivatives of 2-substituted-6-fluorobenzo[d]thiazoles as cholinesterase inhibitors, *Bioorg. Med. Chem.*, 2013, **21**(7), 1735–1748, DOI: **10.1016/j.bmc.2013.01.052**.

200 G. H. Elgemeie, A. M. Salah, N. S. Abbas, H. A. Hussein and R. A. Mohamed, Nucleic acid components and their analogs: design and synthesis of novel cytosine thioglycoside analogs, *Nucleosides, Nucleotides Nucleic Acids*, 2017, **36**(2), 139–150, DOI: **10.1080/15257770.2016.1231318**.

201 G. H. Elgemeie and R. A. Mohamed, Application of dimethyl *N*-cyanodithioiminocarbonate in synthesis of fused heterocycles and in biological chemistry, *Heterocycl. Commun.*, 2014, **20**(6), 313–331, DOI: **10.1515/hc-2014-0156**.

202 G. H. Elgemeie and R. A. Mohamed, Discovery and synthesis of novel bio-isostere of purine analogues inhibiting SARS-CoV-2, *Egypt. J. Chem.*, 2023, **66**(7), 657–666, DOI: **10.21608/EJCHEM.2023.196504.7681**.

203 R. A. Mohamed-Ezzat, G. H. Elgemeie and P. G. Jones, An unexpected tautomer: synthesis and crystal structure of N-[6-amino-4-(methylsulfanyl)-1,2-dihydro-1,3,5-triazin-2-yl-idene]benzenesulfonamide, *Acta Crystallogr., Sect. E: Crystallogr. Commun.*, 2024, **80**, 120–124.

204 R. A. Mohamed-Ezzat and G. H. Elgemeie, Novel synthesis of the first new class of triazine sulfonamide thioglycosides and the evaluation of their anti-tumor and anti-viral activities against human coronavirus, *Nucleosides, Nucleotides Nucleic Acids*, 2024, **43**(12), 1511–1528.

205 R. A. Mohamed-Ezzat and G. H. Elgemeie, Novel synthesis of new triazine sulfonamides with antitumor, anti-microbial and anti-SARS-CoV-2 activities, *BMC Chem.*, 2024, **18**, 58, DOI: **10.1186/s13065-024-01164-9**.

206 S. Nalawade, V. Deshmukh and S. Chaudhari, Design, microwave assisted synthesis and pharmacological activities of substituted pyrimido[2,1-b][1,3]benzothiazole-

3-carboxylate derivatives, *J. Pharm. Res.*, 2013, **7**, 433–438, DOI: **10.1016/j.jopr.2013.04.045**.

207 G. S. Waghmare, A. B. Chidrawar, V. N. Bhosale, G. R. Shendarkar and S. V. Kuberkar, Synthesis and in-vitro anticancer activity of 3-cyano-6,9-dimethyl-4-imino 2-methylthio4H-pyrimido[2,1-*b*][1,3]benzothiazole and its 2-substituted derivatives, *J. Pharm. Res.*, 2013, **7**, 823–827, DOI: **10.1016/j.jopr.2013.08.028**.

208 G. H. Elgemeie, A. H. Elghandour and G. W. A. Elaziz, Novel Cyanoketene N,S-Acetals and Pyrazole Derivatives using Potassium 2-Cyanoethylene-1-thiolates, *Synth. Commun.*, 2007, **37**(17), 2827–2834, DOI: **10.1080/00397910701473317**.

209 R. A. Mohamed-Ezzat, G. H. Elgemeie and P. G. Jones, 2,3,4,6-Tetra-O-acetyl-1-[(dimethylcarbamothioyl)sulfanyl]-β-d-galacto-pyran-ose, *IUCrData*, 2025, **10**(6), x250544, DOI: **10.1107/S2414314625005449**.

210 G. H. Elgemeie, A. M. Salah, R. A. Mohamed and P. G. Jones, Crystal structure of (*E*)-2-amino-4-methylsulfanyl-6-oxo-1-{[(thiophen-2-yl)methylidene] amino}-1,6-dihydropyrimidine-5-carbonitrile, *Acta Crystallogr., Sect. E: Crystallogr. Commun.*, 2015, **71**, 1319–1321, DOI: **10.1107/S205698901501885X**.

211 L. Nagarapu, S. Vanaparthi, R. Bantu and C. G. Kumar, Synthesis of novel benzo[4,5]thiazolo[1,2-a]pyrimidine-3-carboxylate derivatives and biological evaluation as potential anticancer agents, *Eur. J. Med. Chem.*, 2013, **69**, 817–822, DOI: **10.1016/j.ejmech.2013.08.024**.

212 A. Andreani, M. Granaiola, A. Leoni, A. Locatelli, R. Morigi, M. Rambaldi, L. Varoli, D. Lannigan, J. Smith, D. Scudiero, S. Kondapaka and R. H. Shoemaker, Imidazo[2,1-b]thiazole guanylhydrazones as RSK2 inhibitors, *Eur. J. Med. Chem.*, 2011, **46**(9), 4311–4323, DOI: **10.1016/j.ejmech.2011.07.001**.

213 R. M. Kumbhare, K. Vijay Kumar, M. Janaki Ramaiah, T. Dadmal, S. N. Pushpavalli, D. Mukhopadhyay, B. Divya, T. Anjana Devi, U. Kosurkar and M. Pal-Bhadra, Synthesis and biological evaluation of novel Mannich bases of 2-arylimidazo[2,1-b]benzothiazoles as potential anti-cancer agents, *Eur. J. Med. Chem.*, 2011, **46**(9), 4258–4266, DOI: **10.1016/j.ejmech.2011.06.031**.

214 N. Chandak, M. Ceruso, C. T. Supuran and P. K. Sharma, Novel sulfonamide bearing coumarin scaffolds as selective inhibitors of tumor associated carbonic anhydrase isoforms IX and XII, *Bioorg. Med. Chem.*, 2016, **24**(13), 2882–2886, DOI: **10.1016/j.bmc.2016.04.052**.

215 G. Trapani, M. Franco, A. Latrofa, A. Reho and G. Liso, Synthesis, in vitro and in vivo cytotoxicity, and prediction of the intestinal absorption of substituted 2-ethoxycarbonyl-imidazo[2,1-b]benzothiazoles, *Eur. J. Pharm. Sci.*, 2001, **14**(3), 209–216, DOI: **10.1016/s0928-0987(01)00173-7**.

216 R. Alizadeh, M. Afzal and F. Arjmand, In vitro DNA binding, pBR322 plasmid cleavage and molecular modeling study of chiral benzothiazole Schiff-base-valine Cu(II) and Zn(II) complexes to evaluate their enantiomeric biological disposition for molecular target DNA, *Spectrochim. Acta, Part A*, 2014, **131**, 625–635, DOI: **10.1016/j.saa.2014.04.051**.

217 X. Fua, G. Wenga, D. Liua and X. Lea, Synthesis, characterization, DNA binding and cleavage, HAS interaction and cytotoxicity of a new copper(II) complex derived from 2-(2'-pyridyl)benzothiazole and glycylglycine, *J. Photochem. Photobiol., A*, 2013, **276**, 83–95, DOI: **10.1016/j.jphotochem.2013.12.002**.

218 S. S. AlNeyadi, A. A. Salem, M. A. Ghattas, N. Atatreh and I. M. Abdou, Antibacterial activity and mechanism of action of the benzazole acrylonitrile-based compounds: In vitro, spectroscopic, and docking studies, *Eur. J. Med. Chem.*, 2017, **136**, 270–282, DOI: **10.1016/j.ejmech.2017.05.010**.

219 D. Seenaiah, P. R. Reddy, G. M. Reddy, A. Padmaja, V. Padmavathi and N. S. Krishna, Synthesis, antimicrobial and cytotoxic activities of pyrimidinyl benzoxazole, benzothiazole and benzimidazole, *Eur. J. Med. Chem.*, 2014, **77**, 1–7, DOI: **10.1016/j.ejmech.2014.02.050**.

220 G. H. Elgemeie and R. A. Mohamed, Microwave chemistry: Synthesis of purine and pyrimidine nucleosides using microwave radiation, *J. Carbohydr. Chem.*, 2019, **38**, 1–47.

221 G. H. Elgemeie, S. A. Alkhursani and R. A. Mohamed, New synthetic strategies for acyclic and cyclic pyrimidinethione nucleosides and their analogues, *Nucleosides Nucleotides*, 2009, **38**, 12–87.

222 R. A. Mohamed-Ezzat, A. H. Hashem and S. Dacrory, Synthetic strategy towards novel composite based on substituted pyrido[2,1-*b*][1,3,4]oxadiazine-dialdehyde chitosan conjugate with antimicrobial and anticancer activities, *BMC Chem.*, 2023, **17**, 88, DOI: **10.1186/s13065-023-01005-1**.

223 R. A. Mohamed-Ezzat, Z. A. Elshahid, S. A. Gouhar, *et al.*, Synthesis of heterocycle based carboxymethyl cellulose conjugates as novel anticancer agents targeting HCT116, MCF7, PC3 and A549 cells, *Sci. Rep.*, 2025, **15**, 29196, DOI: **10.1038/s41598-025-14146-1**.

224 Y. K. Gupta, V. Gupta and S. Singh, Synthesis, characterization and antimicrobial activity of pyrimidine based derivatives, *J. Pharm. Res.*, 2013, **7**(6), 491–495, DOI: **10.1016/j.jopr.2013.05.020**.

225 R. A. Azzam, R. E. Elsayed and G. H. Elgemeie, Design, synthesis, and antimicrobial evaluation of a new series of *N*-sulfonamide 2-pyridones as dual inhibitors of DHPS and DHFR enzymes, *ACS Omega*, 2020, **5**, 10401–10414, DOI: **10.1021/acsomega.0c00280**.

226 A. Kamal, Y. V. Srikanth, M. Naseer Ahmed Khan, M. Ashraf, M. Kashi Reddy, F. Sultana, T. Kaur, G. Chashoo, N. Suri, I. Sehar, Z. A. Wani, A. Saxena, P. R. Sharma, S. Bhushan, D. M. Mondhe and A. K. Saxena, 2-Anilinonicotinyl linked 2-aminobenzothiazoles and [1,2,4]triazolo[1,5-*b*][1,2,4] benzothiadiazine conjugates as potential mitochondrial apoptotic inducers, *Bioorg. Med. Chem.*, 2011, **19**(23), 7136–7150, DOI: **10.1016/j.bmc.2011.09.060**.

227 M. Piplani, H. Rajak and P. C. Sharma, Synthesis and characterization of N-Mannich based prodrugs of ciprofloxacin and norfloxacin: In vitro anthelmintic and

cytotoxic evaluation, *J. Adv. Res.*, 2017, **8**(4), 463–470, DOI: 10.1016/j.jare.2017.06.003.

228 R. A. Azzam, H. A. Elboshi and G. H. Elgemeie, Synthesis, physicochemical properties, and molecular docking of new benzothiazole derivatives as antimicrobial agents targeting DHPS enzyme, *Antibiotics*, 2022, **11**(12), 1799, DOI: 10.3390/antibiotics11121799.

229 A. M. Sweed, S. S. Ragab, M. Fikry, R. A. Mohamed-Ezzat and Y. M. Shaker, Click approach for the synthesis of 1,4-disubstituted-1,2,3-triazoles of porphyrin-isatin/sulfa drug conjugates based on m-THPP, *J. Porphyrins Phthalocyanines*, 2024, **28**(08), 503–514.

230 H. A. Elfahham, K. U. Sadek, G. E. H. Elgemeie and M. H. Elnagdi, Novel synthesis of pyrazolo[5,1-c]-1,2,4-triazoles, imidazo[1,2-b]pyrazoles, and [1,2,4]-triazolo[4,3-a]benzimidazoles. Reaction of nitrite imines with amino- and oxo-substituted diazoles, *J. Chem. Soc., Perkin Trans. 1*, 1982, 2663–2666.

231 B. Soni, M. S. Ranawat, R. Sharma, A. Bhandari and S. Sharma, Synthesis and evaluation of some new benzothiazole derivatives as potential antimicrobial agents, *Eur. J. Med. Chem.*, 2010, **45**(7), 2938–2942, DOI: 10.1016/j.ejmech.2010.03.019.

232 S. Maračić, T. G. Kraljević, H. Č. Paljetak, M. Perić, M. Matijašić, D. Verbanac, M. Cetina and S. Raić-Malić, 1,2,3-Triazole pharmacophore-based benzofused nitrogen/sulfur heterocycles with potential anti-Moraxella catarrhalis activity, *Bioorg. Med. Chem.*, 2015, **23**(23), 7448–7463, DOI: 10.1016/j.bmc.2015.10.042.

233 S. Shafi, M. M. Alam, N. Mulakayala, C. Mulakayala, G. Vanaja, A. M. Kalle, R. Pallu and M. S. Alam, Synthesis of novel 2-mercapto benzothiazole and 1,2,3-triazole based bis-heterocycles: their anti-inflammatory and anti-nociceptive activities, *Eur. J. Med. Chem.*, 2012, **49**, 324–333, DOI: 10.1016/j.ejmech.2012.01.032.

234 F. Mir, S. Shafi, M. S. Zaman, N. P. Kalia, V. S. Rajput, C. Mulakayala, N. Mulakayala, I. A. Khan and M. S. Alam, Sulfur rich 2-mercaptobenzothiazole and 1,2,3-triazole conjugates as novel antitubercular agents, *Eur. J. Med. Chem.*, 2014, **76**, 274–283, DOI: 10.1016/j.ejmech.2014.02.017.

235 M. K. Singh, R. Tilak, G. Nath, S. K. Awasthi and A. Agarwal, Design, synthesis and antimicrobial activity of novel benzothiazole analogs, *Eur. J. Med. Chem.*, 2013, **63**, 635–644, DOI: 10.1016/j.ejmech.2013.02.027.

236 E. Deau, C. Dubouilh-Benard, V. Levacher and T. Besson, Microwave-assisted synthesis of novel N-(4-phenylthiazol-2-yl)-benzo[d]thiazole-, thiazolo[4,5-b]pyridine-, thiazolo[5,4-b]pyridine- and benzo[d]oxazole-2-carboximidamides inspired by marine topsentines and nortopsentines, *Tetrahedron*, 2014, **70**(35), 5532–5540, DOI: 10.1016/j.tet.2014.06.102.

237 P. Vicini, A. Geronikaki, M. Incerti, F. Zani, J. Dearden and M. Hewitt, 2-Heteroarylimino-5-benzylidene-4-thiazolidinones analogues of 2-thiazolylimino-5-benzylidene-4-thiazolidinones with antimicrobial activity: synthesis and structure-activity relationship, *Bioorg. Med. Chem.*, 2008, **16**(7), 3714–3724, DOI: 10.1016/j.bmc.2008.02.001.

238 S. Sarkar, J. Dwivedi and R. Chauhan, Synthesis of 1-[2 (substituted phenyl)-4-oxothiazolidin-3-yl]-3-(6-fluro-7-chloro-1,3-benzothiazol-2-yl)-ureas as anthelmintic agent, *J. Pharm. Res.*, 2013, **7**, 439–442.

239 S. Zhao, L. Zhao, X. Zhang, C. Liu, C. Hao, H. Xie, B. Sun, D. Zhao and M. Cheng, Design, synthesis, and structure-activity relationship studies of benzothiazole derivatives as antifungal agents, *Eur. J. Med. Chem.*, 2016, **123**, 514–522, DOI: 10.1016/j.ejmech.2016.07.067.

240 L. Racané, V. Tralić-Kulenović, Z. Mihalić, G. Pavlović and G. Karminski-Zamola, Synthesis of new amidino-substituted 2-aminothiophenoles: mild basic ring opening of benzothiazole, *Tetrahedron*, 2008, **64**, 11594–11602.

241 Y. Sun and Y. Cui, The synthesis, structure and spectroscopic properties of novel oxazolone-, pyrazolone- and pyrazoline-containing heterocycle chromophores, *Dyes Pigm.*, 2009, **81**, 27–34, DOI: 10.1016/j.dyepig.2008.08.010.

242 B. K. Çavuşoğlu, L. Yurttaş and Z. Cantürk, The synthesis, antifungal and apoptotic effects of triazole-oxadiazoles against Candida species, *Eur. J. Med. Chem.*, 2018, **144**, 255–261, DOI: 10.1016/j.ejmech.2017.12.020.

243 R. V. Patel, P. K. Patel, P. Kumari, D. P. Rajani and K. H. Chikhalia, Synthesis of benzimidazolyl-1,3,4-oxadiazol-2ylthio-N-phenyl (benzothiazolyl) acetamides as antibacterial, antifungal and antituberculosis agents, *Eur. J. Med. Chem.*, 2012, **53**, 41–51, DOI: 10.1016/j.ejmech.2012.03.033.

244 E. Chugunova, C. Boga, I. Sazykin, S. Cino, G. Micheletti, A. Mazzanti, M. Sazykina, A. Burilov, L. Khmelevtsova and N. Kostina, Synthesis and antimicrobial activity of novel structural hybrids of benzofuroxan and benzothiazole derivatives, *Eur. J. Med. Chem.*, 2015, **93**, 349–359, DOI: 10.1016/j.ejmech.2015.02.023.

245 M. Zajac, P. Hrobárik, P. Magdolen, P. Foltínová and P. Zahradník, Donor–π-acceptor benzothiazole-derived dyes with an extended heteroaryl-containing conjugated system: synthesis, DFT study and antimicrobial activity, *Tetrahedron*, 2008, **64**, 10605–10618, DOI: 10.1016/j.tet.2008.08.064.

246 Y. Ping, Z. Chen, Q. Ding, Q. Zheng, Y. Lin and Y. Peng, Ru-catalyzed *ortho*-oxidative alkenylation of 2-arylbenzo[d] thiazoles in aqueous solution of anionic surfactant sodium dodecylbenzenesulfonate (SDBS), *Tetrahedron*, 2017, **73**, 594–603, DOI: 10.1016/j.tet.2016.12.050.

247 F. Naaz, R. Srivastava, A. Singh, N. Singh, R. Verma, V. K. Singh and R. K. Singh, Molecular modeling, synthesis, antibacterial and cytotoxicity evaluation of sulfonamide derivatives of benzimidazole, indazole, benzothiazole and thiazole, *Bioorg. Med. Chem.*, 2018, **26**(12), 3414–3428, DOI: 10.1016/j.bmc.2018.05.015.

248 V. Murugesan, M. Saravanabhavan, A. Chandramohan, G. Raja and M. Sekar, Pharmacological investigation of 2-aminobenzothiazolium-4-methylbenzenesulphonate:

Synthesis, spectral characterization and structural elucidation, *J. Photochem. Photobiol., B*, 2015, **151**, 248–255, DOI: 10.1016/j.jphotobiol.2015.08.011.

249 A. Zablotskaya, I. Segal, A. Geronikaki, T. Eremkina, S. Belyakov, M. Petrova, I. Shestakova, L. Zvejniece and V. Nikolajeva, Synthesis, physicochemical characterization, cytotoxicity, antimicrobial, anti-inflammatory and psychotropic activity of new *N*-[1,3-(benzo)thiazol-2-yl]-ω-[3,4-dihydroisoquinolin-2(1*H*)-yl] alkanamides, *Eur. J. Med. Chem.*, 2013, **70**, 846–856, DOI: 10.1016/j.ejmech.2013.10.008.

250 E. İnkaya, Synthesis, X-ray structure, FT-IR, NMR (13C/1H), UV–Vis spectroscopy, TG/DTA study and DFT calculations on 2-(benzo[d]thiazol-2-ylthio)-1-((1s, 3s)-3-mesityl-3-methylcyclobutyl) ethan-1-one, *J. Mol. Struct.*, 2018, **1173**, 148–156, DOI: 10.1016/j.molstruc.2018.06.080.

251 P. Borowiecki, M. Fabisiak and Z. Ochal, Lipase-catalyzed kinetic resolution of 1-(1,3-benzothiazol-2-ylsulfanyl) propan-2-ol with antifungal activity: a comparative study of transesterification versus hydrolysis, *Tetrahedron*, 2013, **69**(23), 4597–4602, DOI: 10.1016/j.tet.2013.04.014.

252 E. Tanrıverdi Eçik, E. Şenkuytu, H. İbişoğlu, Y. Zorlu and Ç. Yenilmez Çiftçi, Synthesis and fluorescence properties of cyclophosphazenes containing thiazole or thiadiazole rings, *Polyhedron*, 2017, **135**, 296–302, DOI: 10.1016/j.poly.2017.07.017.

253 V. Kamat, A. Kotian, A. Nevrekar, K. Naik, D. Kokare and V. K. Revankar, In situ oxidation triggered heteroleptically deprotonated cobalt(III) and homoleptic nickel(II) complexes of diacetyl monoxime derived tri-nitrogen chelators; Synthesis, molecular structures and biological assay, *Inorg. Chim. Acta*, 2017, **466**, 625–631, DOI: 10.1016/j.ica.2017.07.036.

254 M. Bao, B. Jiang, H. Wang and L. Li, Three-component [3+2+1] cyclizations leading to densely functionalized benzo[4,5]thiazolo[1,2-a]pyrimidines, *Tetrahedron*, 2016, **72**(7), 1011–1017, DOI: 10.1016/j.tet.2015.12.075.

255 P. K. Sahu, P. K. Sahu, S. K. Gupta, D. Thavaselvam and D. D. Agarwal, Synthesis and evaluation of antimicrobial activity of 4H-pyrimido[2,1-b]benzothiazole, pyrazole and benzylidene derivatives of curcumin, *Eur. J. Med. Chem.*, 2012, **54**, 366–378, DOI: 10.1016/j.ejmech.2012.05.020.

256 A. Aboelmagd, I. A. Ali, E. M. Salem and M. Abdel-Razik, Synthesis and antifungal activity of some s-mercaptotriazolobenzothiazolyl amino acid derivatives, *Eur. J. Med. Chem.*, 2013, **60**, 503–511, DOI: 10.1016/j.ejmech.2012.10.033.

257 T. H. Al-Tel, R. A. Al-Qawasmeh and R. Zaarour, Design, synthesis and in vitro antimicrobial evaluation of novel Imidazo[1,2-a]pyridine and imidazo[2,1-b][1,3] benzothiazole motifs, *Eur. J. Med. Chem.*, 2011, **46**(5), 1874–1881, DOI: 10.1016/j.ejmech.2011.02.051.

258 S. P. Shaik, M. V. P. S. Vishnuvardhan, F. Sultana, A. V. Subba Rao, C. Bagul, D. Bhattacharjee, J. S. Kapure, N. Jain and A. Kamal, Design and synthesis of 1,2,3-triazolo linked benzo[d]imidazo[2,1-b]thiazole conjugates as tubulin polymerization inhibitors, *Bioorg. Med. Chem.*, 2017, **25**(13), 3285–3297, DOI: 10.1016/j.bmc.2017.04.013.

259 M. Shakir, S. Hanif, M. A. Sherwani, O. Mohammad, M. Azam and S. I. Al-Resayes, Pharmacophore hybrid approach of new modulated bis-diimine Cu(II)/Zn(II) complexes based on 5-chloro Isatin Schiff base derivatives: Synthesis, spectral studies and comparative biological assessment, *J. Photochem. Photobiol., B*, 2016, **157**, 39–56, DOI: 10.1016/j.jphotobiol.2016.01.019.

260 J. Joseph and G. Boomadevi Janaki, Synthesis, structural characterization and biological studies of copper complexes with 2-aminobenzothiazole derivatives, *J. Mol. Struct.*, 2014, **1063**, 160–169, DOI: 10.1016/j.molstruc.2014.01.028.

261 R. A. Ammar, A. S. Alturiqi, A. N. Alaghaz and M. E. Zayed, Synthesis, spectral characterization, quantum chemical calculations, in-vitro antimicrobial and DNA activity studies of 2-(2′-mercaptophenyl) benzothiazole complexes, *J. Mol. Struct.*, 2018, **1168**, 250–263, DOI: 10.1016/j.molstruc.2018.05.043.

262 N. M. Mallikarjuna, J. Keshavayya and B. N. Ravi, Synthesis, spectroscopic characterization, antimicrobial, antitubercular and DNA cleavage studies of 2-(1H-indol-3-yldiazenyl)-4,5,6,7-tetrahydro-1,3-benzothiazole and its metal complexes, *J. Mol. Struct.*, 2018, **1173**, 557–566, DOI: 10.1016/j.molstruc.2018.07.007.

263 A. Rambabu, M. Pradeep Kumar, S. Tejaswi and N. Vamsikrishna, Shivaraj, DNA interaction, antimicrobial studies of newly synthesized copper(II) complexes with 2-amino-6-(trifluoromethoxy)benzothiazole Schiff base ligands, *J. Photochem. Photobiol., B*, 2016, **165**, 147–156, DOI: 10.1016/j.jphotobiol.2016.10.027.

264 A. Aktaş, M. Durmuş and I. Değirmencioğlu, Self-assembling novel phthalocyanines containing a rigid benzothiazole skeleton with a 1,4-benzene linker: Synthesis, spectroscopic and spectral properties, and photochemical/photophysical affinity, *Polyhedron*, 2012, **48**(1), 80–91, DOI: 10.1016/j.poly.2012.08.074.

265 H. Gulab, Z. Shah, M. Mahmood, S. Raza Shah, S. Ali, M. Iqbal, M. N. Khan, U. Fl∈orke and S. A. Khan, Synthesis, characterization and antibacterial activity of a new calcium complex using sodium 2-mercaptobenzothiazole and 1,10-phenanthroline as ligands, *J. Mol. Struct.*, 2018, **1154**, 140–144, DOI: 10.1016/j.molstruc.2017.10.045.

266 E. Dube, D. O. Oluwole, N. Nwaji and T. Nyokong, Glycosylated zinc phthalocyanine-gold nanoparticle conjugates for photodynamic therapy: Effect of nanoparticle shape, *Spectrochim. Acta, Part A*, 2018, **203**, 85–95, DOI: 10.1016/j.saa.2018.05.081.

267 R. A. Azzam, R. R. Osman and G. H. Elgemeie, Efficient Synthesis and Docking Studies of Novel Benzothiazole-Based Pyrimidinesulfonamide Scaffolds as New Antiviral Agents and Hsp90α Inhibitors, *ACS Omega*, 2020, **5**(3), 1640–1655, DOI: 10.1021/acsomega.9b03706.

268 R. A. Azzam, H. A. Elboshi and G. H. Elgemeie, Novel Synthesis and Antiviral Evaluation of New Benzothiazole-

Bearing *N*-Sulfonamide 2-Pyridone Derivatives as USP7 Enzyme Inhibitors, *ACS Omega*, 2020, **5**, 30023–30036, DOI: **10.1021/acsomega.0c04424**.

269 M. A. Khedr, W. A. Zaghary, G. E. Elsherif, R. A. Azzam and G. H. Elgemeie, Purine Analogues as Potential CDK9 Inhibitors: New Pyrazolopyrimidines as Anti-Avian Influenza Virus, *Nucleosides, Nucleotides Nucleic Acids*, 2022, **41**(7), 643–670, DOI: **10.1080/15257770.2022.2059674**.

270 R. Chikhale, S. Thorat, A. Pant, A. Jadhav, K. C. Thatipamula, R. Bansode, G. Bhargavi, N. Karodia, M. V. Rajasekharan, A. Paradkar and P. Khedekar, Design, synthesis and pharmacological evaluation of pyrimidobenzothiazole-3-carboxylate derivatives as selective L-type calcium channel blockers, *Bioorg. Med. Chem.*, 2015, **23**(20), 6689–6713, DOI: **10.1016/j.bmc.2015.09.009**.

271 A. Arasappan, F. Bennett, V. Girijavallabhan, Y. Huang, R. Huelgas, C. Alvarez, L. Chen, S. Gavalas, S. H. Kim, A. Kosinski, P. Pinto, R. Rizvi, R. Rossman, B. Shankar, L. Tong, F. Velazquez, S. Venkatraman, V. A. Verma, J. Kozlowski, N. Y. Shih, J. J. Piwinski, M. MacCoss, C. D. Kwong, J. L. Clark, A. T. Fowler, F. Geng, H. S. Kezar 3rd, A. Roychowdhury, R. C. Reynolds, J. A. Maddry, S. Ananthan, J. A. Secrist 3rd, C. Li, R. Chase, S. Curry, H. C. Huang, X. Tong and F. G. Njoroge, 5-Benzothiazole substituted pyrimidine derivatives as HCV replication (replicase) inhibitors, *Bioorg. Med. Chem. Lett.*, 2012, **22**(9), 3229–3234, DOI: **10.1016/j.bmcl.2012.03.036**.

272 A. C. Krueger, J. T. Randolph, D. A. DeGoey, P. L. Donner, C. A. Flentge, D. K. Hutchinson, D. Liu, C. E. Motter, T. W. Rockway, R. Wagner, D. W. Beno, G. Koev, H. B. Lim, J. M. Beyer, R. M. Mondal, Y. Liu, W. M. Kati, K. L. Longenecker, A. Molla, K. D. Stewart and C. J. Maring, Aryl uracil inhibitors of hepatitis C virus NS5B polymerase: synthesis and characterization of analogs with a fused 5,6-bicyclic ring motif, *Bioorg. Med. Chem. Lett.*, 2013, **23**(12), 3487–3490, DOI: **10.1016/j.bmcl.2013.04.057**.

273 D. Rajaraman, A. Kamaraj, G. Sundararajan, S. H. Saleem and K. Krishnasamy, Synthesis, computational and spectroscopic analysis on (*E*)-(4-(2-(benzo[*d*]thiazol-2-yl) hydrazono)methyl-2,6-diphenylpiperidine-1-yl)(phenyl) methanone using DFT Approach, *Spectrochim. Acta, Part A*, 2015, **151**, 480–489, DOI: **10.1016/j.saa.2015.06.037**.

274 A. E. M. Abdallah, S. A. Abdel-Latif and G. H. Elgemeie, Novel Fluorescent Benzothiazolyl-Coumarin Hybrids as Anti-SARS-CoV-2 Agents Supported by Molecular Docking Studies: Design, Synthesis, X-ray Crystal Structures, DFT, and TD-DFT/PCM Calculations, *ACS Omega*, 2023, **8**, 19587–19602, DOI: **10.1021/acsomega.3c02418**.

275 R. A. Azzam, N. M. Gad and G. H. Elgemeie, Novel Thiophene Thioglycosides Substituted with the Benzothiazole Moiety: Synthesis, Characterization, Antiviral and Anticancer Evaluations, and NS3/4A and USP7 Enzyme Inhibitions, *ACS Omega*, 2022, **7**, 35656–35667, DOI: **10.1021/cs5c01627**.

276 P. Thanigaimalai, S. Konno, T. Yamamoto, Y. Koiwai, A. Taguchi, K. Takayama, F. Yakushiji, K. Akaji, S. E. Chen, A. Naser-Tavakolian, A. Schön, E. Freire and Y. Hayashi, Development of potent dipeptide-type SARS-CoV 3CL protease inhibitors with novel P3 scaffolds: design, synthesis, biological evaluation, and docking studies, *Eur. J. Med. Chem.*, 2013, **68**, 372–384, DOI: **10.1016/j.ejmech.2013.07.037**.

277 S. R. Nagarajan, G. A. De Crescenzo, D. P. Getman, H. F. Lu, J. A. Sikorski, J. L. Walker, J. J. McDonald, K. A. Houseman, G. P. Kocan, N. Kishore, P. P. Mehta, C. L. Funkes-Shippy and L. Blystone, Discovery of novel benzothiazolesulfonamides as potent inhibitors of HIV-1 protease, *Bioorg. Med. Chem.*, 2003, **11**(22), 4769–4777, DOI: **10.1016/j.bmc.2003.07.001**.

278 G. Manfroni, F. Meschini, M. L. Barreca, P. Leyssen, A. Samuele, N. Iraci, S. Sabatini, S. Massari, G. Maga, J. Neyts and V. Cecchetti, Pyridobenzothiazole derivatives as new chemotype targeting the HCV NS5B polymerase, *Bioorg. Med. Chem.*, 2012, **20**(2), 866–876, DOI: **10.1016/j.bmc.2011.11.061**.